SPATIAL TUNING STUDIES OF THE PATTERN EVOKED ELECTRORETINOGRAM

DOROTHY ANN THOMPSON

Doctor of Philosophy

THE UNIVERSITY OF ASTON IN BIRMINGHAM

October 1987

The University of Aston in Birmingham

SPATIAL TUNING STUDIES OF THE PATTERN EVOKED ELECTRORETINOGRAM

Dorothy Ann Thompson

Doctor of Philosophy

October 1987

SUMMARY

The locus of origin of the pattern evoked electroretinogram, (PERG), has been the subject of considerable discussion. A novel approach was adopted in this study to further elaborate the nature of the PERG evoked by pattern onset / offset presentation.

The PERG was found to be linearly related to stimulus contrast and in particular was linearly related to the temporal contrast of the retinal image, when elicited by patterns of low spatial frequency. At high spatial frequencies the retinal image contrast is significantly reduced because of optical degradation. This is described by the eye's modulation transfer function (MTF).

The retinal contrasts of square wave grating and chequerboard patterns of increasing spatial frequency were found by filtering their Fourier transforms by the MTF. The filtered pattern harmonics were then resynthesised to constitute a profile of retinal image illuminance from which the temporal and spatial contrast of the image could be calculated.

If the PERG is a pure illuminance response it should be spatially insensitive and dependent upon the temporal contrast of stimulation. The calculated loss of temporal contrast for finer patterns was expressed as a space-averaged temporal contrast attenuation factor. This factor, applied to PERGs evoked by low spatial frequency patterns, was used to predict the retinal illuminance response elicited by a finer pattern. The predicted response was subtracted from the recorded signal and the residual waveform was proposed to represent pattern specific activity. An additional correction for the attenuation of spatial contrast was applied to the extracted pattern specific response. Pattern specific responses computed for different spatial frequency patterns in this way are the predicted result of iso-contrast retinal pattern stimulation.

The pattern specific responses demonstrate a striking bandpass spatial selectivity which peaks at higher spatial frequencies in the more central retina. The variation of spatial sensitivity with eccentricity corresponds closely with estimated ganglion receptive field centre separation and psychophysical data. The variation of retinal structure with eccentricity, in the form of the volumes of the nuclear layers, was compared with the amplitudes of the computed retinal illuminance and pattern specific responses. The retinal illuminance response corresponds more closely to the outer and inner nuclear layers whilst the pattern specific response appears more closely related to the ganglion cell layer. In general the negative response transients correspond to the more proximal retinal layers.

This thesis therefore supports the proposed contribution of proximal retinal cell activity to the PERG and describes techniques which may be further elaborated for more detailed studies of retinal receptive field dimensions.

KEY WORDS: pattern electroretinogram, spatial selectivity, ganglion cells, PERG, pattern onset-offset

to my parents

CECILIA AND ROY THOMPSON

ACKNOWLEDGEMENTS

I would like to especially thank Neville Drasdo, my supervisor, for his advice, discussion and lively encouragement throughout this project.

I am also grateful to the following for their assistance during the research and compilation of this thesis:

the technical staff of the Clinical Neurophysiology Unit of Vision Sciences, Aston University, particularly Paul Furlong, for technical instruction and advice.

Bill Cox for his mathematical computations that played an important role in the development of the study.

Dr Richard Clement for his programming advice on the Pathfinder computer.

Mark Rosenfield, Robin Deeley and Dr Peter Francois for their willing discussion and assistance with computer graphics and statistical methods.

Professor Geoffrey Arden for his discussions and loan of equipment and to Chris Hogg, of Moorfields Electrodiagnostic Department, for his technical help.

Debbie Clueitt for her patience in typing the reference section

Caroline Thompson for her co'operation and assistance constructing the optical stimulator and advice whilst writing this thesis.

Professor Graham Harding for his support and the Department of Vision Sciences, Aston University for access to facilities.

and many thanks to my friends and colleagues in the Department of Vision Sciences, particularly those who volunteered to act as subjects

CONTENTS

LIST OF FIGURES

CHAPTER 5 FIGURES

TABLES

CHAPTER 4 TABLES

CHAPTER 5 TABLES

CHAPTER 7 TABLES

APPENDICES

APPENDIX 1 - CHAPTER 4

APPENDIX 2 - CHAPTER 5

CHAPTER 1.

THE ANATOMY AND PHYSIOLOGY OF THE RETINA

1.1. INTRODUCTION.

The retina encodes the visual scene into a neural representation that is successively transformed at various levels of the visual system. The visual pathway begins with the photoreceptors, the transducers, and via neuronal networks in the retina, optic nerve, optic chiasma, optic tracts, lateral geniculate nuclei, midbrain and geniculo-calcarine tracts terminates in the cerebral cortex (Duke- Elder and Wybar 1961).

In common with other vertebrates man has an inverted retina (Wirth et al 1984). Light must therefore pass through all the retinal layers before it reaches the photoreceptors. The retina is thickest at the optic disc, where ganglion cell axons leave the eye to form the optic nerve, and gradually thins towards the periphery. The variation in retinal layer thickness with eccentricity is illustrated by drawings and photomicrographs of human retinae sections (Polyak 1941; Van Buren 1963a). The retina may be generally divided into central and peripheral regions. The central region contains the foveola, fovea and macula. The peripheral region may be further subdivided into near and far periphery and ora serrata. The retina terminates at the ora serrata which is the only strong morphological connection between neuroglia and pigment epithelium aside from the optic disc where the retina is firmly attached to the choroid layer (Duke Elder and Wybar 1961; Polyak 1941, 1957; Davson 1980). The retina may be differentiated into ten layers which are illustrated in figure 1.1. by a transverse section of the near periphery region of human retina.

Most data on the anatomy and physiology of the visual system has been gained from studies on higher mammals particularly cat and monkey. The information is extrapolated to man with some caution, but is nonetheless valuable when considering comparative neurocircuitry (Rodieck 1979; Lennie 1980).

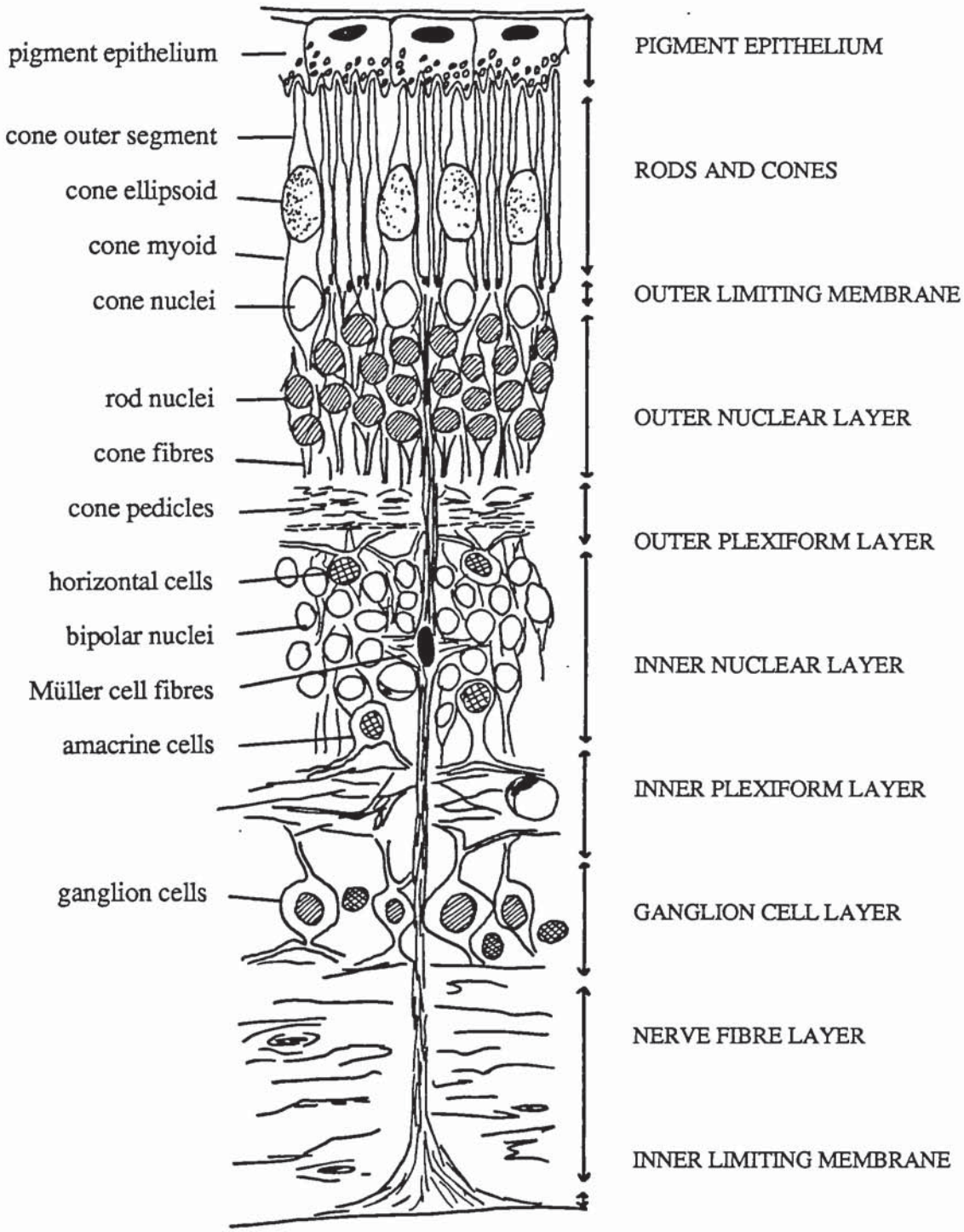

Fig 1.1 Schematic drawing of the human retina; transverse section of the near periphery.

1.2. THE PIGMENT EPITHELIUM and PHOTORECEPTORS.

The photoreceptors detect light and the pigment epithelial cells provide their metabolic support. The hexaganocuboidal pigment cells contain melanin which strongly absorbs light in the range 400 - 800nm. The pigment epithelium therefore serves to limit the amount of light reflected or scattered within the eye. In addition the pigment epithelium is involved in the active transport of metabolites, the provision of a blood-retinal barrier and the regeneration of photoreceptor pigments and phagocytosis (Spalton et al 1986).

The duplex system of rods and cones was first described by Schultze (1866). Rods are characterised by an extensive convergence onto ganglion cells (Polyak 1957). This optimises their sensitivity, but the large receptive field sizes result in poor spatial resolution. Cones on the other hand have relatively direct pathways to ganglion cells. Cone sensitivity is comparatively reduced, but the spatial resolution via smaller receptive fields is greater (D'Zmura and Lennie 1987). Cones mediate colour vision at higher light intensities. Individual cones contain one of three visual pigments whose absorption spectra are maximal for red, green or blue of wavelengths 570nm, 535nm and 445nm respectively (Davson 1980).

Anatomically both rods and cones may be differentiated into inner and outer segments which are connected by a thin cytoplasmic bridge. Light sensitive pigments are located in the outer segments on an elaborate system of stacked membraneous discs that interdigitate with the pigment epithelium. These numerous membraneous invaginations increase the effective surface area of photopigment molecules and facilitates the maximum interaction with light. Cone discs remain connected with the surface membrane. Rod discs separate from the outer membrane and undergo constant renewal. They disintegrate at their apical surface and are phagocytosed by the pigment epithelium. New discs migrate from the basal pole to replace those lost. The photoreceptor cell bodies make up the outer nuclear layer.

Rods contain the photopigment rhodopsin. Rhodopsin has two components; retinal, a light absorbing molecule closely related to vitamin A, attached to opsin a protein moiety that has differing forms. Light absorption breaks rhodopsin down into these two components. The transduction cascade causes a decrease in Na^+ conductance in the outer segment plasma membrane. (for a review see Pugh and Cobbs 1986; Lamb 1986). Light therefore prevents the leakage of Na^+ and the receptor hyperpolarises. Excitation is conveyed in the retina as an initial inhibitory, graded hyperpolarisation of the receptors.

The inner segments transmit information to the bipolar and horizontal cells. The synaptic bodies are called rod spherules or cone pedicles. The synaptic layer is termed the outer plexiform layer. Cones send out processes that end on nearby cone pedicles and rod spherules. These inter-terminal receptor contacts resemble gap junctions and allow an electrotonic spread of current between adjacent cells. There is also evidence in the macula region that other connections occur across receptor inner segments, but the nature of the contact has not been defined (Cohen 1987).

In the cat retina transmitter release is mediated at the cone axon terminal. The source of the input is not important; thus under photopic conditions the cone outer segment transduces light. In low luminance the transduction occurs in the rod outer segment and is conveyed to the cone terminal via gap junctions. Initially therefore there is not much change in the ganglion cell receptive field. However with dark adaptation the surround antagonism weakens and the ganglion cell receptive field centre becomes very sensitive. The ganglion cell may then linearly spatially summate quantal events that arise in individual rods. This suggests that the rod / cone gap junction closes after prolonged dark adaptation and the rod to rod bipolar synapse conducts the information (Sterling et al 1986). (see section 1.3, 1.4). The relative distribution of rods and cones across the retina is illustrated by Osterberg's data; figure 1.2.

Fig 1.2 Diagram showing the distribution of rods and cones in the human retina [after Østerberg (1935)]. {distribution of rods and cones on the nasal side of the fovea are not given, but would be approximately the same as the distribution on the temporal side

The human fovea morphologically matures to form the foveal depression via the peripheral 'migration of displacement' of the inner retinal layers. The full extent of the depression in humans is ≈ 5° arc or 1.5mm on the retina. The central rod free zone decreases to less than 0.4 mm^2 (54' arc extent) in adult retinae following a central 'migration of displacement' of cones. A concomitant elongation and thinning of the foveal cones also serves to increase cone packing (Yuodelis and Hendrikson 1986). The photoreceptor axons, the Henle fibres, are swept horizontally as they leave the foveal area. The horizontal and bipolar cells with which they interact and the amacrine and ganglion cells that receive information from the foveal cones are also centrifugally and laterally displaced (Cohen 1987). There is considerable evidence to suggest that the packing density of adult primate foveal photoreceptors sets the limit for the transmission of spatial frequency by the retina (Green 1970; Williams 1986).

Estimates of cone populations in human retinae have been made, but only from one eye, eg. Østerberg (1935); Polyak (1941). Curcio et al (1987) analysed the topographic distribution in 4 human eyes and produced the first photoreceptor maps since Østerberg's (1935) study. A comparison of cone distributions of the 4 eyes in this study and the eye examined by Østerberg (1935) revealed an extensive overlap in the peripheral retina and a marked variability in the fovea. Peak cone density ranged from 96,900 cones mm^{-2} to 281,000 mm^{-2}. The mean peak density was 161,900 mm^{-2} compared with Østerberg's (1935) estimate of 147,000 mm^{-2} (Curcio et al 1987). Isodensity plots were elliptical and aligned with the horizontal meridian. The cone density falls off more quickly in the vertical meridian. Cone density is higher in the nasal than temporal retina (see also Østerberg 1935; Perry and Cowey 1985). However the naso-temporal asymmetry was not consistently present until outside the optic disc (Curcio et al 1987). The individual differences in foveal architecture, possibly reflecting differences in foveal maturation, have been suggested as contributing factors to individual differences in behavioural acuity (Curcio et al 1985; Yuodelis and Hendrikson 1986).

Another approach to determining the cone spacing in the human eye uses the sampling theorem of regularly arrayed elements (William 1986). The sampling theorem states that an inter-element spacing, d, allows the unambiguous reconstruction of signals that are bandlimited to frequencies of 0.5 x d. This is the Nyquist limit for the array. Signals above the Nyquist limit result in sampling artefact or aliasing.

The cones are packed in a fairly regular triangular mosaic (Borwein et al 1980; Hirsch and Hylton 1984). Often the mosaic is described as hexagonal: technically a line drawn through the centre of adjacent elements form triangles, although each cone may be surrounded by six others (Williams 1986). Using Moiré patterns produced by laser interference fringes on the cone mosaic the spacing and packing of foveal cones can be estimated in the living eye. The contrast of these fringes is unaffected by diffraction and optical aberration (Campbell and Green 1965). For most observers the experimental estimate of the spacing between rows of cones occurs at $\approx 0.5'$ arc which is in good agreement with the anatomical measurements of a minimum centre-centre spacing between cones of 2.8-3.0 μm (Østerberg 1935; Miller 1979; Yellot 1982). This implies the highest spatial frequency that can be resolved without aliasing distortion is 50-60 cycles per degree. The regularity of the cone mosaic rapidly degenerates with eccentricity due to the intrusion of rods. Yellot (1983) proposed the extrafoveal irregular lattice is designed to remove aliasing distortion. Others however argue that it is disadvantageous (Williams 1986).

The role of neural mechanisms in limiting foveal acuity subsequent to cone sampling is reported to be comparable to the effect of optic blur in optimum conditions (Williams 1985).

1.3 INNER NUCLEAR LAYER

The inner nuclear layer contains the cell bodies of the horizontal, bipolars and amacrine cells.

1.3.1 HORIZONTAL CELLS

In man the bodies of the horizontal cells lie in the outer part of the inner nuclear layer whilst the axons and dendrites lie in the inner part of the outer plexiform layer. The cells are fewer and have shorter dendrites centrally where they are more densely packed (Duke-Elder and Wybar 1961). Cajal (1933) morphologically distinguished three types of horizontal cell in the teleost fish;

i) the *external horizontal cells* which are closest to the photoreceptors and receive an exclusive input from cones. They may be subdivided into distal luminosity L-type cells that hyperpolarise to all wavelengths, and more proximal chromaticity C-type horizontal cells which depolarise to some colours and hyperpolarise to others (MacNichol and Svaetchin 1958)

ii) the *intermediate horizontal cells* that receive an exclusive rod input and modify transmission from rod bipolars.

iii) and *internal horizontal cells* which are now considered the processes of the external horizontal cells.

Two morphological types of horizontal cell have been identified in mammal termed H1 and H2 (Kolb et al 1980). In rhesus monkey the dendrites and axons of H2 and the dendrites of H1 only contact cones whilst the axons of H1 cells only contact rods. At the monkey fovea H1 cells contact ≈ 7 cones, H2 dendrites contact about 11-14 cones. Across the retina the dendritic field size of H2 is twice that of H1. In both cat and monkey there are two populations of horizontal cells connecting to the same cones but having a ratio of dendritic field size and numbers of cones contacted of 1.5-2. However monkey retinae has more horizontal cells at each point than cat. Boycott et al (1987) suggest this is a reflection of superior spatial resolution in the monkey.

Svaetchin (1956) was the first to describe a graded potential recorded from teleost

horizontal cells; the S-potential. The cells do not produce any spike discharges, but behave electrically as a laminar conducting medium limited by a pair of high resistance membranes - the S-space (Naka and Rushton 1967; Lamb 1976). Early investigators suggested the properties of the horizontal cells would allow them to modify or control signal transmission within the retina (Svaetchin and MacNichol 1958), but Maksimova (1969) provided the first evidence of direct horizontal cell involvement in retinal processing. She discovered that an artificial injection of current into horizontal cells resulted in spike discharges from ganglion cells.

Davis and Naka (1980) reported that all the bipolar cells in catfish formed concentric receptive fields whose surrounds had the same spatial dimensions as the horizontal cell soma receptive field. Naka (1982) proposed that the bipolar cell received two independent inputs; one a local receptoral signal, the other a global integrated signal from the horizontal cell soma. Signals of average luminance could be removed at the bipolar level and consequently produce the antagonistic surround of the bipolar receptive field (Kaneko 1973).

A horizontal cell feedback mechanism (Baylor et al 1971) is thought to improve the response range of the photoreceptors and also to contribute to colour opponency (Marmarelis and Naka 1973). Like receptor to receptor contacts the horizontal cell would increase the effective field of a single receptive cell beyond the area of its outer segment.

1.3.2 BIPOLAR CELLS.

Bipolar cells are the commonest type of neurone in the inner nuclear layer and are synaptically related to the photoreceptors. The synapses may be one of three basic forms;

1) *ribbon synapses:* These synapses have an electron dense bar called the pre-synaptic ribbon which is perpendicularly oriented to the pre-synaptic membrane. This ribbon is intimately associated with synaptic vesicles. The bipolar making this synaptic

connection deeply invaginates the pedicle or spherule and is consequently named the invaginating bipolar cell. Typically ribbon synapses involve three post synaptic elements. The triad is formed by two horizontal cells laterally and a invaginating bipolar cell centrally (Dowling and Boycott 1966).

2) *superficial or flat synapses:* Flat synapses only involve one non-invaginating post synaptic element.

3) *conventional or electrical synapses:* These are gap junctions which can occur between receptors and at their terminals (Kandel and Schwartz 1982).

Cajal defined the basic neurocircuitry subserving high visual acuity as a bipolar to ganglion cell chain that is connected to a cone in a one to one fashion (Duke Elder and Wybar 1961). In primate retinae this network is represented by the midget bipolar and midget ganglion cells that synapse with individual cones (Polyak 1941).

Kolb et al (1969) characterised the cone midget pathway in monkey by the type of contact made with the cone pedicle; invaginating midget and flat midget bipolar cells. Other bipolars, flat and invaginating, were diffuse and contacted several cones. In rhesus monkey the midget bipolar cells appear to relate to red and green cones (Kolb et al 1984). A flat bistratified bipolar that contacts several cones has been proposed as a candidate for blue cone synapses (Mariani 1984; Kolb et al 1984).

These morphologically distinct bipolars are thought to correspond to two functional classes (Nelson et al 1978). Thus in cat retinae the axons of invaginating bipolars terminate in sublamina b of the inner plexiform layer, closest to the ganglion cells. Flat bipolar cell axons terminate in the more distal sublamina a. This branching pattern corresponds to the different stratification of ganglion cells (Polyak 1941; Kolb et al 1981). Indeed Nelson et al (1978) have concluded that invaginating cone bipolars support the depolarising ON-pathways in the cat retina, whilst the flat cone bipolars subserve the hyperpolarising OFF-pathway. A neuron is assigned to a pathway by the polarity of its response to the onset of light in its receptive field centre. An opposite

effect occurs with light offset. Cells that exhibit on-off behaviour are thought to connect to both information streams (Cohen 1987).

There is morphological evidence that the dichotomy exists in the monkey retina: parallel ON and OFF channels, signalling brightness and darkness, are mediated by invaginating and flat midget bipolars respectively (Kolb et al 1981). The relationship between the receptive field centre sign (ON or OFF) is discussed in greater detail with reference to ganglion cells (see section 1.4). It is likely that the two bipolar classes (depolarising and hyperpolarising) differ in their responsitivity to the same photoreceptor transmitter (Cohen 1987).

In both cat and monkey there appears to be only one type of rod contacting bipolar which makes an invaginating ribbon related synapse with the rod spherule. The rod bipolars do not seem to directly contact the ganglion cells, but use interneurones eg. amacrine cells (Famiglietti 1983). Unusually in cat retina a direct ganglion cell contact is effected through shared cone pathways, via horizontal cells or via direct gap junctions with cones (Nelson et al 1975; Nelson 1977). In rhesus monkey retina $\approx$ 2% of the ganglion cells have long dendritic processes that bypass the bipolar cells and directly contact the rods (Mariani 1981).

In human retina Missotten (1974) determined the ratio of cone pedicles to neurones in the fovea. The observations are consistent with a single cone providing the input to the receptive field centre of a foveal ganglion cell. However the number of bipolar cells in the inner nuclear layer exceeds the cones by a factor of 2-3. Thus the mean estimates for each cone pedicle were 2-3 bipolars, $\pm$ 0.6 horizontal cells, $\pm$ 0.7 amacrine cells and 0.9 ganglion cells (see section 1.7).

Confronted by the enormous variation in the number of retinal cells and the pattern of their processes Cajal (1893) divided the inner plexiform layer into 5 layers of approximately equal width. These were designated 1 to 5 in a sclerad to vitread order.

This classification of lamina relied on Golgi staining and its functional significance was not accepted (Boycott and Dowling 1969). However more recent data relating the morphological and physiological characterstics of retinal cells has renewed interest in a functional laminal classification (Karten and Brecha 1983). To this end Nelson et al (1978) introduced a bisublaminar nomenclature describing the cat's inner plexiform layer, where sublamina a is distal and b more proximal. Cajal's classification is more usually applied in the description of retinal neurotransmitter location (section 1.8).

1.3.3 AMACRINE CELLS.

Amacrines act as intermediaries between bipolar and ganglion cells. They may synapse individually with each cell type or contact both simultaneously in a dyad. They may also contact other amacrines serially (Boycott and Dowling 1969). Amacrine cells are usually classified according to their dendritic field size and stratification (Boycott and Dowling 1969; Nelson et al 1978; Famiglietti 1983).

In catfish two amacrine cells types have been distinguished. There is a sustained or true amacrine that lacks an axon and produces slow sustained potentials without spike activity. The sustained amacrine communicates with both ON and OFF ganglion cells. Naka (1976) demonstrated that the sustained catfish amacrine is inhibitory to both ON- and OFF-centre cells. There are also transient amacrine cells that are bistratified and act as frequency doublers giving non-linear responses. The transient amacrines have been described as intraretinal ganglion cells (Gallega 1971; Chan and Naka 1976).

It seems probable that the nature of the amacrine cell response will depend on the inner plexiform layer sublamina in which it receives its functional input i.e.on the centre sign of the bipolar or ganglion cell (Nelson and Kolb 1983). Wide field amacrines seem to interact in a lateral network within a single sublamina synapsing with ganglion cell dendrites in that strata. Bistratified amacrines have a distinct neurocircuitry for each of the two sublamina in which they ramify, but appear to be involved in information flow in a vertical rather than lateral direction (Kolb and Nelson 1981). Other amacrines

make reciprocal synapses with neighbouring bipolar cells and probably participate in feedback circuits (Nakatsuka and Hamasaki 1985). Indeed studies on cat retinae suggest there may be a different neurocircuitry for each morphological type of amacrine cell. This is in keeping with the large number of putative neurotransmitters associated with amacrine cells (Pycock 1985).

Of particular significance is the rod amacrine that makes contact with the rod bipolar (Famiglietti and Kolb 1975). It is atypically vertically organised and possibly unique in having separate pre- and post-synaptic processes. Rod amacrines like rod bipolars are of a single type, but show an increase in receptive field size with eccentricity. In this way a degree of dendritic overlap is maintained that compensates for the fall in cell density with eccentricity. The rod amacrine is also unique in its bifunctional output. It distributes rod input from a single type of rod bipolar to ganglion cells of both polarities (Famiglietti 1983). Thus it makes direct chemical synapse with OFF beta and alpha ganglion cells in the OFF sublamina, but indirectly contacts the ON ganglion cells via numerous large gap junctions with the axon terminals of the cone bipolar.

One interesting product of the rod amacrine in the convergence of the rod pathway is the introduction of an additional array. It is postulated that continuous noise inherent in the rod outer segment may be suppressed by a thresholding mechanism at each step in the pathway array (Sterling et al 1986). Quantal noise would otherwise tend to increase at each synaptic stage and swamp the ganglion cell signal.

Amacrine cells have been implicated in retinal phenomena that require signal propagation over large retinal areas (Hochstein and Shapley 1976; Barlow et al 1977). For example the movement of a small disc in the visual field of a cat far from the classically defined receptive field increases the steady discharge from the ganglion cell. This became known as the 'peripheral effect' (McIllwain 1966). A similar result occurs in response to an abrupt movement; the 'shift effect' (Kruger and Fisher 1973). The 'shift effect' has been found in almost all Y-cells tested, but in X-cells is weaker

or absent (Cleland et al 1971).

Derrington et al (1979) have studied the 'peripheral effect' and the 'shift effect'. They concluded that the responsible mechanisms must integrate the effect of light over areas of 1° diameter and must originate from densely packed possibly overlapping units. These mechanisms have thresholds, combine non-linearly and generate signals that are rapidly saturating functions of luminance. Several of these properties parallel those of the rectifying subunits which were proposed to account for non-linear spatial summation in Y-cells and the contrast gain control of both X- and Y-cells (Hochstein and Shapley 1976; Shapley and Victor 1979). Structurally the wide lateral interactions of the amacrine cells would allow their participation in these phenomena. Derrington et al (1979) specifically suggested the involvement of the transient amacrine, reputedly present in most vertebrates, because it always gives frequency doubled responses to sinusoidal stimulation and its generated responses are independent of stimulus size and intensity over a wide range (Chan and Naka 1976).

1.4. GANGLION CELL LAYER.

Hartline was awarded the Nobel Prize in 1967 for his investigation of ganglion cell receptive fields. The receptive field defines the spatial characteristic of a ganglion cell (Rodieck and Stone 1965a,b; Robson 1986). Examining the mammalian eye Küffler (1953) described symmetrically concentric centre-surround cat ganglion cell receptive fields. The ganglion cells responded to a light spot with either an excitatory ON-centre or an inhibitory OFF-centre whilst the surround receptive field gave an antagonistic or opposite response. In the simplest receptive field model the signals from the centre surround mechanisms with radially Gaussian weighting functions are summed to provide the output of the ganglion cells (Enroth-Cugell et al 1983). A delay in the surround signal relative to the centre signal is necessarily introduced in such models to explain the spatio-temporal interactions of a cell, although the general form of its temporal frequency response characteristic are probably provided by the characteristics of elements common to both centre and surround (Enroth-Cugell et al 1983).

Using receptive field properties and axonal velocity characteristics cat ganglion cells have been physiologically classified as X- and Y-cells (Enroth-Cugell and Robson 1966), or W-cells (Stone and Hoffman 1972). Using morphological criteria cat's ganglion cells are classified as alpha, beta or gamma cells, (Boycott and Wassle 1974) or numerically G1-G23, (Kolb et al, 1981; Hughes 1981). It has been generally accepted that alpha, beta and gamma cells are the morphological correlates of the Y-, X- and W- cell respectively (Fukuda et al,1985). A review of cat ganglion cell properties has been tabulated and referenced by Grüsser (1979). The major distinguishing characteristics are described here.

X-cells are the physiological correlates of the cat's beta-cells and compose some 55% of the ganglion cell population (Peichl and Wassle 1979). The X-cells have small concentric receptive fields of ≈ 20' arc centre size in the central retina. The receptive fields display linear spatial summation. Thus a pattern may be positioned within the receptive field such that signals arising from all points sum to zero (Enroth-Cugell and Robson 1966). The cell response is sustained to standing contrast (Cleland and Levick 1974). Non-linearity of the X-cell is reported to become obvious at low temporal frequencies (below 2Hz).

Y-cells , alpha cell correlates, account for 2-3% of the cell population. They give transient responses to standing contrast and their antagonistic receptive fields demonstrate non-linear summation (Cleland et al, 1975).

The alpha-cell collects contacts from many more cone bipolars than the beta cell and has a characteristically wide receptive field centre; centre sizes estimated at 50' arc in the central retina (Cleland et al, 1975). However the stimulus exciting the alpha-cell does so by exciting the centres of several cone bipolar cells. The same stimulus also falls on the surrounds of many other cone bipolars and therefore tends to suppress their excitement of the alpha cell. This disfacilitation would occur with some delay and would tend to cut short the excitation to the alpha cell resulting in the transient

response (Sterling et al 1986).

To explain the non-linear spatial summation Hochstein and Shapley (1976) have proposed a model comprising a series of rectifying subunits distributed throughout and beyond the classical receptive field. Each subunit would sum photoreceptor signals across an area smaller than the classic receptive field centre, but would only respond with an increase in discharge. These subunits will not be synchronously activated by a moving grating and therefore the summed response will be an unmodulated steady increase in average discharge (Shapley 1982). More recent data suggests that multiple functional subunits are present in the receptive field centres of both X- and Y-cells. In X-cells it was suggested that the linearly summing, spatially separate subunits correspond to individual cone bipolar inputs (Soodak et al 1987). However in Y-cells the number of subunits was substantially less than the bipolar to ganglion cell convergence and a clustering of bipolar input has been suggested (Soodak et al 1987).

W-cells, the physiological correlates of gamma cells, make up a large heterogenous group whose responses may be sustained or transient, but tend to be slower than X- or Y-cells and have been termed sluggish (Cleland and Levick 1974). The group includes direction sensitive neurons, movement sensitive neurons, colour coded neurons, uniformity selectors and others (Grüsser 1979). Thus some cells have a concentric centre-surround receptive field construction; others have a very different organisation.

In cat the ganglion cells, irrespective of classification, exhibit a dichotomy of inner plexiform layer branching which mirrors their bipolar input. Thus ON-centre cells have dendrites that branch in sublamina b and OFF-centre cells that branch in sublamina a (Famiglietti and Kolb 1976; Nelson et al 1978). In addition the two morphological groups appear to occur as paramorphic pairs across the retina terminating in either ON or OFF sublaminas, (b or a) (Boycott and Wassle 1974).

The importance of colour vision in primate results in some marked differences in the ganglion cell receptive field properties (Lennie 1980). Over thirty different types of ganglion cell have been isolated in monkey retina which fall into three main classifications; spectrally opponent, spectrally non-opponent and atypical ganglion cells (de Monasterio 1978a,b,c). Perry and Cowey (1984) and Perry et al (1984) have described two types of ganglion cell P.alpha and P.beta, the prefix represents primate. Each group forms a relatively homogeneous class whose morphological characteristics change in a systematic, gradual manner with increasing retinal eccentricity.

The colour opponent cells have concentrically organised receptive fields. One cone type mediates the centre response and the antagonistic surround receives input from a different type(s). de Monasterio (1978) has called these Type I cells. Perry et al (1984) relate P.beta cells to Type I cells as a substrate for the X-like colour opponent system.

Thus the Type I cell response is generally sustained and demonstrates linear spatial summation. The cell axons are slowly conducting and project to the parvocellular layers of the dorsal lateral geniculate nucleus (Schiller and Malpeli 1977). Type I ganglion cells are most frequent in the fovea, composing ≈ 90% of the cell units. Their receptive fields have the smallest centre sizes: cells receiving input from red or green cones are 2-3 times smaller than those driven by blue cones (de Monasterio and Gouras 1975; de Monasterio 1978). Type II cells are colour opponent cells that lack spatial oppponency. Their receptive fields consist of two coextensive regions that have different spectral sensitivities.

Spectrally non-opponent cells have concentric receptive fields and give transient responses to all wavelengths. Most, the Type III cells, have the same two cone mechanisms mediating the centre and surround. (Schiller and Malpeli 1977; de Monasterio 1978). The receptive fields display non-linear spatial summation. Type IV cells have different surround and centre spectral sensitivity, but also give non-linear responses. Both cell types have receptive field sizes which increase with eccentricity

and are larger than the corresponding Type 1 cells. Perry et al (1984) relate the Y-like properties of these groups to the morphological substrate P.alpha projecting to the magnocellular layers of the dorsal lateral geniculate nucleus (Dreher et al 1976; Schiller and Malpeli 1977).

The receptive field sizes of both P.beta and P.alpha ganglion cells are consistently larger than the dendritic field size; probably because the dendritic field size of the pre-synaptic neurones exceeds the borders of the ganglion cell dendritic field (Perry et al 1984). The coverage factor is a measure of the degree of receptive field centre overlap and describes how many ganglion cells sample a particular point in the visual field (Cleland et al 1975). The coverage factor for the P.beta cell class was lower at 1.4-2.3 than for P. alpha cells at 2-7. Consequently P.beta cells are thought to represent the midget ganglion cells that subserve high spatial resolution (Perry et al 1984).

Chromatic and achromatic contrast sensitivity measures have been made in monkeys treated with a neurotoxicant that selectively damages the medium size ganglion cell pathway (Merigan and Eskin 1986). The findings support the proposition that the medium cell, P.beta, retino-geniculate pathway contributes primarily to the detection of achromatic high spatial, low temporal frequencies and chromatic vision. The larger cell pathway, equivalent to the P.alpha cell network, appears sensitive to lower spatial and higher temporal frequencies. Nonetheless there is a substantial overlap in spatio-temporal contrast sensitivity of P- and M- cells (Merigan 1987).

Of the atypical receptive field organisations there are edge detectors or ON-OFF units, direction selective units and uniformity detectors (Stone and Fukuda 1974; Lennie 1980). Edge detectors lack a distinct concentric receptive field and respond with increased discharge to the onset and offset of light: ie give transient rectified responses (Hochstein and Shapley 1976). In monkey such units give frequency doubled ON-OFF responses to flickering stimuli in the central part of their receptive field

In catfish retinae ganglion cells have been found to have pre-synaptic dendrites. Thus in addition to the proximal dendrites that receive input from bipolar and amacrine cells, distal dendrites make synapses on vesicle containing amacrine or ganglion cell dendrites and ribbon containing processes as on bipolar axon terminals (Shepherd 1986). This pattern of synaptic connection was only ellucidated on large field ganglion cells of varying property. No distal terminal clusters were seen around narrow field ganglion cells (Sakai et al 1986). Ganglion cells are known to lack recurrent axon collaterals and have been believed to function entirely as a follower cell, driven by its inputs from bipolar and amacrine cells. Evidence of local distal dendritic processing suggests that ganglion cells can at least in part shape their own response.

1.5. NEUROGLIA AND MÜLLER CELLS.

Glial tissue may be distinguished from neurones in that:

a) it neither generates action potentials nor receives synaptic input

b) glia membrane potentials are more negative than those of neurones - they depend on a potassium ion gradient predicted by the Nernst equation.

c) neighbouring glia cells are electrically coupled

(Duke Elder and Wybar 1961).

Müller cells are the principle glial element in the vertebrate retina. They are radially directed and span the thickness of the retina; their processes fill most of the extra-neural space (Conner et al 1985). Their exact function isn't known. Biochemical studies suggest that they are involved in the inactivation of chemical transmitters and the removal of metabolic products (Sarthy 1983). They are electrically coupled via intracellular channels associated with gap junctions that allow cytoplasmic continuity. Ions and small metabolites may be exchanged between cells providing a possible mechanism for ionic homeostasis in the retina (Conner et al 1985) The Müller cells are of particular interest in electroretinography because of their proposed involvement in the spatial buffering of potassium ions (Newman 1980,84; Ripps and Witkovsky 1985). (refer to section 2.2.3).

1.6. CENTRIFUGAL FIBRES AND INTERPLEXIFORM CELLS

Cajal reported thin fibres in dog retina that extended from neurones in the superior colliculus to the inner plexiform layer (Duke Elder and Wybar 1961). These centrifugal fibres are postulated as providing a pathway for a central control of retinal function (Jacobsen and Gestring 1958). There is still some debate about their existence in human retinae (Wachtmeister and Azazi 1985). Some studies have reported 'supernormal' electrical responses from the retinae of subjects suffering optic nerve lesions. This may reflect a loss of central inhibitory influence mediated by a centrifugal network (eg Arden et al 1982 - section 3.4.2.). Adopting a more pragmatic approach Perry et al (1984) reason that the human retina most probably resembles other vertebrates and does possess centrifugal fibres.

Interplexiform cell bodies are located at the innermost border of the inner nuclear layer, but their processes extend into both inner and outer plexiform layers (Dowling 1979). They appear to provide an information route from inner to outer retina. Their presence in primate retina has been disputed, but they have been isolated in human retina (Frederick et al 1982). The input to interplexiform cells is exclusively from amacrine cells. The output occurs in both plexiform layers particularly in the outer plexiform layer with synapses onto horizontal cells and some bipolar cell dendrites (Ryan and Hendrickson 1987). The interplexiform cell does not directly contact photoreceptors or ganglion cells. It has been suggested that interplexiform cells regulate centre-surround antagonism in the outer plexiform layer: thus the centre response of a bipolar would be enhanced whilst the lateral inhibitory effects initiated by the horizontal cells is depressed (Berson 1987).

1.7. PARALLEL PATHWAYS AND NEURAL CIRCUITS.

The parallel conduction of visual information along for example ON and OFF, sustained and transient channels, or the more recent proposition of achromatic and chromatic pathways receives support from both anatomical and physiological studies.

For example two types of cone bipolars contact the ON beta ganglion cell in cat retina and another two types contact the OFF beta ganglion cell. At least one member of each pair also connects with a corresponding alpha cell. Hence the observation of Missotten (1974) of more foveal bipolars than cones or ganglion cells (see section 1.3). The cone bipolars feeding the ON beta cell are driven by light in opposite directions (Nelson and Kolb 1983). As yet there is no evidence that a cone bipolar uses an inhibitory transmitter (Sterling et al 1986). Thus it is probable that cone bipolar hyperpolarisation and depolarisation are accompanied by a decrease and increase in transmitter release respectively. ON beta cell response is caused by increased excitation from one cone bipolar and decreased inhibition from another. This complementary action is advantageous because it allows the input of a linear signal to the ganglion cell over a wider range and can provide more gain than a single ended mechanism. The cone bipolar pair connected to the OFF beta cell are believed to behave similarly; centre excitation and disinhibition occur when light is switched off.

The dichotomy that occurs in the stratification of ON- and OFF- centre neurons in the inner plexiform layer initialises the processing of visual information in parallel channels (Massey 1983). Indeed Schiller (1984) reports the ON and OFF channels originating in monkey retina appear to remain functionally separate at the lateral geniculate nucleus. In this way both an increase and decrease in light can be signalled as an excitatory process to the higher visual centres. Parallel processing along separate neural channels has been reported in every vertebrate investigated (Lennie 1980). These visual channels have different functions, cell types and organisations (Kaplan and Shapley 1986).

A feature of the visual system is the convergence of $\approx$ 130 million photoreceptors onto $\approx$ 1.2 million ganglion cells (Sanchez et al 1986). Different arrays of connection are constructed in the retina which function under different stimulus conditions.

One concept of parallel visual channels is based on the model that the visual system

performs a type of Fourier analysis of the visual environment. Thus it is assumed that the visual system contains a number of channels each responding to a selective range of spatial frequencies (Campbell and Robson 1968). To be effective the distribution of the size tuned mechanisms must show a systematic variation with eccentricity and several mechanisms of different size tuning must coexist at each retinal eccentricity (Wilson 1978).

Neuroanatomical evidence supports the concept of a few receptive field sizes centred at each retinal point. Thus at the bipolar level midget bipolars receive input from single cones. Flat top cone bipolars pool signals from a hexagonal array of ≈ 7 neighbouring cones (Boycott and Dowling 1969). The cone mosaic may therefore sample with a field diameter of 3:1, perhaps sampled in parallel by two groups of ganglion cells (Wilson and Bergen 1979). At ganglion cell level another receptive field organisation can arise indirectly from amacrine cell action.

However inspite of the well documented small receptive field size of tonic, P.beta-type, ganglion cells Lee et al (1985) report that tonic and phasic ganglion cells in monkey have similar spatial resolution. This is contrary to work on cat neurons which suggests that spatial resolution is reciprocal to receptive field size (Shapley and Lennie 1985). Kaplan and Shapley (1986) have explained this discrepancy by considering the interaction of a cell's contrast gain with its receptive field size. Thus the higher gain of phasic, P.alpha-type, cells can explain their high resolution.

Two parallel channels that relate to the projection of ganglion cells to the lateral geniculate nucleus have been isolated (Kaplan and Shapley 1986). Thus ganglion cells of higher sensitivity, project to the magnocellular layers and function near threshold for isochromatic luminance patterns. Lower sensitivity cells, projecting to the parvocellular layers are recruited at higher contrasts when the responses of the high sensitivity group become saturated.

In this way a classification of monkey ganglion cells can be introduced that describes their projection to the LGN. P-cells project to the parvocellular layers of the LGN, have small receptive fields, are wavelength sensitive and are insensitive to contrast. M-cells project to the magnocellular layers and have larger receptive fields. They are not wavelength selective, but are very sensitive to contrast (Shapley and Perry 1986). Of monkey ganglion cells P-cells are the most numerous and give a sustained response to light at the peak of their spectral sensitivity curve. However they respond phasically to white light or other broad band illumination (de Monasterio 1978). M-cells resemble P-cells in their transient response to broad band illumination.

Shapley and Perry (1986) have measured the contrast sensitivity of the M- and P-ganglion cells. They report that M-cells are composed of two groups that correspond to X and Y cells in cat. M_X are more numerous than M_Y cells. The high gain and high sensitivity of the M-cell pathway are probably important for pattern perception at low contrasts and low to intermediate frequencies. At high contrast the P-cells may extend the dynamic range of vision, because the M-cell responses will have saturated (Shapley and Perry 1986). Merigan (1987) however concludes that there is a wide overlap in the spatio-temporal properties of M- and P-cells.

The mean P-cell receptive field size near the fovea is 3.6' arc diameter. The mean M-cell receptive field diameter is 7.2' arc (Shapley and Perry 1986). The dimensions of the P-cell do not alter significantly within the central 5° (de Monasterio 1978). A modified ganglion cell classification in monkey based on visual and spatial filtering properties has been suggested in an effort to relate cell types with those encountered in cat. Thus P-cells seem to form a subgroup concerned with colour vision.

Shapley and Perry (1986) place great importance on the constant P-cell dendritic tree size in the central 8° of the fovea whilst the M-cell show a spatial scaling of dendritic tree and receptive field size with retinal eccentricity that corresponds to psychophysical spatial scaling. Mullen (1985) has shown that human colour perception is a low gain,

low resolution system. It is suggested that the very small 'midget' P-cell receptive field sizes could provide a way of preserving wavelength specificity in the central retina via one-one connections with bipolar and ganglion cells.

This system of nomenclature conflicts with data presented by Rodieck et al (1985) on two Golgi stained flat mounted human retinae. They counted the ganglion cells that stratified within a narrow band of the inner plexiform layer. At any eccentricity there was no overlap between the group with the large receptive fields and the group with the smaller receptive fields. Rodieck et al (1985) relate the large field cells to Polyak's (1941) parasol cells and Perry and Cowey's (1984) P.alpha cells in monkey. The small field cells were related to the midget ganglion cell of Polyak (1941) and the P.beta cells of Perry et al (1984). Neither the parasol nor midget cells demonstrate a plateau in dendritic field diameter within the central 8° as Shapley and Perry (1986) reported in monkey retina. However the midget ganglion cells appear to increase in dendritic field diameter more rapidly with eccentricity than the parasol cells (direct inspection of the scatter plot) (Rodieck et al 1985).

There have been theroretical attempts to relate the retinal ganglion cell density to the cortical scaling of the visual field to derive a cortical magnification factor M. These studies have collated all available counts of ganglion cells in both primate and human retinae. Several difficulties are encountered in these manipulations: different techniques of mounting sections, accounting for cell shrinkage and methods of counting nuclei. The displacement of foveal ganglion cells requires an additional estimation which is most commonly based on the foveal cone density.

Thus Drasdo (1977) pooled empirical estimates of the human ganglion cell density from three studies on 12 eyes and selected a central density which equated the integrated receptive fields with ganglion cell somata inside 12.5°. He reported that this density coincided with Polyak's (1957) data for centremost cones. An equation expressing the variation of ganglion cell receptive field density per solid degree with

eccentricity was derived:

$$V=k[1+0.59\emptyset]$$

where $V= 1/\sqrt{Dr}$, Dr = receptive field density and $\emptyset$ = peripheral angle

There is some debate about the accuracy of the centremost cone estimate; some workers advocating a lower value. This effectively reduces the gradient of decline of ganglion cell receptive field density with eccentricity (Rovamo and Virsu 1979). However available data does not yet account for differential scaling of human ganglion cell classes which may correlate with psychophysical results more sensitively.

1.8. RETINAL NEUROTRANSMITTERS.

The isolation and recognition of neurotransmitters has clarified some of the mechanisms and pathways that occur in the retina. Some isolated chemicals are putative transmitters and their function has not yet been elaborated. Currently available data may be schematically summarised in figure 1.3.

Most of the identified substances are associated with the amacrine cells. The large number may minimise cross-talk in a system that is not particularly well insulated and may relate to the many morphological different amacrine cells (see section 1.4). Reviews of current transmitter data have been made by Ehinger (1983), Pycock (1985) and Marc (1986). A few of the well investigated substances are described. Some have been applied experimentally to isolate and so examine the function of specific retinal cells.

TAURINE is concentrated mostly in the photoreceptor layer, but it also occurs in significant amounts in the inner nuclear layer and the inner plexiform layer. It appears able to separate ON and OFF channels. Strychnine is able to rapidly reverse taurine's depressive effects. Taurine has been implicated in the temporal organisation of ganglion cell receptive fields (Bonadventure and Wioland 1978). In rat retinae taurine is released at the withdrawal of a depolarising stimulus and thus demonstrates an OFF effect. (Pycock 1985). Taurine mediated cells may therefore fire at the cessation of a light stimulus possibly to stabilise neural elements.

Fig 1.3 Schematic diagram showing the distribution of putative neurotransmitters of the vertebrate retina. [After Ehinger 1983; Pycock 1985]

DOPAMINE is usually found in the distal part of the inner nuclear layer (Cajal's sublamina 1.). Dopaminergic neurones are located among the amacrine cells of investigated species (Ehinger 1983). Ultrastructure studies show that dopaminergic neurones make conventional synapses but only with other amacrines.

In cat retina dopamine has been associated with a wide field amacrine (Kolb et al 1981). The dopaminergic amacrine is thought to control the convergence of the rod pathway into the cone pathway via connections with the rod amacrine (Pourcho 1982). Indeed in monkey retina dopaminergic amacrine cells parallel rods in their spatial distribution. This supports suggestions of its involvement in rod circuitry (Mariani et al 1984). It is possible that the activation of tyrosine hydroxylase, which increases the concentration of dopamine during light adaptation could uncouple the rod and cone system in the inner plexiform layer.

Thier and Adler (1984) found that dopamine suppressed the spontaneous activity of ganglion cells which could relate to a reduced rod contribution. In light adapted retina Maguire and Smith (1985) noted that dopaminergic amacrines affected the OFF more than the ON pathway. The receptive field centre of the OFF ganglion cell became more sustained and its spatial summation more linear. Considering the lateral organisation of dopaminergic neurons it is unlikely that dopamine is involved in pattern vision. The association of dopaminergic neurons with rods suggests a role in adaptation and modulation of retinal response.

GLUTAMATE is a most likely transmitter for the photoreceptors (Pycock 1985). A glutamate analogue APB, (2 amino-4 phosphonobutyric acid), selectively blocks the depolarising bipolar cell response in Mudpuppy (Slaughter and Miller 1981). APB is therefore highly specific for the ON pathway and has been used in electrophysiological experiments (see section 2.2.3.).

L-ASPARTATE enhanced the excitatory firing rate of sustained ganglion cells in cat

irrespective of their centre sign (Ikeda and Sheardown 1983). This suggests that aspartate is released by both ON and OFF bipolars when they depolarise.

ACETYLCHOLINE is synthesised and released by a sparse group of amacrines that symmetrically line both margins of the inner plexiform layer of rabbit retinae (Masland 1980). It has also been isolated in retinal fractions containing bipolar cell, but across a variety of species most commonly occurs in association with the amacrine cells (Hutchins 1987).

Ganglion cells resolve smaller stimuli than the dendritic fields of the amacrines that excite them. This led Masland and Tauchi (1986) to suggest that local regions of amacrine cell's dendritic tree may be capable of spatially autonomous release of neurotransmitter.

Ganglion cells only have a partial dependence on the cholinergic input and the action of acetylcholine, (ACh), is consequently diffuse. In cat retina ACh has been found to mediate the excitatory input of transient or phasic ganglion cells irrespective of their centre polarity (Ikeda and Sheardown 1983).

gamma-AMINOBUTYRIC ACID, (GABA), is accumulated by horizontal, amacrine and possibly ganglion cells as well as Müller cells in various vertebrate species (Karten and Brecha 1983). GABA appears the most likely mediator of feedback loops and lateral inhibition in the retina. It has been shown to counteract ganglion cells excitation and intensify spontaneous and light evoked inhibition (Pycock 1985). In Mudpuppy GABA hyperpolarised ganglion cells and similarly inhibited cat ganglion cells (Miller et al 1981; Ikeda and Sheardown 1983). In frog retina picrotoxin specifically antagonises the inhibitory action of GABA and was found to induce a spatial re-organisation of the ON-OFF ganglion cell receptive field (Bonadventure and Wioland 1978). In cat retina GABA caused a modification of the Y-cell centre/surround balance to the detriment of the surround (Kirkby and

Enroth-Cugell 1976). Thus it appears that GABA participates in the structure of the centre/surround antagonism.

GLYCINE release is sensitive to potassium ion concentration. The direct application of glycine to ganglion cells strongly suppresses spontaneous and light evoked activity irrespective of cell class.

Ikeda and Sheardown (1983) found both GABA and glycine to be inhibitory, but proposed a dichotomy of ganglion cell action: GABA mediates inhibition of both sustained and transient ON-centre cells whilst glycine mediates inhibition of sustained and transient OFF-centre cells. GABA is therefore released to suppress ON cells when OFF centre cells are activated by dark objects and glycine is released to suppress OFF cells when ON cells are firing (Ikeda and Robbins 1987). The hypothetical physical separation of GABA-ergic and glycinergic pathways was also proposed by Miller et al (1977). They found two populations of on/off amacrine cells one releasing GABA the other glycine. The separation correlates with the location of glycine concentrations in sublamina a. of the monkey's inner plexiform layer and GABA concentrations in sublamina b. (Berger et al 1977). Ariel and Daw (1982a,b) examined the effects of GABA and glycine on rabbit ganglion cells. They appeared to cause a response specificity in some cells to the size, direction, orientation and velocity of a moving stimulus that would be in keeping with an inhibitory effect.

There is much debate about the exact functions of individual transmitters and also about their interaction with one another: e.g. in rat retinae there is evidence for the tonic GABA mediated inhibition of dopamine cells in both ON and OFF pathways when the cells are dark adapted (Kamp and Morgen 1981). Component analysis in electroretinographic studies have most frequently employed glutamate analogues to pharmacologically dissociate the retinal pathway.

CHAPTER 2

THE ELECTRORETINOGRAM

2.1 HISTORY AND DEVELOPMENT OF THE ERG

The demonstration of a steady positive-negative, corneo-retinal potential by du Bois Reymond in 1849 heralded an examination of the eye's electrical response to light and the first stages of visual processing (Armington 1974; Riggs 1977; Henkes 1984).

The electroretinogram, (ERG), is a measure of the transient changes in the eye's resting potential that occur in response to light. It was independently discovered and reported by Holmgren (1865) in Sweden and Dewar and M'Kendrik (1873) in Scotland. However it was Einthoven and Jolly (1908) who produced a permanent record of the ERG from a dark adapted frog's eye and first designated portions of the curve by letter. They displayed a corneal positive potential change as an upward deflection; a convention adhered to today. The earliest negative deflection was termed the a-wave, the following larger positive the b-wave and the more slowly developing positive the c-wave. Occasionally they also noted a corneal positive d-wave or OFF effect at the cessation of the light stimulus (Henkes 1984).

Many of the early workers realised that the ERG was likely to be a composite of more than one separate process (eg Einthoven and Jolly 1908; Piper 1911). However the search for agents with selective effects on different ERG components did not begin until 1932 (Granit 1963). Granit (1933) investigated the ERG under conditions of ether anaesthesia and in his now classical analysis deduced the presence of three processes termed PI, PII and PIII. The processes were labelled in order of their successive disappearance under anaesthesia, PIII being the most resistant. PI is a slowly developing positive change which tends to disappear after light adaptation or with intense light stimuli. PII is also positive, but it arises rapidly and appears responsible for the b-wave. PIII is a rapidly generated, negative component consistent

with the a-wave.

The morphology of the ERG alters with the level of light adaptation and the intensity of stimulation. It also depends on the anatomy of the stimulated retina. Granit (1935) classified retinas as E-type which are predominantly comprised of rods and I-type which are mainly composed of cones. The response envelope becomes faster as the ambient illumination increases. This reflects a shift in operating characteristics from the slower, more sensitive rod system to the faster, less sensitive cone system.

The schema, shown in figures 2.1a and b [after Granit (1933) and Ripps and Witkovsky (1985)], describes how the summation of several light evoked potentials of different polarity, duration, amplitude and latency result in the recorded ERG envelope. However the simple schema belie the underlying complexity of ionic shifts that generate the extra-cellular field current. The improvement of microelectrode technology in hand with recording methods has facilitated an understanding of the processes involved at each retinal level. There is good evidence that the electrical potentials result from light induced changes in extracellular potassium ions, (K^+_0), acting passively on the membranes of the non-neuronal elements (Ripps and Witkovsky 1985). It is appropriate therefore to consider some of the developments and investigations that have contributed to the understanding of the retina's electrophysiology.

2.2 COMPONENT ANALYSIS OF THE ERG

2.2.1. The early receptor potential, (ERP).

The ERP is a diphasic response of extremely short latency that is recorded from the junction between inner and outer segments of the receptors (Brown and Murakami 1964). The initial small positive wave (R1) is followed by a larger negative wave (R2) which leads into the a-wave (Galloway 1967). The ERP may only be recorded to very intense light flashes and in the human occurs within 1.5 ms of stimulus onset. Cone and Cobbs (1969) showed that the ERP changed its form at successive intervals

FIG 2.1a) after GRANIT (1933)

FIG 2.1b) after RIPPS AND WITKOVSKY (1985)

Fig 2.1a) Schema showing Granit's (1933) analysis of the ERG recorded from an E -type retina to a light of high intensity. The three processes are labelled PI, PII and PIII in order of their increasing resistance to ether anaesthesia.

Fig 2.1b) Simplified schema demonstrating the summation of potentials of different amplitude, polarity, duration and latency which results in the recorded ERG envelope. The probable origin of each component is indicated. [after Ripps and Witkovsky (1985)]

following a bleaching exposure. The currently accepted hypothesis is that the potential arises from a change in orientation or magnitude of the electric dipole of the visual pigment molecule as it undergoes isomerisation (Davson 1980).

2.2.2 The a-wave.

In Granit's analysis the a-wave corresponds to PIII which is most resistant to ether and anoxia and has a short implicit time. He concluded that it had a photoreceptor origin rather than a neural origin (Granit 1933). Piéron and Segal (1939) supported Granit's conclusion when they found the a-wave to be insensitive to temperature changes. This has been confirmed by Adolph (1985) in the isolated turtle retina.

Examining this proposition Noell (1954) carried out a series of innovative experiments using chemical agents. He produced optic nerve blockage by injecting iodoacetic acid into a rabbit eye. He found the a-wave was most resistant to this treatment and was only affected when repeated applications of the chemical had destroyed considerable numbers of photoreceptors. Potts et al (1960) treated the eyes of newborn mice with sodium glutamate to produce retinae purely of receptor cells. The only ERG component they were able to record from such retinae was the a-wave. Thus evidence accumulated that the a-wave generator was the photoreceptor layer.

Brown and Watanabe (1962) found the ERG recorded from the fovea, an area where the retina is composed mainly of photoreceptors, to have a large a-wave. More peripheral regions, with more prominent inner nuclear layers, generated an ERG with a diminished a-wave, but larger b-wave. Brown and Watanabe (1962) also demonstrated that clamping the retinal circulation in monkey diminished the b-wave whilst the a-wave remained. Since the photoreceptors and pigment epithelium are supplied by the chorio-capillaris the remaining negativity must reflect rod and cone physiology. Indeed Brown et al (1965) called the residual response the late receptor potential.

In frog PIII has been separated into two fractions using micropipette recording techniques; one fraction is recorded distally from the receptor layer and the other more proximally from the inner nuclear layer (Murakami and Kaneko 1966). The faster, receptoral PIII comprises the initial negativity. Microelectrode recordings across rat rods has shown this faster component to be the result of radial interstitial currents generated by the light evoked closure of Na^+ channels along the plasma membrane of the receptor outer segments (Penn and Hagins 1969). Valeton and van Norren (1982) applied a statistical method of component analysis to intracellular depth recordings obtained with a bipolar microelectrode and isolated a receptor response from cone outer segments in the intact rhesus monkey eye.

A photoreceptor origin was difficult to reconcile with the negative polarity of the a-wave unless the receptors hyperpolarise in light ie become positive (Tomita 1970). In darkness sodium ions, (Na^+), enter the photoreceptor outer segment and are actively removed from the inner segment producing the "dark current". Pump activity also transports potassium ions, (K^+), into the cell that passively leave via the inner segment cell membrane (Davson 1980). Matsuura et al (1978) reasoned that light does not affect the Na^+/K^+ active transport mechanism, but reduces the passive entry of Na^+ and the exit of K^+. The net result is a decrease in the level of extracellular K^+. In human eye Yonemura and Kawasaki (1978) found that the latency and slope of the leading edge of the a-wave corresponds to the late receptor potential which in turn reflects the distal PIII.

The 'slower', more proximal, PIII is thought to be a reflection of the concomitant decrease in K_0^+ caused by the suppression of the 'dark current'. In mammals it is generally much smaller than the fast receptoral PIII, although Marg (1955) has reported its proportionality to the a-wave. The 'slow' PIII, the afterpotential manifest after the b-wave, is particularly clear with periodic stimuli and becomes larger as the stimulus luminance is increased (Armington 1974). In isolated rat retina Arden (1977) has produced evidence of Müller cell involvement in the 'slow' PIII genesis. A 'slow' PIII

component has also been isolated in primate by Valeton and van Norren (1982) using component analysis. They precluded a receptoral or pigment epithelial origin of 'slow' PIII because it did not reverse in polarity when the pigment epithelium was penetrated by the recording electrode. More recent work by Nilsson (1984) supports the Müller cell hypothesis of 'slow' PIII generation. He reports an increase in c-wave amplitude after the slow PIII is reduced or abolished by the administration of alpha-AAA, (amino-adipic acid). The PI is then able to form the c-wave without counteraction.

The schema of Ripps and Witkovsky (1985) demonstrates how only a small proportion of the fast transient of the receptor potential contributes to the leading edge of the a-wave. The rising phase of the b-wave and later potentials masks the remainder of the receptor response.

2.2.3 The b-wave.

The b-wave is the large positive ERG component seen as the expression of Granit's PII. There is little doubt that it arises from elements situated postsynaptically to the photoreceptors as the b-wave is blocked by virtually any agent that impairs synaptic transmission between the photoreceptors and their second order neurons (Ripps and Witkovsky 1985).

Intraretinal recordings of the intact cat eye suggested PII was composed of two parts: a graded, positive plateau of rectangular waveform, the DC-component, which acquires a positive, phasic component on its rising phase at high stimulus intensity (Brown and Wiesel 1961a,b). Both components were located at maximal amplitude in the inner nuclear layer. However they could be differentiated by low intensity stimuli that markedly reduced the transient component, but did not alter the DC-component.

It was Faber (1969), working in Noell's laboratory, who first suggested that the b-wave reflects extracellular currents that result from the depolarisation of the radially orientated Müller cells. His current source density analysis of rabbit retinae indicated a

current sink, *(a locus of K^+ efflux from active retinal neurones where current flows into the Müller cell)*, located in the outer plexiform layer with current sources, *(where K^+ flows out of the Müller cell)*, both proximal and distal to that locus extending to the inner margin of the retina. He concluded that the only element with a spatial distribution consistent with the distribution of the b-wave sources and sinks is the Müller cell.

In 1970 Miller and Dowling reported a similarity of latency and waveform of the intracellularly recorded Müller cell of Mudpuppy and the extracellularly recorded b-wave. They also suggested that the Müller cell generated the b-wave via a K^+ regulated mechanism. Miller and Dowling (1970) provided evidence that potassium serves as the intracellular messenger mediating glia cell depolarisation. Dick and Miller (1978) and Kline et al (1978) found two sites of light evoked K^+ change in Mudpuppy and Skate retinae respectively. The faster more transient distal site occured in the outer plexiform layer with pharmacological properties indicating it is post receptoral in origin and probably reflects depolarising bipolar cell activity. The other site was located proximally at the amacrine cell level with pharmacological properties indicative of a largely post bipolar origin. More recent data from Stockton and Slaughter (1987) has employed highly specific glutamate analogues and other pharmacological agents to functionally dissociate the retinal network. (see section 1.8). They have associated the light response of the ON-centre, depolarising, bipolar cell with the potassium flux in the inner and outer retina and with the b-wave of the ERG.

The concept of the b-wave as the extracellular expression of radial current flow generated by a K^+ mediated depolarisation forms the basis of "the Muller-cell hypothesis". Recent versions of the Müller cell hypothesis have tried to assess the interactions of extracellular currents generated by the light induced increases in extracellular K^+ (Kline et al 1978; Newman 1980; Newman and Odette 1984). Such interactions critically depend upon the conductivity of the glia cell and its regional heterogeneities.

Newman (1984) has examined the isolated Müller cells of Salamander and has found the proximal endfoot membrane to be most permeable to K^+. This suggests any K^+ entering the cell will tend to flow out of the vitreal end of the cell creating a strong current source. This agrees well with the model of b-wave generation proposed by Newman (1980) where both distal and proximal effluxes of K^+ contribute to the positivity of the b-wave (Fig 2.2). The distal increase appears to be more transient and has a longer extracellular return path against consequently greater interstitial resistance. It would be expected to contribute the major portion of the b-wave at its response peak. The more sustained proximal K^+ release produces a current loop confined to the inner retina and encounters considerably less interstitial resistance along a shorter return path. It is expected to be primarily manifest during the falling phase of the b-wave. This model is quantitatively expressed in Newman and Odette (1984). However in this model the current dipoles have the same polarity. This causes some problem in the explanation of polarity reversal at different retinal depths during intra-retinal electrode penetration. In explanation of this anomaly Newman and Odette (1984) have considered extra-retinal shunts which could result in spurious polarity reversal according to the site of the reference electrode.

An alternative more qualitative model which includes the current sources arising in the distal retina has been proposed by Kline et al (1978) (Fig 2.3). According to this model currents can also flow distally through the Müller cell and return proximally in the extracellular space. In this way subtractive as well as additive processes mould the trans-retinal response. However Kline et al (1978) also conclude that the asymmetrically positioned distal sink is the major b-wave contributor and the distal efflux is initiated by depolarising cell activity. The inclusion of currents of opposite polarity could be sufficient to contribute to the falling phase of the response. Kline's model does not require the spatial segregation of the Skate glia cell that has been reported to occur in isolated Salamander Müller cells and therefore affords a degree of flexibility in the interpretation of experimental findings.

Fig 2.2 This diagram illustrates the pattern of current flow around Müller cells initiated by light increases in extracellular potassium ions, K^+, that occur in the distal (outer plexiform layer) and proximal (inner plexiform layer) retina.

Newman (1980) considers that the currents which enter the cell in regions of increased K^+ leave the cell almost exclusively through the endfoot region. The current flow is therefore unidirectional and both distal and proximal current loops contribute to the positivity of the b-wave. R.distal and R.proximal represent the interstitial resistance. The extracellular return pathway of the distal current loop is longer thus R.distal > R.proximal.
[after Ripps and Witkovsky 1985].

KLINE et al's MODEL (1978)

Fig 2.3 Kline et al (1978) include the current paths suggested by Newman (1980). These are represented by A. and B. However they also consider distributed current sources in the distal retina that set up counter currents, C. and D.

These may contribute potentials of opposite polarity which allows the transretinal b-wave to be shaped by subtractive and additive processes. Their model suggests that currents of opposite polarity may be substantial enough to contribute to the falling phase of the response.
[after Ripps and Witkovsky 1985].

The activities of the spike generating neurons of the retina (amacrine and ganglion cells) have been strongly implicated in the K_0^+ efflux in the proximal synaptic zone. In mudpuppy retina Karwoski and Proenza (1978) found the depth profile of this efflux closely matched that of the proximal negative response (PNR). The PNR is an extracellular response whose properties closely match the firing pattern of amacrine cells (Burkhardt 1970). In addition the proximal increase is elicited by both onset and offset of illumination and exhibits centre surround antagonism, features which are evident in the responses of amacrines and ganglion cells (Ripps and Witkovsky 1985). Although these cells produce action spike potentials their depolarising synaptic potentials are the probable source of the efflux.

The distal increase in K^+ ions may be distinguished from the proximal increase using pharmacological agents. Thus Dick and Miller (1978) used ethanol, alone and in combination with GABA, to selectively enhance the distal increase whilst simultaneously decreasing the proximal increase. (see section 1.8). These changes were associated with an increase in b-wave amplitude and a significant reduction in the magnitude and decay of the falling phase of the response

When Karwoski and Proenza (1977,78,80) compared the intracellular Müller cell response (M-wave) in Mudpuppy with the b-wave they found it to be much slower, particularly during the falling phase. They suggested that the fast transients of the PNR and the slower M-wave summate at ON and OFF to result in the composite extracellular response. In intracellular recordings of cat retinae Sieving et al (1986) distinguished the M-wave from PII (b-wave and DC component) by its form, depth distribution (more proximal) and its exhibited spatial tuning.

Other studies have disputed the Müller cell contribution in the models described. Vogel and Green (1980) recorded K^+ concentration and simultaneous local ERGs in frog retina, but found the two were neither spatially nor temporally identical. They concluded that any Müller cell participation is in conjunction with other retinal cells and

proposed the principal b-wave source is an active neurone, namely the bipolar. They suggest the extended range of the depth profile is due to the summation of extracellular currents from two or more neurone populations eg. bipolar and amacrine cells. Szamier et al (1980) used chemical agents to selectively interfer with the neuroglia of Skate retina. Extensive Müller cell damage was caused particularly in the inner nuclear layers together with some change to the amacrine cells. Surprisingly they recorded a recovery of the b-wave inspite of persistent Müller cell damage. This implies the involvement of other cells in b-wave generation.

Dowling (1970) examined the retinal activity of Skate under dark and light adapted conditions. He found a similarity in b-wave behaviour and ganglion cell activity. However Miller et al (1977b) showed that antidromic stimulation of axolotl, (Salamander), ganglion cells caused Müller cell depolarisation, ie. a proximal increase in K_0^+, and a reduction in the Müller cell response to light. There was no effect on the recorded light evoked b-wave, and in the absence of photic stimulation the potential recorded at the surface of the retina was of opposite polarity to that of the b-wave (Miller et al 1977b).

Other experiments have also dissociated the b-wave response from the retinal neurones. Thus Masland and Ames (1975) demonstrated that after brief periods of anoxia or exposure to Ca^{2+} Ringers solution, both the compound action potential of rabbit optic nerve and the discharge of ON-centre ganglion cells returned quickly to normal, whereas the b-wave response remained grossly depressed. Studies in chicken and frog have shown the ganglion cell discharge and the tectum evoked response to be unchanged after Müller cell disruption and loss of the b-wave (Bonaventure et al 1981). It is possible that the chemical agents used in these studies are not exclusive and a lowering of the interstitial resistance occurs. The transretinal voltages generated by neuronal elements would then be shunted: however it seems unlikely that the marked b-wave suppression, but accompanying increase in other components (a- and c-wave) is due to shunting (Welinder 1982).

Using current source density analysis Heynen and van Norren (1985b) in macaque eye were unable to isolate a proximal sink of K^+ described previously in mudpuppy and skate, (Dick and Miller 1978; Kline et al 1978). They found a distal sink and a diffuse proximal source. They concluded that in primate the proximal K^+ efflux is very small or even absent. In agreement with Miller et al (1977b) they found the likely site of DC-component generation to be the Müller cells. The b-wave origin was the same in dark and light adapted conditions. Interspecies variation is attributed to the more extensive signal processing that occurs in the retinae of lower order species.

The weight of available evidence favours the Müller cell hypotheses: that the distal efflux of potassium ions generates the extracellular currents that give rise to the large positive peak of the b-wave.

2.2.4 The c-wave.

The c-wave is represented by PI in Granit's analysis. Granit and Munsterhjelm (1937) found the spectral sensitivity of the dark adapted c-wave matched the absorption spectra of rhodopsin and not melanin which is located in the pigment epithelium. However Noell (1954) used sodium iodate to selectively destroy the pigment epithelium and noted a reduction in the c-wave amplitude. Following an intravenous injection of sodium iodate Imaizumi et al (1972) observed initial changes in the receptor outer segments as well as the pigment epithelium of the rabbit retina. The inner layers were also later affected.

Microelectrode studies also indicate the pigment epithelium as the site of c-wave generation. Brown and Tasaki (1961) recorded maximum c-wave amplitude on the pigment side of Bruch's membrane. Steinberg et al (1970) also noted intracellularly the cat pigment epithelium has similar response waveform and latency to the c-wave. Electrical changes induced by bleaching rod pigments must affect the pigment epithelium. Lurie (1976) has applied this model to the more simplified c-wave of frog and suggests the c-wave is related to a change in the resting potential. Under steady

illumination the the c-effect becomes a changed standing potential, when the light is extinguished the decline in steady potential closely matches the regeneration of rhodopsin. The pigment epithelium may thus have the ability to signal the degree of bleaching of the visual pigment in the retina.

In conclusion the c-wave depends on the integrity and complementary functioning of the pigment epithelium and the rods.

2.2.5 The d-wave, Off-effect and e-wave.

The pioneer workers in the field of electroretinography had noticed a change in the retinal potential when light was switched off (Holmgren 1865; Dewar and McKendrick 1873). They observed that whenever the a-wave was of large amplitude the d-wave was also large. It was suggested that the d-wave was the result of interference of the OFF responses of the a-,b-, and c-waves. Brown and Wiesel (1961a,b) attributed the OFF-effect of the cat's ERG to the cessation of the DC-component of the PII process. The DC- component reaches a plateau of negativity as the illumination is increased and declines abruptly as light is switched off.

Thereupon the Off-effect was considered the interaction of two individual Off-effects: the initial part of the falling wave due to the receptor OFF response and the rising edge after the d-wave dip due to the OFF response of the DC-component. Heynen and van Norren (1985a,b) were unable to demonstrate an On-effect of the DC- component of macaque and have assumed it gradually increases in amplitude after stimulus onset. This is at odds with the original assumption of fast ON/OFF transients, but is in line with findings in primate ERG by Valeton and van Norren (1982).

As each photoreceptor system, rods and cones appears able to generate its own response so it is possible by chromatic adaptation to record the averaged ERG produced by separate cone subsystems. Evers and Gouras (1986) found the S-cone mechanism (short-wave length), resembles an E- or rod-like ERG, whilst the

remaining cone mechanism resembles the I- or classic cone ERG in primate. They suggest the similarity of S-cone and rod ERG is because they are each subserved only by On-centre bipolars. The Off-effect of I-retinae is positive, the Off-effect for E-retinae is negative.

Evers and Gouras (1986) applied APB (a glutamate analogue that selectively blocks transmission from receptors to the on bipolar cells, (Slaughter and Miller 1981) to the primate eye. The S-cone ERG was blocked, but in the I-type retina a large a-wave remains. This may be the result of L- and M-cone hyperpolarisation (long and medium wavelength) respectively and/or the hyperpolarisation of Off bipolars. Off bipolars could contribute to the greater efflux of K^+ at the bipolar level resulting in a larger a-wave and positive Off response. For E-retinae without the Off system the a-wave would be smaller and the Off effect or d-wave negative.

The e-wave is a delayed OFF, negative-going, field potential which is a component of the vertebrate electroretinogram (Karwoski and Newman 1987). It is recorded maximally intra-retinally in the proximal layers. The properties of the e-wave closely resemble those of the delayed OFF K_0^+ concentration increase that similarly occurs in the distal half of the inner plexiform layer. Current source density analysis has revealed a current sink distributed throughout the proximal retina, a current source sharply located at the retinal surface and a weaker source distributed through the mid retina. Karwoski and Newman (1987) have modelled the e-wave generation: delayed OFF activity (both action and graded potentials) in neurons of the proximal retina causes the release of K^+ which in turn induces a spatial buffer in Müller cells. This current enters the Müller cells in the inner plexiform layer and exits these cells primarily via their endfoot. The return current flow through the extracellular space gives rise to the e-wave.

2.2.6. The oscillatory potentials, OPs

The OPs are a series of rapid rhythmic wavelets superimposed on the b-wave (Wachtmeister 1972). Their number and amplitude depend on the level of adaptation and intensity of stimulation. Thus they are maximal when photopically driven i.e. with red light and under mesopic adaptation conditions. Although the OPs can reflect scotopic as well as photopic spectral sensitivity (Wachmeister 1974, Watnabe and Toyama 1979). The higher the adapting illumination the greater the intensity flash required to elicit the OPs (Denden 1978). They have been recorded from many species. Ogden (1973) has reported the maximal amplitude of the first three OPs of monkey retina to arise in the inner nuclear layer. Indeed the OPs have been shown to be vulnerable to any compromise of the retinal circulation that supplies this lamina (Ikeda 1976). Ogden (1973) proposed that the axon terminals of bipolar, amacrine and ganglion cells could be responsible for these wavelets.

In Mudpuppy retina Wachtmeister and Dowling (1979) found the OPs reversed in polarity at different retinal depths and suggested they reflected radial current flow in the retina. The earlier OPs arose more proximally than the later OPs. The laterally extending tangential current flow from amacrine cells did not reverse in polarity during electrode penetration and Wachtmeister and Dowling (1979) concluded that these neurons did not therefore contribute to the OPs. Heynen et al (1985) reported the current distribution of oscillatory potentials differed from that of receptoral and b-wave components. They used principal component analysis to study the oscillatory potentials (OPs), at different retinal depths and concluded that the OPs represented radial current flow.

Yonemura et al (1979) administered glycine, ß-alamine, taurine and GABA intravitreally to rabbits and monkeys and noted a decrease in the amplitude of the OPs. They were able to restore the OPs by the application of antagonistic drugs that released the suppressive effects of the above agents. This also suggested a neuronal network in the OP genesis. The concept developed that the OPs represent synaptic feedback loops

extending radially through the retina.

Ogden (1973) had also noticed that optic nerve section abolished the OPs, supporting the participation of ganglion cells in their generation. However in cases of optic atrophy with assumed retrograde ganglion cell impairment Wachtmeister and Azazi (1985) have been unable to demonstrate any selective OP reduction. Gur et al (1987) have found some alteration in the OPs of patients with unilateral glaucoma. However irregularities in the retinal circulation, rather than ganglion cell damage may account for some of the deficit.

More recently using mathematical modelling Lachapelle (1985) and Lachapelle and Molotchnikoff (1986) have postulated that the b-wave is made up of many OPs which have effectively coalesced.

2.2.7. Summary of intra retinal ionic currents

Na^+ ions mediate the tonic depolarisation of the photoreceptors in darkness; Na^+ enters the receptor's outer segment and is actively removed from the inner segment. This radial interstitial ionic exchange constitutes the "dark current". Light stimulation results in a blockage of the Na^+ channels found along the plasma membrane of the outer segment. Recent data suggests that the photic hydrolysis of cytoplasmic cGMP in the outer segment causes fewer channels to open (Yau and Nakatani 1985). (cGMP is cyclic guanosine 3'-5'-monophosphate). The prominent changes in calcium concentration are considered to reflect the modulation in the cell's cyclic nucleotide metabolism. The entry of both Ca^+ and Na^+ into the outer segment is blocked, but a sodium/calcium exchange mechanism which returns Ca^+ to the external medium continues to operate. The calcium activity in the outer segment is thus reduced. A detailed description is given by Lamb (1986) and Pugh and Cobbs (1986).

Whatever the mechanism light decreases the membrane current and the receptor hyperpolarises. This is thought to result in the recorded receptor potential, the a-wave.

It is unusual for excitation in the nervous system to be conducted via a hyperpolarisation. The receptors are thought to release transmitters in the dark and membrane hyperpolaristion reduces the rate of transmitter release. The synapses between the receptors and the bipolar cells do not appear to have a clear threshold for transmitter release. Transmitters are constantly released and the change in membrane potential modifies this background activity. The same transmitters from receptors must influence both depolarising and hyperpolarising bipolars. It has been proposed that they have a different mode of action on each post-synaptic terminal (Cohen 1987).

There is a concomitant decrease in extracellular potassium as the dark current is reduced. The pump activity that transports the sodium ions from the inner segment also takes K^+ ions into the cell, which leaves passively through the inner segment. Although light does not interfer with the Na^+/K^+ active pump it prevents Na^+ entering the cell and impedes the passive exit of K^+. The net result is a reduction in extracellular potassium ions - the distal decrease.

Glia cells are exquisitely sensitive to the concentration of K^+ ions. As light increases the retinal glia, the Müller cells, depolarise. This is probably due to the distal K^+ efflux by the depolarising bipolars - the distal increase (eg. Knapp and Schiller 1984). The passive electrotonic spread of current through the cell results in the extracellularly returning K^+ current which is manifest as the recorded b-wave. The mechanism of the current flow through the Müller cell has been described by several models. (eg Kline et al 1978, Newman and Odette 1984). The heterogenity of the Müller cell will determine the nature of the recorded potential. A proximal K^+ efflux has also been found in some species, but its contribution to the b-wave is thought to be minimal because of the shorter K^+ return path against significantly less resistance. Its contribution will be expressed during the falling phase of the b-wave potential.

2.3. DEVELOPMENT OF ERG RECORDING ELECTRODES

In order for the ERG to have a clinical application a non-invasive method of response

recording is necessary. The maximal response potential occurs at the cornea when referenced at the back or posterior pole of the eye. In practice the closest a reference electrode may be positioned is on the temple near to the outer canthus [Korth (1984), has recorded pattern evoked ERGs with a naso-pharyngeal reference electrode, but reports a reluctance on the part of volunteer subjects to participate!].

The method of obtaining a relatively direct corneal contact also poses a considerable problem. One of the first attempts to record from the cornea employed a saline soaked moist thread. This reputedly painful procedure provided unstable electrical contact because of drying and eye movements (Henkes 1984). To increase stability Hartline (1925) used a pair of tightly fitting goggles filled with conducting solution with an electrode/ conductor fitted inside. However it was not until the design of contact lenses and their successful fitting in the correction of refractive errors that significant progress in the realm of clinical recording was made. Riggs (1941) and Karpe (1945) independently introduced almost identical glass contact lenses that incorporated a metallic conductor to record the corneal ERG. Many modified designs have followed eg. Henkes (1951); Burian and Allen (1954), but most are reported to give comparable recordings (Sundmark 1959; Armington 1974).

Contact lens borne electrodes have the inherent problem of achieving a universal fit. Discomfort can be overcome using topical anaesthetics. However repeated instillation can result in a softening and desquamation of the corneal epithelium making it more susceptible to insult through poor fitting characteristics (O'Connor Davies 1976). These considerations preclude extended use. Air bubbles under the lens that interfere with electrical contact may be reduced by fenestration (Armington 1974). A comparison of four different types of contact lens electrode in common use has been made by Gjotterberg (1986)(see also Kooijman 1987).

The development of hydrogel 'soft' contact lens materials has led to their use as a cushion underneath 'hard' plastic electrode bearing contact lenses, (Dawson 1974) or

directly in conjunction with conductive materials (eg Barber et al 1976; Bloom and Sokol 1977; Honda et al 1986).

Attempts have also been made to record the ERG using non-corneal electrodes attached usually to the lower eyelid or the outer canthus. The recorded amplitude is markedly reduced and the results are subject to greater muscle artefacts. However this is still a valuable method of obtaining responses when corneal recording is contra-indicated, eg in cases of corneal infection or recent ocular surgery (Giltrow-Tyler et al 1978; Sierpinski-Bart et al 1978; Skalka 1979; Leguire and Rogers 1985)

More recent innovations have moved away from conventional contact lens design. Ziv (1961) used a ring of gold placed directly on the cornea. This concept has been modified into a thin strip of metal-coated plastic foil which may be inserted within the sac between the globe and the lower lid (Chase et al 1976; Borda et al 1978). Gold foil electrodes have the advantage of extended wear over aluminium coated electrodes and are suitable for use in cases of corneal pathology (Arden et al 1979).

Another material with properties similar to the gold foil electrode is the "DTL" electrode (Dawson et al 1979). This is an extremely low mass conductive thread composed of nylon monofilaments impregnated with silver. There have been several suggested methods of application (Dawson et al 1982; Spekreijse et al 1986, Thompson and Drasdo 1987). All of which depend on the fibre making contact between the tear film and an adjacent metal conductor, although the latter technique provides a disposable system. The "DTL" fibre causes minimal visual disturbance and has a wide patient acceptability without corneal anaesthesia.

Such electrodes can produce signals of slightly lower amplitude and slightly higher noise levels, but the increasing use of sophisticated averaging devices tends to compensate for these minimal disadvantages (Riggs 1986). However some investigators have advocated special care in the positioning of extraocular reference

electrodes to prevent contamination from potentials evoked in the fellow eye or volume conducted visually-evoked cortical potentials (Peachey et al 1983; Seiple and Siegel 1983; Hobson et al 1984; Arden 1986).

2.4 RECORDING TECHNIQUES

2.4.1 Stimulation

The ERG is a potential summed across the entire retina. Asher (1951) recorded a normal ERG when he focused a light spot onto the optic nerve. This illustrated the large contribution of stray and scattered light to the summated response. A Ganzfield stimulus is most commonly used to standardise the potential measurements However under these conditions the ERG may only give a coarse, overall evaluation of retinal function.

In order to increase ERG sensitivity a more qualitative assessment of localised retinal regions is necessary. To this end Brindley and Westheimer (1965) designed an "Enhancetron". This device acts as a brightly illuminated surround that floods the eye with steady illumination. The ERG response threshold of the peripheral retina is thus raised above the level of light scattered from the central stimulus field. Above 10% (1/11) of the mean stimulus field luminance as surround luminance was shown to localise the response.

Riggs et al (1964) introduced the counterphase grating stimulus as a method of limiting stray light. When a black and white pattern of identical element size phase-reverses, the mean space-averaged luminance of each stimulus position is equal. There is therefore no change in the scattered light that falls outside the stimulus area. If the ERG was a completely integrating system the result should be a cancellation of the positive and negative response. This is not the case and some type of rectification appears to take place (Riggs 1986). At that time the pattern-evoked ERG was tacitly assumed to have the same site of generation as the more conventionally recorded flash, unpatterned ERG.

The striped pattern was first used clinically to evoke ERGs by Lawwill (1974). The resulting signal was small, of the order of several microvolts, compared with the scotopic ERG b-wave amplitude of ≈ 300 μV. The signal to noise ratio of small signal responses may be improved by response averaging (Dawson 1951). Orthodox methods give a reduction in random noise proportional to $1/\sqrt{n}$ where n = the number of averages (eg Armington et al 1961; Regan and Spekreijse 1986). The technical problems involved in the collection of small signal data impeded the routine electroretinographic use of pattern stimuli.

Pattern evoked ERGs were also uncommon because of the image degradation caused by contact lens recording electrodes. Metal strip electrodes, eg. gold foil electrode and the "DTL" electrode (Arden et al 1979; Dawson et al 1979), do not compromise the quality of the retinal image and their development allowed a systematic assessment of the ERG response to patterned stimuli.

2.4.2 Stimulus presentation

A pattern containing equal numbers of black and white or luminance balanced coloured elements of equal size may be presented in one of three ways:

a) a flashed presentation of the pattern.

The response to this stimulation mode is unlikely to differ significantly from the ERG evoked by a conventional light flash. Contamination by stray light is inherent in this technique. (Barber and Galloway 1974)

b) counterphase or reversal of the pattern.

This technique minimises stray light modulation (Riggs et al 1964; Johnson et al 1966). The light and dark elements interchange rhythmically at twice the modulation frequency. Response components are only seen at even multiples of the stimulus modulation frequency. Spekreijse et al (1973a,b) describe the response energy as being concentrated at the second harmonic of the fundamental presentation rate. A fundamental response is seen only if the stimulus field does not contain an even number of elements symmetrically distributed about the fixation point (Hess and Baker

1984; Riemslag et al 1985).

c) pattern appearance / disappearance.

In this presentation the pattern appears from and disappears into a uniform background of the same mean luminance. The pattern appears and disappears to leave a blank field once each stimulus cycle without any change in overall luminance (Spekreijse 1966; Lawwill 1984).

2.4.3 Response analysis - Steady state and Transient responses.

Systems analysis is a technique widely used in engineering (Spekreijse and Apkarian 1986). A system refers to an assembly of functional units or mechanisms that together produce a controlled result. System analysis investigates the relationship between input and output ie stimulus and response. In electroretinography the input is the light stimulus; the output the ERG itself. This approach to ERG analysis has been adopted by Spekreijse et al (1973b); Riemslag et al (1985); Hess and Baker (1984); Baker and Hess (1984). When the input is sinusoidal and the stimulus presentation rate is above $\approx$ 8 Hz , a steady state response occurs. A transient response occurs to a step input.

If the response to an alternating pattern was linearly related to luminance the net result would be a cancellation of response. The response has been postulated as coming from a non-linearity in the luminance response which gives rise to a 2nd harmonic distortion, ie a response at twice the frequency of modulation (Riemslag et al 1985). In Fourier terms the fundamental and odd harmonics will cancel and the even harmonics will summate. There are two principal lines of supporting evidence for this model of pattern ERG generation (Plant and Hess 1986)

i) a 2nd harmonic component has been found in the response to luminance modulation (van der Tweel 1961)

ii) when the ERG is evoked by the appearance or disappearance of a pattern with an associated change in mean luminance the ERG response is determined by the increase in luminance independent of whether the contrast has increased or decreased (Ringo et al 1984 -in cat, Riemslag et al 1985-in man)

However a pattern or contrast specific response will also occur at twice the modulation frequency, because the elements contrast reverse twice in this period. Therefore pattern responses will also be maximal at the 2nd harmonic of the modulation frequency. The pattern ERG could be a 2nd harmonic, non-linear component of a luminance or pattern response.

The generator of a nonlinear component only produces 2nd harmonic components and therefore acts as an even symmetric filter. It produces the same sign output to inputs of opposite sign e.g. full wave rectification. An odd-symmetric transfer function produces an output of opposite sign, for inputs of opposite polarity and vice versa. A linear system is a special case of this. The odd-symmetric component reflects any modulation of space averaged luminance. Thus it contributes to uniform field responses, but makes no contribution to responses to contrast reversing or pattern on-off stimuli.

Baker and Hess (1984) set out to establish a relationship between linear and non-linear responses to pattern reversal and uniform field stimulation in transient and steady state modes of presentation. They compared the temporal frequency dependence of each response. Two response peaks were noticeable; one at 1-2 Hz and another at 8-10 Hz. Under their conditions a typical pattern reversal response consisted of a fast diphasic component and a slow monophasic response. They related the time course of the fast transient reponses to the steady state response peak at 8-10 Hz and the transient slow wave to the steady state response peak at 1-2 Hz.

The contrast reversing stimulus produces a substantially larger peak at 8 Hz than at 1-2 Hz. The fast wave is accordingly more prominent in the transient response. The reverse is true to the uniform field stimulation. Baker and Hess (1984) therefore related the 8 Hz sinusoidal response to the fast component of the transient response.
N.B. this is possible with small signal analysis, however with larger amplitude stimulation there may not be a clear relationship between sinusoidal and transient

responses.

A correspondence has thus been drawn between the 2nd harmonic of the steady state response to the modulation of a uniform field and the predominant 2nd harmonic recorded to counterphase pattern stimulation (van der Tweel 1961; Spekreijse et al 1973b; Reimslag et al 1985). Any study designed to examine the behaviour of the retina to luminance and pattern stimulation should compare the 2nd harmonic component of the steady state response to each stimulation mode (Plant and Hess 1986).

The amplitude of a transient evoked response is most commonly measured from peak to peak. The convention is to label the peak according to its polarity and latency. Thus under Holder's (1987) clinical protocol a pattern reversal positive peak occurs at ≈ 50ms followed by a negative peak at ≈ 95ms; these are labelled p50 and n95 respectively and amplitude is measured from peak to peak. Others refer to the successive peaks and troughs response by letter eg p,q and r (Kirkham and Coupland 1982/83)

Some workers have consistently measured the positive going potential, p50 equivalent, of the pattern reversal ERG in a similar manner to the b-wave measurement of the conventional luminance ERG. The negative 'after-potential' of the response has not been considered in many studies (Armington et al 1971).

Korth and Rix (1985) advocate a baseline to peak amplitude measure of the negative going transient. However it can be difficult to determine the baseline in electrical potential recordings In order to avoid distortion because of an obscured baseline it is possible to measure the major positive peak from a perpendicular line drawn from the peak to a line connecting the adjacent negative troughs (after Algvere and Westbeck 1972).

Arden and Vaegan (1983) have used this method and additionally computed an index that compares the amplitude of the pattern evoked ERG with that of the focal luminance ERG. In a similar manner Holder (1987) suggests using the ratio of p50/n95 amplitude as an index of retinal function (see also Porciatti and von Berger 1984).

Different systems of nomenclature have been employed to describe the pattern evoked ERG. This is paralled by the variation in the amplitude measures taken of the transient response. The term pattern electroretinogram or PERG will be used in the remainder of the text. As when prefixes are applied to the ERG for example flicker or flash ERG, pattern is descriptively applied to the ERG and relates to the mode of stimulation. The locus of origin of the PERG is in no way indicated by the use of this term. The debate introduced in this chapter about the composition of the PERG, from luminance or pattern component responses, is explored in detail in Chapter 3.

CHAPTER 3

THE PATTERN EVOKED ELECTRORETINOGRAM

3.1 INTRODUCTION

When a counterphase patterned stimulus was first introduced in electroretinography the resulting localised signal was considered to have the same retinal origin as the flash ERG (section 2.4.1). More recently however, it has been suggested that the PERG includes pattern specific responses from more proximal retinal cells, particularly ganglion cells (Maffei and Fiorentini 1981; Lawill 1984). The characteristics of the PERG have consequently become the subject of vigorous investigation, both experimentally and clinically. Nonetheless there is still considerable debate about the retinal origin and nature of the PERG. The results of some these investigative studies are described in the following sections.

3.2. INTRA-RETINAL RECORDING OF THE PERG

Holden and Vaegan (1983b) compared the ERG and the PERG of the central yellow field of the pigeon retina using vitreal and intra-retinal recordings. A depth profile comparison of the PERG and the sum of the on-off ERG suggested that the two have a common electroretinographic location.

They proposed that the PERG and summed focal ERG form a smooth continuum as a function of spatial frequency, and their generators occupy closely similar anatomical locations within the retina. The spatial filter so formed would contain both low pass and bandpass components: the bandpass component would emerge at higher spatial frequencies (Holden and Vaegan 1983b).

In cat retinae however the intra-retinal electroretinographic recordings to phase reversing square wave gratings were maximal in the proximal retina (Sieving and Steinberg 1985). The depth profile was composed of a negative potential at stimulus onset and a faster

negative potential at stimulus offset. A smaller sustained negative response was observed deeper in the retina which seemed to correspond to the DC-component of PII (Brown and Wiesel 1961a,b, see section 2.2.3).

The proximal intracellular profile and spatial sensitivity of the PERG closely resembled the characteristics the M-wave, first identified in the retinae of cold blooded vertebrates (Burkhardt 1970, see section 2.2.3). This prompted Sieving and Steinberg (1985) to suggest that the M-wave contributes to the PERG: the relative contribution of amacrine and ganglion cells to the response is not known. The authors however stress that a contribution of PII component activity to the PERG is not excluded by their data.

Riemslag and Heynen (1984) have recorded the intra-retinal responses from an intact macaque eye to patterned and unpatterned stimuli using a bipolar electrode. The PERG showed a depth profile comparable to the 2nd harmonic luminance b-wave profile. They conclude that the PERG does not yield any additional information to the luminance ERG and might be presumed to have the same retinal origin.

3.3. THE PERG IN CASES OF EXPERIMENTALLY INDUCED RETINAL PATHOLOGY

In 1981 Maffei and Fiorentini suggested the PERG depended on more proximal retinal cells than the flash ERG, specifically mooting ganglion cell participation in PERG genesis. They had noticed a selective reduction in the PERG recorded from a cat's eye following optic nerve section. Furthermore the time course of the response reduction paralleled that of retrograde degeneration and ganglion cell loss. The flicker ERG from the same eye remained unaltered throughout the experiment. Their conclusion that ganglion cell activity is a major source of the PERG provoked a resurgence of interest in electroretinography.

Maffei and Fiorentini (1981) had also noted that the PERG was attenuated more quickly at lower spatial frequencies suggesting the earlier impairment of larger receptive field

ganglion cells. The first changes were noted at 3 weeks in one cat and at 4 and 6 weeks in others. Degenerative changes might first occur in the cat's Y-cells (Enroth-Cugell and Robson 1984). After 8 weeks some attenuation at medium spatial frequencies was reported. Unfortunately at the time of the report they were unable to supply any supporting histological evidence.

Hollander et al (1984) attemped to correlate the disappearance of the PERG with the process of ganglion cell degeneration and in particular addressed the question of which class of cell degenerates first. Quantitative analysis of wholemounted cat retinae showed that ganglion cell shrinkage (20%) and loss (30%) begins in the temporal periphery, 3 weeks after section. The earliest loss is among medium size ganglion cells, probably beta-cells that comprise ≈ 50% of the retinal ganglion cell population. Beta-cells and alpha-cells are the substrates for the X- and Y-system respectively, (Boycott and Wassle 1974). The alpha cells, making up ≈ 5% of the population (Hughes 1978,81), only showed some shrinkage after 3 months. This is in agreement with previous work in which thinner axons of the optic tract degenerate faster that thicker ones (Eysel and Grusser 1974), but at odds with Maffei's supposition of Y-cell involvement. It would seem unlikely however, that such a small cell population, (≈ 5%), contributes vastly to the gross response or mediates pattern vision. Ikeda et al (1978) found some evidence of impaired bipolar cell function following retrograde degeneration in cat retinae.

Interspecies differences are always a problem in the extrapolation of experimental results, particularly the comparison of PERG in cat and man (Hess et al 1986). As a more appropriate model of human visual function Maffei et al (1985) repeated their experiment in monkeys using intracranial optic nerve section. They demonstrated the same progressive and selective PERG reduction with time that occured in cat. Histological examination of 2 whole-mounted Macaque retinae, 6 and 8 weeks after section, showed severe degeneration with ganglion cell loss and glia reaction. The degeneration was most pronounced in the temporal hemiretina, but there was no evidence of a different vulnerability among ganglion cells of different pericarial sizes.

Dawson et al (1986) induced local retrograde degeneration of retinal ganglion cells in 4 rhesus monkeys by microdiathermy fibrelayer burns at the nasal and temporal edges of the optic disc. Local ERG recordings established the ability of rhesus monkey outer retina to produce normal signals in areas where the inner layers are atrophic. Within 9 weeks the signals recorded from retinae with temporal lesions were markedly reduced to high spatial frequencies. There was histological evidence for extensive ganglion cell loss after 30 weeks. They concluded that their results provide strong evidence for local ganglion cell dependent electrical potentials to be produced by selected stimuli.

Earlier studies on trans-synaptic retrograde degenerative changes in human retinae by van Buren (1963b) produced evidence of cystic degeneration in the inner nuclear layer. Dawson et al (1986) noted similar cystic changes and suggested they relate to the degeneration of displaced ganglion cells. It must be with some caution therefore that selective retrograde ganglion cell changes are presumed. Degenerative changes in the inner nuclear layer with possible bipolar cell, (Ikeda et al 1978) and glia cell reaction, (Maffei et al 1985) may confound electroretinographic studies.

Porciatti et al (1987) have recently recorded PERG and focal ERGs from pigeon retinae after the intravitreal administration of two glutamate analogues; 2 -amino phosphono butyric acid, APB and cis 2,3- piperidin dicarboxylic acid, PDA. APB selectively blocks depolarising ON-channels by mimicing the effect of the photoreceptor transmitter. (Slaughter and Miller 1981). PDA blocks the cone input to OFF bipolars and horizontal cells, while the ON bipolars are relatively unaffected (Slaughter and Miller 1983). APB reversibly abolishes the b-wave of the flash ERG (see section 2.2.3.), but PIII and the d-wave of the pigeon were enhanced. The PERG and the tectal response, monitoring retinal output, remained stable. PDA on the other hand enhanced the focal b-wave, but reduced the d-wave, PERG and tectal response. The authors conclude that the b-wave of the focal ERG and the PERG are different retinal events and that ON activity is not necessary for PERG generation.

3.4 REVIEW OF CLINICAL USE OF PERG IN CASES OF POSSIBLE RETINAL DYSFUNCTION

A selective test of proximal retinal function would have a powerful diagnostic and prognostic application. Indeed with the supposition of ganglion cell participation in its generation (Maffei and Fiorentini 1981), the PERG is now routinely included as a visual electrodiagnostic test in some centres (e.g. Holder 1987). Its sensitivity as a measure of retinal dysfunction has been assessed with different clinical protocols over a range of ophthalmological conditions.

3.4.1 Optic Nerve Dysfunction

i) Optic atrophy

The reaction of the optic nerve to traumatic, degenerative or inflammatory insult is fundamentally the same. Degenerative changes occur centrally and peripherally in the direction of the ganglion cells and the optic disc becomes atrophied. Atrophy describes pallor of the optic disc associated with a loss of optic nerve function; it may occur within 14 days or 3 months after injury, (Duke Elder and Scott 1971).

Dawson et al (1982) reported the absence of the PERG in a patient who had suffered a traumatic section of the optic nerve 15 months prior to recording. Similarly May et al (1982) could not obtain PERGs from a patient with a well documented unilateral optic nerve dysfunction. In both instances the flash ERG was normal in the affected eye. Mashimo and Oguchi (1985) examined two patients who had suffered fracture of the optic nerve canal 12 months prior to testing. The PERG exhibited some deficit, but was not completely diminished. This prompted Mashimo and Oguchi (1985) to suggest that the PERG contains both luminance and contrast components in varying proportions.

Harrison et al (1987) have recorded steady state PERG signals from an eye whose optic nerve was surgically transected 30 months previously in order to remove a glioma. The responses to checks smaller than 3° 23' were reduced in amplitude compared with responses from the fellow eye. Larger checks and diffuse flashes produced

approximately equal responses in the two eyes. They conclude that there may be a contribution to the PERG from ganglion cells in addition to other retinal cells.

However Sherman (1982) reported that 7 patients with long standing optic nerve disease did not present grossly abnormal PERGs and in another study obtained relatively normal PERGs in a further 3 patients having traumatic optic atrophy (Sherman and Richardson 1982).

In cases of absolute bitemporal hemianopia a loss of ganglion cell function on the nasal hemiretina can be anticipated via retrograde degenerative changes. Caruso and Higgins (1987) examined 6 patients with bitemporal hemianopia and report a reduction, but not absence, of the transient PERG recorded from the nasal retina whilst the temporal retina gave PERGs within normal limits. They postulate that the PERG has two components; one which depends on the functional integrity of the ganglion cell layer and the other which persists after ganglion cell atrophy probably originating from the distal retinal layers.

A similar study analysed the 2nd harmonic responses from the steady state PERGs recorded from patients suffering homonymous field defects (Stoerig and Zrenner 1987). They found the activity from the nasal retina to be systematically higher than the activity from the temporal retina, which they suggest may reflect nasotemporal ganglion cell density differences. Activity from the functional hemifield were in accordance with a normal subject's responses. Responses from the nasal retina, the patients blind side, showed a shift in the peak activity towards lower temporal frequencies. The nasal retina was reduced to the same amplitude of activity as the temporal retina. Skrandies et al (1987) report the PERG is only affected in long standing cases of optic nerve dysfunction. The luminance ERG was unaffected in these cases which suggest the PERG depends on ganglion cell function.

ii) Optic neuritis

Optic neuritis refers to a clinical syndrome in which visual impairment develops over a couple of days usually accompanied by discomfort in or around the eye that increases on eye movement. (Macdonald 1983,1986). At the height of the illness there is a central scotoma, a swollen optic disc in rather less than 50% of patients and a colour vision deficit in almost all cases. In the U.K. ≈ 2/3 rds patients with optic neuritis develop Multiple Sclerosis (M.S.). 70% patients with M.S. will have an episode of optic neuritis. There is some evidence of retinal vascular abnormality in acute M.S. that precedes demyelination of the optic nerve (Macdonald 1986).

Fiorentini et al (1981) found the steady state PERG diminished or absent in patients with retrobulbar neuritis and temporary occlusion of the optic artery. The flash and flicker ERGs in these patients were normal. Porciatti and von Berger (1984) studied the PERG in the acute stages of optic neuritis in 8 patients and monitored their progress over the following year. The so called "after-potential" the positive to negative peak (p-n) of the transient response was more affected than the early negative to positive (n-p). An earlier impairment of the response to low and medium spatial frequencies was noted.

Porciatti and von Berger (1984) suggested the PERG was a complex response in which luminance and contrast responses contribute with different weighting to the waveform. They infer that the after-potential has a different origin to the positive going transient. Holder (1987) has a similar view. He uses a ratio of positive p50 peak to peak amplitude: negative n95 peak to peak amplitude as an index of retinal function. He suggests the selective involvement of p50 and n95 in different pathological states indicates their generation in different retinal layers. Holder (1987) postulates the n95 is an sensitive indicator of optic nerve dysfunction whilst the p50 reflects generalised retinal or macular dysfunction. Indeed 81% of the patients he examined with optic nerve dysfunction displayed a selective abnormality of the n95 component.

Examining a larger patient group, (n=16), with unilateral optic nerve lesions of varying

severity Sieple et al (1983) found the PERG was reduced in proportion to the visual deficit. In cases with good Snellen acuity, (6/6-6/30), however, it was difficult to demonstrate a consistent pattern of PERG variation. To increase test sensitivity Sieple et al (1983) examined the contrast level at which the PERG response disappeared. In all cases the PERG from the affected eye disappeared at a higher contrast level than from the unaffected contralateral eye.

Persson and Wanger (1984) studied 15 patients with a clinical diagnosis of M.S. who were in a stable state. All had a prolonged pattern reversal visual evoked cortical potential as a sign of demyelination in the optic nerves (Halliday 1982). Loss of axons takes place in chronic plaques of demyelination. Nerve fibre defects indicative of secondary axonal degeneration in the retinal papillomacular bundles were demonstrated by red free fundus photography (Frisen and Hoyt 1974). The PERG amplitudes were reduced in 50% of eyes that showed signs of optic nerve demyelination. The results were supposed by the investigators to represent secondary ganglion cell dysfunction.

Celesia and Kaufman (1985) report two patients suffering from M.S. who presented with optic atrophy secondary to retro-bulbar neuritis who produced normal PERGs. A third patient showed a normal PERG to a 31' check, but the response was absent 15' checks. This could indicate a gradual involvement of retinal cells with an earlier impairment located in the foveola. Again the more severe the visual impairment Celesia and Kaufman (1985) report the greater possibility of PERG abnormality. Serra et al (1984) showed significantly reduced PERGs in 7/20 cases of multiple sclerosis.

However Kirkham and Coupland (1982/83) could not find any significant differences in the PERG in 28 M.S. patients compared to a control group without M.S. Similarly Bobak et al (1983) found normal PERGs in 8/10 M.S. patients. Ota and Mikaye (1986) also found the PERG to be extremely limited in its aid to the detection of unilateral optic nerve disease in a sample of 29 patients.

Ringens et al (1986b) found no difference between the PERG recorded from 54 patients in the acute phase of optic neuritis and a group of normal subjects. Although disturbed PERG findings may relate to ganglion cell changes which happen secondarily to demyelination, Ringens et al (1986b) point out that in the acute stages of the disease these changes have not yet occured. Arden et al (1982) were also unable to detect a reduction of the pattern ERG in the acute stages of optic neuritis. As vision returned 2-7 weeks after the attack the PERG amplitude was larger in the affected eye. This seemed to suggest a phase of hyperexcitability of neurons on the point of degeneration (Gills 1966; Feinsod et al 1971. - see Section 1.6). Still later the PERG was reduced in the affected eye. Arden et al (1982) believe this observation was consistent with some retrograde degeneration of the optic nerve.

Galloway et al (1986) conducted serial studies on 2 patients with unilateral optic nerve disease. One patient with optic neuritis showed a gradual PERG reduction over 4 months. The other patient had suffered an optic nerve trauma. Similarly the PERG response was initially within normal limits from the affected eye, but gradually reduced in amplitude over 11 weeks. Galloway et al (1986) related the progressive amplitude reduction to ophthalmoscopic changes in the optic disc.

Plant and Hess (1986) studied 32 eyes, 24 of which had a history of optic neuritis of varying severity and residual visual function. All had been quiescent in visual symptomology for the last 6 months prior to testing. The amplitude of the 2nd harmonic retinal response to alternating sinusoidal gratings was significantly reduced in the group as a whole compared to a control group of 40 eyes. However they concluded that the sensitivity of the PERG in the detection of optic neuritis is low.

In retrograde degeneration it is important to remember that there may also be an interference in other retinal layers and possible anomalies in the retinal circulation in the acute phase of optic neuritis (Macdonald 1986).

3.4.2 Glaucoma

The PERG has been extensively applied in cases of glaucoma in attempts to correlate field loss with response amplitude. Indeed the PERG has been proposed as an adjunct to the commencement of therapy. (personal communication; Holder 1987). Open angle glaucoma (chronic simple) has an insiduous onset and is diagnosed as an elevated intra-ocular pressure, with changes to the optic nerve head and characteristic visual field defects. (Duke-Elder and Scott 1971; Spalton 1986). Glaucomatous damage to ganglion cells seems to occur via a combination of mechanical pressure resulting in impaired axoplasmatic transport (Quigley and Addicks 1980) and diminished retinal perfusion (Papst et al 1984a,b). Histological studies have shown 40-50% of the nerve fibres to be degenerated in incipient visual field defects (Quigley et al 1983).

Monkey models have been used to simulate the progress of glaucoma in humans. Laser induced glaucoma in primates produces an elevation in intra-ocular pressure with cup/disc ratio changes that are similar to those accompanying primary open angle glaucoma in humans except they are accelerated over a period of 2-3 months (Marx et al 1986). In monkey a significant and consistent reduction in the PERG amplitude was noticed to lower spatial frequency stimuli; 0.51 cpd compared with 1.25 cpd (Marx et al 1986).

Examining the steady state PERGs in 4 patients suffering with open angle glaucoma Bobak et al (1983) found abnormal 2nd harmonic response amplitude in 3/4 when the Fourier power spectrum of the raw data was analysed.

Wanger and Persson (1983) investigated 11 patients who had manifest unilateral glaucoma according to conventional criteria (raised IOP, cup/disc ratio increase and field defect). The PERGs to a 24' phase reversing checkerboard were reduced in amplitude compared to the fellow eye in all cases and were below the level of normal deviation in 10/11 cases. A statistically significant relation between PERG amplitude and the visual field defect was established. A later presentation by the same authors of 7 cases of

unilateral ocular hypertensives (increased IOP, but no disc changes or field defects) reported a reduction in the PERG amplitude in 4 cases that was below the normal level when compared with the normotensive fellow eye. Three of these four patients went on to develop excavation of the optic disc 6-15 months after the PERG recording (Wanger and Persson 1985). They suggest the transient PERG is a useful objective test for the early detection of functional damage in eyes with increased IOP.

Papst et al (1984b) recorded transient PERGs from 8 patients suffering from protracted elevation of intraocular pressure. They found intraocular pressures of 30mm Hg or more result in an reduction in PERG amplitude. At intraocular pressures lower than 26mm Hg PERGs amplitude fell within the normal range. They suggest the findings are an expression of impaired function at the ganglion cell level due to a reduction in retinal blood flow and consequent reduction in ganglion cell activity. They also demonstrated an amplitude reduction in patients exhibiting positive field defects.

Van Lith et al (1984) has found a disturbance of the PERG in cases of glaucoma, but could only systematically correlate the reduction with cup/disc ratio. They selected a large sample, (n=75), of mild cases having normal visual acuity. A longitudinal study of these patients would be valuable in assessing the sensitivity of the technique. Arden et al (1982) also reports some reduction in PERG amplitude recorded from glaucomatous eyes. Holder (1987) has shown a selective reduction in the p50 component in 3/3 glaucoma patients.

Porciatti and von Berger (1984) studied the PERG in 4 cases of open angle glaucoma and found the largest intraocular amplitude difference in the medium range of spatial frequencies. No improvement of the PERG was noticeable over the following 12 months which they suggest is indicative of irreversible retinal damage. Trick (1985) reported an equal reduction in PERG amplitude at all tested spatial frequencies in 32 patients with open angle glaucoma.

Trick (1985) also examined the temporal characteristics of the PERG in these patients. The high temporal frequency roll off is shifted to lower temporal frequencies in glaucoma patients. (see also Stoerig and Zrenner (1987) section 3.4.1). Trick (1985) proposes this evidence as support for an increased vulnerability of Y-type cells to glaucoma induced damage.

Van den Berg et al (1986) felt that optical factors might play an important confounding role in the response reduction described in many reports. They have conducted a study using 6 asymmetrical glaucoma patients who still maintain a high level of visual acuity. Their responses were compared with normative data collected from 11 young volunteers. They concluded that visual field defects are not reflected in the steady state PERG. However in many studies the effects of pupil size due to miotic therapy and the clarity of the optical media have been taken into account (eg Arden et al 1982; Wanger and Persson 1983; Papst et al 1984).

Conte and Brodie (1987) have also used Fourier techniques to isolate the even harmonic response evoked by contrast reversing and uniform field stimulation. In agreement with work by Reimslag et al (1985) and Hess and Baker (1984a) in normal eyes they found the 2nd harmonic component response from luminance stimulation closely resembled that from pattern. However there was a clear distinction in glaucomatous eyes; the pattern evoked 2nd harmonic was reduced. These findings imply the loss of the pattern ERG, in glaucoma at least, is not due to a linearisation of the local response to luminance and suggests a dissociation between the non-linear response to luminance and pattern ERG.

Kolker et al (1987) have reported the initial baseline results of a 5 year prospective study of ocular hypertensives using steady state pattern reversal stimulation. They have found the degree of PERG abnormality varied with check size. It appears that there is an optimum or maximally sensitive spatial frequency around which the relative abnormality declines. Korth et al (1987a), in one of the first clinical studies to employ the pattern

onset stimulus, also noted the most frequent PERG abnormality occured at the peak spatial frequency of the onset response in glaucoma patients. They were able to correlate the PERG amplitude with the cup/disc ratio. They conclude that the PERG is a ganglion cell response which is of value in the screening and examination of glaucoma patients.

The consensus would therefore suggest a anomaly in the PERGs recorded from glaucomatous eyes that depends on the severity of the disease process.

3.4.3 Amblyopia

Ambylopia is a usually uniocular reduction in spatial resolution established during childhood, (Shapero 1971). The loss of visual acuity has been considered to be cortical in origin (Hubel and Wiesel 1965; Wiesel and Hubel 1965; Blakemore et al 1978; Blakemore and Vital-Durand 1979). In monkeys following total pattern deprivation no neurophysiological reduction in spatial resolution occurs before the visual cortex although behaviour tests reveal a significant impairment (Blakemore and Vital-Durand 1979). However in kittens uniocular penalisation by surgical or pharmacological means causes some alteration in the properties of retinal ganglion cells in the area centralis (Ikeda and Tremain 1978,1979). Indeed Ikeda and Tremain (1979) suggested that inadequate stimulation causes a retinal defect that accounts for the reduced visual acuity from which the well established cortical anomaly may be derived. Both views imply that a modification of the visual input results in amblyopia although the proposed sites of amblyopic change differ.

Amblyopia has therefore become a topic for investigation using pattern electroretinography in an attempt to demonstrate a retinal deficit, at the ganglion cell layer for example.

Jacobsen et al (1979) ellicited focal cone ERGs using a hand held ophthalmoscope stimulator to minimise focusing and fixational errors. Their conclusions suggest normal pre-ganglionic cell function in strabismic amblyopia.

Sokol and Nadler (1979) recorded PERGs from 3 adult amblyopes. A reduction in the amplitude of the PERGs from the amblyopic eyes of all subjects was noticeable, but the after potential (p-n) was more sensitive than the positive going (n-p) component. They claim this as the first report of PERGs being more affected than the conventional flash ERG in amblyopia. Tuttle (1973) used alternating square wave gratings to ellicit PERGs from 4 adult amblyopes and reported no difference in the amplitude of the 'b-wave' of the ERGs recorded from amblyopic and normal eyes. The subjects only had a mild loss of visual acuity [6/12 $^{-3}$, 6/12, 6/18 and 6/30].

Arden et al (1980) published a preliminary report on 13 amblyopic subjects and concluded that retinae in the region of amblyopic suppression produce very little electrical activity. The amplitude of PERGs recorded from amblyopic eyes were 50% or less than those produced by the fellow eye. The fixation position was adjusted for strabismic subjects. Vaegan et al (1982) demonstrated that the intraocular difference in PERG amplitude between amblyopic and contralateral eye increased with decreasing check size. Arden & Wooding (1985) reported the results of a more extensive study involving 62 subjects, many of them children who had undergone orthoptic therapy. They found only 3 of the sample who did not show any PERG deficit. However they acknowledge a relationship of greater complexity must exist in adult amblyopia between contrast sensitivity, visual acuity and PERG loss. They suggest the relationship may depend on the type of amblyopia. Arden & Wooding (1985) also noted that occlusion therapy at an early age reduces the PERG in the occluded eye whilst orthoptic exercise increases it.

Persson and Wanger (1982) recorded PERGs in 10 adult patients with strabismic amblyopia. They were previously unable to demonstrate any reduction in the PERG when up to 4° of eccentric fixation was simulated in normal subjects. Eccentric fixation of 4° or less in the amblyopic patients was not therefore corrected. The amblyopic patients were also carefully refracted until no further improvement in PERG amplitude

could be achieved. The PERG amplitudes were significantly lower in all amblyopic eyes compared with their fellows. The report supports the view of a functional retinal impairment in strabismic ambylopia. Wanger and Persson (1984) investigated whether there was also an effect on the oscillatory potentials and flash ERG in amblyopic patients. They concluded that there was no pre-ganglionic retinal dysfunction evidenced by the normal flash ERG and oscillatory potential responses. The PERG was however again found to be significantly reduced in 8/8 adult amblyopic eyes compared with their fellows.

Hess et al (1985) used steady state PERG techniques to compare the psychophysical losses exhibited by 14 amblyopic adults with the retinal response to stimuli of the same spatial frequency. They emphasise the need for fixation control and accurate refraction. The maximum PERG response was used to judge the optimum optical prescription and the direction of gaze required to correct eccentric fixation. The artefact reject rate was used to indicate fixation stability. When these factors had been individually optimised Hess et al (1985) were unable to find any PERG deficit in the spatial frequency range where there were obvious psychophysical deficits.

In attempt to marry the disparate results obtained with steady state and transient PERG techniques by Hess and Baker (1984b), Hess et al (1985) and Arden and Wooding (1985), respectively, Gottlob and Welge-Lussen (1987) carried out a transient PERG study on 14 patients using the same stimulus parameters as Arden and Wooding (1985), but including an adjustment for fixation until the PERG achieved maximum amplitude (Hess et al 1985). They were unable to find any abnormality in the amblyopic eye compared to its fellow nor when compared with the normal variation between right and left eyes.

3.4.4 Maculopathy

The localised nature of the pattern ERG makes it ideal for the examination of the macula region. The conventional flash ERG can only give a gross appraisal of retinal function

and may be insensitive to a focal retinal lesion (Sokol and Bloom 1977).

Support for the role of ganglion cell participation in PERG genesis was provided by Kirkham and Coupland (1981). An abnormal PERG was recorded from a patient with cherry red spot myoclonus syndrome. This condition is a visible abnormality which indicates the storage of abnormal white neurolipid metabolic products by retinal ganglion cells. The flash ERG was normal in this patient.

Arden et al (1984) report an abnormal PERG in all but 3 of 40 cases of maculopathy and were able to relate the degree of reduction to the loss of visual acuity. The PERG was thus shown to be a sensitive index of retinal abnormalities. In a group of Stargardt's patients the focal luminance ERG was not reduced to the same extent as the PERG. This is interesting because the condition originates in the photoreceptor/pigment epithelium complex and must affect both processes. The authors suggest that the discrepancy may arise through degradation of the optical image by deposits, but do not cite the results as evidence of a different locus of generation.

Celesia and Kaufman (1985) recorded transient and steady state PERGs to 15' and 30' phase reversing checkerboards in a group of 7 patients having predominantly unilateral maculopathies. They found a greater percentage abnormality to smaller checks using a transient recording method. Their findings suggest the a role for the PERG in the early detection of maculopathy. Indeed Holder (1987) reports all patients examined with maculopathy exhibited an abnormality in the p50 component.

3.3.5 Retinal manifestation of systemic disease

The PERG is reduced below normal values in diabetic retinopathy when cotton wool spots and angiographic evidence of capillary non-perfusion are present (Arden et al 1986). Similar, but more variable, changes occured to the oscillatory potentials in these patients.

Nightingale et al (1986) found the amplitudes of cortical and retinal evoked potentials

were significantly reduced in Parkinson disease patients compared with a matched control group. The retina is rich in dopamine (see Section 1.8) and it has been suggested that a biochemical and physiological disorder in the retina may account for the well documented abnormal cortical potentials. Nightingale's group established a significant relationship between PERG amplitude and the latency of the major positive response of the cortical evoked potential and proposed that the deficit in the cortical potential was secondary in part at least to a retinal abnormality.

3.4.6. Overview of clinical evidence for a proximal PERG origin

A difference in the behaviour of the focal and pattern ERG in selected ophthalmological conditions can imply a differential locus of response genesis. Many studies have compared the PERG with the flash ERG. The gross summation of the flash ERG however would mask a small localised retinal disturbance. It is more appropriate considering the localised, photopic nature of the PERG to compare the focal luminance ERG (Arden et al 1982), red flicker ERG (Plant and Hess 1986) or in cases of steady state stimulation the 2nd harmonic amplitude of the focal luminance ERG (van den Berg 1986). In the clinical studies where this comparison has been conducted interstudy correlation is hampered by the diversity of clinical protocols employed and the techniques of PERG measurement and analysis.

Transient responses have been measured as both positive and negative going transients (Porciatti and von Berger 1984; Holder 1987). Indeed it has been proposed that these two response components are generated in different retinal layers: the later negative going transient has been found more sensitive to optic nerve dysfunction whilst the earlier positive transient appears to reflect more generalised retinal dysfunction. The measurement of the inappropriate component in some studies might account for some of the disparate findings (e.g. Armington and Brignell 1981).

In the studies of optic nerve dysfunction it is important to consider the effects of trans-synaptic retrograde degeneration. Thus cystic changes occur in the inner nuclear

layer and impaired bipolar cell function has been suggested (van Buren 1963; Ikeda et al 1978). The participation of bipolar cell activity in the luminance ERG might be impaired in these cases and a differential PERG generator may not be necessary to explain some of the results. The inclusion of patients who may have had several attacks of retrobulbar neuritis and have varying degrees of visual deficit needs careful collating of large subject groups into sub-categories to examine the proposition of gradual PERG anomalies occuring after the acute event. In addition there is evidence that ganglion cells may survive up to nine months following intra-cranial optic nerve section, however after intra-orbital section ganglion cell function is compromised sooner because of an impaired blood supply (Madison et al 1984).

Many studies have only employed a limited range of stimuli (e.g. only one check size or square wave grating - Bobak et al 1983; Papst et al 1984a,b; Persson and Wanger 1984). A profile of the PERG amplitude as a function of check size has proved a more effective procedure for revealing neural deficit (Lovasik and Kothe 1986). Thus a differential vulnerability of specific classes of neurones has been suggested by the selective reduction of the PERG to certain spatial frequencies. Celesia and Kaufman (1985) and Harrison et al (1987) found an earlier loss of higher spatial frequency PERG responses effected by retrograde changes. Conversely Maffei and Fiorentini (1981) and Porciatti and von Berger (1984) found medium to lower spatial frequencies were more affected.

There is perhaps a little more agreement that the PERG declines in optic neuritis according to the severity of the visual impairment. (e.g. Arden and Vaegan 1982; Sieple et al 1983; Celesia and Kaufman 1985; Harrison et al 1987). However Sherman (1982) firmly concludes that the PERG is preganglionic in origin and has not found any significant amplitude alteration in cases of optic atrophy.

The general consensus would similarly suggest an anomaly in the PERGs recorded from glaucomatous eyes which depends on the severity of the disease process. There are no systematic longitudinal studies that relate ocular vascular perfusion pressures to the

activity of ganglion cells and thus indirectly to the magnitude of PERG amplitude reduction or latency variation (Lovasik and Kothe 1986). Such information would be of great value in drawing more analytical conclusions about the retinal origin of the PERG. The b-wave of the classical luminance ERG was shown in early studies to be reduced by clamping the retinal circulation (Brown et al 1968 - Section 2.2.3). However several studies have been able to correlate the reduction in PERG amplitude to the ophthalmoscopically determined cup to disc ratio; suggesting a relationship with nerve fibre function and ganglion cells (Van Lith et al 1984; Galloway et al 1986; Korth et al 1987)

Fazio et al (1986) examined 14 patients with advanced open angle glaucoma using flash electroretinography with dilated pupils. They report significant abnormalities in the flash ERG compared with the normal group. They directly attribute the results to a careful standardisation of technique. Abnormal ERGs have also been reported in patients with optic atrophy (Feinsod et al 1971), including some supernormal ERGs. This would lend support to retrograde trans-synaptic degeneration occuring in some optic nerve disease.

The results found in cases of amblyopia are equivocal and the nature of the visual deficit, in adults particularly, is too complex to draw any inferences. In younger amblyopes undergoing orthoptic therapy, however, the PERG seems a sensitive monitor of visual function (Arden and Wooding 1985). However Lachapelle (1985) attempted to relate the reduction of the PERG in response to 1° checks reported in cases of amblyopia by Arden and Wooding (1985) to the size of X-cell receptive field in cat. He proposed that Arden and Wooding (1985) results support Ikeda's (1980) hypothesis that the spatial resolving power of X-type cells is decreased in amblyopia. Arden (1985) in reply is more cautious about the direct extrapolation between species (see also Hess et al 1986). He points out that although the results are consistent with the idea that the PERG responses are driven by mechanisms which drive different types of ganglion cell, these mechanisms may just as well be located in the outer part of the retina.

However the general conclusions that may be drawn from clinical studies suggests the PERG is a composite response depending on the functional integrity of the both distal and proximal retinal layers (Skrandies et al 1987; Caruso and Higgins 1987). Thus luminance and contrast responses contribute with a different weighting to the PERG according to the spatial frequency of the stimulus (e.g. Porciatti and von Berger 1984). Several workers use an index measure of focal to pattern ERG amplitude (e.g. Arden and Vaegan 1983; Holder 1987) which looks for a selective difference between the responses. However isolation of the proximal or pattern component has not been attempted in transient recording.

3.5 REVIEW OF PARAMETRIC STUDIES OF THE PERG

3.5.1 Response latency

Kirkham and Coupland (1982/83) report no peak latency change with different spatial frequencies in the range 15 - 100' arc. Vaegan et al (1982) on the other hand postulate that the emergence of a slower response with smaller check size can be used to characterise the change from a focal response to a pattern response.

3.5.2 Temporal tuning

Odom et al (1982/83) found the maximum PERG amplitude responses occured at lower modulation rates for higher spatial frequencies. At spatial frequencies of 3 cpd or less a temporal rate of 4 Hz, 8 reversals /second, resulted in the greatest magnitude response. Trick and Wintermeyer (1982) also remarked a shift in the maxima of the temporal frequency function to lower rates with higher spatial frequencies: from 7.5 Hz at 0.25-0.5 cpd to 3.75 Hz for higher spatial frequencies [1-4 cpd]. Odom and Norcia (1984) later reported multiple temporal maxima that vary with spatial frequency.

On the other hand Hess and Baker (1984a) found a higher spatial frequency grating, 1.7 cpd, produced 2 definite peaks at 2 Hz and 8 Hz. The signal had a larger amplitude at the faster modulation rate. A lower spatial frequency of 0.17 cpd similarly produced two defined peaks at these frequencies, but of reduced amplitude. As discussed in section

2.4.3. this was the basis of their postulate of two mechanisms contributing to the PERG. Berninger and Schuurmans (1985) reported the temporal peak of the PERG to a 50' pattern reversing check occured at lower temporal frequency ≈ 1 reversal /second if the, p-n, negative going transient was measured. This component diminished as the temporal frequency increased. The positive component, n-p, peaked at ≈ 2 reversals /second and displayed a slow attenuation at lower and higher temporal frequencies. Sokol et al (1983) however found temporal tuning peaks at the two faster rates tested 3.75 and 7.5 Hz.

3.5.3 Spatial tuning

Spatial tuning is the presence of an optimum spatial frequency around which, at higher and lower spatial frequency, there is response attenuation. It is a property of a generator whose receptive fields display spatial antagonism and is used to characterise a pattern specific response (Padmos et al 1973). In the retina the receptive fields of ganglion cells and to a lesser extent bipolar cells display centre/surround antagonism that is mediated by amacrine and horizontal cells respectively (Kuffler 1953; Kaneko 1973; Missotten 1974).

The amplitude of the pattern reversal ERG as a function of pattern size has been extensively studied, (Armington et al 1971; Groneberg 1980; Groneberg and Teping 1980; Armington and Brignell 1981; Maffei and Fiorentini 1981, 1982; Arden et al 1982; Kirkham and Coupland 1982/83; Odom et al 1982/83; Trick and Wintermeyer 1982; Vaegan et al 1982; Arden and Vaegan 1983; Sokol et al 1983; Korth 1983; Ringo et al 1984; Hess and Baker 1984; Riemslag et al 1985; Korth and Rix 1985; Korth et al 1987).

As is common place in PERG studies there are quite diverse opinions about the resulting spatial tuning functions. Again differences in methodology can account for some discrepancy. The peak of any spatial tuning function might be expected to vary with the temporal frequency of stimulation, the extent of the stimulated retina and the luminance and contrast of the stimulus used. Some factors can be expected to alter the extent of

retinal cell receptive field sizes, as occurs with light adaptation (Shapley and Enroth-Cugell 1984; Korth and Ilschner 1986). Other factors will govern the effectivity and selectivity of the stimulation for particular classes of retinal cell (eg Kaplan and Shapley 1986).

One of the earliest investigations of the ERG's spatial characteristics was carried out by Nelson et al (1979) on the perfused eyecup of cat. Using hexagonally arrayed multispot patterns they found that the b-wave was sensitive to the diameters of spots. The ratio of light : dark stimulation area was kept constant throughout. As the spot diameter was increased, with a concomitant increase in spot separation, the b-wave response was found to rapidly diminish. Defocusing the pattern caused an immediate return of the response. Diehl and Zrenner (1980) developed and applied this concept to man. They used a circularly concentric spot pattern. They demonstrated that the a- and b-wave amplitude decreased by 33% in comparison with the defocused state. A receptive field organisation of the b-wave process was suggested to account for these observations.

Trick and Wintermeyer (1982) did not observe a low spatial frequency roll off in their data. They suggest this is because the pattern-reversal retinal potential is influenced by both contrast specific and luminance specific retinal responses. The luminance specific response contributes most strongly at low spatial frequency and possibly obscures the low spatial frequency attenuation due to the contrast specific response. Sokol et al (1983) only found the PERG to be spatially tuned at high contrast and fast modulation rates.

Holden and Vaegan (1983a) reported a bandpass spatial tuning of the PERG in pigeon and developed the concept that the PERG forms part of a spatial filter, (see section 3.2). A bell shaped tuning function that peaked at ≈1cpd was demonstrated in man by Arden and Vaegan (1983) using small stimulus fields 4.74° x 7.5°. The stimulus was a high contrast checkerboard modulated at 3 Hz. Larger stimulus fields produced peaks at lower spatial frequencies ≈ 0.5cpd. The focal luminance ERG recorded under identical conditions was larger than the optimum PERG at all but the smallest field size. Arden

and Vaegan (1983) affirm that comparable results were obtained if the relative surround luminance was increased. These observations would suggest that low spatial frequency attenuation is not due to the destructive interference of slower stray light responses from other parts of the retina. (cf. Reimslag et al 1985 - discussion).

Berninger and Schuurmans (1985) demonstrated spatial tuning of the negative wave of the pattern reversal response across several temporal frequencies. The positive component however was not specific to distribution changes in retinal contrast, (Berninger and Schuurmans 1985). Korth et al (1985) also showed the negative transient of the pattern reversal PERG to be spatially tuned; peaking at 4 cpd. This tuning was more pronounced at lower contrast levels. At low contrasts the positive wave also exhibited some spatial selectivity.

Korth et al (1985) measured the positive component from the first negative trough to the following positive peak. The negative potential was measured from the baseline (see also Armington et al 1971). Korth and Rix (1985) suggest that when the negative transient is measured peak to peak the inclusion of the positive transient amplitude in the measure will mask any spatial tuning. They propose this explanation for the results of Armington (1970), Groneberg (1980), and Kirkham and Coupland (1982/1983). Other workers who have been unable to demonstrate any spatial selectivity of the response have most often measured the positive transient (e.g. Armington and Brignell 1981).

Odom et al (1982/83) analysed the 2nd harmonic component and demonstrated a low spatial frequency attenuation of the PERG using low contrast sinusoidal gratings. The tuning function peaked at 0.68 and 2.22 cpd at a temporal modulation of 4 Hz. Odom et al (1982/83) suggest the failure to demonstrate spatial tuning in previous studies relates to the choice of high luminance and high contrast levels. They suggest the PERG resembles the visually evoked cortical potential and is composed of two types of response (Regan 1972; Padmos et al 1973):

i) a pattern contrast response with bandpass filter-like characteristics (Hess and Baker

1984a)

ii) a local luminance response with low pass filter like characteristics (Spekreijse et al 1973a,b). Conditions that reduce the local luminance contribution more than the pattern contrast response would result in greater spatial tuning.

Riemslag et al (1985) repeated the experiments of Spekreijse et al (1973) using a DTL electrode. Smaller patterns could therefore be employed without optical interference from a contact lens electrode. High contrast checks were modulated at 4 Hz in a 12° field of high mean luminance and the amplitude of the 2nd harmonic PERG responses to various check sizes was examined. Spekreijse et al (1973) had concluded that the PERG could be accounted for by the summation of local luminance responses and contained very little if any contrast specific response. Reimslag et al (1985) reaffirmed this view concluding that the ERG varies little with check size and does not differ significantly from the luminance 2nd harmonic response.

Hess and Baker (1984a) in agreement with Spekreijse (1973), have shown that the 2nd harmonic of the steady state response to counterphase pattern stimuli and uniform field stimuli have similar properties wrt temporal frequency and the effect of luminance. However they found it to be clearly sensitive to stimulus pattern parameters ie. spatial frequency.

Using a very small field size and a modulation rate of 8 Hz, Hess and Baker (1984a) demonstrated a clear peak in the PERG at 2-5 cpd. The bandpass function was persistent under square wave or sinusoidal modes of presentation. The ERGs to low spatial frequency patterns were evoked under different conditions of surround luminance. The low spatial frequency roll off was present in all cases (see also Arden and Vaegan 1983). Response magnitude was reduced, but this could be attributed to a loss of stimulus contrast due to scattered light from the surround. Hess and Baker (1984a) concluded that the response is not purely due to local luminance (cf. Spekreijse et al 1973), but displays some sensitivity to differences of luminance across the retina.

Baker and Hess (1984) proposed that two mechanisms contribute to the PERG:

1) An odd-symmetric response which behaves linearly and is independent of spatial frequency

2) An even-symmetric response that by definition is non-linear, but displays a bandpass spatial frequency dependence

The spatial tuning of the 2nd harmonic strongly suggests a post receptoral origin for this component of the contrast response. Indeed Baker and Hess (1984) additionally suggest a possible correspondence between the distal and proximal fluctuations in potassium and the odd and even components respectively.

Note: although the response to contrast reversing stimuli by definition contains no odd-symmetric harmonics it is still possible that the underlying local generators may exhibit odd-symmetric components (half wave rectification rather than full wave rectification). However in the ERG recorded from the whole eye it is likely that spatial symmetries in the whole pattern together with separate parallel sets of generators having on- and off- centre receptive fields will tend to cancel these out.

Plant and Hess (1986) proposed a subtle modification of previous models to explain most of the experimental data:- the width of the bandpass response is such that it can be driven by uniform field stimulation. Thus the 2nd harmonic response in the uniform field condition is driven by an identical post receptoral element as the pattern response and is equivalent to a low spatial frequency pattern.

3.5.4 Pattern onset-offset responses

The majority of clinical studies have used the pattern reversal mode of presentation to elicit PERGs. An alternative presentation method, first investigated by Spekreijse (1966), is the appearance-disappearance of a pattern from a background of mean luminance (see Section 2.4.1). In the study of cortical evoked potentials the onset-offset mode of stimulus presentation has proved most efficient in separating pattern from

luminance related responses (Korth 1983). A corneal positive response occurs at the onset and offset of a patterned stimulus. However there is an asymmetry in the response magnitude which may be enhanced by altering the spatial frequency of the pattern. Thus at higher spatial frequencies the onset response exceeds the offset, but at low spatial frequency the offset response increases in amplitude until it exceeds the onset signal (Arden and Vaegan 1983; Korth et al 1985).

Korth (1983) found the negative wave of the onset response was spatially tuned at ≈ 3-4 cpd. However the offset response seemed to be luminance mediated; the signal amplitude decreasing monotonically with increasing spatial frequency (Padmos et al 1973). Korth et al (1987b) were only able to demonstrate fundamentally different mechanisms between onset and offset responses with light adaptation and they suggest that in part the two responses may be generated by the same non-antagonistic units at low intensity.

The spatial selectivity of the PERG has been explained in terms of lateral inhibitory activity of spatially antagonistic centre surround receptive fields. The spatial antagonism of the receptive fields can change with the state of adaptation. In the dark adapted state surround antagonism is less effective; the reduction in inhibitory effect between centre and surround effectively increases the size of the centre field (Barlow 1957; Davson 1980). Korth et al (1987) therefore investigated the effect of different adaptation levels on the PERGs spatial selectivity. They found with increasing dark adaptation the spatial tuning peaked at increasingly lower spatial frequencies. They suggest this relates to the functioning of larger receptive fields in the dark and lends further support to the assumption that the PERG is associated with contrast processing mechanisms.

3.5.5 Effect of retinal position

As described by Brindley and Westheimer (1965) retinal responses from adjacent retinal areas summate (Armington and Brignell 1981; Arden and Vaegan 1983; Hess and Baker 1984a). If the reported bandpass spatial tuning characteristic (Hess and Baker 1984a) is

the consequence of centre-surround antagonistic receptive fields its peak might be expected to occur at lower spatial frequencies with increasing retinal eccentricity. Larger receptive fields occur in more peripheral regions (e.g. Cleland and Levick 1974). Hess and Baker (1984a) found this was indeed the case. Arden and Vaegan (1983) also provided evidence of differential sensitivity of central and peripheral regions by comparing the ratio of response amplitude from centre: annular surround to 7.5' and 30' checks. (cf. Riemslag et al 1985). Thus the centre field was more sensitive to the smaller check size. The central response was also larger than from the equi-area annular field. The PERG therefore demonstrates macula over-representation (Armington and Brignell 1981; Arden and Vaegan 1983; Hess and Baker 1984a).

3.5.6 Stimulus Contrast

The pattern evoked ERG has been reported to be linearly related to stimulus contrast as defined by the Michelson contrast ratio for the visibility of interference fringes

(Lmax - Lmin) / (Lmax + Lmin),

where Lmax is the luminance of a bright element and Lmin the luminance of a dark element (Michelson 1891). This equation is most commonly applied to spatially repetitive stimuli, e.g. sinusoidal gratings, (Arden and Vaegan 1983; Hess and Baker 1984a; Korth et al 1985).

3.5.7 Colour contrast

Riggs et al (1964) first reported that ERGs could be recorded to changes in hue without changes in luminosity. Arden and Vaegan (1983) also remarked that the ERG evoked by large uniform field changing from red to green differed in morphology from the responses seen when a red/green checkerboard reverses in hue. The colours were adjusted to be isoluminant. Therefore if the ERG mechanism had CIE spectral sensitivity no response would have been expected. The amplitude of the pattern reversal red/green ERG was similar to the focal on/off ERG. The authors therefore suggest that no lateral interactions need be postulated to account for the size of the PERG (Arden and Vaegan 1983).

Riemslag et al (1985) combined two independently generated red (Wratten 25) and green (Wratten 58) checkerboards. Each generator could produce either pattern reversal or luminance stimulation. The 2nd harmonic responses to each condition were compared. The PERG response to 20' checks presented at 8.3 reversals s^{-1} in an 6° field was found to be indistinguishable from the 2nd harmonic response to a homogenous red/green exchange. They similarly concluded that the ERG in response to a red/green checkerboard is determined by local chromatic change.

3.5.8 Pupil size and defocus

Holder and Huber (1984) examined the effect of unilateral miosis on the PERG using pilocarpine. Pilocarpine is a direct acting parasympathomimetic ie has a direct muscarinic action on the sphincter pupillae. At the time of recording the treated pupil diameter was ≤ 2.0 mm, the fellow eye pupillary diameter was in the range 4-6mm. The authors could not discern any interocular amplitude asymmetry in 5/6 subjects as measured by the interocular ratio. They concluded that miosis appears to have very little effect on PERG amplitude, but recognise that further studies are required to assess the additional pharmacological effects of the miotic eg accomodative spasm of the ciliary muscle. In most cases natural pupils are used in PERG recording to ensure accurate focusing without any impairment of ciliary muscle function.

Hess and Baker (1984a) and Korth (1983) have both assessed the influence of the slow iris potentials on the PERG recording. Korth (1983) studied the effect of stimulus intensity on the wave shape of the pattern onset-offset ERG. At low intensity levels a slow broad wave of positive polarity was observed at higher spatial frequencies. Korth (1983) suggested this relates to slow iris potentials caused by pupillary movements. The experiment was repeated with an immobilised dilated pupil following the topical administration of tropicamide, an antimuscarinic drug. The broad wave was eliminated. Slooter and van Norren (1980) showed that the human pupil responded with a constriction following a pattern onset stimulus while only a little pupillary movement

was noted following pattern offset. Korth (1983) concludes that the slow wave following pattern onset is an iris potential associated with pupillary constriction. However Baker and Hess (1984) found the slow, low frequency wave response was greater when responses were recorded with a fixed dilated pupil and a centred 4mm artificial pupil.

The PERG has been shown to be very sensitive to defocus (Sokol and Bloom 1977; Arden and Vaegan 1983; Hess and Baker 1984a). The disparity in the effect of blur in each of these studies reflects the spatial freqencies used to evoke the response. The higher the spatial frequency the greater the amplitude reduction; thus Hess and Baker (1984a) noted a 50% reduction to the PERG recorded to a 4cpd grating with 0.50 dioptres blur.

3.5.9 Raster responses

A television picture is written on the screen by the raster which takes 20 ms to scroll from top edge to bottom opposite edge. Every point on the screen is bright for a brief instant although the flyback time is short - the screen is dark for only 7% of the duty cycle. However a fast focal ERG has been recorded to the blank screen by Arden et al (1982). Using a fast TV run at 119 Hz they were unable to record a response to the raster, but when the screen brightness alternated on every frame (ie 59 Hz stimulation) they did; they conclude that the raster response disappears at about the frequency where flicker can no longer be discerned (Arden et al 1982). The time taken to traverse the screen could effectively round or smooth the PERG response as the stimulation of each retinal locus will be slightly out of phase with its neighbour and summate into the final field response.

3.6 AIM OF THE PRESENT STUDY

As evidenced by the clinical investigations and parametric studies a purely luminance model of PERG generation is not compatible with many findings. For example the selective reduction of PERG following optic nerve section or optic nerve dysfunction

and the absence of a PERG in specific ganglion cell disease are difficult to understand if the mode of PERG generation is identical to the local flash ERG. A compromise proposal from Hess and Baker (1984a) suggests luminance and pattern evoked ERGs share a common generator which is preferentially stimulated by patterns of higher spatial frequency. A uniform field would in this case behave as a very low spatial frequency pattern. Others have similarly suggested the PERG forms part of a spatial filter; the PERG and focal luminance ERG forming a smooth continuum as a function of spatial frequency (Holden and Vaegan 1983a). The response would therefore be composed of bandpass and lowpass elements whose effectiveness varies with spatial frequency (Trick and Wintermeyer 1982).

The aim of the present study was to attempt to separate the two proposed mechanisms of luminance mediated and pattern mediated responses or at least to preferentially enhance the contribution of the postulated pattern component so that its retinal generator could be more readily examined.

One of the more persuasive arguments for a more proximal retinal cell contribution to the PERG is the demonstration of bandpass spatial tuning. A luminance response is described as one which is essentially spatially insensitive (Padmos et al 1973). Bandpass spatial selectivity on the other hand characterises a pattern response and may be explained by a spatially antagonistic receptive field model of response generation (Padmos et al 1973). In the retina ganglion cells and to a lesser extent bipolar cells could contibute to such a response (section 3.5.3). A high spatial frequency attenuation may be in part accounted for by optical degradation of the retinal image (Campbell and Green 1965; Hess and Baker 1984a). Low spatial frequency response attenuation becomes the criterion on which the presence of a pattern specific response is defined. The experimental paradigms were designed to examining the spatial selectivity or pattern response of the retina at different eccentricities.

CHAPTER 4.

SPATIAL TUNING STUDIES OF THE PERG.

4.1 EXPERIMENTAL DESIGN

The properties of the cellular elements involved in the initiation and generation of an evoked potential are likely to characterise the recorded signal. Thus a pattern specific response generated by elements having spatially antagonistic receptive fields will demonstrate bandpass spatial tuning (Padmos et al 1973). In an effort to elucidate the origin and nature of the PERG a study was designed to examine the variation of its spatial sensitivity with retinal eccentricity. Any variation in spatial selectivity across the retina might then be related to changes in cell population, size and density.

Pattern onset-offset stimulation has been fruitful in distinguishing the pattern specific and luminance components of the pattern evoked cortical potential (Spekreijse et al 1966; Korth 1983). It was adopted in this study to similarly provide a more analytical method of investigating the pattern evoked retinal response.

4.1.1 Recording Electrodes

DTL fibre was chosen as the active recording electrode (Dawson et al 1979). It could be used without corneal anaesthesia and could be tolerated comfortably for recording sessions of 1 - 2 hours duration. Initial attempts to attach the fibre to a silver wire conductor employed 'araldite'. (see also Spekreijse and Apkarian 1986). However the conductivity of the 'DTL' fibre was found to be disturbed after autoclaving. A disposable system of fibre application was subsequently developed. A fresh length of fibre is used for each subject. The design of the fibre holder is shown in Fig 4.1. The extensible properties of the Perisil sleeving secure the fibre into the silver wire hook (Thompson and Drasdo 1987). The holder is positioned on the subjects temple, the fibre stretched across the inferior cornea and tethered at the nasal canthus. The spiral construction of the fibre prevents corneal trauma on blinking or eye movement.

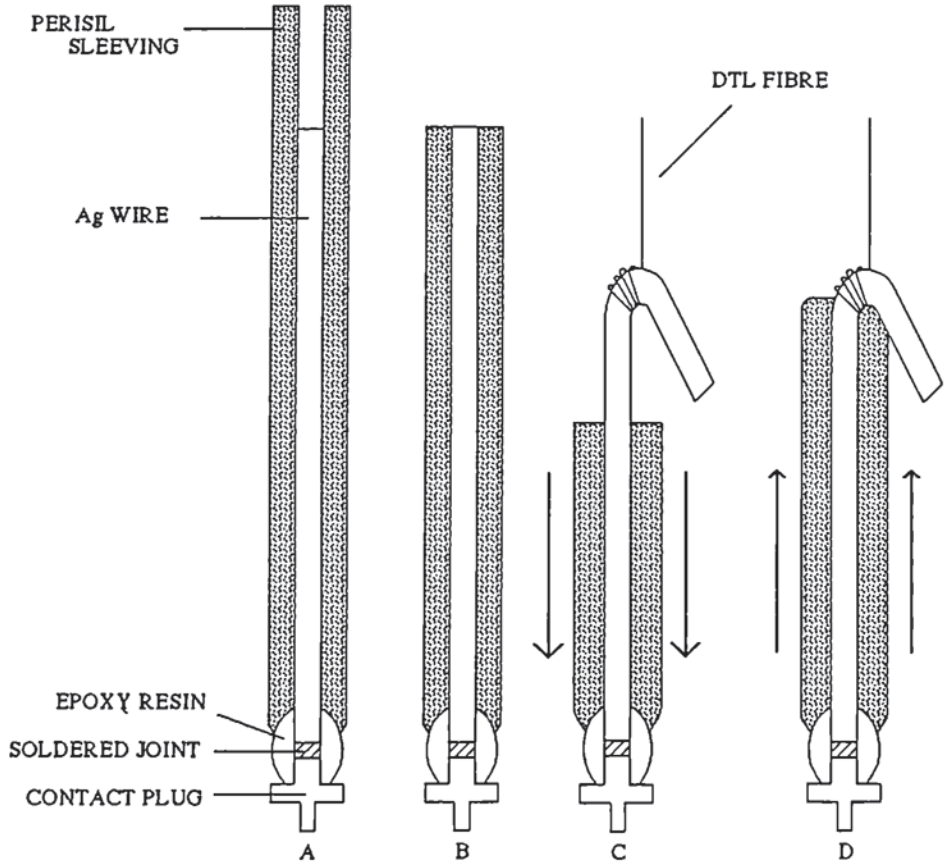

A) A 5 cm length of siver wire is silver soldered onto a 1mm contact plug and the joint sealed with araldite. A length of Perisil sleeving is passed over the wire and embedded into the araldite. The holder may be autoclaved.

B) The Perisil sleeving is cut flush with the end of the silver wire.

C) The sleeving is then pushed away from the free end of wire. A hook is bent into the wire around which the DTL fibre is wound.

D) The sleeving is then released forcing the DTL fibre tightly into the junction of the hook, the angle of which is then made more acute.

Fig 4.1 Diagram illustrating the construction of a silver wire' DTL' fibre holder designed for easy replacement of fibre.

4.1.2 Pattern stimulator

An optical stimulator was preferred over a TV system for its superior image quality, fast rise time and its versatilty of pattern presentation. TV generators produce a large electric field which surrounds the monitor and the evoked potentials can be easily confounded by electrical 'mains' interference. An optical pattern stimulator was built according to dimensions elaborated by C.M.Thompson (1987). Details of its construction are given in appendix 1. Slide mounted achromatic patterns were back projected and reflected along a series of front silvered mirrors onto a screen covered with diffusing material. The first mirror in the system was mounted on a pen motor and the pattern elements could be displaced by a variable amplitude thus effecting pattern reversal. Also attached to the pen motor was a diffusing shutter which had a fast rise time of 4.2 ms (Drasdo 1982). It was therefore also possible to present the slides in an onset-offset mode or even as a combination of both reversal and appearance (see Chapter 7). The pen motor timing was controlled via a *Digitimer* generating a series of electrical pulses. The mean contrast of the patterns on the screen was 75%, the mean luminance 250cdm^{-2}.

4.1.3 Stimulus fields.

The recent literature has suggested the participation of ganglion cells in the generation of the PERG (Maffei and Fiorentini 1981; Maffei et al 1985). The PERG might therefore be expected to reflect the spatial properties of retinal ganglion cells and to relate to ganglion cell density. The stimulus fields in this study were therefore chosen to contain equal ganglion cell densities. Using equation 2 of Drasdo (1977):

$$C = \int_0^{\varnothing} \frac{2\pi \varnothing d\varnothing}{[k(1 + S\varnothing)]^2} = \frac{2\pi}{(kS)^2} \left\{ \log_e(1 + S\varnothing) + \frac{1}{(1 + S\varnothing)} - 1 \right\}$$

C is the cumulative count, S determines the initial slope of the regression curve that fit the ganglion cell data and k is the inverse of the square root of the receptive field density.

The calculated stimulus zones contained approximately 25% of the total ganglion cell population and were used in a concentric array. White cardboard masks were placed in front of the projection screen to produce a central field of 0-5.1° radius, a mid-peripheral field of 5.6-12.6° annular radii and a peripheral zone that subtended 12.3-26.6°. The width of the projection screen coupled with viewing distances of 126cm, 50cm and 22.5cm respectively, acted as limiting factors.

4.1.4 Amplifier and averager settings

PERG data were recorded using a Nicolet Pathfinder II 8-channel averager. Its software processing capability permits data storage and subsequent analysis. A computer program describing the recording parameters was written onto the Winchester disc and summoned for each experimental trial. The parameters remained constant within an experimental series.

The pattern onset-offset ERG was initially recorded with a wide filter setting; 0.1 -300 Hz. The resulting waveform was Fourier analysed and the major power of the response was complete at 35 Hz and the recording bandpass was accordingly set at 0.5 - 70 Hz; 3db down, 12 db/octave. A 50 Hz notch filter was additionally introduced into each recording program to help remove electrical noise. Amplifier sensitivity was set at 100 μV/± 50 μV. An artifact reject system operated if a signal was over 96% of the full scale deflection ie ± 96% x 50 μV.

The electrooculogram was simultaneously recorded with the PERG. Ag EEG cup electrodes were positioned on the nasal and temporal canthus for this purpose (Galloway 1975). The small amount of eye movement artefact that accompanies fixation was found to be minimal at this amplifier sensitivity (see Appendix 1) For most subjects 100 μV sensitivity resulted in a rejection : average ratio of 1:3.

The initial PERG studies incorporated an interrupt button which allowed the subject to control the length of the recording epoch. Volunteers were thus instructed to restrict

averaging to between blinks. The resulting traces were compared with those obtained when the artefact reject system alone controlled the averaging. There did not appear to be a significant difference in the signal to noise ratio in the two conditions. The interrupt system was therefore used only in the first study. However in clinical situations with cooperative, but naive observers the interrupt button may offer some advantage (e.g. Holder 1987).

4.1.5 Temporal rate of stimulation

The amplitude of the PERG has been noted to vary with the temporal frequency of stimulation (section 3.5.2). However there is little agreement on the optimal rate, probably because of other differences in employed protocols. Slower presentation rates result in transient responses, the positive and negative components of which have been reported to differ (Korth and Rix 1985; Berninger and Schuurmans1985; Holder 1987). This information is masked in a steady state response that approximates to a sinusoid and requires Fourier harmonic analysis. Transient responses were therefore chosen for investigation and a temporal frequency selected which would minimise recording time.

Pattern ERGs were recorded to onset-offset stimulation. Typically a peak onset response occured at 40-50 ms. The fastest rate compatible with transient signal analysis was 5 Hz. Thus the pattern was presented for 105ms followed by a blank screen for 106ms. The choice of timing was calculated to induce drift with respect to mains frequency and aid electrical noise reduction through averaging.

4.1.6 The effect of defocus

As described in section 3.5.8 the amplitude of the PERG is very sensitive to defocus. In all these experiments the volunteer subjects wore their latest spectacle correction or contact lenses as appropriate and were capable of right and left eye 6/6 visual acuity. There were no significant binocular anomalies or eccentric fixators in any subject group.

4.1.7 Response Measurement

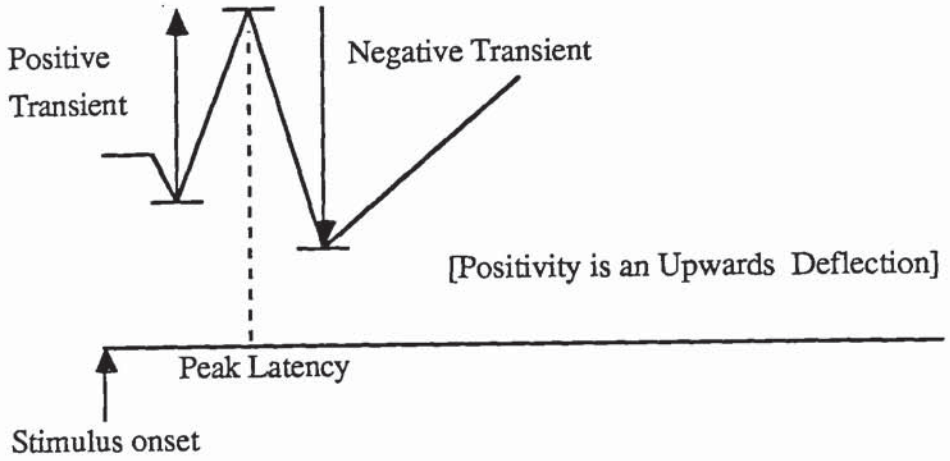

Fig 4.2 Schematic diagram illustrating the peak to peak response amplitude and peak latency measures referred to in subsequent results sections.

4.2 METHOD - SPATIAL TUNING STUDY

The following protocol was adopted to examine the spatial selectivity of the retinal response to patterned stimulation:

Pattern onset-offset ERGs were recorded binocularly from 4 informed volunteers whose ages ranged from 22-52 yrs of age. All wore spectacle corrections if appropriate and were capable of 6/6 or better acuity right and left. Achromatic square wave gratings and chequerboard patterns of varying spatial frequency were presented in three contiguous zones using a back projection optical system. The zones subtended 0-5.1°, 5.6-12.6° and 12.3-25.6° at viewing distances of 126cm, 50cm and 22.5cm respectively. The patterned stimuli appeared for 105ms and disappeared into a uniform background of mean luminance for 106ms.

Responses were recorded with a 'DTL' fibre electrode referenced to an Ag EEG cup electrode positioned on the ipsilateral outer canthus. A mid-frontal Ag EEG electrode acted as an earth. At least 100 sweeps were recorded on a Nicolet Pathfinder II averager with a bandpass 5 -70 Hz, time window 200 ms. Averaging was controlled by the use of an interrupt button which subjects were instructed to use when blinking. Subjects were asked to fixate a target positioned in the centre of the stimulus field,

which in the central field coincided with the intersection of four checks. The room and mask luminance were maintained at approximately 10% (25-50 $cdm^{-2)}$ of the mean screen luminance of 250 cdm^{-2} (Brindley and Westheimer 1965) to reduce the effects of stray light. Stimulus contrast defined by the Michelson equation;
C = (Lmax-Lmin) / (Lmax+Lmin) was 75%.

Controls were incorporated into each experimental trial. A monocular stimulus run was included to check for the confounding presence of volume conducted visual evoked cortical potential in the signal from the occluded eye (Peachey et al 1983; Seiple and Siegel 1983; Hobson et al 1984; Arden 1986). A run without a pattern, but with a neutral density filter reducing the luminance by 50%, was carried out to assess any confounding effects of slight luminance mismatch via the diffusing shutter - (see appendix 1)

4.3 RESULTS

4.3.1 Amplitude variation with spatial frequency

In each stimulus condition the data for the 4 subjects was group averaged and the resulting traces have been displayed in Figure 4.3 and 4.4 for square wave grating and chequerboard stimuli respectively. Positivity is shown as an upward deflection in accordance with ERG convention. The *group average* data for the three stimulus zones are grouped according to the type of stimulus pattern. The display gain for each group of traces is shown in the legend. Typically the standard error of an amplitude measure did not exceed 15 - 20% of the mean. The peak to peak amplitudes of the positive and negative going transients of the *group averaged* PERG signal are plotted as functions of spatial frequency in figures 4.5 and 4.6., and demonstrate a broad spatial tuning in all but 2 stimulus conditions.

The results of an analysis of variance carried out on the *individually* measured peak to peak amplitudes that compose the group average confirms the significance of the tuned functions.

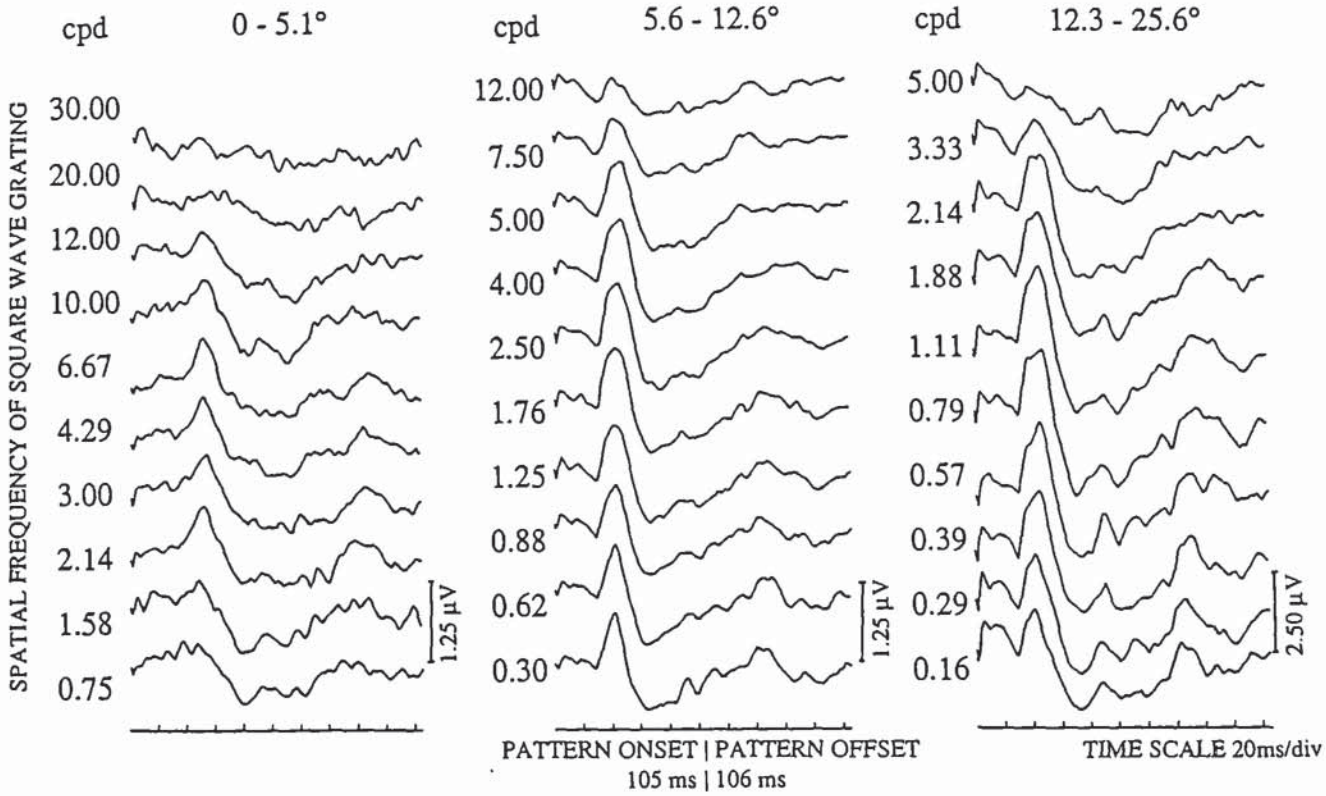

Fig 4.3 Group averaged PERG data (n=4), recorded in response to square wave gratings presented in an onset-offset mode in three stimulus zones. NB the display gain for the peripheral field is lower than for the more central zones.

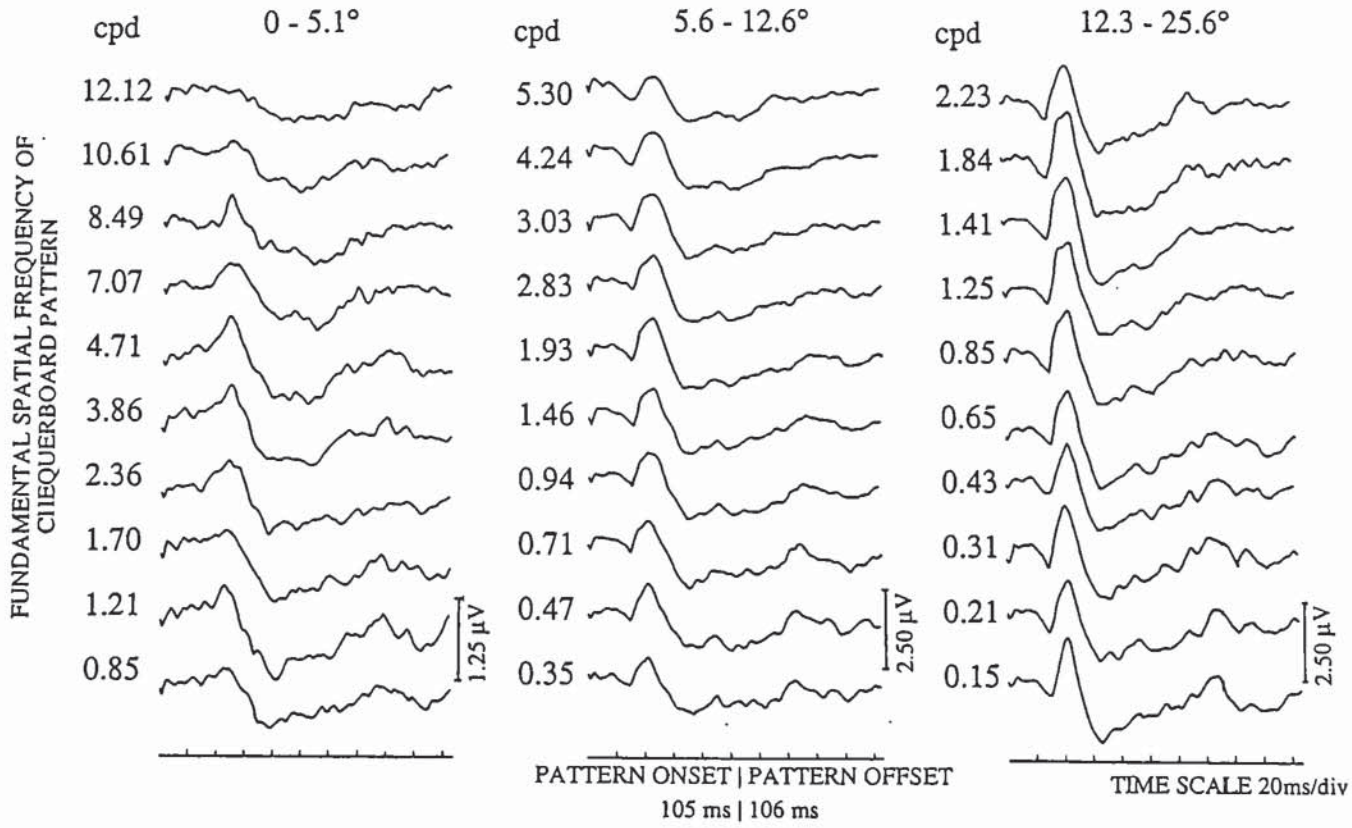

Fig 4.4 Group averaged PERG data (n=4), recorded in response to chequerboard patterns presented in three different stimulus fields in an onset-offset mode. NB the display gain for the central field is higher than for the more peripheral zones.

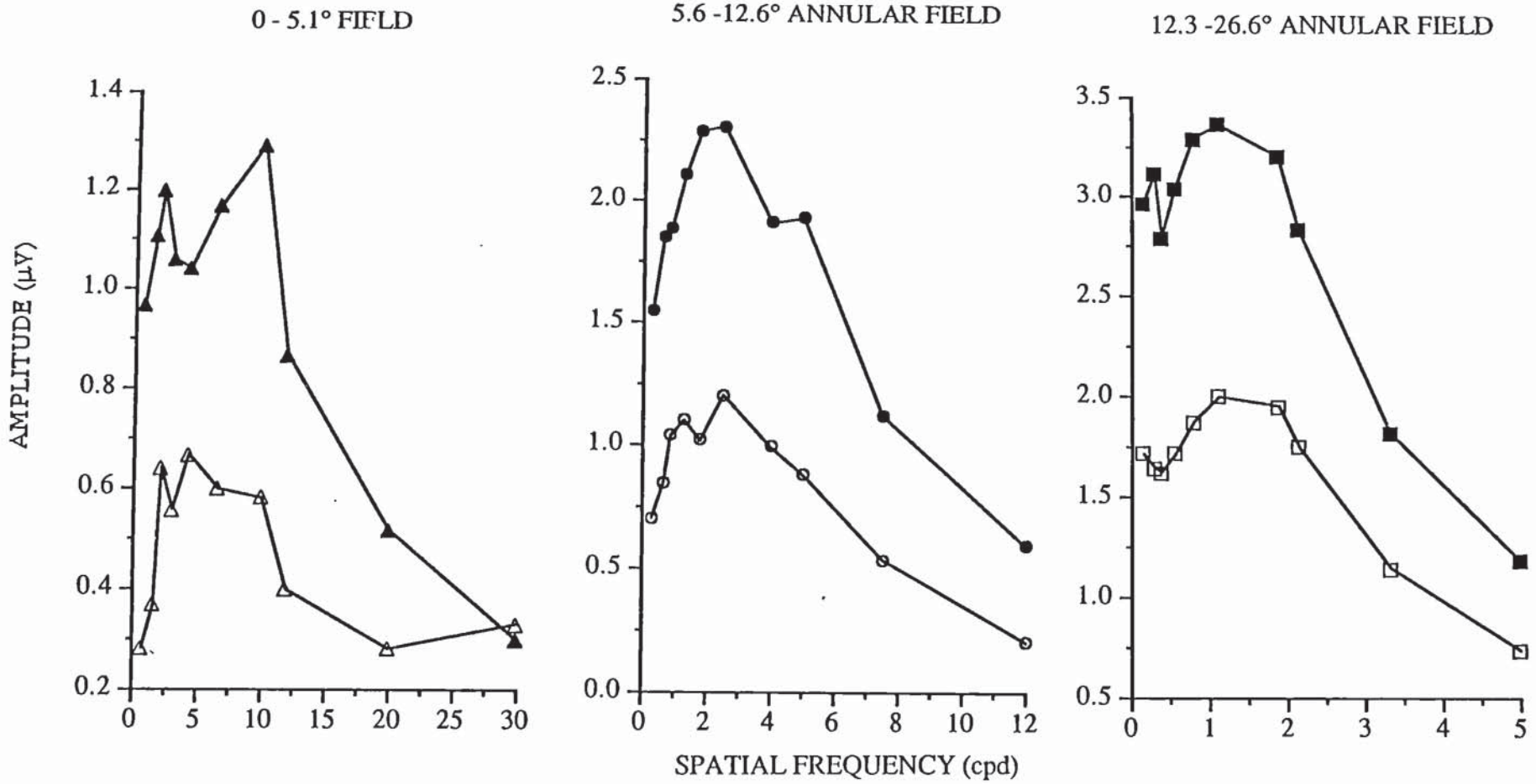

Fig 4.5 The peak to peak amplitudes of the group averaged PERG waveforms recorded to square wave gratings are plotted as a function of spatial frequency. Positive transients are shown as open symbols, negative transients as solid symbols.

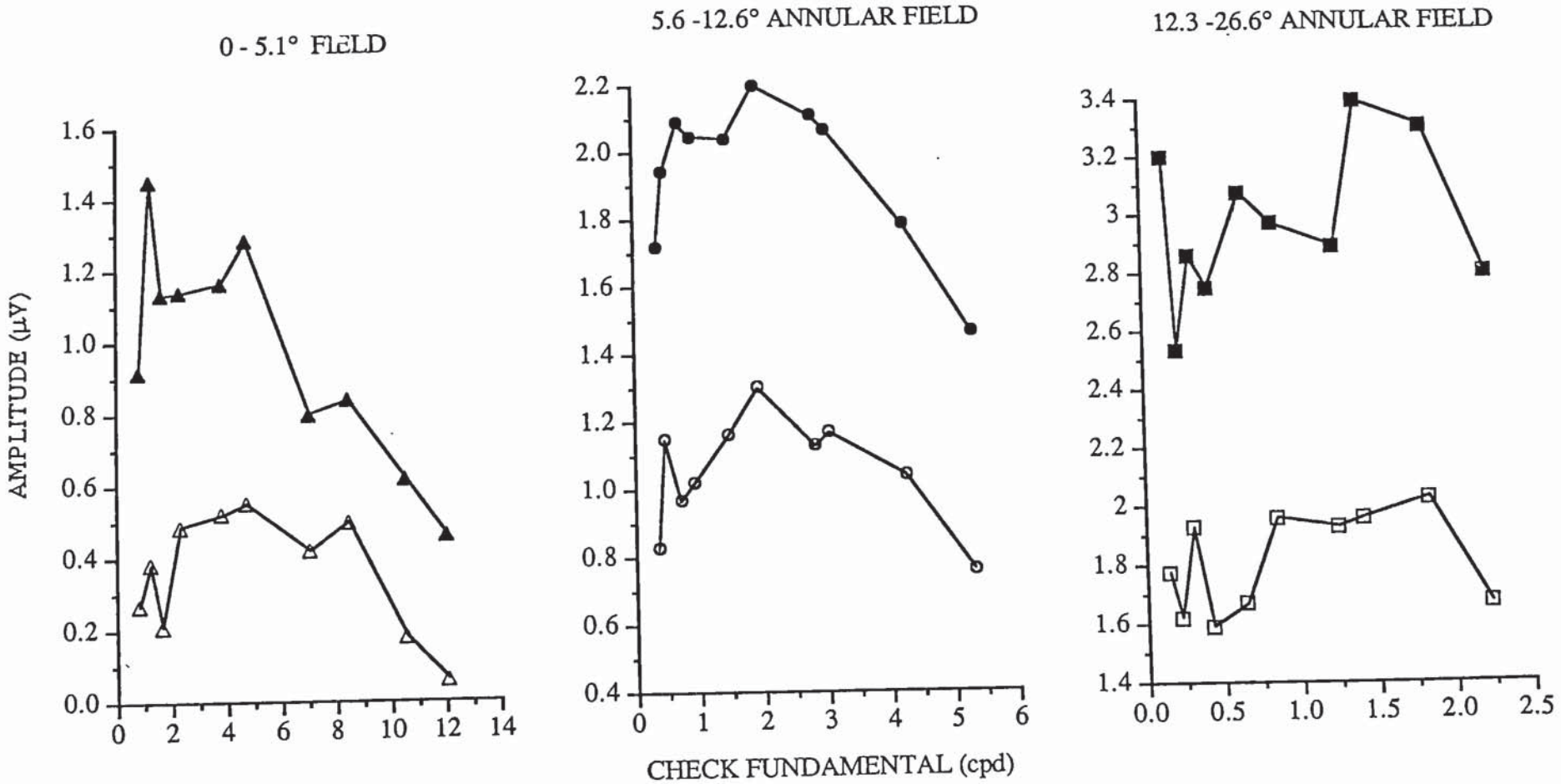

Fig 4.6 The peak to peak amplitudes of the group averaged PERG waveforms recorded to chequerboard stimuli displayed as a function of fundamental check spatial frequency. Positive transients are shown as open symbols, negative transients as solid symbols.

Table 4.1 Results of an analysis of variance carried out on the individually measured amplitude PERG data illustrated in Figs 4.5 and 4.6.

Line Gratings

0 - 5.1° zone: F=1.69, df = 9,30 p = 0.14 [*]

5.6 -12.6° zone: F= 4.99 df = 9,30 $p \leq 6 \times 10^{-5}$

12.3 -25.6° zone: F = 10.48, df = 9,30 $p \leq 1 \times 10^{-5}$

Checkerboards

0 - 5.1° zone: F=3.48, df = 9,30 p = 0.005

5.6 -12.6° zone: F= 3.45, df = 9,30 p = 0.0045

12.3 -25.6° zone: F= 0.7, df 9,30 p = 0.70 [*]

[* not significant]

4.3.2 Variation of peak latency with spatial frequency

Latency showed a tendency to increase with spatial frequency; an effect that was most pronounced in the peripheral field. The *group averaged* peak latency obtained for chequerboard patterns have been shown graphically below in figures 4.7, 4.8 and 4.9.

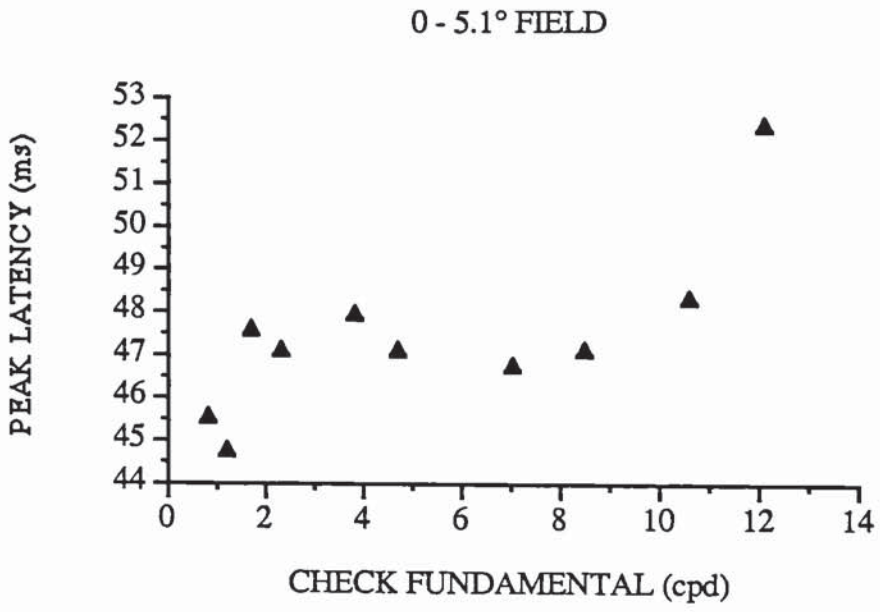

Fig 4.7. PERG onset peak latency in the central region, **y = 47.4 - 0.16 x**, r = 0.15; df 1, 38 p = 0.35*

Straight lines have been fitted to the *individual* data points that make up the group average, by the method of least squares. The regression equation for each zone is shown in the individual legend. The trend is not significant in the central field fig. 4.7.

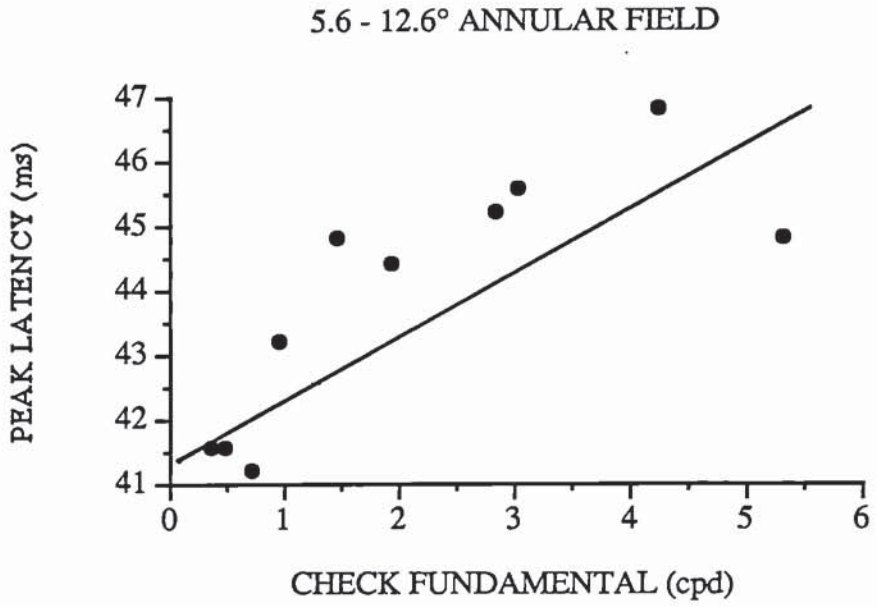

Fig 4.8. PERG onset peak latency in the mid-peripheral zone, **y = 41.8 + 0.82x,** r = 0.5; df 1, 38 p = 0.001

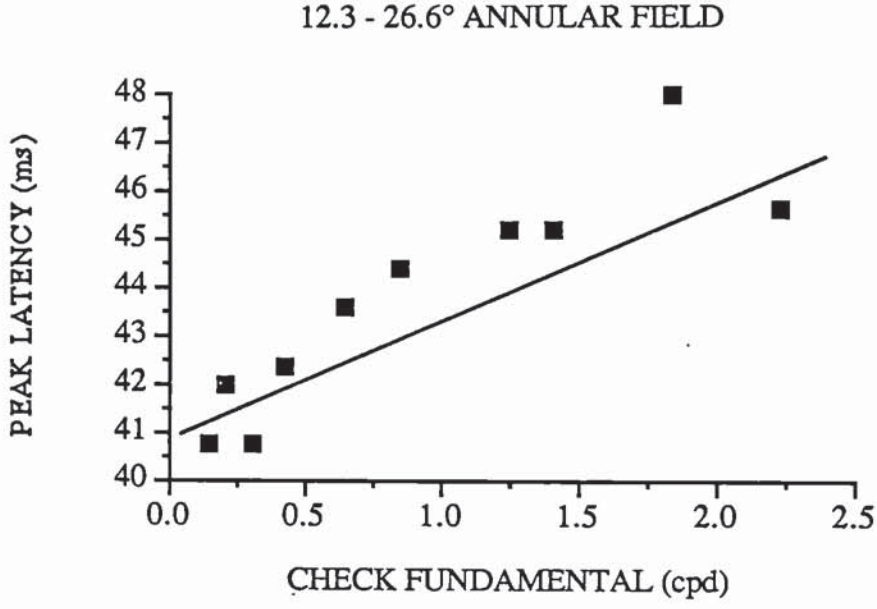

F:g 4.9 PERG onset peak latency in the peripheral zone, **y = 40.9 + 2.33 x,** r = 0.6; df 1, 38 p = .00004

If the gradients of regression equations are compared an increase in implicit time with higher spatial frequency is most noticeable in the peripheral zone. Also it appears that the implicit time of the response tends to become earlier with increasing eccentricity. However there are insufficient corresponding spatial frequencies in each zone to allow statistical analysis of this trend.

4.4 DISCUSSION

The morphology of the PERG waveform alters with eccentricity; figs 4.3 and 4.4. In the central zone at lower spatial frequencies the positive transient of the onset response is much smaller than the negative transient. A greater amplitude negative transient in the PERG recorded from the central retina has also been noted in pattern reversal studies (Berninger and Schuurmans 1985). Berninger and Schuurmans (1985) suggest the tuning of the negative transient relates to a ganglion cell response as does Holder (1987). The negative transient of the flash ERG was identified as the 'afterpotential' by Armington (1974) (section 2.3). Armington's (1974) investigations of the flash ERG also report a difference in waveform morphology in the central compared with peripheral retina. He suggests this afterpotential reflects the same processes as the a-wave or PIII and has related its magnitude to the concentration of cones in the central retina. The falling phase of the PERG may however reflect proximal K_o^+ effluxes discussed in earlier chapters or the 'slow' PIII response (Ripps and Witkovsky 1985).

The amplitude of the onset response exceeds the offset. This observation will be explored in more detail in Chapter 6. The variation in PERG amplitude with eccentricity is surprising if the original premise of ganglion cell origin is assumed. Equal numbers of ganglion cells might be expected to result in equal amplitude responses. However the data takes no account of the relative sizes of ganglion cells in each zone and this may have caused the increased amplitude. Additionally the ganglion cells may not be the sole generators and the luminance and pattern components of the PERG demand separate consideration.

The PERG has been reported to produce linear areal summation, but over representation of the macula region (Hess and Baker 1984a). The ratio of the stimulation areas with eccentricity is 1 : 4.8 : 21.4 central to peripheral field. The peak responses in each zone have a ratio 1 : 1.9 : 2.8. Reasons for the 'macula overrepresentation' are discussed in Chapter 5.

Chequerboards would be anticipated as being a more effective stimulus than the line gratings because they more closely approximate to the ideal stimulation for a circularly arranged centre/ surround receptive field. This is not immediately apparent in the group averaged results. Both conditions show the same trend in morphology with eccentricity and both have similar amplitudes at corresponding fundamental spatial frequencies. (cf. Vaegan and Arden (1987)). However a broad band pass spatial tuning is present in the group average traces which suggests some contribution from spatially antagonistic elements.

The increased latency with higher spatial frequency could relate to the generation of slower responses by thinner neurons. Smaller soma sizes, which would be expected to respond preferentially to smaller pattern elements, are known to generate slower responses (Ikeda and Wright 1972; Kandel and James 1985; Robson 1986). Therefore responses from the central region would be anticipated to have longer implicit times than responses from the peripheral annulus (Cleland and Levick 1974). Empirically this is the case but this experiment does not allow this to be statistically verified. Alternatively the increased latency may reflect the reduced retinal stimulation caused by optical degradation of higher spatial frequencies (eg Hess and Baker 1984). Latency would thus increase as contrast is decreased. However we will subsequently see that this is not the case, (see Chapter 5).

In these results no account has been taken of the proportion of luminance response that might be expected to be contained in the PERG. Distal and proximal elements are contributing to the recorded signal and any pattern specific responses will be generated or initiated by the more proximal elements. The amplitude measures thus reflect the interaction of both pattern and luminance processes. To investigate the PERG further it is necessary to attempt to isolate any pattern specific component. To achieve this the effect of optical degradation on the retinal image has been calculated.

4.5 DEVELOPED TECHNIQUE of PERG ANALYSIS

A pattern response might be expected to depend on the spatial contrast of the stimulus as well as its spatial frequency. A luminance response on the other hand would be expected to depend on the temporal contrast of the stimulation and to be insensitive to spatial frequency. It is known that the retinal contrast is reduced at higher spatial frequencies because of optical degradation (Charman 1983). The amount of contrast attenuation is described by the eye's modulation transfer function (MTF) and will vary according to the size of the pupil (Campbell and Gubisch 1966).

Attempts to measure the eye's modulation transfer function have been made psychophysically using sinusoidal interference fringes produced by laser optics. The coherence of the monochromatic laser light means that the contrast of the fringes is independent of most optical defects (Campbell and Green 1965). By comparing the subjectively matched contrast of sine wave gratings imaged on the retina in the usual way with laser interference fringes, the contrast decrease caused by the optics alone can be deduced.

An alternative method that employs 'polychromatic' white light is to directly measure the fundal reflection of a line source (Flamant 1955). These measurements combine the effects of optical imaging and retinal stray light. Campbell and Gubisch (1966) have used this technique to estimate the MTFs of three subjects for six different pupil sizes. They make a correction for the double traverse of the light through the eye and their data has been generally accepted as the best available (Westheimer 1985). Using a model suggested by Johnson (1973) for measuring the MTF of photo-electric devices the data of Campbell and Gubisch (1966) for a 5mm pupil has been described by a two parameter equation of the form:

$$MTF = \exp - [\, f / \, f_c \,]^{n}$$

where f is spatial frequency, f_c is the frequency constant and n is the MTF index. In the case of a 4.9 mm pupil this equation becomes:

$$MTF = \exp - [\, f / 8.4 \,]^{0.8}$$

The major ocular aberrations are diffraction, spherical aberration and chromatic aberration; all of which depend on the pupil size. The eye is very nearly diffraction limited in monochromatic light for pupil diameters ≤ 2.0 mm (Campbell and Gubisch 1966). The Stiles Crawford (S-C) effect relates the luminous efficiency of a light beam to the position of the entrance pupil in the eye (van Blokland 1986). This is widely accepted to be a consequence of the directional sensitivity of cones particularly in the fovea. The effectivity of incident light is reduced if it strikes a cone obliquely (Le Grand 1968). The S-C effect thus diminishes the influence of aberrations or scattered light.

The optically derived MTF taken from the data of Campbell and Gubisch (1966) might overestimate the attenuation of retinal contrast because of S-C apodization. However recent evidence suggests that reflected retinal light varies in intensity with its position in the pupil in roughly the same manner as the S-C effect (van Blokland 1986). Thus the optically derived MTF may in fact represent an underestimate which will partly counterbalance the S-C effect (Deeley and Drasdo 1987). In addition theoretical calculations by van Meeteren (1974) imply that S-C apodization can be neglected at small pupil sizes and has slight effect on aberration at larger pupil sizes.

The most powerful descriptions of ocular images that adequately include all sources of image degradation are based on the actual distribution of retinal irradiance (Charman 1983). Every point source is imaged as a patch of light of finite distribution called a point spread function. More practically a line spread function is used. The Fourier transform of a line produces a spatial frequency spectrum, each spatial frequency attenuated by the optical transfer function. The Fourier transform of the line spread function therefore yields the optical transfer function. In principle the image of any object can be determined by taking the Fourier transform of its irradiance distribution to obtain its spatial frequency spectrum. Each spatial frequency is then multiplied by the optical transfer function to yield the image spectrum. The inverse Fourier transform will then give the image irradiance distribution (Charman 1983).

In order to assess the retinal contrast of the stimuli employed in this study the Fourier components of square wave gratings and chequerboard patterns have been filtered by the eye's MTF. The mean pupil diameter of the participant subjects was approximately 5 mm. Therefore the data of Campbell and Gubisch (1966) describing a 4.9 mm pupil were used.

The one dimensional array of the square wave data is described by the expression:

$$E_d = E_m + \frac{4I}{\pi}\left[\cos d - 1/3 \cos 3d + 1/5 \cos 5d - 1/7 \cos 7d \ldots\right]$$

where E_m is the mean luminance, I is the mean of the extreme deviations in light intensity and d is the width of a grating/ bar at 90° to its long axis in radians

The two dimensional Fourier transform of the unattenuated chequerboard has been described by Kelly (1976) and may be expressed by the following equation:

$$E(x,y) = E_m + \frac{8}{\pi^2} \sum_{m,n=0}^{\infty} \frac{(-1)^{m+n}}{\beta_m \beta_n} \left[\cos\left[\frac{\pi}{L}(\beta_m x + \beta_n y)\right] + \cos\left[\frac{\pi}{L}(\beta_m x - \beta_n y)\right]\right]$$

where E_m is the mean luminance, L is side length of check with x and y axes parallel to the edges and $\beta_m = 2m+1$

The MTF in a suitable form for filtering this equation is:

$$b_{mn} = \exp\left[-\frac{\sqrt{(\beta_m^2 + \beta_n^2)}\, 0.8}{16.8\ L}\right]$$

where b_{mn} is the amplitude attenuating factor for the m,n harmonic

The expression: $\cos\left[\frac{\pi}{L}(\beta_m x \pm \beta_n y)\right]$

describes the unidirectional harmonic components. Each component has a spatial frequency F, of the form:

$$F_{m,n} = \frac{\sqrt{(\beta_m^2 + \beta_n^2)}}{2L}$$

The reader is referred to Drasdo and Cox (1987) for further mathematical details of the procedure and nomenclature of the above formula. The filtering procedure was carried out for all stimulus spatial frequencies used in the study. The Fourier components

were filtered up to the 100th harmonic in the first instance. However little significant alteration was noticed after the 20th harmonic of the chequerboard had been filtered and this was subsequently adopted as an end point. The filtered components were then resynthesised to compose a retinal illuminance profile of the stimulus image. This is shown for both square wave gratings and checkerboards in Figures 4.10, 4.11.

It is now possible to calculate the effective retinal contrast of each stimulus from its retinal illuminance profile. Spatial contrast is specified most usually by the Michelson equation (1891) originally devised for sinusoidal waveforms, but is currently used for all types of spatially repetitive stimulus (Westheimer 1985). A similar formula is used to describe temporal contrast (De Lange 1958).

Spatial contrast depends on illuminance levels at different points in space at the same time; using the same formula temporal contrast applies to the same point at different times. It is of interest that according to this definition the temporal contrast at every point on a phase reversing pattern is equal to the spatial contrast of the pattern. However the temporal contrast during onset-offset stimulation is not related to the spatial contrast by a fixed ratio.

The appearance of a black square from a mean background results in three times the contrast change produced by the appearance of the corresponding white square at 100% modulation. Thus the proportional contrast change is 3:1, black to white. This is illustrated schematically by the spatial cycle of luminance in the pattern, (Figure 4.12). As the initial stimulus contrast is reduced towards the mean value the difference between the two presentation modes gradually approaches 50%.

To specify the temporal contrast in the onset /offset mode of stimulation it is thus necessary to take an average value. When the retinal image is degraded this is even more obviously necessary since the temporal contrast varies at many different points

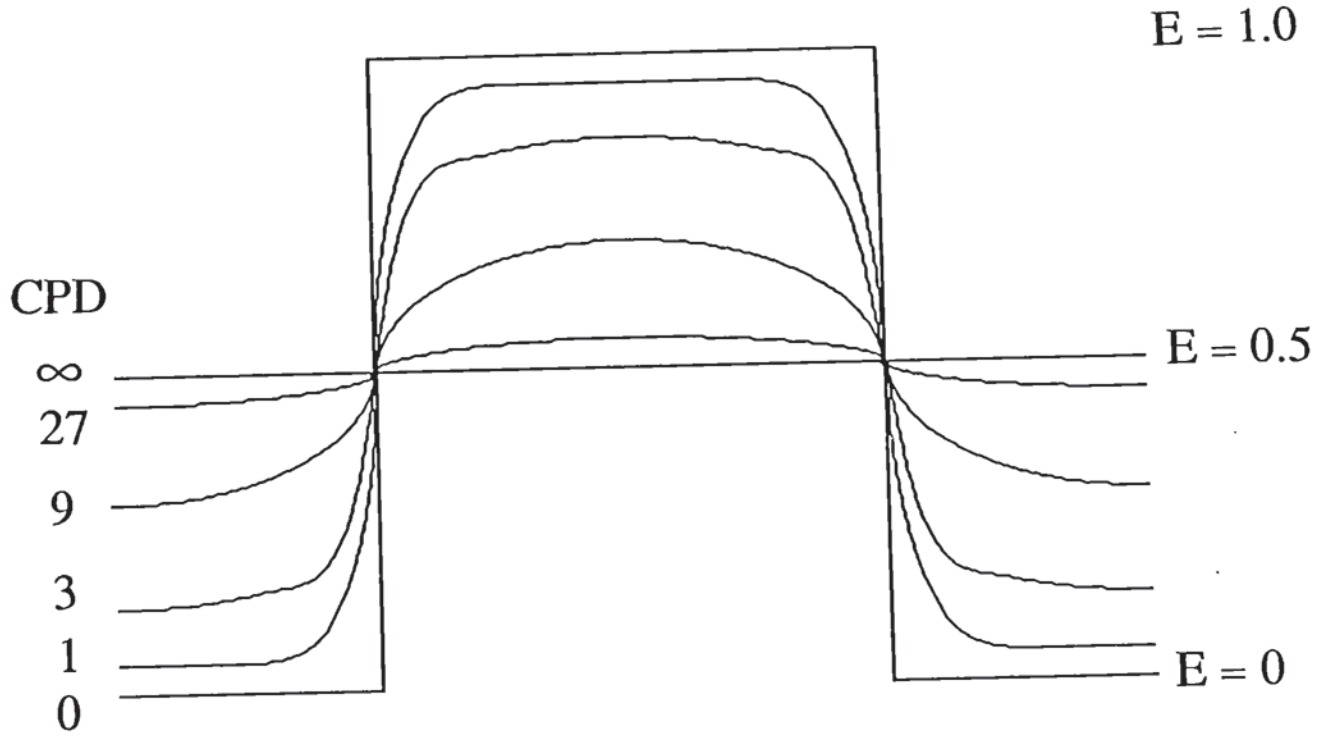

Fig 4.10 Diagrammatic representation of the retinal illuminance profile of a one-dimensional square wave grating, over one spatially normalised cycle. Spatial frequency (cpd) is indicated adjacent to each profile and E represents the normalised retinal illuminance

Fig 4.11 Schematic three dimensional representation of the retinal illuminance profile for chequerboard patterns. This is shown for checks of ≈ 2', 10' and 50' arc angular subtense in descending order. The distribution is shown for a white and black element above and below the mean level; where maximum < +1, mean = 0 and minimum > -1. The peak and trough values of illuminance are shown with illuminance contours at 1/3 and 2/3 levels over a spatially normalised cycle. [after Drasdo and Cox 1987]

on a spatially repetitive element of the pattern. The resulting value computed by integration is referred to as space averaged temporal contrast.

Fig 4.12. The bold line represents the intial stimulus profile which changes to the fine line situation following reversal and onset presentation.Three luminance levels are shown, the mean level being 0.5.The spatial contrast (SC) is determined by the maximum and minimum luminances, 0 and 1, indicated by a light and dark element and is the same in both conditions. Temporal contrast only equals spatial contrast in the pattern reversal mode of presentation. This does not occur in the pattern onset condition. (after Drasdo, Cox and Thompson 1987).

The attenuation in space averaged temporal contrast calculated from the degraded retinal image profile of each square wave and chequerboard pattern employed is graphically illustrated in Figure 4.13 for pattern onset presentation of 75% stimulus contrast (defined by the Michelson equation.).

If the retinal responses to pattern stimuli of low spatial frequency are linearly related to stimulus contrast as has been reported in several studies (e.g. Arden and Vaegan 1982; Hess and Baker 1984; Korth et al 1985) the proportion of the response that is due to luminance processing might be computed from the retinal space averaged temporal contrast for a particular stimulus condition. Thus a luminance generated response may be expected to vary in amplitude in a manner described by the MTF i.e. a low pass function.

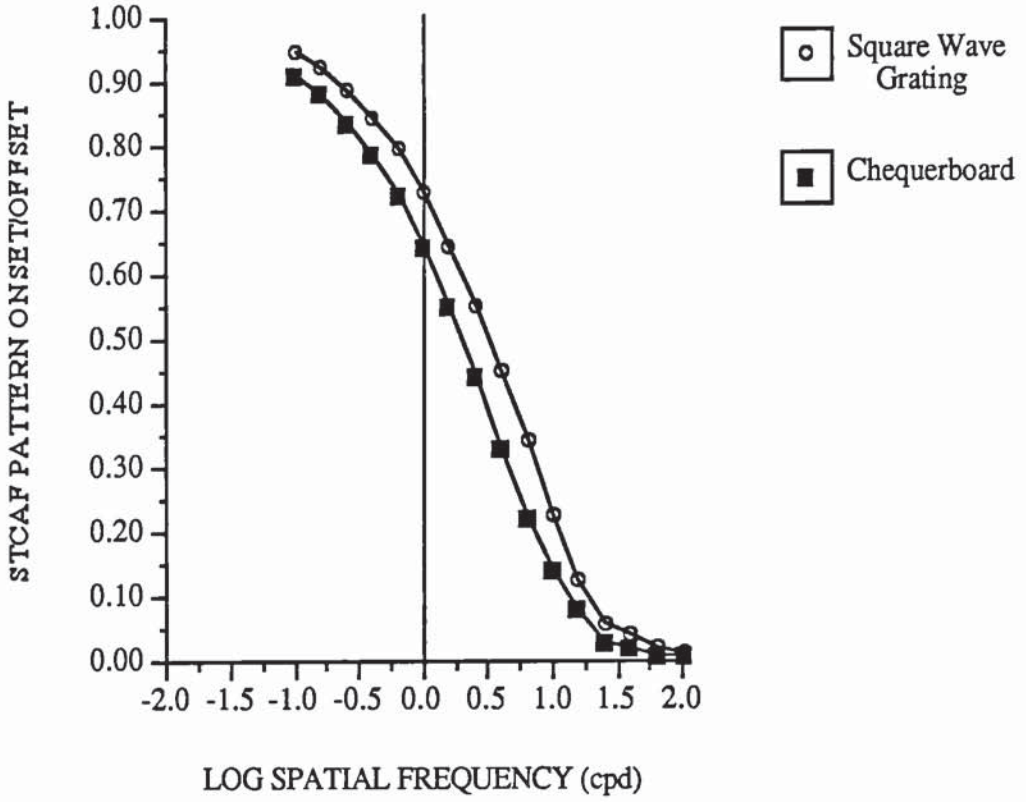

Fig 4.13. Graph illustrating the normalised space averaged temporal contrast attenuation factors, STCAF, for square wave gratings and chequerboards of 75% stimulus contrast presented in a pattern onset-offset mode. (N.B. the spatial frequency refers to the check side not the fundamental).

This data has been used to determine the proportion of PERG that might be expected from luminance processing. To this end the lowest spatial frequency in each stimulus zone, assumed representative of a luminance response in amplitude and morphology, has been attenuated by the space averaged temporal contrast attenuation factor appropriate for each spatial frequency. The computed retinal illuminance responses (RIR) have been subtracted from the group averaged responses and the resultant waveform is assumed to represent additional processing in the retina due to pattern specific responses. Examples of this process applied to the results obtained with line grating stimuli from each stimulus zone are shown in figures 4.14, 4.15 and 4.16. The extracted pattern specific response has a necessarily enhanced bandpass tuning which occurs at higher spatial frequency with increasing peripheral angle.

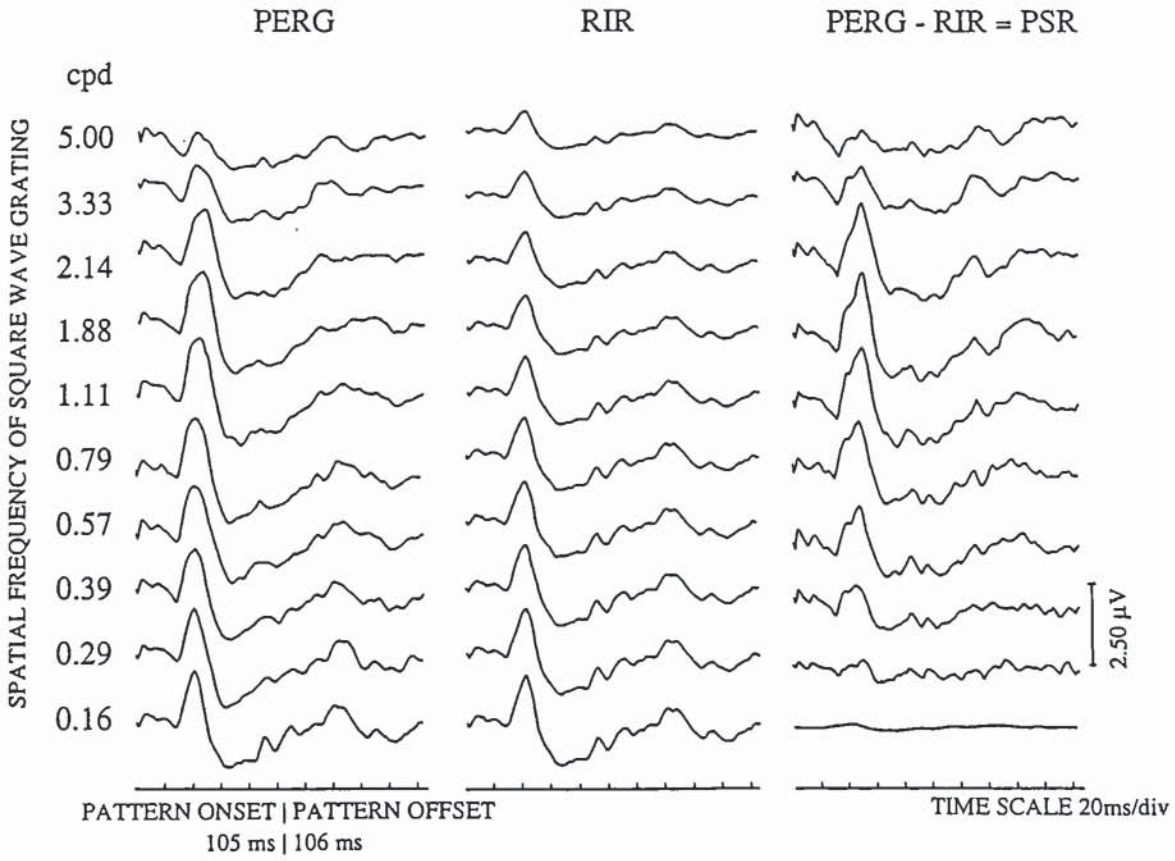

Fig.4.14 The computed retinal illuminance responses, RIR, for the grating spatial frequencies presented in the most peripheral annular field are shown in the second column. The result of the subtraction from the group averaged PERG is displayed in the third column. This represents the pattern specific response PSR.

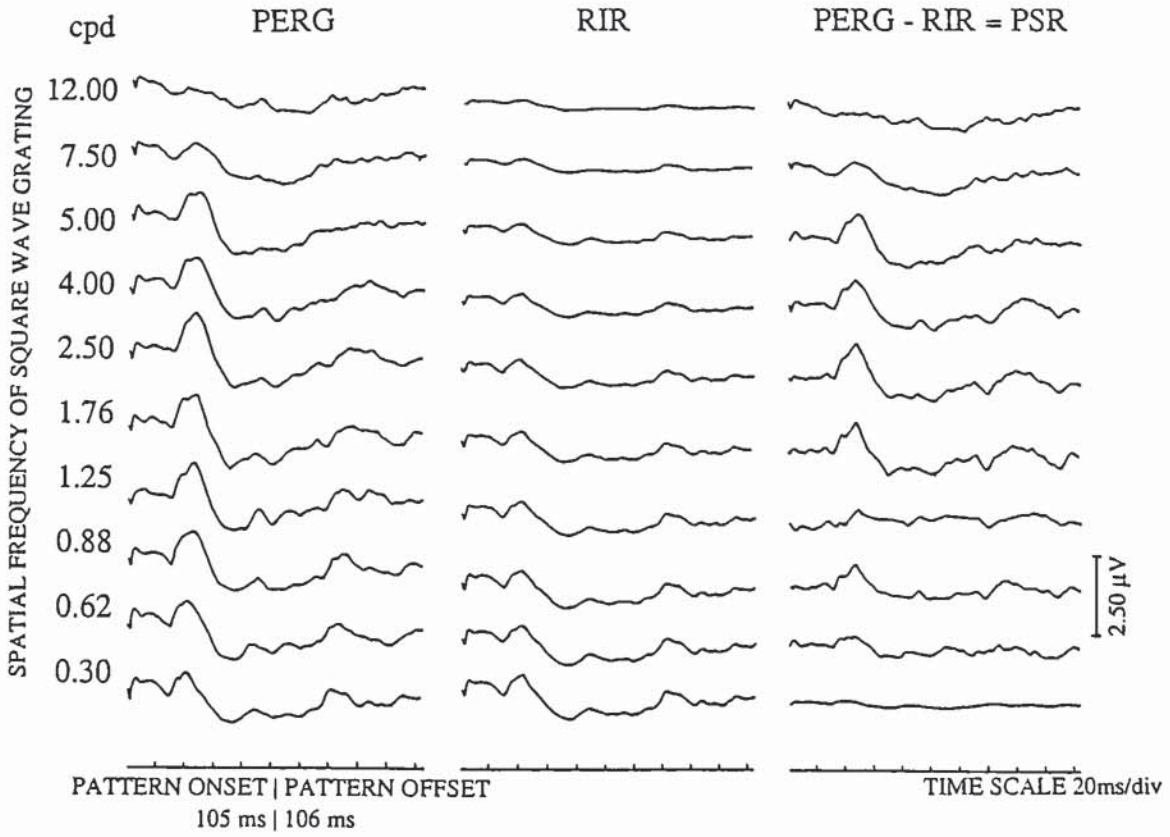

Fig 4.15 The computed retinal illuminance responses, RIR, for the bar grating spatial frequencies presented in the 5.6 -12.6° annular field are shown in the second column. The result of the subtraction from the group averaged PERG is displayed in the third column. This represents the pattern specific response PSR.

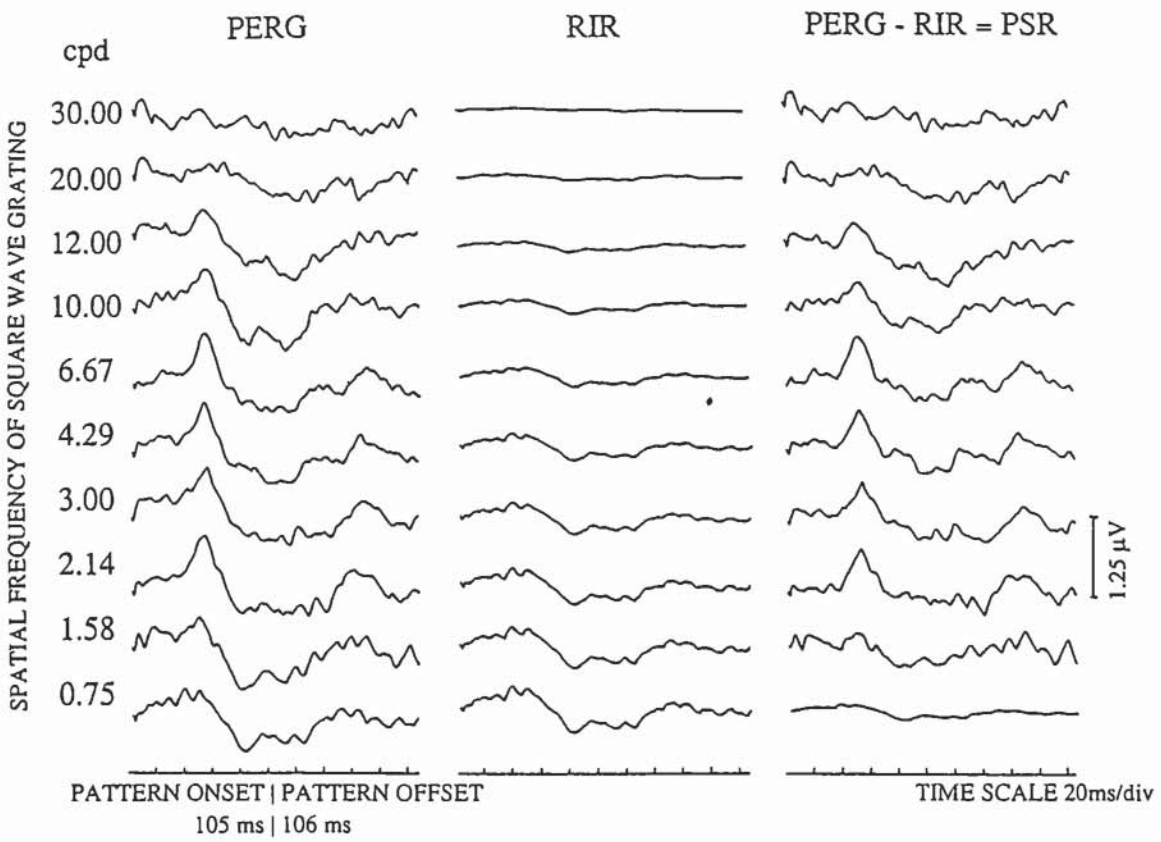

Fig 4.16 The computed retinal illuminance responses, RIR, for the bar grating spatial frequencies presented in the central field are shown in the second column. The result of the subtraction from the group averaged PERG is displayed in the third column. This represents the pattern specific response PSR.

Figures 4.17 and 4.18 show the measured -ve and +ve peak to peak amplitudes of the pattern specific response recorded to square wave gratings.

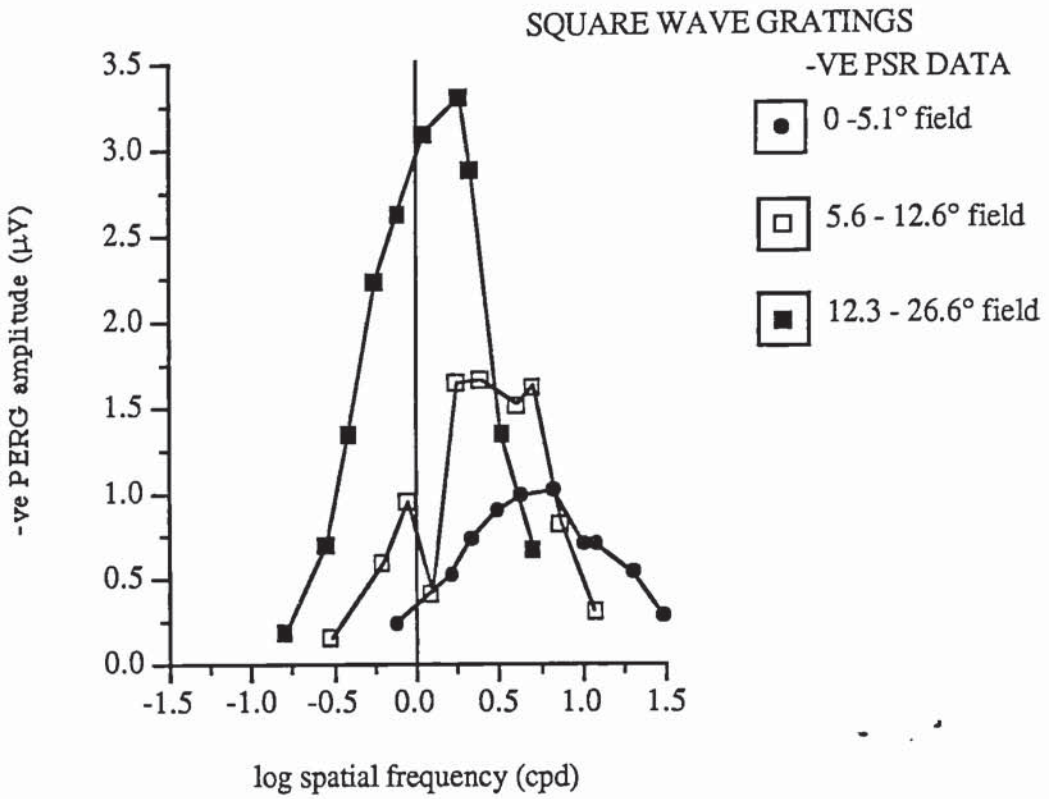

Fig 4.17 Graph showing -ve PSR amplitude as a function of square wave spatial frequency in the three stimulus zones. The smaller amplitude responses from the central field peak at higher spatial frequency than those from the more peripheral fields

4.5 DISCUSSION AND CONCLUSIONS

Therefore it appears possible to isolate a pattern specific response from the retinal response to pattern stimulation if the optical properties of the eye are considered. The eye's MTF used in the calculation makes no provision of the phase transfer function. The only data available suggests this is very variable inter individual and thus in group averaged data may have minimal effect (Jennings and Charman 1981).

The analysis technique rests on a number of assumptions. The computation of the expected response to illuminance processing relies on the presence of a linear relationship with temporal contrast. This has been inferred from the data of other workers with stimulus spatial contrast, but not under our conditions specifically for

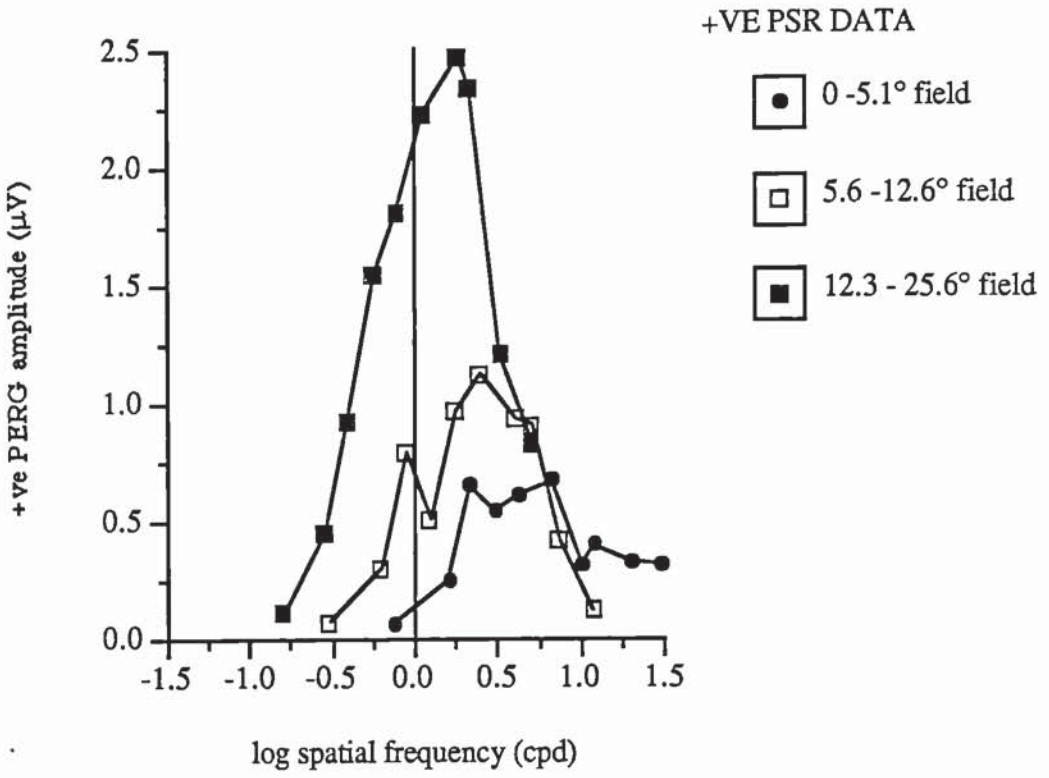

Fig 4.18 Graph showing corresponding +ve PSR data for the three stimulus fields as a function of spatial frequency.

temporal contrast. In addition the subtraction has been carried out at fixed latency; there is little available data regarding the latency variation with contrast.

This preliminary data suggests the spatial characteristics of the pattern specific response vary across the retina in a manner that indicates the participation of smaller receptive field generators in the central region. This is compatible with known retinal anatomy and physiology (e.g. section 1.4 Ganglion cells). However the PSR described here does not represent an iso-contrast response; optical degradation also reduces the spatial contrast of the retinal image. A further correction factor might therefore be applicable before the amplitude of the PSR may be correlated with retinal cell populations. A further study was therefore designed to examine the assumptions made with respect to PERG behaviour with contrast.

CHAPTER 5.

THE PERG AND CONTRAST

5.1 INTRODUCTION

The analysis technique developed in Chapter 4 regards the retinal response evoked by a patterned stimulus as a composite of illuminance and pattern specific responses: the proportion of each component varies according to the spatial frequency of the stimulating pattern. An illuminance response would be spatially insensitive and depend on temporal modulations of local luminance ie. the temporal contrast of stimulation. A pattern specific response would be expected to vary with the spatial contrast and spatial frequency of the patterned stimulus.

The proposed method of analysis makes two assumptions about the behaviour of the PERG with contrast level; that the amplitude of a PERG evoked by a low spatial frequency pattern varies linearly with the temporal contrast of the retinal image and the implicit time of the response does not alter with contrast level.

This study therefore set out to establish the relationship between retinal contrast and the amplitude of the pattern onset ERGs evoked by different spatial frequencies and to also examine any variation of peak response latency with contrast level. The consensus of previous investigations indicates a linear relationship between PERG amplitude and the spatial contrast of the stimulus (Arden & Vaegan 1983, Hess & Baker 1984a, using pattern reversal stimulation; Korth and Rix 1983 using pattern onset / offset stimulation).

Attempts were made to construct photographic slides of different contrast using double exposure photographic techniques. However it proved difficult to maintain an accurate mean luminance level and this method was eventually abandoned. A simple method of altering contrast was then attempted using neutral density filters in the light path of the

projector. Again the steps of filter used were difficult to balance and only produced a small range of contrasts and the heat of the projector eventually altered the quality of the interposing filter which in turn affected the quality of the screen image. The inevitable hot spot obtained with back projection optical stimulators also confounded the measurement of contrast over a wide field which is necessary to obtain a measurable signal at low contrast. Thus it was appropriate to use a television monitor driven by a function generator to display achromatic checkerboards. In all these experiments contrast levels have been defined by the Michelson equation;

$$\text{Contrast} = (L_{max} - L_{min}) / (L_{max} + L_{min}),$$

where L is the luminance of the stimulus.

5.2 METHOD

Pattern onset / offset ERGs (PERGs) were recorded to black and white chequerboard stimuli. The chequerboard was presented for 140 ms followed by a blank screen of mean luminance for 120 ms. The mean screen luminance matched the surround luminance at 100 cdm^{-2}. Luminance levels were measured by a spot photometer. The black and white chequerboard was produced by a TV monitor connected to an IOL generator which had been modified to include an independent fine control of mean luminance. Great care was taken to maintain a constant mean luminance level; thus any alteration in response amplitude was not confounded by decreases in mean luminance. The monitor operated at 100 Hz refresh rate as described by Arden et al (1982).

The PERGs were recorded binocularly from 10 subjects using a DTL electrode applied to the cornea referred to an EEG Ag cup electrode positioned on the ipsilateral temple close to the outer canthus. An EEG Ag cup electrode placed on the forehead acted as a ground. Spectacle prescriptions were worn as necessary. All subjects had R &L visual acuities of 6/6, were orthophoric at the test distance and were capable of steady fixation. The signals were recorded on a Nicolet Pathfinder II averager and stored for later analysis. The bandpass filters were set at 0.5-50 Hz. The timebase was 250ms

and 200 averages were recorded from each subject for each stimulus condition. The circular stimulus field subtended 15 degrees in diameter. The check sides subtended 10', 30' and 7°30'; the lowest spatial frequency effectively divided the stimulus field into quadrants. Five stimulus contrast levels of 13%, 30%, 50%, 65% and 80% were used.

5.3 RESULTS

5.3.1 Amplitude variation with contrast

The *group averaged* responses of 10 subjects (20 eyes) for each stimulus condition are displayed in Fig. 5.1. Direct inspection shows the onset response is smaller than the offset at the low spatial frequency used, whilst the reverse is true for the response to the 10' checks [cf Korth and Rix (1983); Arden and Vaegan (1983)]. Indeed the responses illustrate a low spatial frequency attenuation when the amplitudes of these two onset responses are compared; measuring the negative going transient of the 80% contrast response = 1.37 μV for the 10" check cf 0.74 μV for the 7° 30" check, a difference of more than 4 sem.

The amplitude of the negative going transient of the *group averaged* onset response has been plotted as a function of stimulus contrast for each spatial frequency and straight lines have been fitted by linear regression techniques. (Fig. 5.2, 5.3 and 5.4). Each is significant at the $p \leq 0.01$ level. The slope of the function steepens as the spatial frequency increases, (this is more noticeable when the results are analysed as a function of temporal contrast, see p.132.) which again illustrates the low spatial frequency attenuation.

The positive transient amplitude of the *group averaged onset* data was also well fitted by the method of least squares:

10' check: $y = 0.015x + 0.186$, $r=0.96$; df 1,3; $p=0.011$

30' check: $y = 0.018x - 0.118$, $r=0.97$; df 1,3; $p=0.005$

7°30' check: $y = 0.01x - 0.044$, $r=0.899$; df 1,3; $p=0.044$

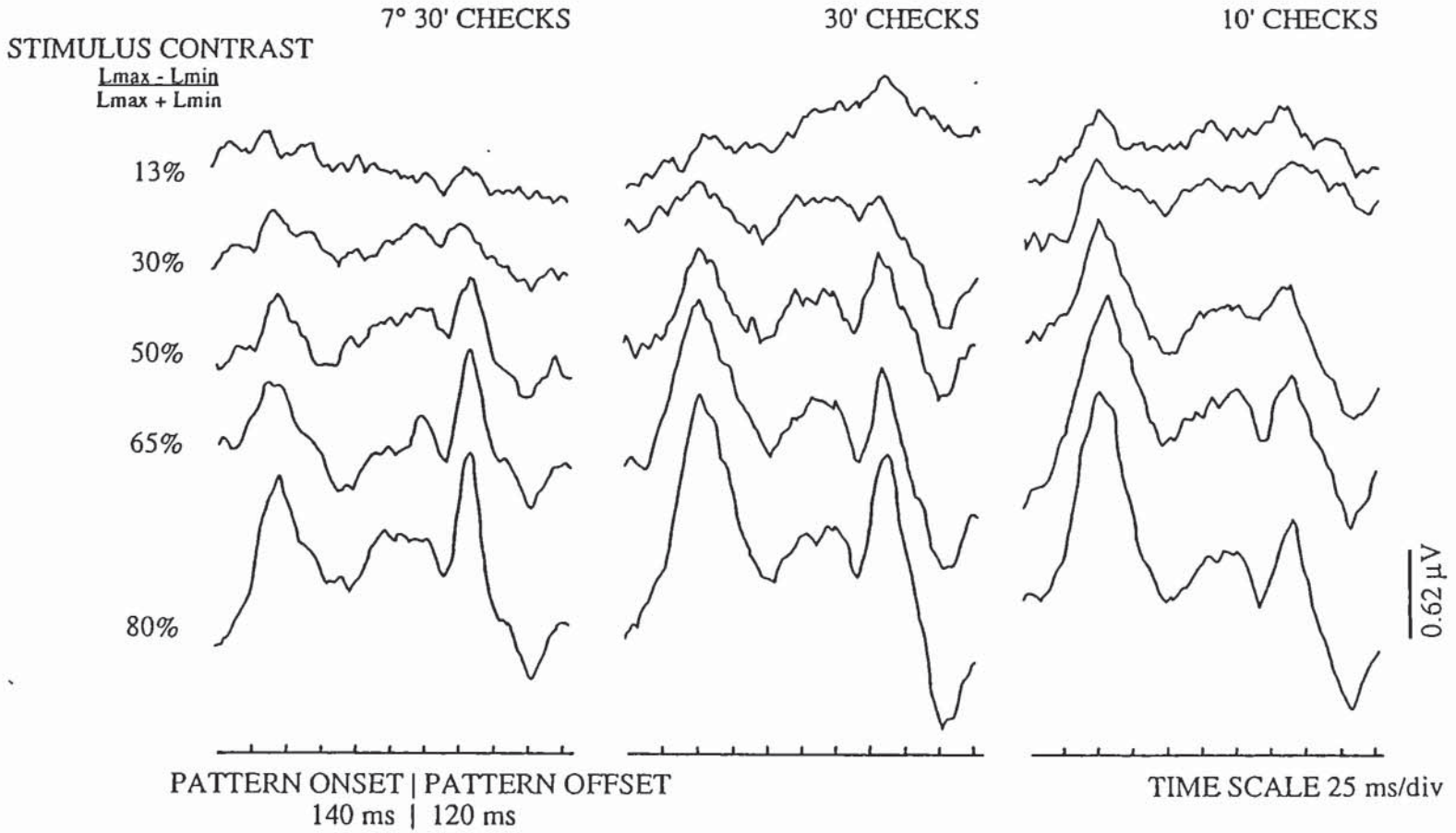

Fig 5.1 Group averaged PERG waveforms (n=10), recorded to three different check sizes presented at a range of stimulus contrasts defined by the Michelson equation.

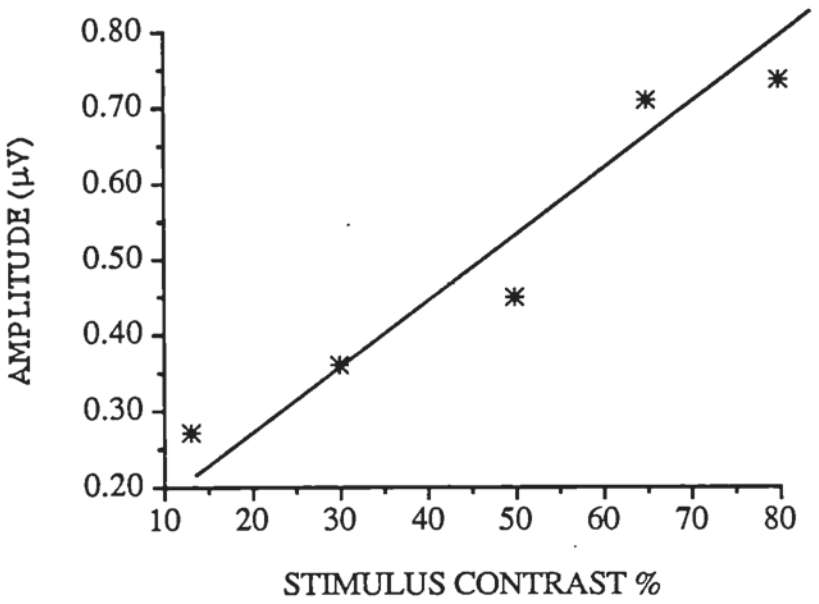

Fig 5.2 The negative transient amplitude of the PERG evoked by the onset of a 7° 30' check pattern is displayed as a function of stimulus contrast:
y = 0.008x + 0.145, r = 0.97; df 1,3; p= 0.007

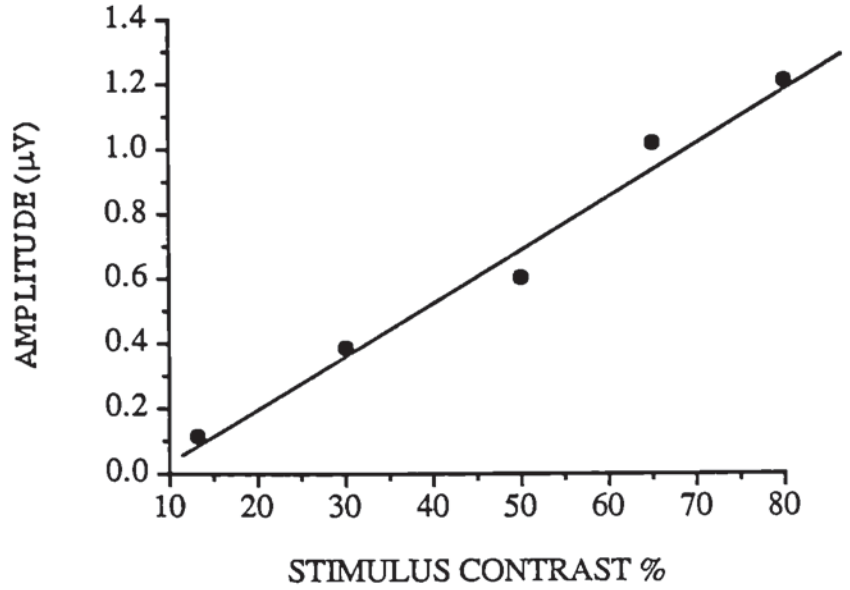

Fig 5.3 Solid symbols show the amplitude of the -ve PERG evoked by the appearance of a 30' check pattern as a function of stimulus contrast. A straight line was fitted by linear regression:
y = 0.017 x - 0.124, r = 0.99; df 1,3; p = 0.001

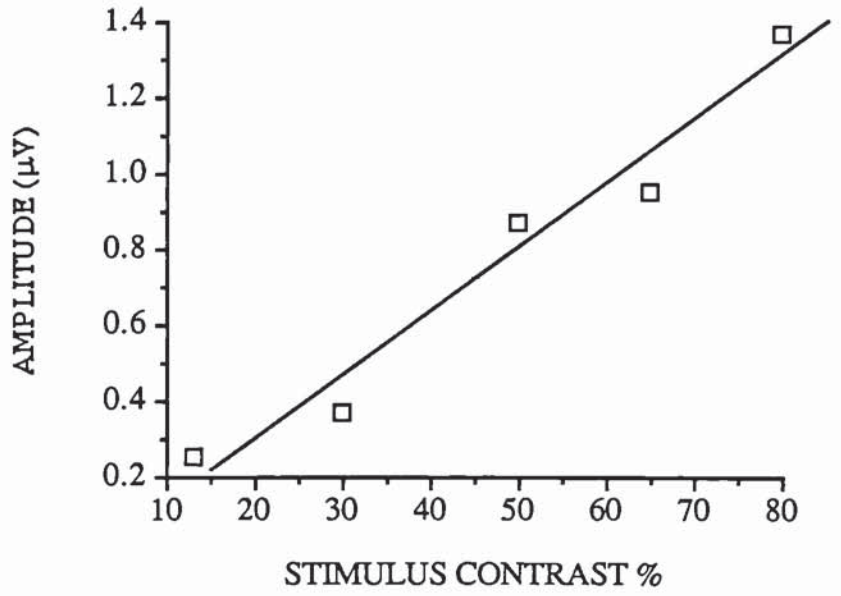

Fig 5.4 The open symbols describe the negative transient amplitude of the PERG evoked by the onset of a 10' chequerboard:
y = 0.17 x - 0.026, r = 0.98; df 1,3; p = 0.003

The offset response measured as +ve and -ve transients is shown in Figs 5.5 & 5.6. The -ve offset transients show a linear relationship with stimulus contrast. However the +ve offset transients do not increase in amplitude until the stimulus contrast reaches 30-50%, (greater for the smaller check size). The offset response has been considered a luminance response by Korth and Rix (1983), because it failed to show spatial selectivity except at low contrast.

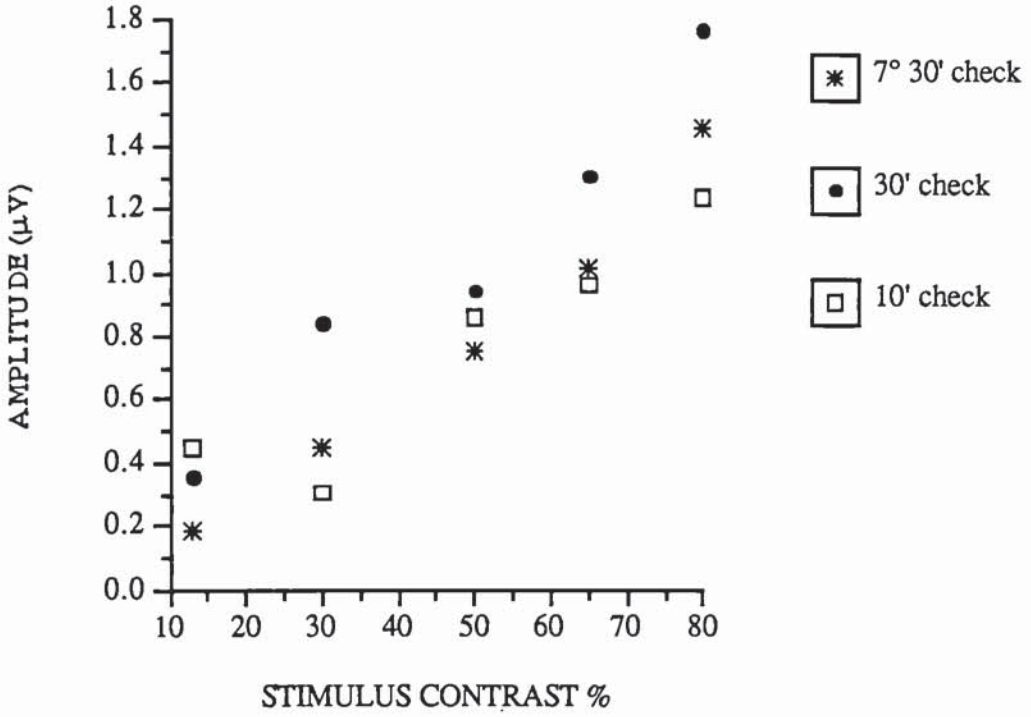

Fig 5.5 Pattern offset PERG negative transient amplitude as a function of stimulus contrast.

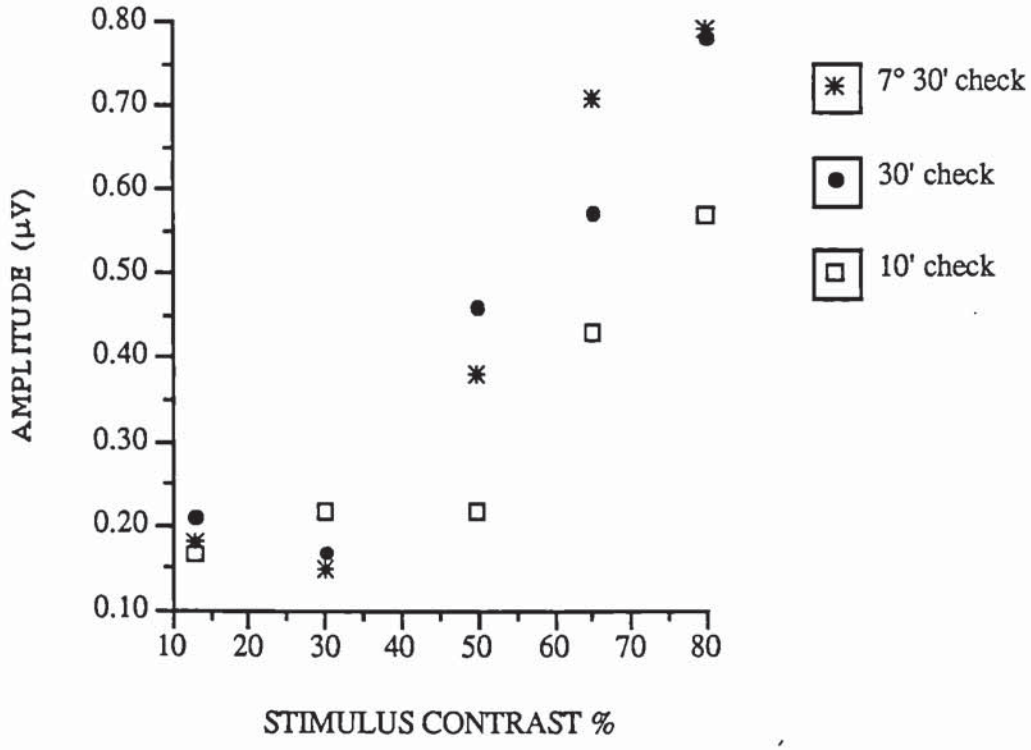

Fig 5.6 Pattern offset ERG positive transient amplitude plotted as a function of stimulus contrast for three check sizes.

3.5.2 Latency variation with contrast

No systematic variation of peak response latency with contrast could be statistically determined for any spatial frequency. The *group averaged* peak latencies have been displayed in figure 5.7. There is however an increase in PERG latency with higher spatial frequency as shown; from a mean of 43ms for a 7° 30' check to a mean of 54ms for a 10' and 30' check. This increase in latency with increasing spatial frequency has been previously reported (e.g. Arden & Vaegan 1983).

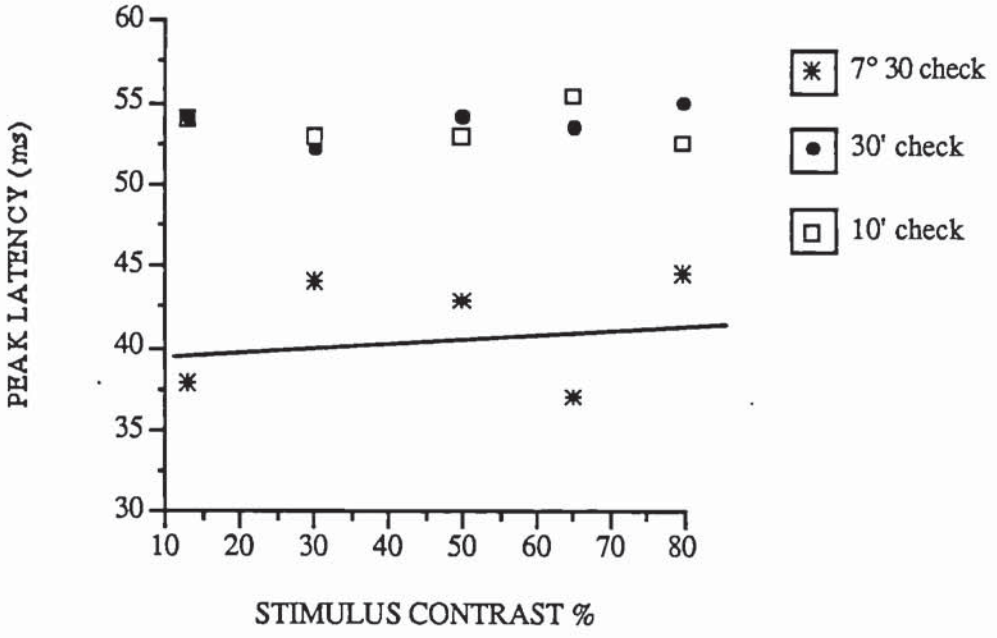

Fig. 5.7 The graph shows the *group averaged* peak latency of the onset PERG as a function of stimulus contrast for each check size.

The *group average* peak latency data shown in Fig 5.7 for the lowest spatial frequency used, 7° 30' has been fitted by linear regression.

The regression equation $y = 0.035 x + 39.65$; $r = 0.26$; df 1,3; $p = 0.67$

The *individual peak* latency data that made up the group average were also analysed and the results for the 7° 30' check are graphically displayed in Fig 5.8. This data was also fitted by linear regression techniques:

$y = - 0.048 x + 47.2$; $r = 0.144$; df 1,48; $p = 0.325$.

Thus one method of analysis yields a positive gradient, 0.035, (Fig 5.7) and the other (Fig 5.8) a negative gradient, -0.048, implying slight latency increases and decreases occur with increasing contrast respectively. However neither were statistically significant and we conclude that no systematic change in peak latency with contrast can be statistically determined.

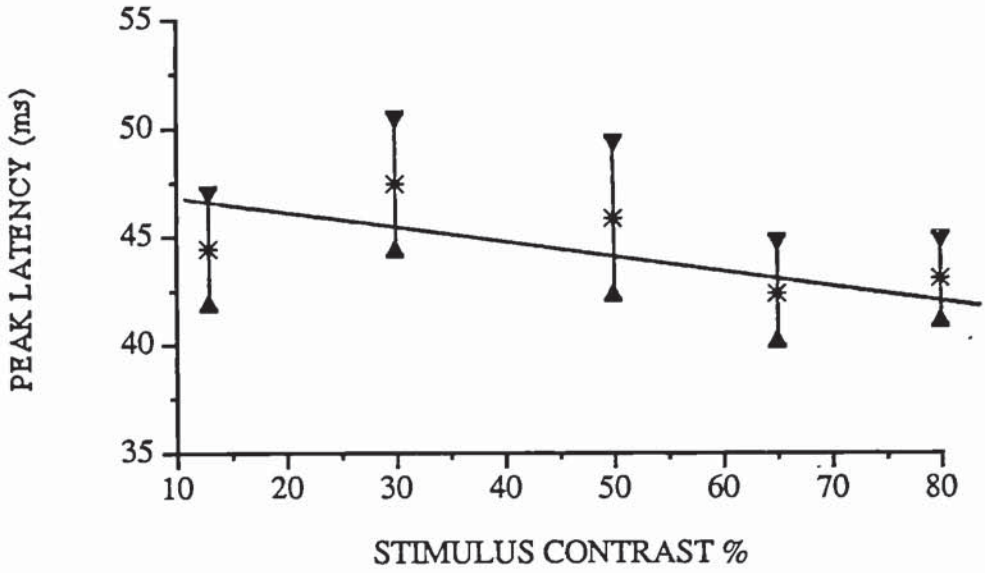

Fig 5.8 The mean of the *individual* peak latencies is shown ± 1sem as a function of stimulus contrast.

The PERG analysis technique assumes a linear relationship between temporal contrast and low spatial frequency response amplitude. The temporal contrast of each check size for each contrast level was calculated as described in the Chapter 4. and normalised to the value for a uniform field in the pattern onset condition; the values are given in tabular form in appendix 2. The responses obtained to the 7°30' chequerboard have been shown as a function of temporal contrast. The function is well described by a straight line; r= 0.97, $p < 0.01$; Figure 5.9. The regression equations for the PERG -ve transient as functions of temporal contrast were all significant at the $p \leq 0.01$ level:-

7°30': $y = 0.66x + 0.17$, **30':** $y = 2.13x - 0.092$, **10':** $y = 5.82x - 0.28$

and demonstrate a steepening gradient with increasing spatial frequency

The appropriate space averaged temporal contrast attenuation factors were applied to the 7°30' waveform for the 10' and 30' check sizes and the retinal illuminance responses RIRs computed and pattern specific responses extracted according to the method described in Chapter 4. The waveforms are shown in appendix 2.

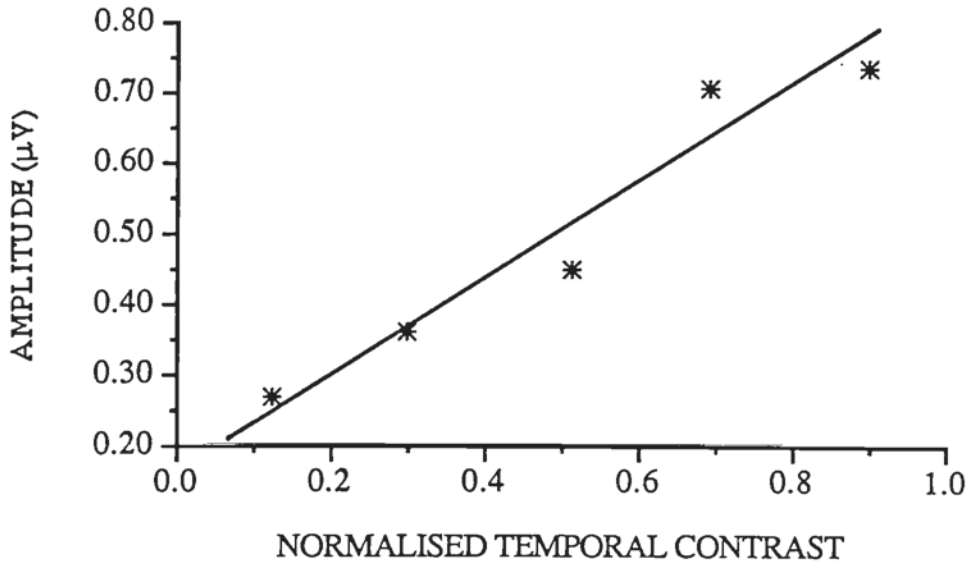

Fig 5.9 Negative transient PERG amplitude shown as a function of space averaged temporal contrast for the 7°30' check

The PSR would be expected to relate to the spatial contrast of the retinal image. The spatial contrast is also attenuated by optical degradation. However as described in Chapter 4 the retinal spatial contrast is the same as in the pattern reversal mode of stimulation and may be represented by the checks fundamental filtered by the eye's MTF. The variation of the extracted PSR amplitudes for the 10' and 30' checks were analysed as a function of effective spatial contrast at the retina. Regression analysis indicates a linear relationship:

10' check PSR : +ve transient	y=2.198 x + 0.153,	r=0.96; df1,3; p=0.01,
-ve transient	y=3.478 x + 0.015,	r= 0.92; df1,3; p=0.03
30' check PSR: +ve transient	y=1.024 x + 0.009,	r=0.91; df1,3; p=0.03,
-ve transient	y=1.383 x - 0.11,	r=0.99; df1,3; p=0.001

The inferred linear relationship with spatial contrast suggests the application of an additional correction factor is appropriate. Therefore to correct the PSR responses for any inequality in spatial contrast stimulation that arises through optical degradation the PSR signals for each spatial frequency may be multiplied by the reciprocal of effective spatial contrast. This manipulation has been carried out on PERG data previously reported in Chapter 4 in response to chequerboard patterns. Figures 5.10, 5.11 and 5.12.

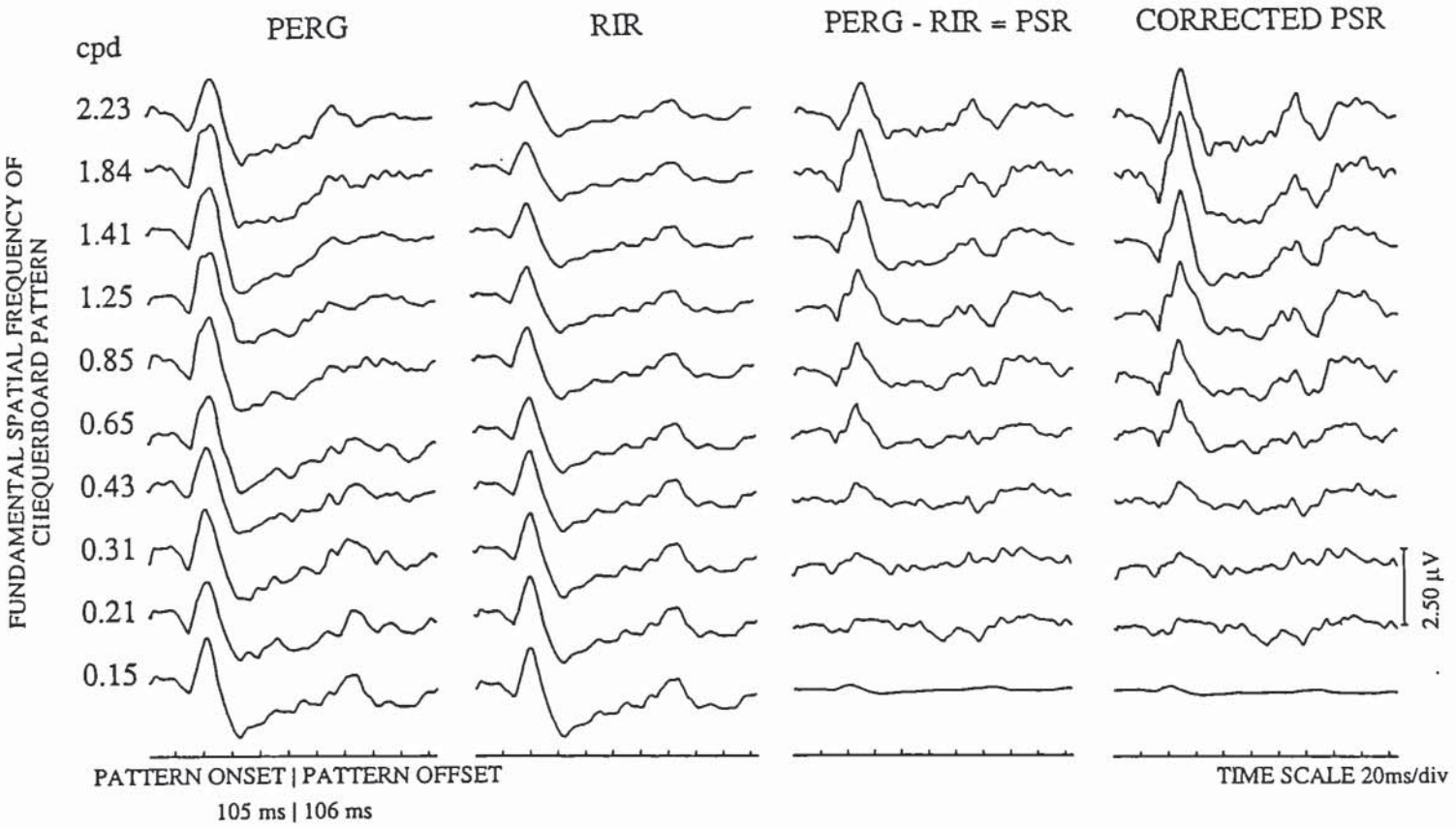

Fig 5.10 The computed retinal illuminance responses, RIR, for the fundamental chequerboard spatial frequencies presented in the 12.3 - 25.6 ° annular field are shown in the second column. The result of the subtraction from the group averaged PERG is displayed in the third column. This represents the pattern specific response, PSR. The fourth column shows the 'iso-contrast' PSR corrected for spatial contrast attenuation.

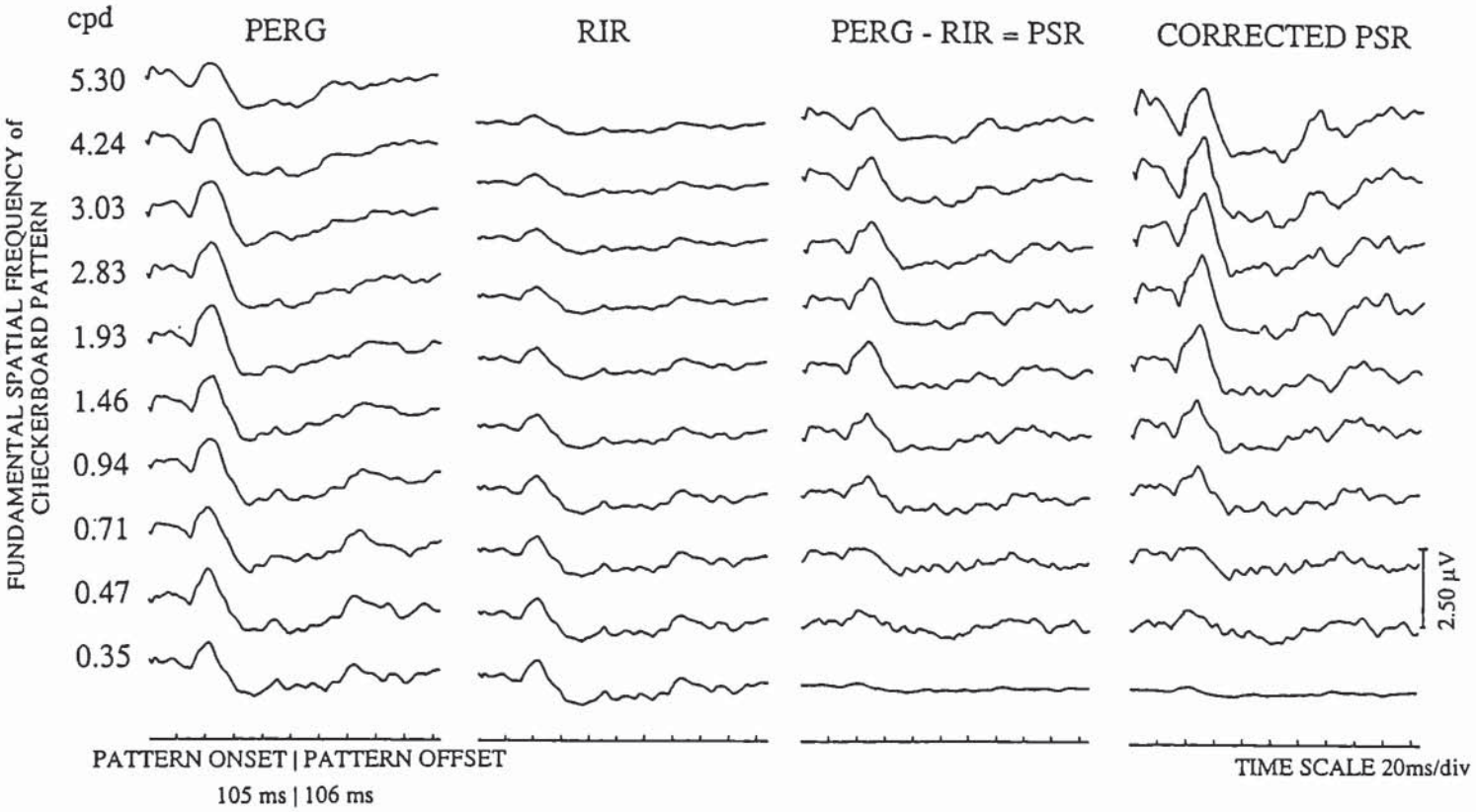

Fig 5.11 As in Fig 5.10, but for the 5.6 - 12.6° annular field, computed retinal illuminance responses, RIR, for the fundamental chequerboard spatial frequencies presented in this zone are shown in the second column. The result of the subtraction from the group averaged PERG the pattern specific response, PSR, is displayed in the third column. The fourth column shows the 'iso-contrast' PSR corrected for spatial contrast attenuation.

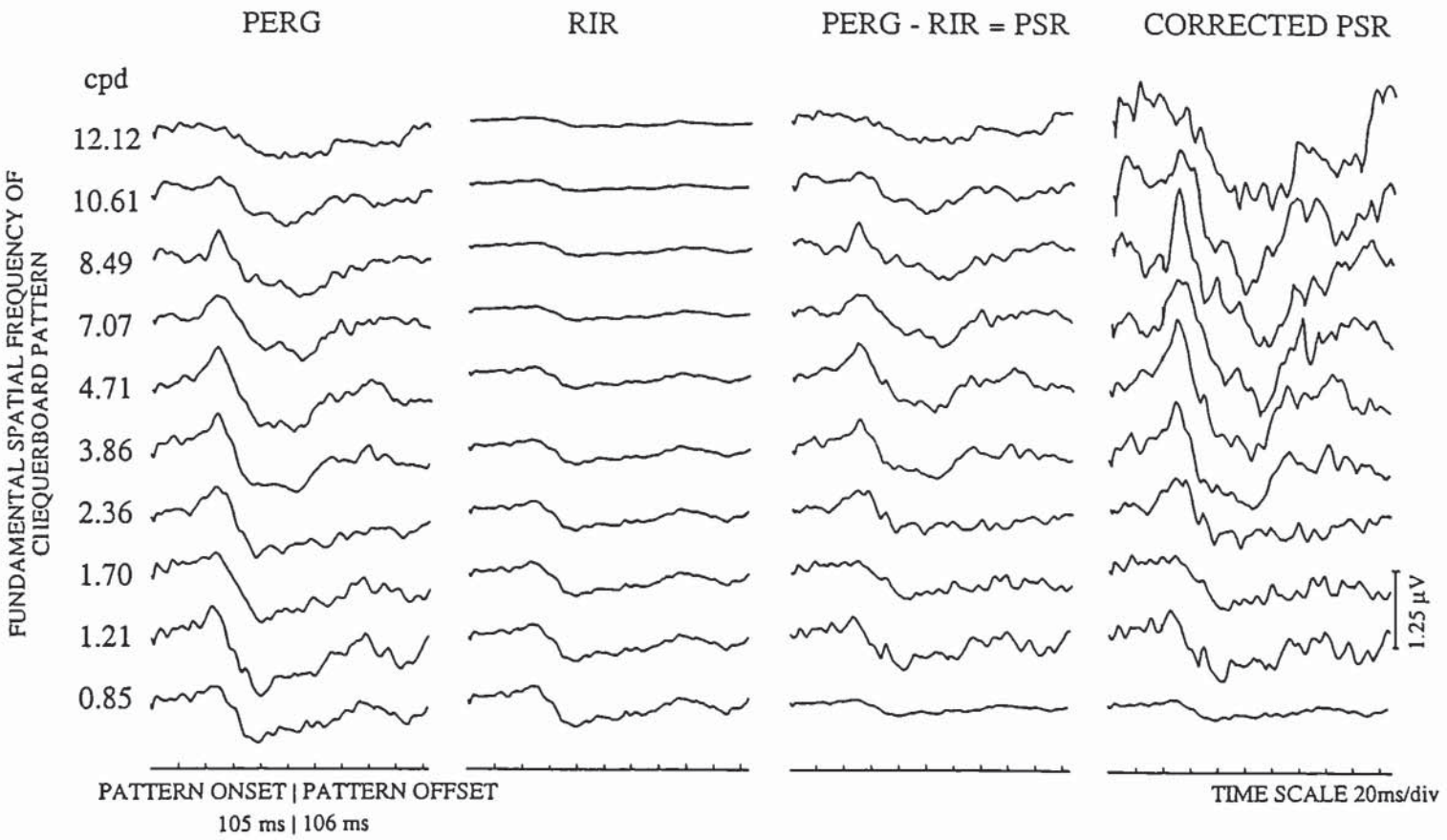

Fig 5.12 As in Fig 5.10, but for the 0 -5.1° central field, computed retinal illuminance responses, RIR, for the fundamental chequerboard spatial frequencies are shown in the second column. The pattern specific response, PSR, that results from the subtraction of the RIR from the group averaged PERG is displayed in the third column. The fourth column shows the 'iso-contrast' PSR corrected for spatial contrast attenuation.

5.4 THE CORRECTED PATTERN SPECIFIC RESPONSE

The negative transients of the corrected PSR waveforms are shown in Fig 5.13 as a function of fundamental check spatial frequency for each zone and the curves fitted by eye.

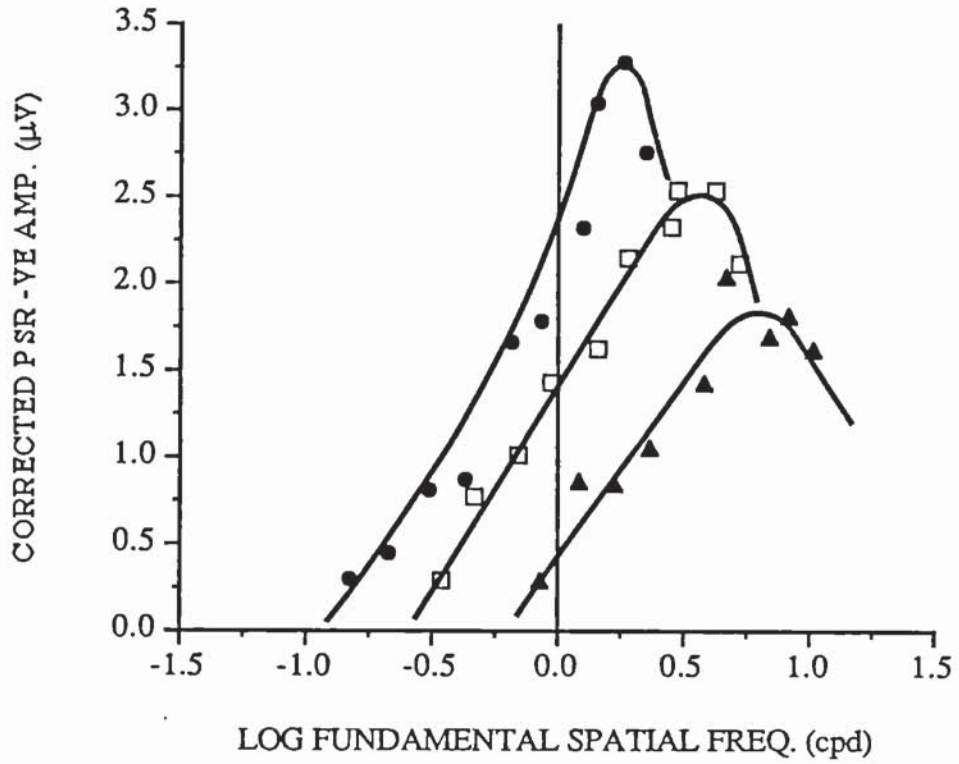

Fig 5.13. This graph demonstrates the variation of corrected PSR amplitude with spatial frequency for each zone. The symbols, closed triangles = 0 -5.1° zone, open squares = 5.6 -12.6° field and closed circles =12.3 - 25.6° annular field show the measured *group averaged* -ve transient amplitudes.

Using the method of least squares quadratic equations have been fitted to the corrected PSR amplitude data points plotted against spatial frequency in each stimulus field, The resulting equations are shown in table 5.1. The data have been graphically displayed in figure 5.14. The resulting equations were differentiated to give the peak spatial frequency, x cpd, (fundamental spatial freq.of chequerboard) for each stimulus zone for both amplitude measures. These values are tabulated in table 5.2.

Table 5.1 Equations fitted to PSR +ve and -ve amplitude vs spatial frequency.

CHECKERBOARDS:	positive transient	negative transient
0 - 5.1° field	$y = -0.266 + 0.0404x - 0.03x^2$ $r = 0.92$; df 2,6; $p = 0.004$	$y = 0.099 + 0.505x - 0.035x^2$ $r = 0.945$; df 2,6; $p = 0.001$
5.6 - 12.6° annulus	$y = -0.72 + 1.026x - 0.137x^2$ $r = 0.978$; df 2,7; $p = 1.77e^{-5}$	$y = 0.081 + 1.396x - 0.192x^2$ $r = 0.986$; df 2,7; $p = 3.51e^{-6}$
12.3 - 25.6° annulus	$y = -0.174 + 2.942x - 0.779x^2$ $r = 0.987$; df 2,7; $p = 2.93e^{-6}$	$y = -0.243 + 3.346x - 0.858x^2$ $r = 0.984$; df 2,7; $p = 5.38e^{-6}$

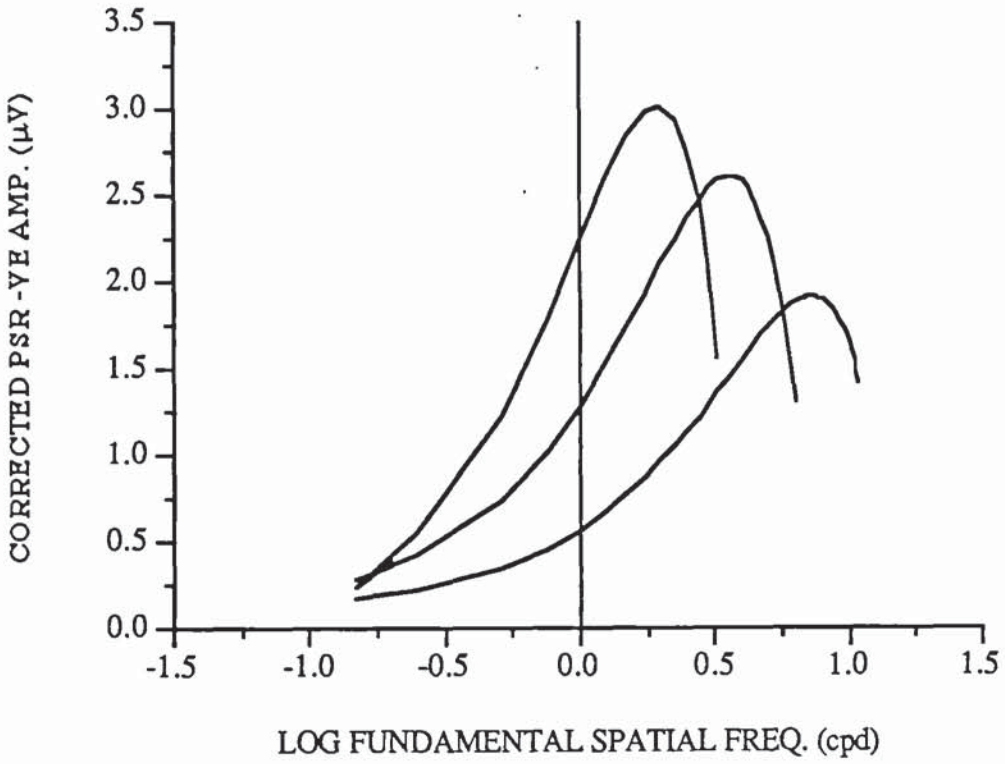

Fig 5.14 Quadratic functions fitted by the method of least squares to the corrected PSR -ve transient amplitude data showing change in peak in peak spatial frequency with peripheral angle.

Table 5.2 Peak spatial frequency in each stimulus zone.

	positive transient dy/dx = 0	negative transient
0 - 5.1° field	x = 6.733 cpd	x = 7.214 cpd
5.6 - 12.6° annulus	x = 3.744 cpd	x = 3.635 cpd
12.3 - 25.6° annulus	x = 1.888 cpd	x = 1.946 cpd

The peak of the corrected pattern specific response spatial tuning function varies with eccentricity and occurs at higher spatial frequencies than previously reported in Chapter 4. The reciprocal of the fundamental spatial frequency ie the peak spatial cycle for the negative transient has been plotted as a function of mean radial peripheral angle in figure 5.15. A straight line has been fitted to the points by linear regression, which is the same for both positive and negative transient amplitudes:

$y = 0.022\ x + 0.082$, for the +ve amplitude: $r = 0.997$; df 1,1; $p = 0.05$

for the -ve amplitude: $r = 1.00$; df1,1; $p = 0.013$

The optimum spatial cycle increases linearly with increasing peripheral angle.

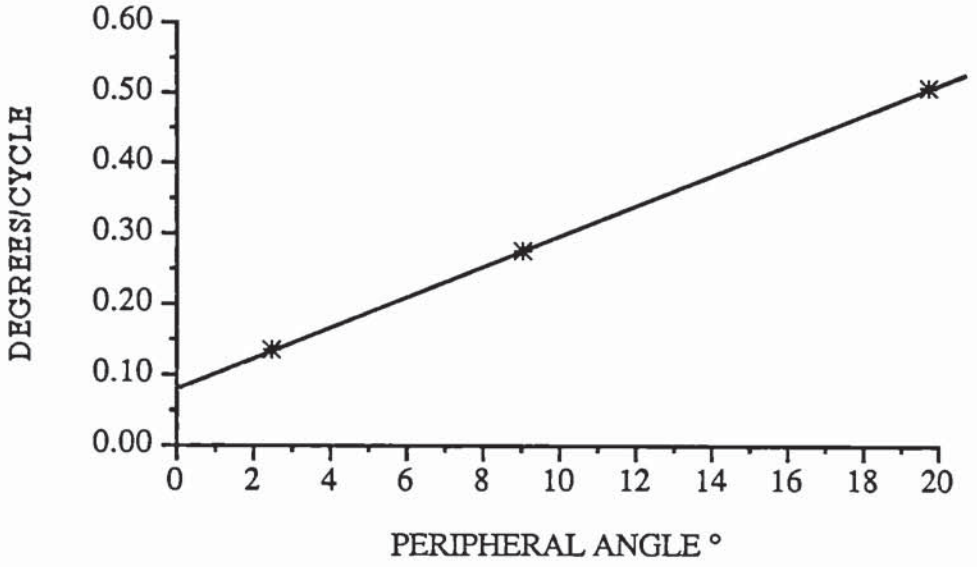

Fig 5.15 The optimum chequerboard stimulus (deg/cycle) in each field is plotted as a function of mean radial peripheral angle.

This equation may be alternatively expressed

$$y = 0.082\ (1 + 0.27\ \emptyset),$$

the gradient, although shallower, is still compatible with that predicted by the equations that describe ganglion cell receptive field centre separation across the retina (Drasdo et al 1977; Rovamo and Virsu 1978). This is most likely due to the participation of bipolars whose receptive fields have weaker surround antagonism, but more importantly whose numbers are more evenly distributed across the retina. Thus their variation of cell centre separation with retinal eccentricity is less steep. The linear

of the function is clearly established and extrapolation appears justifiable giving an estimate of the optimal foveal receptive field. Thus when x = 0, y = 0.082 deg / cycle ie a fundamental cycle of 4.92 min arc. This corresponds to a check side of 3.5 min of arc ie. an optimal foveal stimulus of 3.5 minutes of arc.

Similar linear functions have often been used to relate human psychophysical data with retinal eccentricity and estimated receptive field centre separation (eg Rovamo 1978). Weymouth (1958), for example, plotted the reciprocal of visual acuity, namely minimum angle of resolution, and found that several visual thresholds increased linearly with eccentricity, at least up to 30°. The same is true for the grating acuity data of Wertheim (1894). The reduction in spatial resolution with eccentricity (eg Anstis 1974) is thought to reflect the decline in receptive field and ganglion cell density, the increase in receptive field size and a decrease in the cortical magnification factor (Cleland et al 1979). The latter is a measure of the cortical representation of visual space (Drasdo 1977).

The spatial tuning of the PSR might be expected to relate to receptive field sizes across the retina. However there is very little clear evidence about the dimensions of human ganglion cell receptive fields. The information available is gleaned from histological studies of man and monkey, from psychophysical data, which refers to the visual system as whole and may not necessarily reflect retinal receptive field dimensions, and also from optical and psychophysical line spread functions.

In this study the calculation of the stimulus field diameters was based on collated ganglion cell data, corrected for shrinkage and sampling errors, from three studies, [Vilter (1954), Van Buren (1963) and (Opel 1967)], of twelve human eyes, (Drasdo 1977). However these studies did not distinguish the distribution variation of different ganglion cell classes with eccentricity.

Two of the most recent histological reports of ganglion cell dendritic field diameter and retinal eccentricity are by Perry et al (1984) in macaque and Rodieck et al (1985) in human flat mounted retinae. Dendritic field diameter is not related by a simple rule to the receptive field size (Perry et al 1984); although in cat Piechl and Wässle (1981) found the size and shape of the alpha ganglion cell receptive field centre to be slightly larger, but nonetheless in close correspondence to its dendritic field diameter.

These recent data have distinguished ganglion cell types. In the former study the dendritic field diameters of P.alpha and P.beta ganglion cells of macaque have been graphically displayed as a function of retinal eccentricity (Perry et al 1984). When regression lines were fitted to these data, by eye, the foveal dendritic field diameter could be estimated by extrapolation. Thus in figures 6A and 6B of Perry et al (1984) the intercept for P.beta cells falls between 7.7 and 11.5 μm and the foveal dendritic field diameter of P.alpha cells between 15 -17.5 μm. Using a scale factor of 1.6 mm = 8° for macaque retina (Shapley and Perry 1986) the gradient of dendritic field size with eccentricity was approximated. The foveal P.beta dendritic field approximated to 2.8' arc and the P.alpha dendritic field to 4.5' arc. Our results gave a value of optimum foveal stimulus of 3.5' arc which would seem compatible with the P.beta dendritic field diameter (as dendritic field diameter is generally smaller than receptive field diameter).

The human parasol and midget ganglion cell data has been similarly examined (Rodieck et al 1985). Rodieck et al (1985) related the human parasol cells to the P.alpha cells of macaque (Perry et al 1984) and the midget cells to P.beta cells. Boycott and Dowling (1969) exclusively applied the term midget to ganglion cells with dendritic field diameters of 10 μm or less. Occasionally cells of this magnitude were noted in the retinal periphery. Midget ganglion cells were consequently considered to maintain a constant dendritic field diameter across the retina. de Monasterio (1978) similarly remarked fairly constant P. ganglion cell dimensions within the central 5°. However this data does not agree with Polyak's (1941) original description nor with

that of Rodieck et al (1985).

The best fit straight line was fitted by eye to the data of Rodieck et al (1985) and the mean intercept of four independent appraisals approximated by extrapolation. A larger difference is apparent between parasol and midget cell dendritic field size than had been reported between P.alpha and P.beta cells. Thus the intercept for midget cells was 8 μm and for parasol cells was 81μm. A conversion factor was estimated from the fovea to optic disc distance and the foveal midget dendritic field diameter found to be 1.8' arc at the fovea whilst the parasol dendritic field diameter approximated 18.45' arc.

The midget cell therefore appears most compatible with the experimental results. Also the gradient of human midget dendritic field size with eccentricity expressed in the form:

$$y = 8\ (1 + 0.19Ø)$$

is the closest expression of ganglion cell dendritic diameter variation with eccentricity to the experimentally derived equation that may be derived from these two reports (Perry et al 1984; Rodieck et al 1985). However another report on macaque ganglion cell dendritic field variation with eccentricity suggests a reappraisal of ganglion cell taxonomy is appropriate. Direct inspection and fit of regression lines to the graphical representation of the macaque dendritic field data of Shapley and Perry (1986) [their fig.3.] suggests a M-cell gradient, expressed in similar form as above:

$$y = 15\ (1 + 0.25\ Ø)$$

which is closely compatible with the experimental results. Shapley and Perry (1986) have proposed that the M-cell population can be sub-divided into M_x and M_y - like cells. They suggest that the M cells demonstrate a spatial scaling of dendritic field and receptive field size that is consistent with psychophysical scaling. A flat plateau is evident in the P cell dendritic field diameter in the central retina in this study which is not consistent with psychophysical results, but is similar to the findings of Boycott and Dowling (1969) and de Monasterio (1978).

Studies that examine psychophysical spatial scaling use the concept of perceptive field size. A perceptive field is a hypothetical construct that denotes the psychophysical correlate of a receptive field in human vision. Threshold changes and perceptual effects of spatially interacting stimuli are explained by analogy to receptive field centre/surround antagonism (Ransom-Hogg and Spillman 1980). Westheimer (1965) developed a paradigm that is believed to reflect retinal perceptive field organisation. He measured the incremental threshold for a small test spot which is flashed on steady background discs of varying diameter. The measures are correlated thus: threshold first rises to an increase in background diameter due to areal summation until the background covers the entire receptive field centre. Threshold then decreases as the background invades the inhibitory surround and plateaus when the background becomes larger than the total receptive field.

Oehler (1983) has used Westheimer's paradigm to estimate the variation in perceptive centre field size with eccentricity in rhesus monkey. He found the perceptive field size was larger than the dendritic field size at all eccentricities, but correlated well with the receptive field centres of broad band cells measured by de Monasterio and Gouras (1975). Ransom-Hogg and Spillman (1980) also found perceptive field sizes increased in both centre and total size with eccentricity, but noted a plateau between 10° and 30°. They related this to van Buren's (1963) data where the retinal ganglion cell layer is only one layer thick, but has no intracellular gaps. Ransom-Hogg and Spillman (1980) have graphically collated the data of several other workers (their Fig 7). They find a centre size increases from less than 9' at the fovea to 1° at 10° eccentricity and then rises more slowly. However their central value was constrained by the size of their smallest available test aperture. Troscianko (1982) found a perceptive field centre diameter at the fovea of 15' arc. Spillman (1971) using Hermann grid patterns estimated the centre perceptive field was of the order of 4' whilst the surround was 18' arc. However it must be remembered that most measures are pooled responses from all perceptive fields at any retinal location.

The full summation zone of the retinal receptive field has been reported by Glezer (1965) to range from 4' - 10' arc at the fovea to 15' -30' arc in the periphery. Hallett (1963) has tabulated the spatial estimates of several studies measured under different conditions of adaptation. The smallest estimate suggests a receptive field of 3' arc at 5° eccentricity under photopic conditions.

One of the few studies to avoid optical factors in the assessment of the peripheral retina was conducted by Hilz and Cavonius (1974) who used interference fringes to measure the contrast sensitivity under photopic conditions. The foveal value was 8 cpd i.e. an element size of 3.75' arc. An assessment of the simple processing of the visual system may be obtained from threshold assessment of the foveal point spread function (Vos et al 1976). In this way Bloomhardt and Roufs (1981) obtained a foveal value of 4' arc centre point spread function width.

The consensus of these studies suggests a foveal perceptive field and receptive field size of the order of 3' - 4' arc. This is in close agreement with the data obtained by linear extrapolation of the PSR tuning peaks with eccentricity. The data from Rodieck et al's (1985) study suggests a closer correspondence with the smaller ganglion cells, the midget sub-system in human or P.beta ganglion cells (in macaque) that comprise some 80% of the total population and subserve colour discrimination and the detection of high spatial frequencies at high contrasts. However the data of Shapley and Perry (1986) suggests a correspondence between the experimental findings and M - ganglion cell distribution (i.e. those cells that project to the magno-cellular layers of the lateral geniculate nucleus). Thus the contribution of a specific ganglion cell class to the pattern specific response cannot be inferred from the available data with any confidence.

The three stimulus zones had been calculated to contain equal numbers of ganglion cell receptive fields, (Drasdo 1977), but no data were available on the distribution of bipolar cells in the retina. However the thickness of the three nuclear layers of the

retina have characteristically different distributions. The outer nuclear layer remains fairly constant across the retina, the ganglion cell layer declines rapidly in the periphery and the inner nuclear layer declines at an intermediate rate (Polyak 1957). The variations in layer thickness, averaged over all retinal meridians, were assessed from the radial sections of Van Buren (1963), which were considered to be the most complete and typical data. The volumes relating to each stimulus zone in the experiment were calculated by spherical integration, with due allowance for the displacement factor caused by the foveal excavation of inner nuclear and ganglion cell somata (Drasdo 1977). The outer nuclear layer includes both rods and cones. It is difficult to separate the rod and cone function in ERG recordings with white light. (Carr and Siegal 1972). Thus the pattern ERG may still contain rod contribution, more especially in the retinal illuminance component. Available data describing the variation of different ganglion cell classes with eccentricity is variable and incomplete. For the purposes of this investigation therefore it was decided to include all classes. The nuclear volumes were normalised on the central zone for comparison with corresponding data on the amplitude of the RIR and PSR signals.

The data has been displayed in histogram form in Figure 5.16. (after Drasdo, Thompson and Arden - in preparation.). The results further reinforce the contribution of proximal elements to the PSR, particularly with respect to the negative response transient. As anticipated the positive transient of the RIR, which corresponds to the conventional flash ERG b-wave, appears to relate to the outer and inner nuclear layer representing receptoral and bipolar cell activity (section 2.3). The negative response transients generally appear to relate to the more proximal retinal layers. This may be explained if the PERG arises from the integration in the Müller cell of activity from many kinds of neurone. Potentials will have different implicit times and those due to proximal elements are likely to arise last and affect the later negative response transient. Therefore ganglion cells, especially those with slowly conducting axons and strong inhibition, occuring with a slight phase delay (Enroth-Cugell et al 1983), are likely to contribute most to the falling phase of the recorded field response.

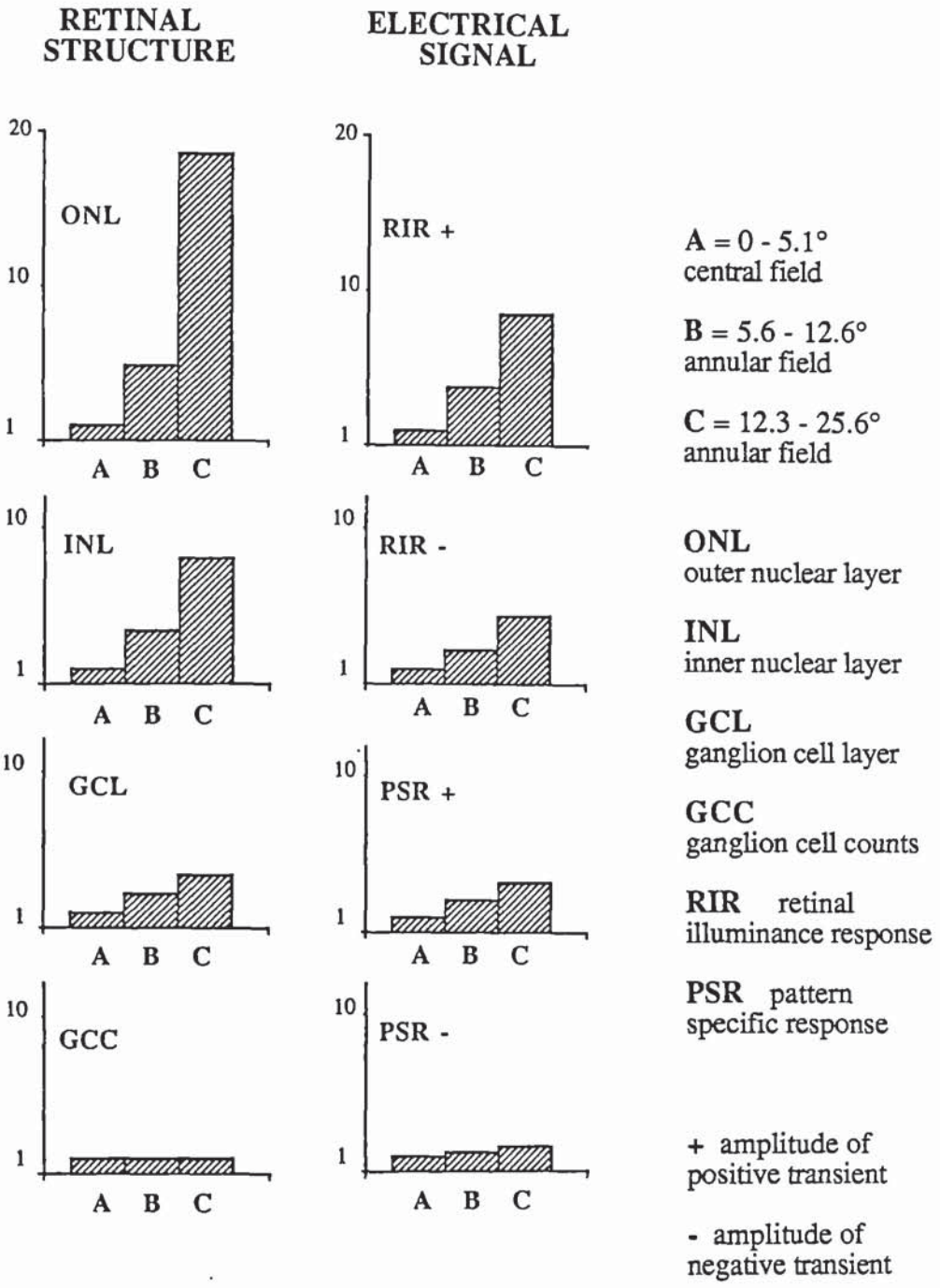

Fig 5.16 The histograms allow a comparison of the structure and electrical function of the stimulus zones. The nuclear layer voulmes were normalised on the central value for comparison with the correspondingly normalised amplitudes of the retinal illuminance RIR, and corrected pattern specific responses PSR.

5.5 CONCLUSION

A linear relationship exists between the PERG and stimulus contrast with no systematic variation in peak latency. An analytical separation of retinal illuminance and pattern specific responses may therefore be carried out via computation of the effective retinal temporal and spatial contrast using the eye's modulation transfer function. The relative proportion of retinal illuminance response diminishes at higher spatial frequencies: the proportion of pattern specific response increases.

The variation of the components alters with eccentricity in manner that has been related to the volumes of the three nuclear layers. The pattern specific response, particularly its negative transient, is related to more proximal layers that include the ganglion cells. As anticipated the retinal illuminance response resembles the conventional flash ERG b-wave and correlates better with the inner nuclear layer containing the bipolar cells; although it's negative transient amplitude also corresponds to the ganglion cell layer. Therefore the contribution of proximal retinal elements to the flash ERG cannot be discounted. Thus the observation of Armington (1974) that the negative 'afterpotential' is greater with periodic patterns may relate to the preferential stimulation of proximal elements ie pattern stimuli tend to emphasise the contribution of more proximal retinal cells in the electrical field response.

These results also contribute to the explanation that the negative transient of the PERG is affected in optic nerve dysfunction (eg Porciatti and von Berger 1984; Holder 1987) is related to the compound action potential of the optic nerve in cat (Schuurmans and Berninger 1984) and more frequently demonstrates spatial selectivity (eg Korth 1983).

CHAPTER 6

SYNTHESIS OF THE ON AND OFF COMPONENTS OF THE RETINAL ILLUMINANCE RESPONSE

6.1 INTRODUCTION

In the preceding chapters a method of analysis has been described which assesses the retinal illuminance response and the corresponding pattern specific response that make up the pattern onset ERG. The retinal illuminance response amplitude depends on the temporal contrast of stimulation. The relative amplitudes of the pattern onset and offset responses vary with spatial frequency (Arden and Vaegan 1983; Korth 1983). If a PERG is evoked only by an increase in local luminance and is the summation of focal luminance ERGs, as suggested by Reimslag et al (1985), the difference between onset and offset amplitude with spatial frequency should be readily explicable and quantifiable in terms of temporal contrast. When luminance increases alone are considered the change in temporal contrast resulting from the disappearance of a dark element into a uniform background of mean luminance is greater than the temporal contrast change resulting from the appearance of a light element from the same mean background. The ratio at 100% modulation is 1:3 light appearance at onset : dark disappearance at offset (as described in Chapter 5).

A PERG evoked by a low spatial frequency pattern approximates to an illuminance response and in this case the offset response is greater than the onset response. This observation may be understood by the greater contribution of dark elements at offset causing a larger signal. However at high spatial frequencies the offset response becomes progressively smaller than the onset response. Although the retinal image of high spatial frequencies patterns is degraded the temporal contrast change due to the disappearance of dark elements is always greater than the the appearance of a light element. The greater onset signal amplitude may therefore be due to the emergence of a pattern specific response.

There have been several attempts to synthesis the PERG from the constituent focal luminance changes (Korth 1983; Arden and Vaegan 1983; Reimslag et al 1983,1985). Korth (1983) separately presented unpatterned increases and decreases in luminance at levels which corresponded to patterned stimuli presentation. The focal responses to luminance change were summed and compared with the signal evoked by patterned stimuli. The summated waveform was dominated by the response to a luminance decrease-increase, but resembled the waveform of responses obtained with patterned stimuli. Using a faster time base the morphology of the synthesised onset response differed from the pattern onset response.

Korth (1983) concluded that pattern onset is not the result of linear summation of two responses evoked by luminance increases and decreases in an homogenous field, but pattern offset is predominantly due to the increase in light in previously dark retinal areas. He proposes that decreases in luminance are essential for the generation of a pattern-related response, but as he mentions his experimental paradigm did result in a change in retinal contrast. Thus pattern offset demonstrates a monotonic amplitude decline with higher spatial frequencies and is reckoned to be a response to local luminance whilst the onset response is pattern related.

Arden and Vaegan (1983) similarly recognised the largest logarithmic increase in local retinal illumination occurs when the dark elements disappear into the mean background. They suggested processes of lateral interaction account for the difference in onset-offset response magnitude at higher spatial frequencies. Arden and Vaegan (1983) attempted to synthesis the waveform, but found they could not achieve this. However they point out that as part of the method the overall flux entering the eye is necessarily increased; this does not occur with a patterned stimulus - the flux remains constant. Stray light effects, iris potentials and adaptation changes might have confounded the results.

Riemslag et al (1983;1985) used stimuli in which an equal contrast change was associated with either an increase or decrease of mean luminance. The cortically evoked responses were similar to each other, the retinal responses however were opposite and depended on the increase in luminance. Ringo et al (1984) proposed an alternative compressive input:output system to explain low spatial frequency attenuation. They suggested a set of small receptive field rectifying subunits feed into a larger receptive field integrator. With low spatial frequency stimuli all the rectifiers of 1/2 the integrators are stimulated; at high spatial frequencies 1/2 the rectifiers of all the integrators are stimulated. The scheme relies upon the integrators producing constant size response when stimulated and the response is initiated only to an increase in luminance. This model offers a possible explanation of spatial selectivity, but does not account for the relatively greater amplitude of pattern onset compared with pattern offset responses evoked by high spatial frequency patterns.

This study therefore set out to examine the composition of the low spatial frequency pattern onset-offset response, the retinal illuminance response, and to examine whether its behaviour could be predicted from data relating to the temporal contrast of stimulation.

6.2 METHOD

A 100 Hz TV monitor was used to evoke focal ERGs (Arden et al 1982). The screen composition was adjusted until half the field of view was light the other half dark. The contrast across the border using the Michelson equation was 80%. Luminance modulated between 180 and 20 cdm^{-2} (as used in the experiment of PERG amplitude variation with stimulus contrast in Chapter 5). Mean luminance and surround luminance were 100 cdm^{-2}. The low spatial frequency pattern / focal ERGs evoked by the luminance change from a mean background were recorded from ten volunteers. All the subjects were capable of 6/6 acuity and fixated a centrally positioned target. The recordings were made binocularly using DTL electrodes referenced to EEG Ag cup electrodes positioned on the ipsilateral outer canthii. The responses were

recorded on a Nicolet Pathfinder II computer averager between a filter bandpass of 0.5 - 50 Hz.

The ERGs evoked by the modulation of 1/2 the field from light to mean and mean to dark were also recorded. The other half of the screen was covered by a white mask in each condition. The responses were group averaged. The TV triggered the averager at pattern onset ie when the screen become light or darker than the mean luminance level.

6.3 RESULTS

The onset and offset responses to both the appearance of white 1/2 and black 1/2 fields were independently group averaged. The ERG recorded to the whole field, low spatial frequency modulation was similarly group averaged. When the response to white 1/2 and black 1/2 field are added or summed the resultant trace should equate to 50% of the whole field ERG. The PERG is known to demonstrate linear areal summation particularly when the stimuli are designed to include equal proportions of macula (Hess and Baker 1984). Using the Pathfinder it was possible to multiply the summated, synthesised focal response by a factor of two. The resultant traces are displayed in figure 6.1. As can be seen there is good correspondence in morphology and amplitude between the synthesised response and the recorded full field focal ERG.

The onset response of the white 1/2 field has a longer implicit time than the onset response of the black 1/2 field. The response to an increase in luminance: white 1/2 field onset and black 1/2 field offset, has a definite early negative component, like an a-wave. The response to a luminance decrement does not. When the amplitude of the white onset and black offset are compared their amplitudes, positive, (b-wave), and negative transients are approximately in the proportion of 1 : 2. The predicted proportion is 1 : 3; response to white check onset : black check offset, which relates to 100% modulation. The disparity may be therefore be due to a stimulus modulation of 80% and the larger experimental error incurred with small amplitude signals.

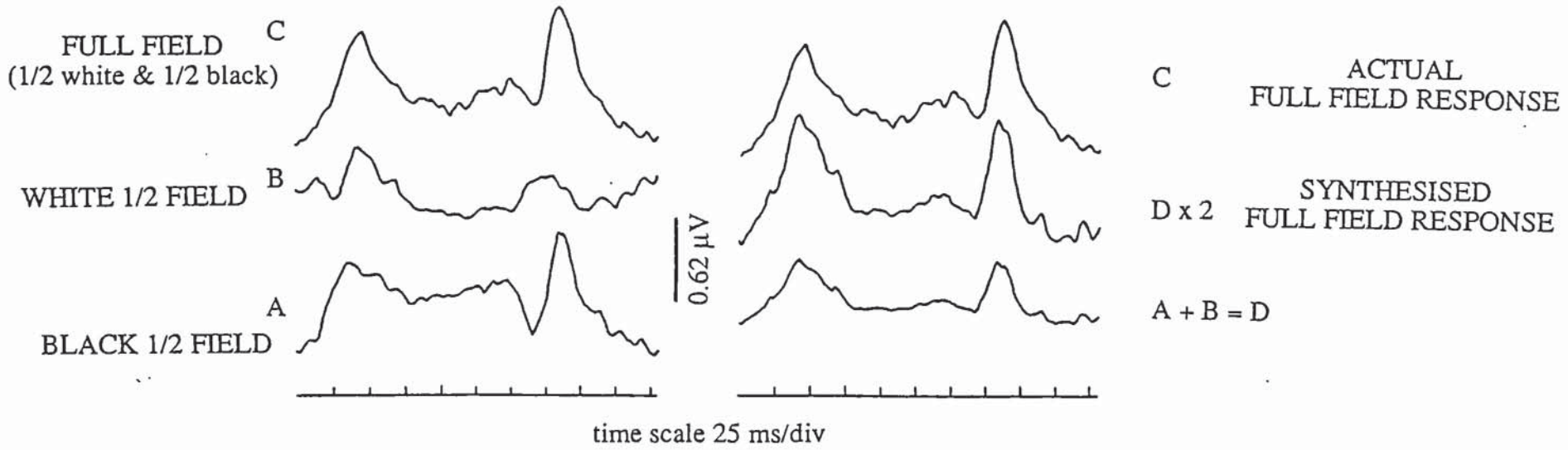

Fig 6.1 Low spatial frequency response D is synthesised from group averaged signals recorded to 1/2 screen white (A) and black element (B) modulation multiplied by a factor of two. The group averaged waveform actually recorded to full screen modulation is C.

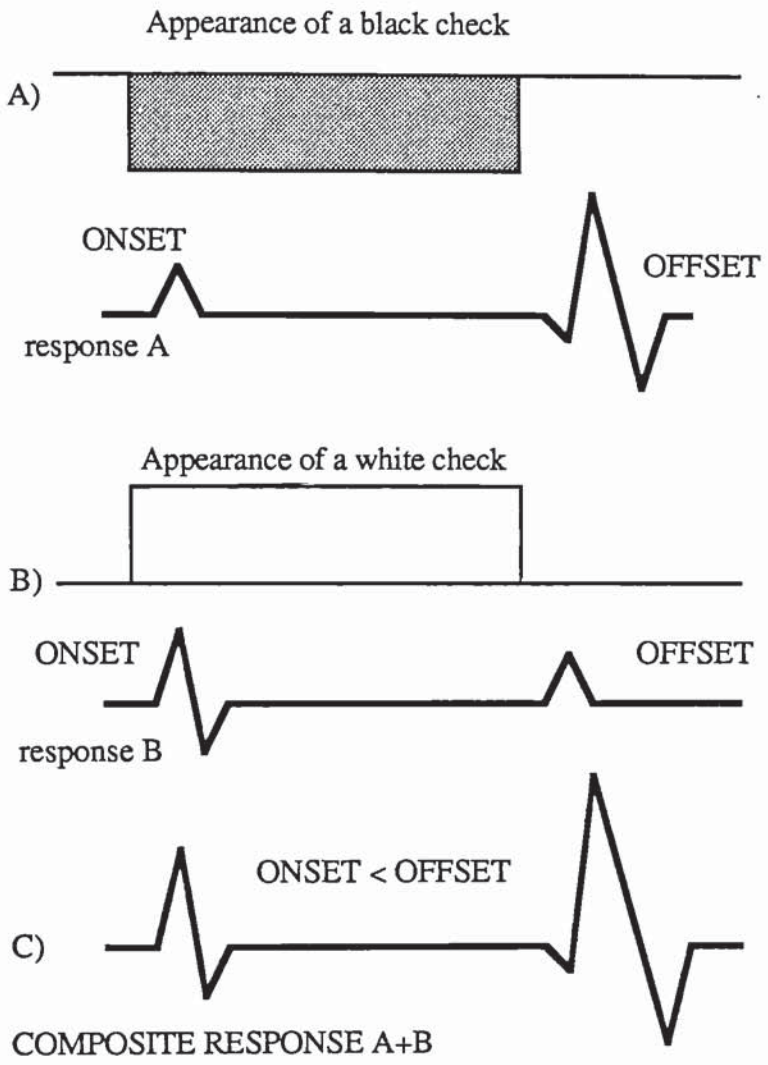

Fig 6.2 Schematic diagram showing the relative amplitude of ERG response expected to light increases due to white and black pattern elements respectively. The waveform is discussed in greater detail in the text. No account is made of latency in this diagram.

Thus it appears that the local luminance responses of the 'pattern' onset-offset retinal illuminance response are rectified and roughly proportional to the temporal contrast. Both the increase and decrease in illuminance results in a positive response at the cornea although the magnitude of the response differs. The increase in illuminance would stimulate the on-centre system and cause the photoreceptors to hyperpolarise. The Müller cell hypothesis for b-wave generation would account for the resulting ERG. When the illuminance decreases the ERG is still positive, but the response is smaller. The off-centre system will be stimulated. Off-centre bipolars will depolarise and change the concentration of K_0^+ which may affect ionic currents in the Müller cell

in a similar manner to the light response of on-centre bipolar cells (Evers and Gouras 1986). The photoreceptors would tend to depolarise and decrease the amount of transmitter release, but they would not participate greatly in the potassium shifts in the distal retina. Thus the corneal negative a-wave is not seen.

The delay in the implicit time of the positive peak appears to be the result of the polarity of the initial deflection. Thus the white 1/2 field onset response begins at the same time as the black onset, but the former develops into a negative response the latter into a broad positive response.

6.4 CONCLUSIONS

The retinal illuminance response examined in this study appears to be approximately proportional to the temporal contrast of the stimulus in the pattern onset-offset mode of presentation. This suggests that the contribution of illuminance responses to retinal responses evoked by patterns of high spatial frequency may be estimated from the temporal contrast of the degraded image. The addition of pattern specific responses, sensitive to the spatial variation of illuminance across the retina, are likely to account for the greater PERG onset amplitude at high spatial frequency.

The responses described in Chapter 5, Fig 5.1 effectively had the same magnitude of modulation at 80%, the same mean luminance level and the same stimulus area of black and white yet the PERG onset response amplitude is much greater for the smaller check size eg 10', than for 1/4 or in this case 1/2 field black/white modulation.

CHAPTER 7

ASSESSMENT OF A STIMULUS PARADIGM TO AVOID EYE MOVEMENT ARTEFACT

7.1 INTRODUCTION

7.1.1 Fixation eye movements

The fixation maintenance system has an inherent and regular instability of position that is quite small but constant (Hart 1987). The eye movements associated with fixation have been resolved into three types namely tremor, flicks and drifts. Tremor describes an irregular, high frequency, (30 to 70 s^{-1}), movement of small excursion ($\approx$ 20 seconds of arc). Flicks or microsaccades occur at irregular intervals ($\approx$1 sec), and tend to be corrective, returning the image detail to the optimum fixation point (Davson 1980). They take $\approx$ 25ms. Slow irregular drifts occur between flicks and can extend up to 6 min of arc. Drifts are monocular and independent between the two eyes (Cornsweet 1956).

Nachmias (1959) has described the probable range of eye movements over a 30 second fixation period and concludes the excursion is not large enough to bring the point image off the fovea. More recent data confirms the maximum probable fixation movement, in a younger person viewing a stationary target, falls within a 25'arc diameter ellipse at the 68% level (Kosnik et al 1986).

These small saccadic movements provide discrete changes in retinal stimulation. If the retinal image is stabilised contrasting contours fade from view, particularly in the periphery - the Troxler phemonenon (Davson 1980). However sensitivity rapidly recovers with eye movement which suggests this is not a localised bleaching effect of the photoreceptors. Rather the rapid mechanism would seem to be neural in basis (Hart 1987).

7.1.2 After-images, eye movements and the ERG

When the eye is exposed to brief flashes of light a subjective sensation lasts for longer than the stimulus; a series of after-images occurs (Brindley 1959). A bright flash of light also increases the detection threshold for a second flash (Crawford 1947). Similarly if an ERG is evoked shortly after the eye has been stimulated by a bright flash its amplitude will be reduced (Burian and Spivey 1959). This is also apparent in the flicker ERG where, with high intensity, the first b-wave has a larger amplitude than successive responses (Arden et al 1960). Schneider and Zrenner (1987) conclude that response depression results from the combination of photochemical bleaching and neural processes. They have suggested a stabilising neural circuitry in the inner retina to compensate for the loss of responsitivity in the outer and middle retinal layers. In this way a feedback mechanism adjusts or scales the strength of the visual signals until until they fall within the centre of the eye' response range - an automatic gain control (Shapley and Enroth-Cugell 1984).

With continuing light stimulation the amplitude of the ERG is markedly attenuated (Armington et al 1967). However if a saccadic eye movement causes the light to fall on a previously unstimulated retinal region ERG amplitude will increases again. Indeed the eyes natural movements have been used in the "method of spontaneous response" which is akin to the technique of alternating stimuli proposed by Riggs et al (1964), (Armington 1974). The size of the element is altered until it corresponds to the size of the saccade therefore producing the maximum luminance change and greatest response (Armington et al 1967; Flamm et al 1971).

Eye movements may be anticipated to similarly effect response amplitude during pattern fixation in PERG recording. In the onset-offset presentation mode the pattern appears in the same place every cycle. Therefore the response evoked by patterns of angular subtense greater than the amplitude of the saccadic fixation movements may be depressed. At higher spatial frequencies, of the same angular subtense or less than the saccadic eye movements, the fixation eye movements may enhance the pattern onset

ERG. This would not occur in pattern reversal stimulation where the pattern position alters twice each cycle. It is possible therefore that the Pattern appearance-disappearance stimulation employed in these studies may have resulted in spurious bandpass spatial tuning of the pattern onset ERG. A stimulation paradigm was designed to examine these effects and the PERG onset responses evoked by chequerboards in three different presentation modes have been compared.

7.2 METHOD

The different presentation modes were set up using a *Digitimer* to control the optical stimulator system, described in Chapter 4. The first presentation method was the previously employed conventional Pattern appearance from a mean background. The second method used the mirror, mounted on the pen motor, to reverse the check positions during every offset phase. Thus a white check appeared for 105ms and disappeared into the uniform screen for 105ms and on the next presentation a dark check appeared in its place as a result of the reversal. In this way the pattern was presented in alternate positions. The third paradigm reversed the pattern elements during every offset phase. The timing intervals of the pulses generated by the Digitimer have been illustrated in Figure 7.1. The shutter operated in all three presentation methods according to the timing shown at the top of the diagram.

If the effects of afterimages and adaptation confound the spatial tuning studies the 'static' pattern appearance mode would be predicted to result in the most pronounced low spatial frequency attenuation. The least noticeable low spatial response attenuation would be anticipated to occur in the pattern appearance mode with reversal every cycle, whilst the stimulation paradigm designed to reverse the image every alternate cycle would result in signals of intermediate amplitude.

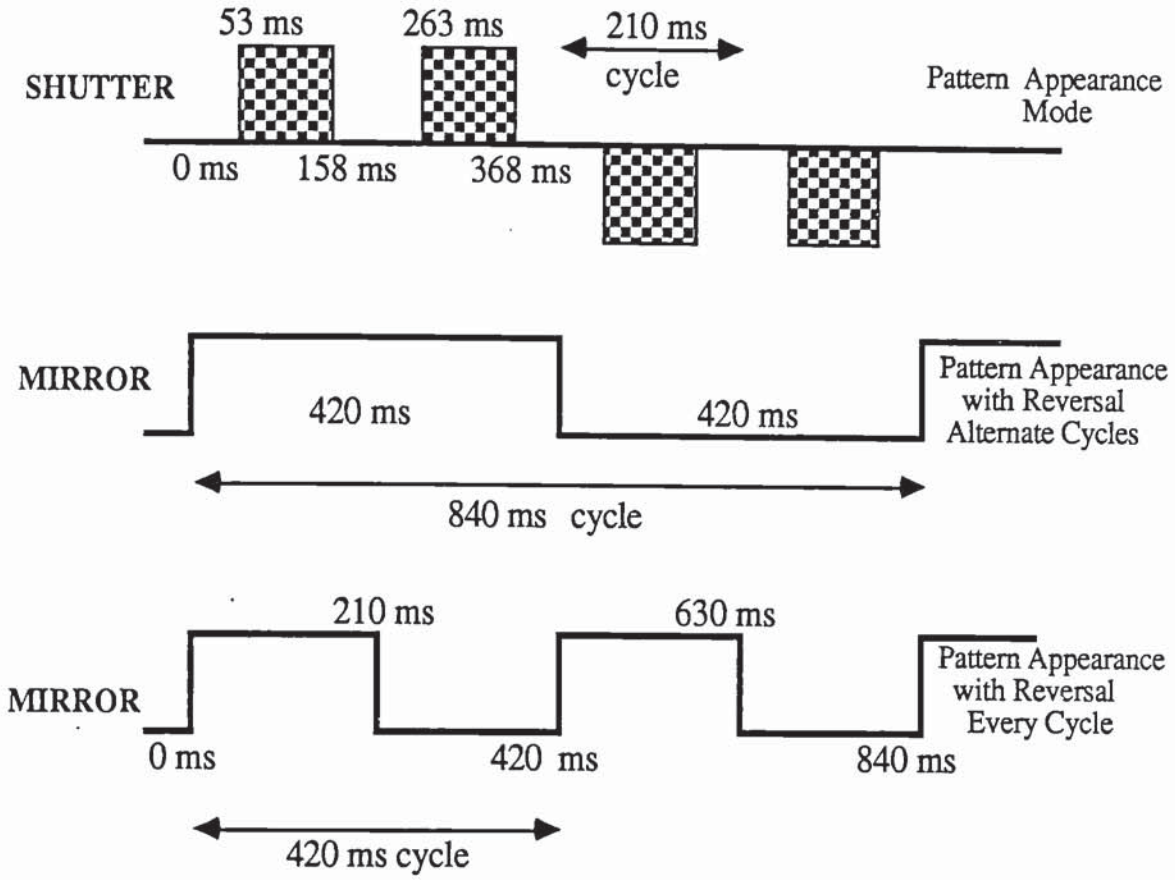

Fig 7.1 Diagram illustrating the timing intervals of *Digitimer* pulses driving the shutter and pen-motor mounted mirror. When the shutter alone was operating the resulting presentation was pattern appearance. When the mirror was introduced the pattern reversed either alternate appearance cycles or every appearance cycle. Reversal occured when the shutter obscured the pattern.

7.2.1 Protocol

A 15° circular stimulus field of mean luminance 275 cdm^{-2} was used. A large white surround of mean luminance 120 cdm^{-2} subtended 65° diameter. Ten subjects mean age 24.5 yrs participated in the study wearing spectacle corrections when appropriate. 200 responses were averaged on a Nicolet Pathfinder II, between a bandpass of 0.5 - 70 Hz, for each subject for each stimulus condition The pattern appeared for 105ms and disappeared for 105ms. The time window was 200 ms. The viewing distance was

100 cm and subjects were instructed to fixate a cross positioned at the intersection of the 4 central checks. Chequerboards in a range of spatial frequencies 7' - 134' of arc were presented in each of the three modes described. An additional stimulus subtending 222' arc was used to evoke pattern onset ERGs in 6 of the 10 subjects.

7.3 RESULTS

The results of the ten subjects were group averaged and are shown in Figure 7.2. As in previous studies the peak to peak amplitude of the negative and positive going transients have been measured. These are graphically displayed as a function of spatial frequency in figures 7.3 and 7.4: the data points relating to the stimulus paradigm of 'pattern reversal alternate cycles of appearance' have been joined by a solid line in each figure.

open squares = Pattern appearance
closed squares = Pattern appearance with reversal every cycle
closed circles = Pattern appearance with reversal alternate cycles (solid line)

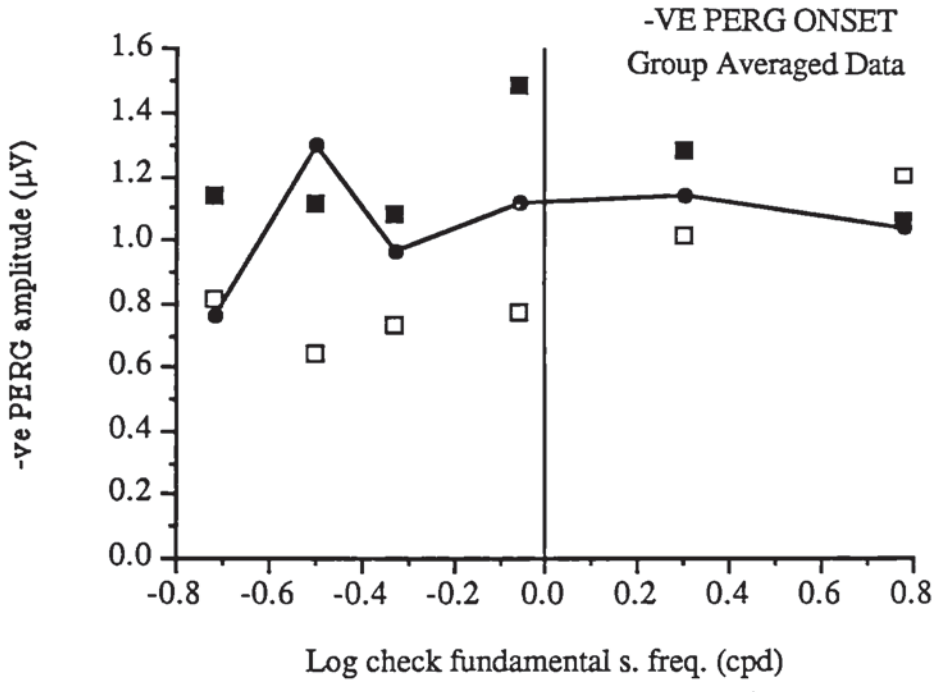

Fig 7.3 This graph shows the negative PERG onset response transient as a function of spatial frequency for each presentation mode.

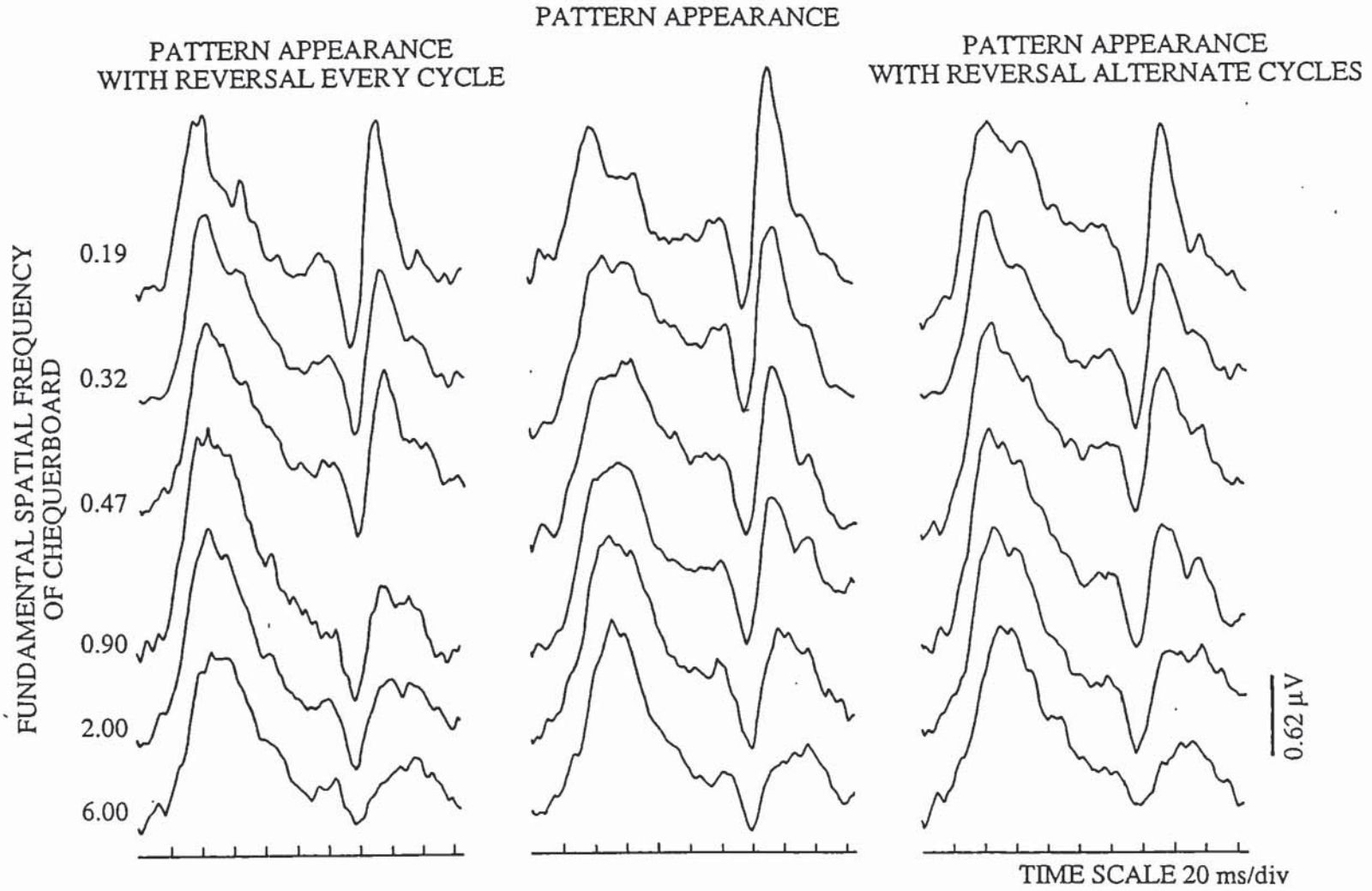

Fig 7.2 Group averaged PERG data for three modes of pattern appearance presentation. The second column shows the responses recorded to conventional pattern onset-offset stimuli.

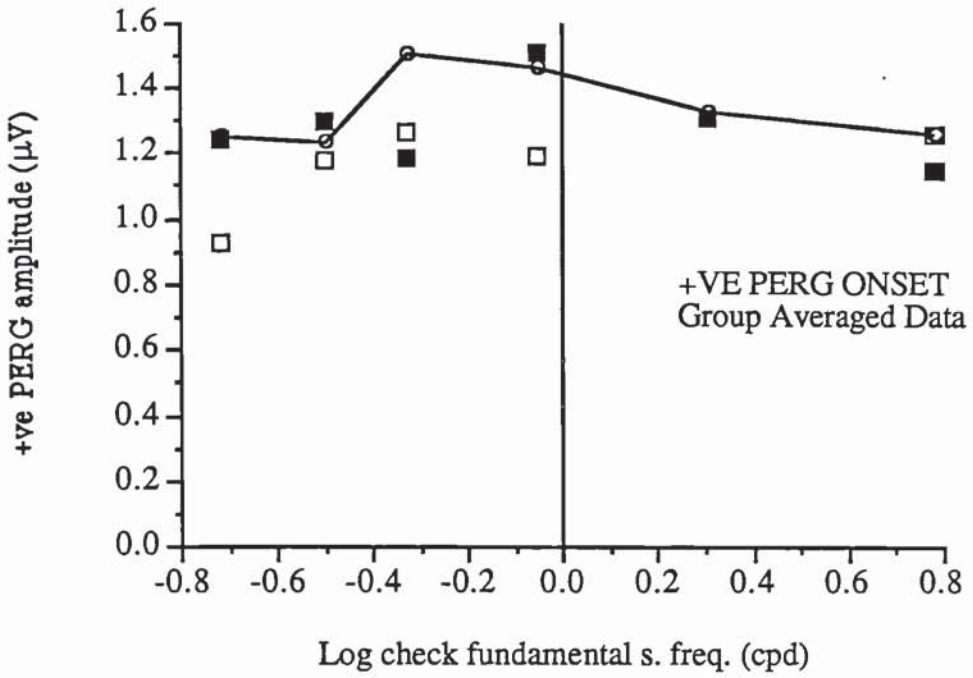

Fig 7.4 The shows the group averaged +ve PERG amplitude for the three stimulus presentation methods.

open squares = Pattern appearance
closed squares = Pattern appearance with reversal once per cycle
open circles = Pattern appearance with reversal alternate cycles

The +ve PERG group average data demonstrates a slight low spatial frequency attenuation in the pattern appearance condition. This is not mirrored in the pattern reversal with appearance modes. The stimulus paradigm, when the pattern reverses every alternate cycle, generally results in amplitudes that fall between the data acquired in the other two modes. This is most readily observable at the high spatial frequency end of the range in the data representing the -ve PERG component in Fig 7.3.

To obtain a statistical concept of the variation in PERG onset behaviour in the three presentation modes the individual data was measured and a two way anaylsis of variance carried out between the 3 presentation modes with spatial frequency. The results are shown in tables 7.1 and 7.2: 7.1 refers to -ve PERG amplitude, 7.2 relates to +ve PERG amplitude.

Table 7.1 **-ve PERG** amplitude analysed as a function of presentation mode and spatial frequency.

SOURCE	sum of squares	df	mean squares	F-ratio	Prob>F
between Mode	1.9	2	0.949	3.04	0.051*
between Check size	1.37	5	0.275	0.88	0.496
Interaction	2.86	10	0.286	0.917	0.52
Error	46.8	130	0.312		
Total	53.0	167			

The only significant variation is marked with an *.

Table 7.2 **+ve PERG** amplitude analysed as a function of presentation mode and spatial frequency.

SOURCE	sum of squares	df	mean squares	F-ratio	Prob>F
between Mode	0.323	2	0. 162	0.556	0.575
between Check size	0.70	5	0.14	0.482	0.789
Interaction	0.715	10	0.0715	0.246	0.991
Error	43.6	150	0.29		
Total	45.3	167			

Thus only the variation of -ve PERG amplitude shows a significant dependence, at the 5% level, on the stimulus presentation mode. The mean -ve PERG transient of individual data is presented graphically for each mode with ± 1 sem error bars in figures 7.6, 7.7 and 7.8. For ease of comparison a composite display of the mean data has been compiled in Figure 7.5. When the composite data is examined there appears to be a tendency for the pattern appearance mode of presentation to result in lower amplitude PERGs at low spatial frequency.

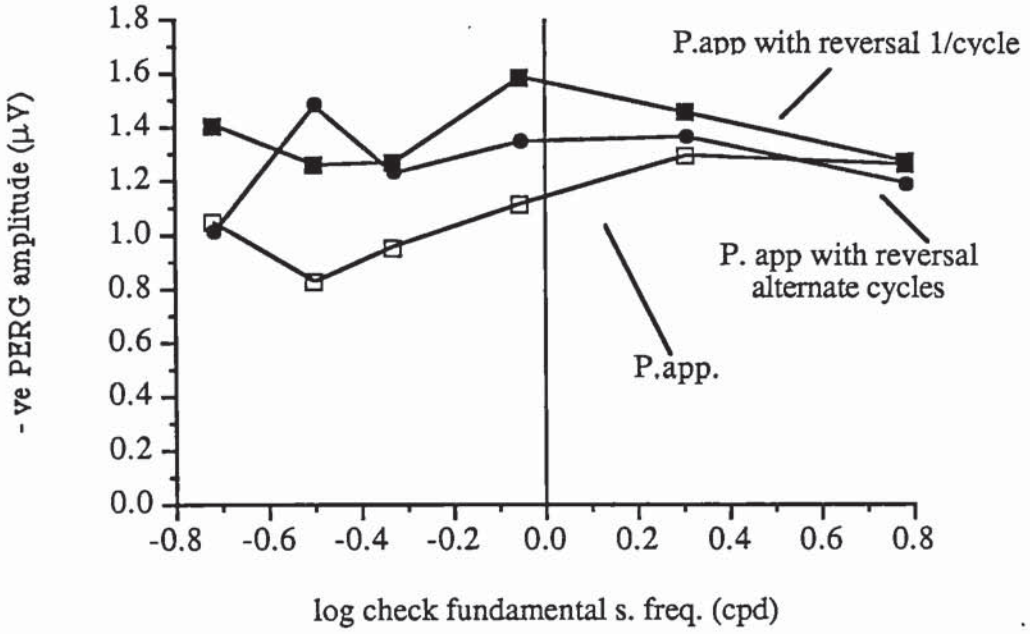

Fig 7.5 Composite graph comparing the mean -ve PERG amplitude of individually measured signals evoked by each presentation mode.

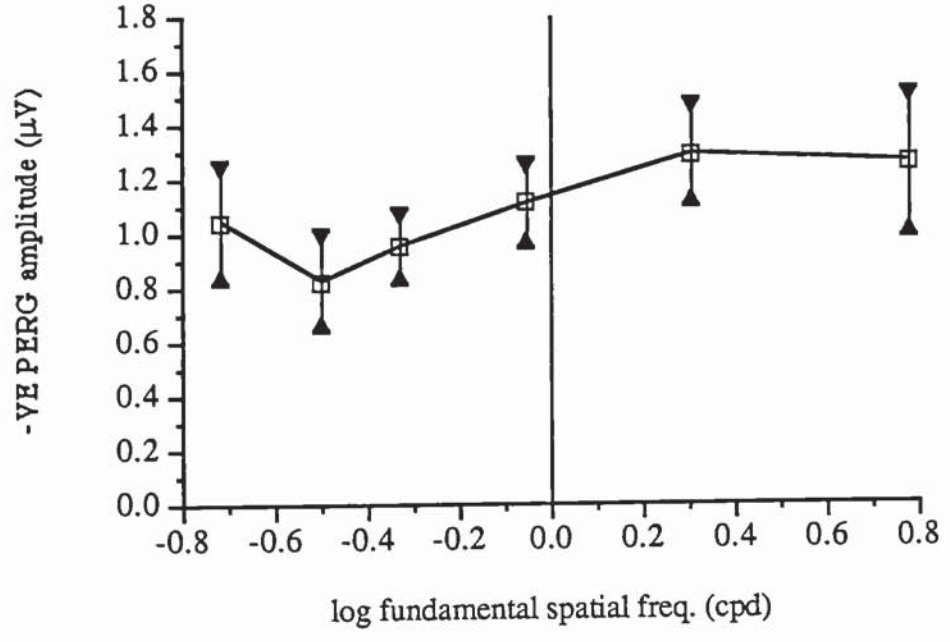

Fig 7.6 Mean -ve PERG amplitude evoked in the pattern appearance mode shown as a function of spatial frequency with ± 1 sem.

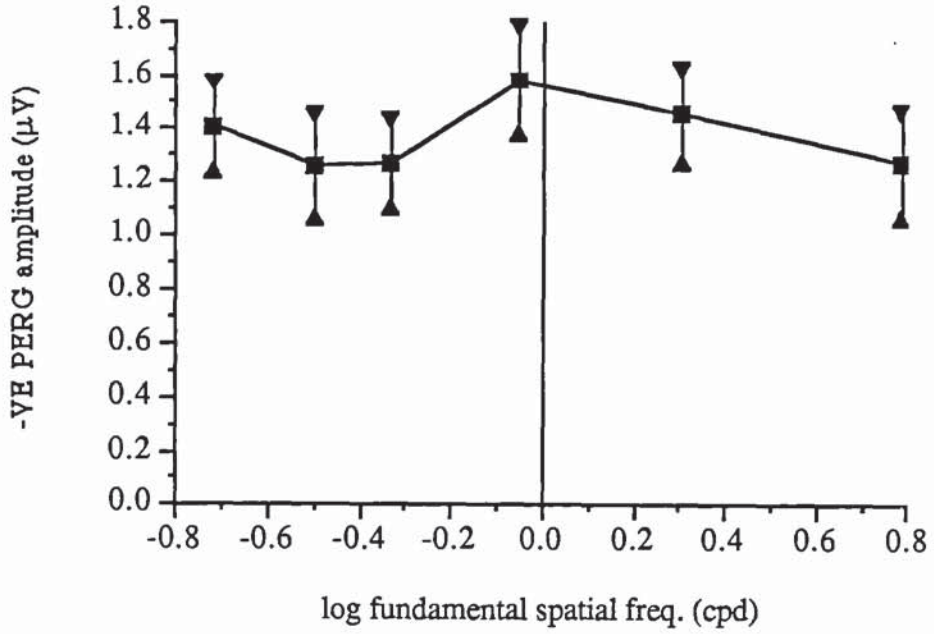

Fig 7.7 Mean -ve PERG data obtained when the pattern appears with a phase reversal every cycle.

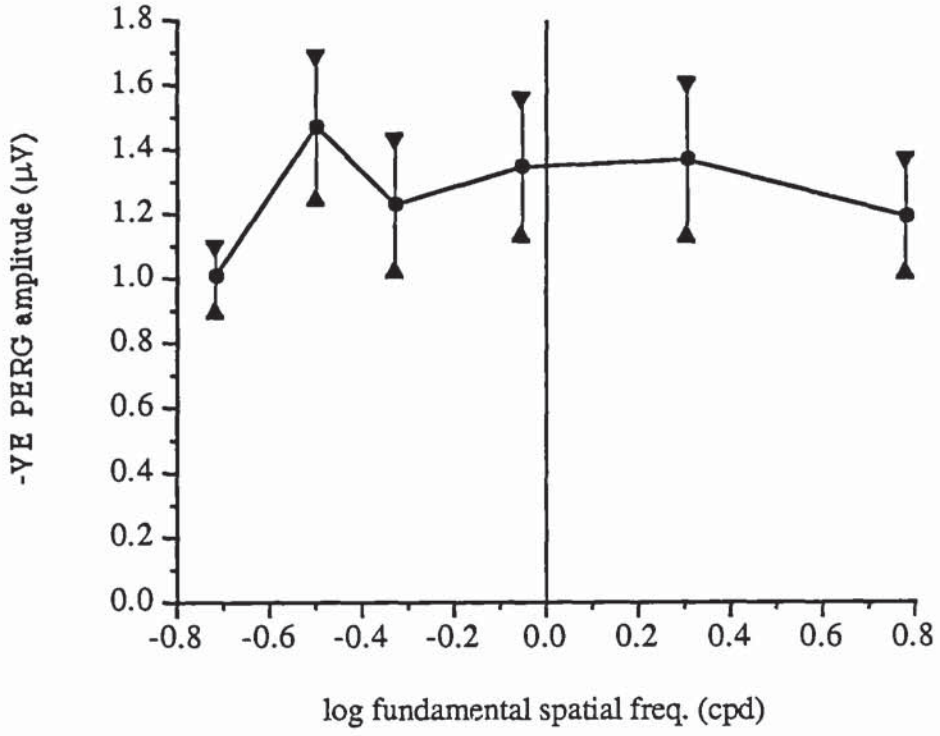

Fig 7.8 Mean -ve PERG amplitudes obtained when the pattern appears and reverses every alternate cycle.

There is very little variation in PERG amplitude across the three methods of stimulus presentation, particularly at higher spatial frequencies. There is a tendency for the devised paradigm, 'pattern appearance with reversal every alternate cycle', to result in PERGs of intermediate amplitudes. However this paradigm results in a larger amplitude response at 134' arc. This was not the result of the inclusion of a single large individual response as evidenced by the similar sized error bars. A change in contrast can generate the impression of movement and phase reversing checkerboards can result in the percept of individual or groups of checks moving (Spekreijse et al 1985). It is possible that in some way the stimulus paradigm and this particular check size interacted at this temporal frequency to evoke the larger response.

There is very little evidence of spatial tuning in the PERG data. This probably reflects the larger stimulus area employed, 15° diameter compared with 10° employed in the spatial tuning with peripheral angle study in Chapter 4. The field inevitably encompasses neurones of considerable dendritic field diameter variation and the response reflects the summation of pooled neuronal responses. A smaller central stimulus zone would be necessary to demonstrate spatial selectivity.

7.4 CONCLUSIONS

At higher spatial frequencies the stimulation paradigm devised to further randomise the effects of saccadic refixation movements results in the anticipated intermediate response amplitude. A slight tendency is exhibited by the -ve transient to low spatial frequency response attenuation. However at the lowest spatial frequency (NB n = 6) the amplitude appears to rise again. This observation is similar to that reported by Arden and Vaegan (1983) for pattern reversal spatial tuning in larger stimulus fields. The differences in the results elicited across the three modes of stimulation are small and the standard errors illustrated in figures 7.5, 7.6 and 7.7. imply that they barely achieve significance. The eye movements of fixation are therefore unlikely to have confounded the spatial tuning study.

CHAPTER 8

THE EFFECT OF PUPIL SIZE ON THE PATTERN ERG

8.1 INTRODUCTION

Optical degradation and intraocular light scatter are determined in part by pupil size (Campbell and Green 1965). The analysis of the pattern specific response described in Chapters 4 and 5 was based on MTF data for a mean pupil size of 4.9mm (Campbell and Gubisch 1966). A decrease in pupil size will reduce light scatter by minimizing the ocular aberrations that degrade the retinal image. A smaller pupillary area thus reduces the contrast attenuation of the retinal image. PERGs of larger amplitude would be consequently anticipated, particularly in response to high spatial frequency patterns. At pupil diameters of about 2.3 mm the eye approaches the optimum optical situation. Any smaller, e.g. 1.8mm, the eye is diffraction limited and the quality of the retinal image is degraded once more. In the diffraction limited condition the eye's MTF approaches a linear function (Charman 1983).

At a constant level of adaptation the neural tuning of a particular retinal area will be the same for different pupillary diameters, even though the amount of optical degradation will alter. When optical degradation is correctly compensated for in the computed retinal illuminance response the tuning function of the pattern specific component can be extracted from the PERG. However the correction for smaller pupils will incur less computational error as the function approaches linearity, than for larger pupils. If the extracted PSR tuning functions are the same for different pupillary diameters, the MTF equations and calculations used in the spatial tuning study will be partially validated.

8.2 METHOD

8.2.1 Topical miotic

Ophthalmic drugs employed in PERG studies to change the pupil size often affect the ciliary muscle and consequently the accommodation mechanism (Korth 1983; Baker

and Hess 1984). Accurate focusing can be compromised in these cases. To produce miosis the sphincter pupillae must be excitated or the dilator inhibited. The former receives parasympathetic innervation the latter predominantly sympathetic innervation. Parasympathomimetics e.g. pilocarpine (Holder and Huber 1983) can result in ciliary muscle spasm (O'Connor Davies 1976). Alpha adrenergic antagonists act on the dilator pupillae and are advantageous because they have no effect on the depth of the anterior chamber and evoke less posterior vector force compared with parasympathomimetics acting on the ciliary muscle (Potter 1981; Saheb 1982).

The alpha adrenergic antagonist thymoxamine was therefore selected as the most suitable miotic. Its maximal pupillary response occurs ≈ 60 minutes after instillation and it has a half life of 10 hours (Lee et al 1983). However the normal human pupil has a variable response to thymoxamine. The variability is due to individual subject differences in drug response as well as differences in the resting sympathetic tone to the pupil that occur even under standard conditions of illumination (Lee et al 1983). The minimum and maximum effective concentration of thymoxamine are 0.01% and1.3% respectively. It is most frequently employed in 0.5% concentration (Smith and Nephew single dose applicators - Minims).

8.2.2 Retinal illuminance

For the two experimental conditions, natural and miotic pupils, to be comparable retinal illuminance must be equated. Retinal illuminance is proportional to pupil size. The reduction in pupillary area will give the percentage reduction in illuminance. A pilot study was conducted to assesss how small the pupil diameter might be after the administration of thymoxamine 0.5%. An initial instillation of benoxinate 0.4% was followed by two drops of thymoxamine 0.5% separated by 5 minutes. Benoxinate is known to improve the passage of a drug across the cornea (O'Connor Davies 1976). It was estimated that the likely reduction in diameter was of the order of 4.5 mm to 2.5 mm.

Using the equation:

$$Se = 1/4\ \pi\ d^2 \left\{ 1 - 0.085\ (d^2/8) + 0.002\ (d^4/48) \right\}$$

the effective pupillary area Se, corrected for Stiles Crawford apodisation was calculated for each pupillary diameter d (Le Grand 1968).

When the luminance L is known the retinal illumination level E = Se x L

ie. the product of pupillary area and luminance;

for $d_2 = 4.5mm$ $Se_2 = 12.2$ sq mm and for $d_1 = 2.5mm$ $Se_1 = 4.82mm$

$$[4.82\ x\ L\ ] / [12.2\ x\ L] = 39.5\%$$

thus E1 = 39.5% E2, a neutral density filter that reduces the transmission to 40% is required before the natural pupil, equivalent to a Wratten neutral density filter ND 0.4. In this way contrast is maintained and the overall retinal illuminance is the same in each condition. Thus the level of retinal adaptation should similarly be constant.

8.2.3 Pupil measurement

There are inherent difficulties in preventing pupillary reactions during and due to the measurement process. A simple subjective method of pupil measurement employs a Scheiner disc with twin pinholes. When this is held close to the eye two entopic images of the pupillary aperture are seen. These images may be separated or overlapping; they will just abutt one another when the distance between pinhole centres equals the pupillary diameter. An alternative technique adapted the advantages of an automated infra red optometer - the Canon Autoref R-1 (a detailed description of this instrument is given by McBrien and Millodot 1985). The instrument target is illuminated with infra red light. Light from the instrument is reflected into the test eye via an angled semi silvered mirror thus affording the subject a largely unrestricted field of view, in the horizontal plane. Using an infra-red tele converter the subjects eye can be seen on a monitor screen in visible light. Having calibrated dimensions on the screen with a mm ruler it was possible to measure the pupil size from the monitor under reasonably 'normal' viewing conditions.

The subjects' pupils were measured by both techniques. When using the pupil gauge they were requested to fixate the pattern projected on the diffusing screen in the laboratory situation. Measurements taken from the Canon Autoref R-1 where taken when subjects viewed a black and white Maltese Cross, of 16 elements, at 100 cm. The target had been designed as a fixation control in ametropia (Dunne 1987), and was back illuminated at an approximately equivalent level to the projection screen. The mean of several readings were taken before and after administration of the drugs. Generally there was good agreement between the two measures, although the degree of accuracy for either technique is likely to be modest (Bennett and Rabbetts 1984).

8.2.4 Protocol

10 subjects participated in the study. Checkerboards were presented using the optical projection system already described. The pattern appeared for 105ms and disappeared into a uniform field of mean luminance for 105ms. The pattern phase shifted with every alternate appearance. This paradigm has been more fully described in Chapter7. A circular stimulus zone subtending 15° was surrounded by a large white mask of mean luminance 120 cdm^{-2} subtending 65°. The viewing distance was 100cm. The recording electrode placement was the same as in previous studies - a DTL electrode referenced to ipsilateral outer canthus. The recording bandwidth was 0.5 -70 Hz, the recording epoch was 200 ms. All subjects wore spectacle corrections if appropriate. The neutral density filter was mounted in a full aperture trial lens holders and placed in a trial frame. Subjects were instructed to fixate a target positioned at the intersection of four checks in the centre of the screen. The signals were group averaged, unfortunately part of the data of the tenth subject was lost due to computer failure during analysis, therefore n =9.

8.3 RESULTS

The group averaged PERG waveforms for each condition have been displayed in Figure 8.1. Displayed graphically as a function of spatial frequency the responses obtained from the miotic eye were slightly greater than from the natural pupil condition

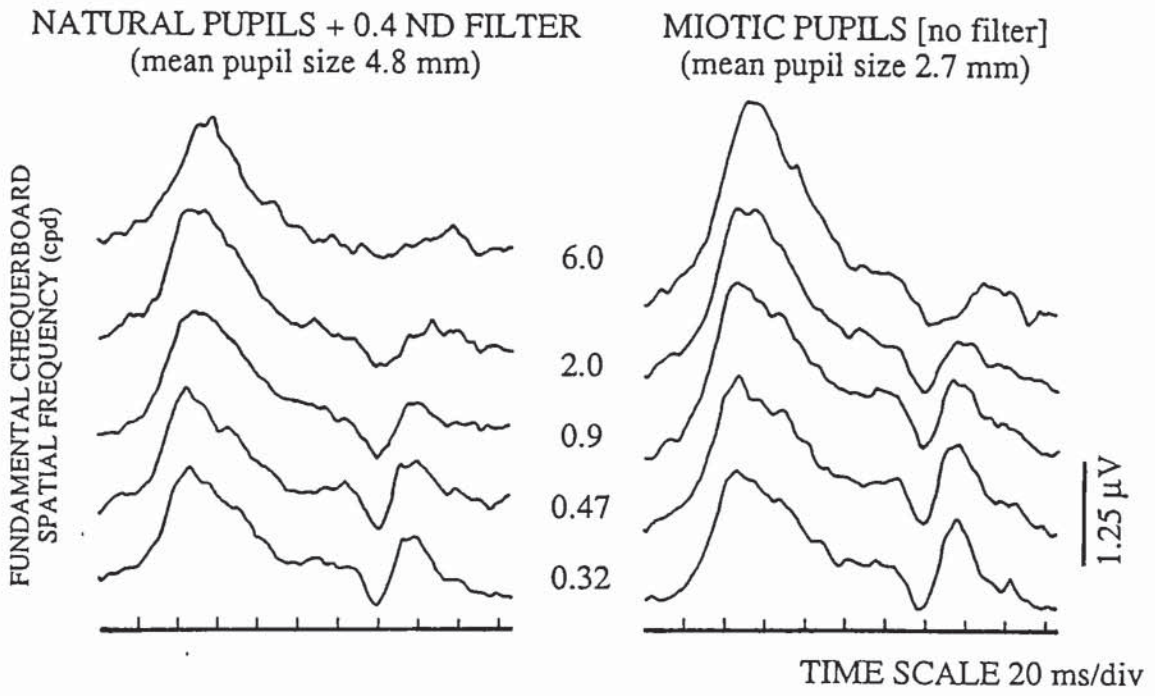

Fig 8.1 Group Averaged PERG waveforms (n=9), recorded with natural pupils with a 0.4 ND filter (mean pupil diameter 4.8 mm) and with miotic pupils without ND filter (mean pupil size 2.7 mm).

particularly at the highest spatial frequency. Figures 8.2 and 8.3 show the group averaged positive and negative PERG onset amplitude variation with spatial frequency.

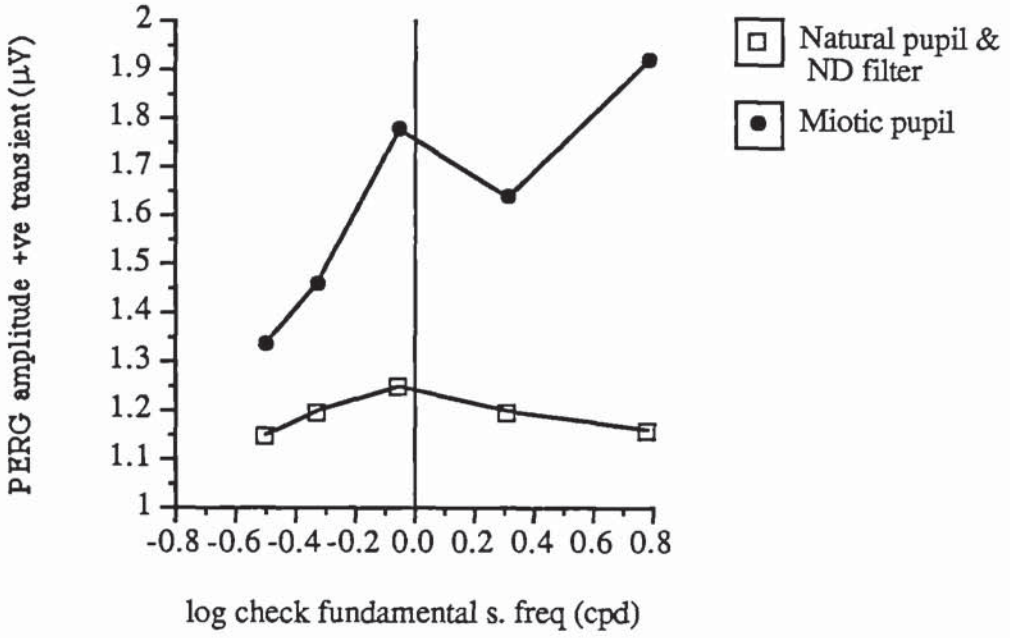

Fig 8.2 **Group averaged +ve PERG** amplitude plotted as a function of log check spatial frequency.

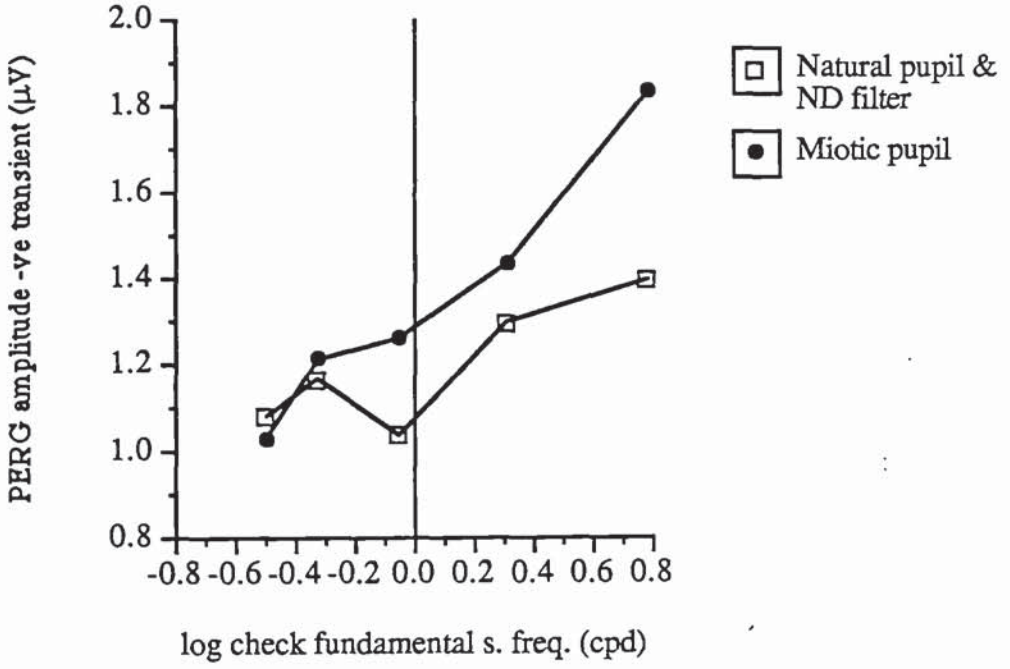

Fig 8.3 **Group averaged -ve PERG** amplitude displayed as a function of spatial frequency. As predicted the PERG has a greater amplitude at the high spatial frequency range in the miosed condition ≈ 0.4 μV

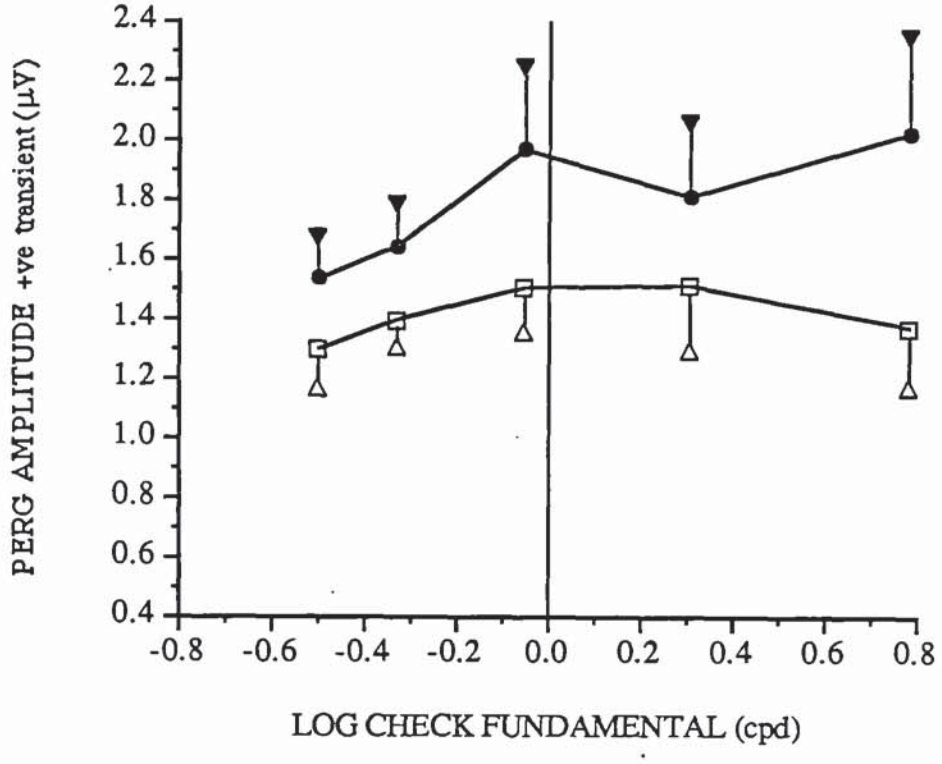

Fig 8.4 The **mean +ve PERG** amplitude of the individually measured traces is displayed as a function of spatial frequency. Error bars = 1 sem (n=9)

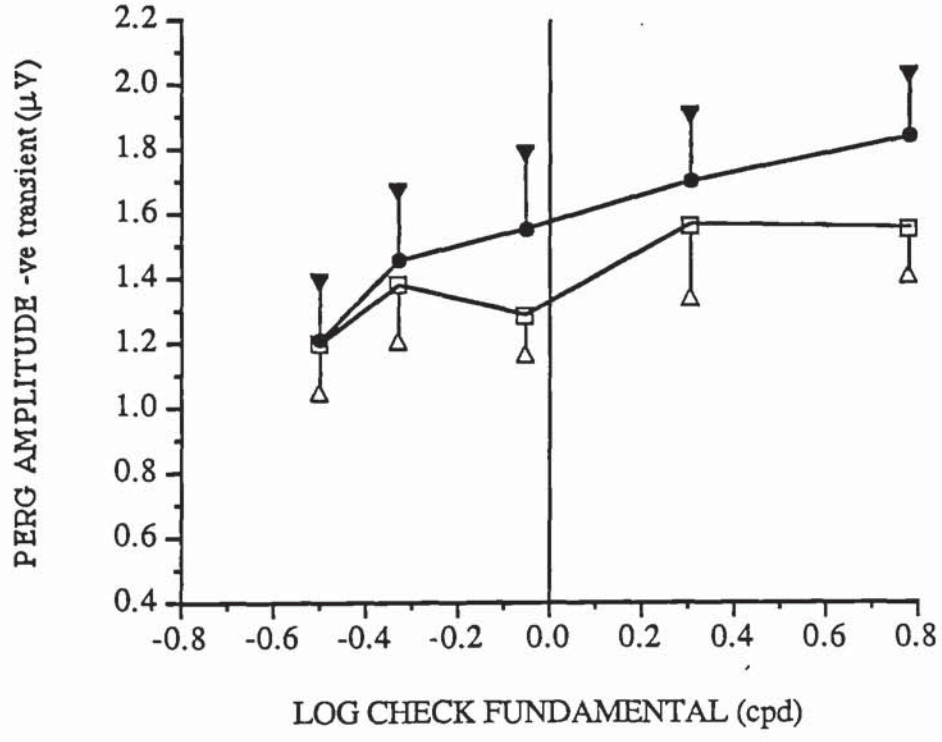

Fig 8.5 The **mean -ve** transient PERG amplitude of the individual data is plotted as a function of fundamental chequerboard spatial frequency (cpd).

Figures 8.4 and 8.5 relate to the mean of the individually measured +ve and -ve transients which are displayed with 1 sem error bars. In all figures the *Closed symbols* relate to data recorded from eyes with miosed pupils and the *Open symbols* to data obtained with 0.4 ND filter in front of the natural pupils to equalise retinal illuminance.

The space averaged temporal contrast attenuation factor STCAF, corresponding to the mean pupil size in the natural and miosed condition were calculated for pattern appearing checkerboards of 75% contrast from MTF data collated by Jennings and Charman (1974). The derived two parameter equation was the same as that derived from Campbell and Gubisch's (1966) data using Johnson's (1970) graphical method. Thus for a 2.5mm pupil the modulation transfer function was expressed by the formula;

$$MTF = \exp - (f/15)^{0.9}$$

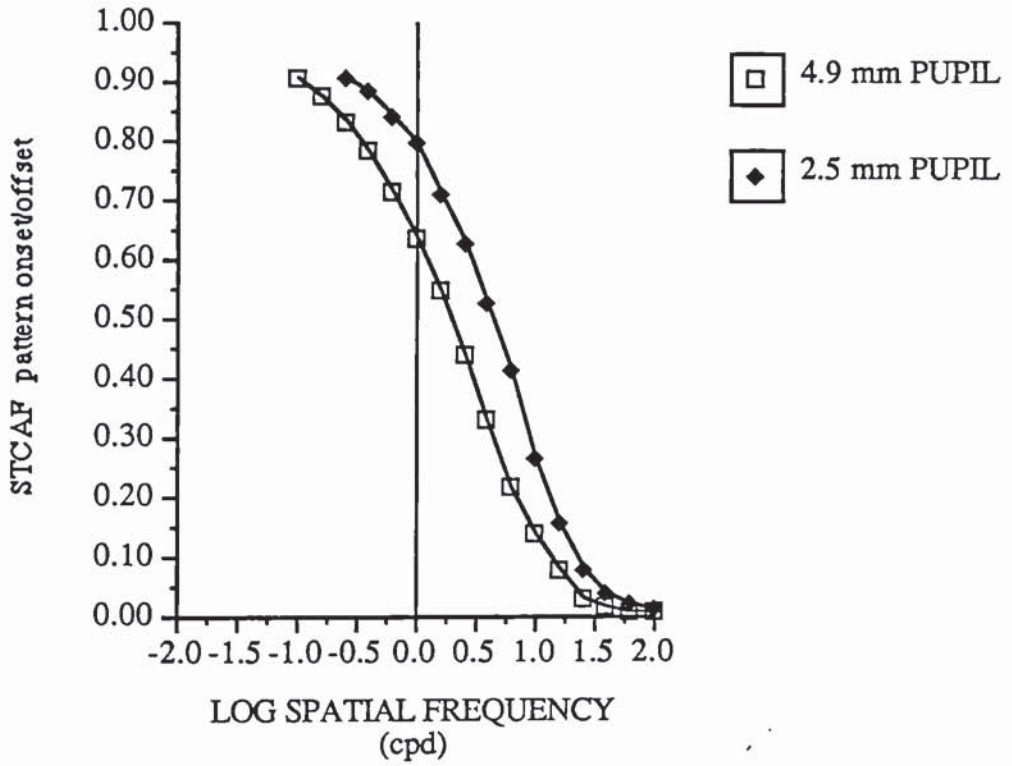

Fig 8.6 Graph describing the change in space averaged temporal conntrast attenuation factor with spatial frequency and pupil size. (NB the spatial frequency refers to the check side measurement not the fundamental)

The Fourier transform of the checkerboard was then filtered by this equation and the retinal illuminance profile resynthesised from the filtered harmonics. A graph showing the computed space-averaged temporal contrast attenuation factor, STCAF, for 2.75mm and 4.9mm pupil diameters is shown in Fig 8.6.

The lowest spatial frequency PERG was used to derive the retinal illuminance response for the other spatial frequencies and the pattern specific responses were extracted from the PERG . The traces are shown in Figures 8.7 and the measured +ve and -ve PSR amplitudes are shown in Figures 8.8 and 8.9 respectively.

The group averaged miotic PERG data displayed in Figures 8.2 and 8.3 demonstrates a slight low spatial frequency attenuation which is more apparent for the -ve transient. It can be seen from the graphs that the PSR amplitudes obtained with miotic and natural pupils are more closely related than the PERG amplitudes in each condition. (cf Figs 8.2 and 8.7; figs 8.3 and 8.8) The group averaged data was subjected to a paired t-test. The +ve and -ve amplitudes in the miotic and natural pupil group were significantly different.

+ve PERG amplitude: t statistic = 4.75, df 4, p = 0.009

-ve PERG amplitude: t statistic = 2.87, df 4, p = 0.046

When the subtracted PSR is similarly analysed the difference is no longer significant.

+ve PSR amplitude: t statistic = 1.51 df 4, p = 0.204

-ve PSR amplitude: t statistic = 0.64 df 4, p = 0.557

The subtracted PSR illustrated above is not however the iso-contrast response (see Chapter 5). Thus an additional correction factor would tend to equalise the amplitudes in each condition a little more; the correction factor being greater for the 4.5mm natural pupil than the 2.5mm miosed pupil.

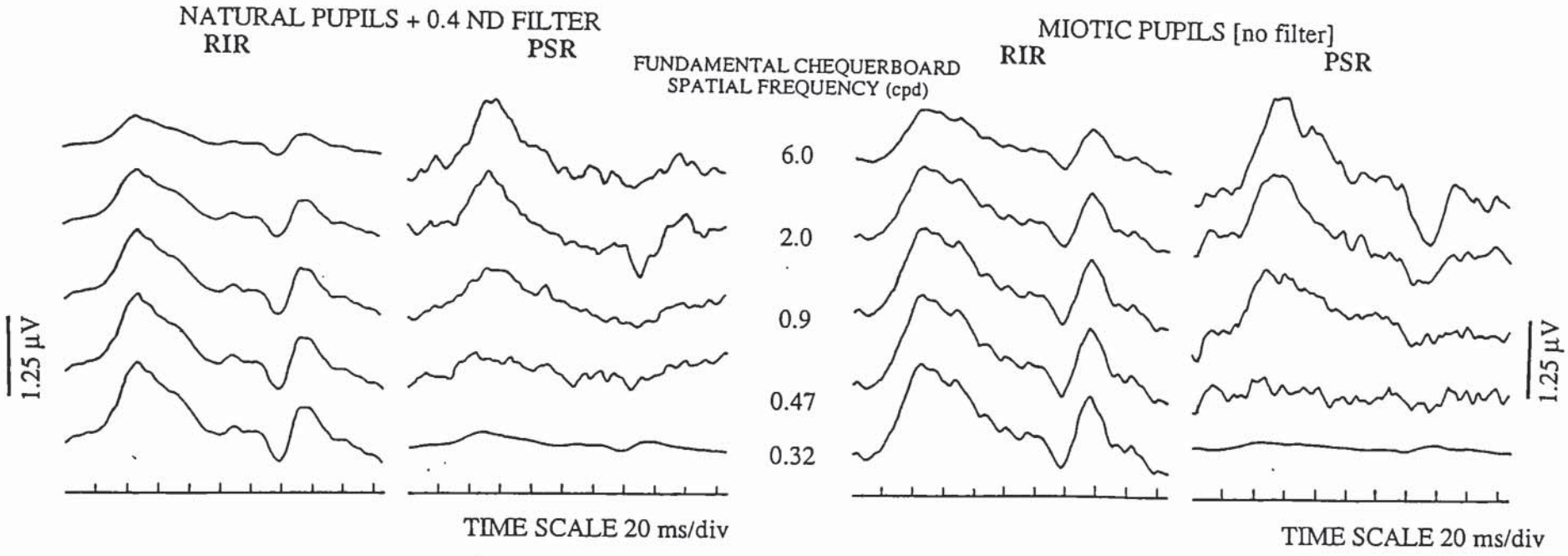

Fig 8.7 Retinal illuminance responses RIR, computed from the group averaged signals (recorded under equi-illuminance conditions) shown in Fig 8.1, and the subtracted pattern specific responses PSR, are displayed for natural and miotic pupils.

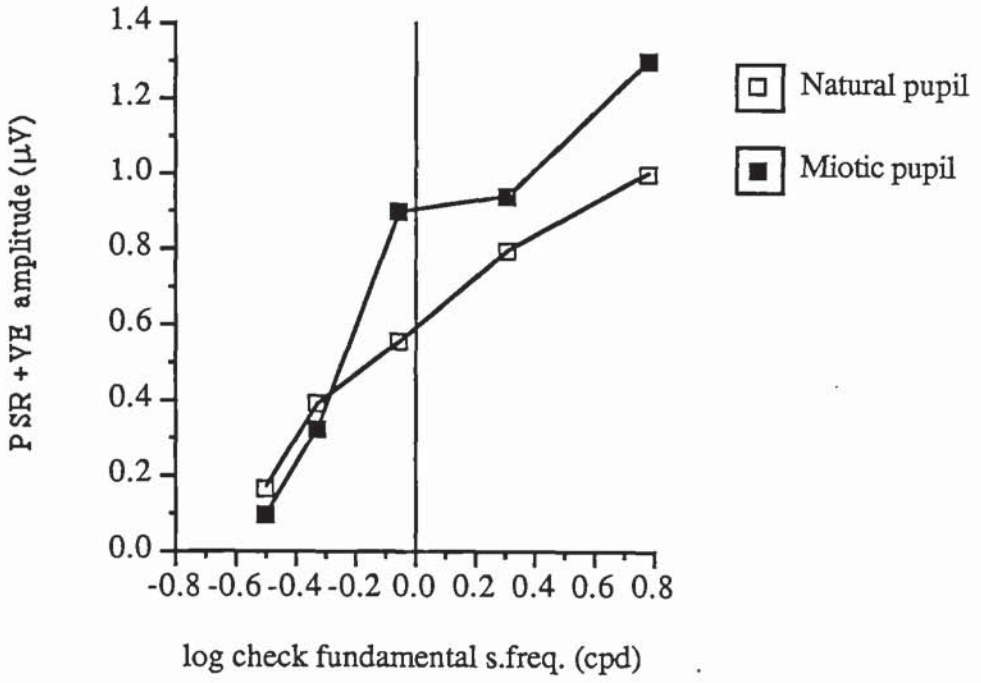

Fig 8.8 **PSR +ve** transient for the miotic and natural pupil condition plotted as a function of check fundamental spatial frequency.

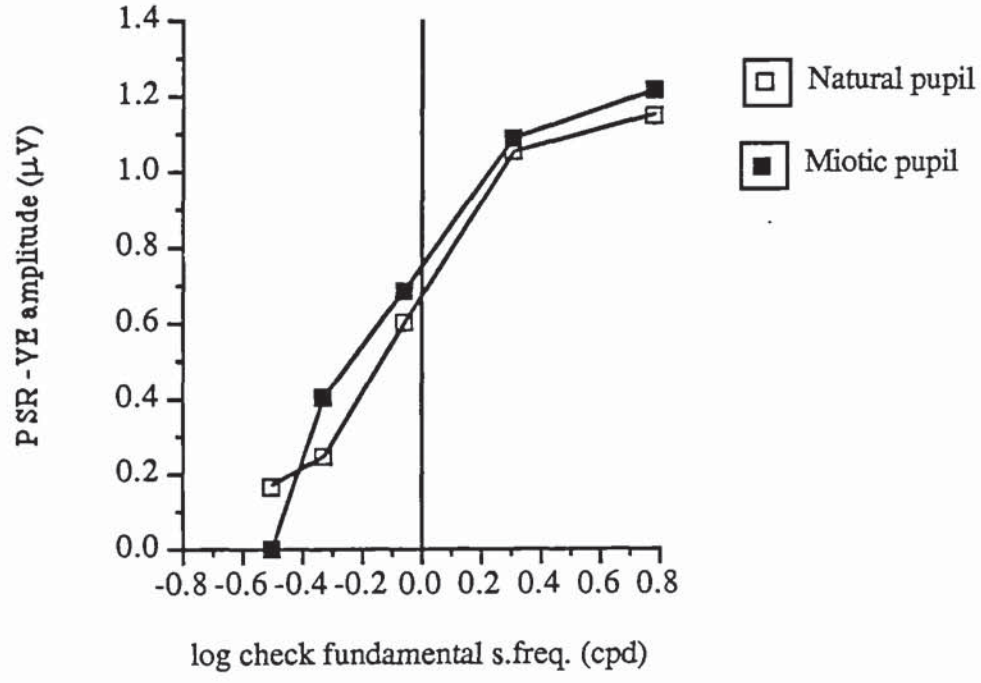

Fig 8.9 **PSR -ve** amplitude as a function of check fundamental spatial frequency

Any approximation in pupil size measure is likely to err on the side of underestimating the filter required and is counterbalance by the slight dilation that may be expected when the ND filter is placed in front of the natural pupils. The PERG data is unlikely therefore to be prejudiced in favour of the small pupil condition.

8.4 CONCLUSIONS

These data affirm that the technique of analysis is based on reasonable assumptions. Thus recording with equi-retinal illuminance, but smaller pupil size will increase the amplitude of the recorded PERG. The application of an appropriate space averaged contrast attenuation factor for pupil size results in pattern specific responses of comparable amplitude in each pupillary condition. These results suggest that the effects of image degradation have been correctly assessed in the MTF computations and further validates the proposed analysis technique.

CHAPTER 9

REVIEW OF RESULTS

9.1 REVIEW of EXPERIMENTAL STUDIES

The retinal origin of the pattern ERG, (PERG), has been the subject of considerable debate. The reduction of PERG amplitude in certain ophthalmological conditions supports the proposal of ganglion cell involvement, but the interpretation of this evidence is influenced by additional aetiological factors (e.g. Porciatti et al 1984; Holder 1987). A technique that examines the function of proximal retinal layers would have significant clinical application in the investigation of retinal disease mechanisms and as a prognostic indicator or monitor of treatment. Therefore to further elaborate the origin of the PERG it is important to construct a profile of its characteristics by complementary parametric manipulations, particularly in the spatial domain where comparisons with existing knowledge of retinal cell anatomy and receptive field physiology can be made. This was the underlying rationale for the investigations carried out in the course of this thesis.

The spatial sensitivity of the PERG was studied at different retinal eccentricities. In agreement with several other studies the PERG signal was found to exhibit a broad bandpass spatial selectivity (e.g. Arden and Vaegan 1983; Hess and Baker 1984a; Berninger and Schuurmans 1985). Pattern specific responses generated by elements having spatially antagonistic receptive fields are characterised by bandpass spatial tuning (Padmos et al 1973). Therefore the results presented and discussed in Chapter 4 may implicate the contribution of ganglion cells, although bipolar cells are also recognised to have receptive fields of this nature, albeit with slightly weaker surround antagonism (Kaneko 1973).

In Chapter 5, the amplitude of the PERG was found to exhibit a linear relationship with stimulus contrast. The retinal image contrast of fine patterns is significantly reduced because of ocular aberrations and intraocular light scatter (Campbell and

Green 1965). When optical degradation is considered an anomaly becomes apparent in those studies in which low spatial frequency PERG response attenuation was not observed. Reimslag et al (1985), for example, found that the PERGs elicited by a high and low spatial frequency pattern had similar amplitudes, yet the retinal contrast of the finer pattern must have been substantially reduced. If the PERG was an illuminance response solely dependent upon temporal contrast the response to the finer pattern should have been significantly attenuated. The supposition of Reimslag et al (1985) [see also Spekreijse et al 1973; Sherman 1982; Ringo et al 1984] that the PERG reflected the summation of local retinal responses to luminance increments was therefore examined more carefully.

Optical degradation is described by the the eye's modulation transfer function (MTF) and in this study was expressed by equations fitted to the data of Campbell and Gubisch (1966) using models proposed by Johnson (1970,73) and Jennings and Charman (1974). The effect of optical degradation on the square wave and chequerboard patterns used in this study was assessed by filtering their Fourier transforms by the MTF equation, [appropriate for the mean pupillary diameter]. The filtered pattern harmonics were resynthesised to produce an illuminance profile of the retinal image (Drasdo and Cox 1987). The temporal (De Lange 1958) and spatial contrasts, defined by the Michelson (1891) equation for spatially repetitive stimuli, were then calculated from the image illuminance profile. The contrast degradation of each pattern was expressed as a space-averaged temporal contrast attenuation factor (STCAF). This is a ratio of the temporal contrast of the degraded retinal image divided by that of a perfect image. Temporal contrast was calculated by integration for each stimulus contrast level; a fixed ratio between spatial and temporal contrast does not occur in the pattern onset presentation mode. (refer to section 4.5 - Fig 4.12). The space-averaged temporal contrast attenuation factor may then be used to predict the response to local illuminance stimulation at each spatial frequency.

For the purposes of computation the PERG recorded to a low spatial frequency pattern

was assumed to represent the morphology and amplitude of a retinal illuminance response. In view of the observed linearity of the PERG amplitude to stimulus contrast, this PERG signal was attenuated by the STCAF to estimate the amplitude of retinal illuminance response likely to be elicited by finer patterns. The amplitude of the computed retinal illuminance responses (RIR) declined monotonically with increasing spatial frequency. This certainly did not resemble the PERG spatial frequency function. The RIR signals were therefore subtracted, at a fixed latency, from the PERGs recorded over a range of pattern sizes in different retinal zones. The residual waveforms are assumed to represent an additional response that is pattern specific, dependent upon spatial frequency and spatial contrast. The extracted pattern specific response displayed an enhanced bandpass spatial selectivity. However in order for this to be an iso-contrast response an additional correction factor compensating for the loss of spatial contrast was also applied. The finally corrected PSR responses for chequerboard stimulation have been illustrated in Chapter 5 (figs 5.10, 5.11and 5.12.)

The spatial tuning function of the corrected pattern specific response peaked at lower spatial frequencies with increasing retinal eccentricity. To illustrate this the peak PSR spatial cycle was plotted as a function of mean radial peripheral angle and fitted with a straight line by the method of least squares (Fig 5.15). Although shallower, the gradient of the regression equation was compatible with gradients used to describe the variation of ganglion cell receptive field centre separation across the retina (Drasdo 1977; Rovamo and Virsu 1979). The inclusion of a weaker, spatially sensitive response from bipolar cells, whose numbers and hence receptive field centre separation ($1/\sqrt{n}$) are more evenly distributed across the retina, could account for the shallower gradient. The linearity of the regression function was clear and it would appear reasonable to extrapolate to ascertain the optimum foveal stimulus. This predicts an optimum size check of 3.5' arc.

Linear functions of this form have long been used to relate human psychophysical data to retinal eccentricity and estimated receptive field centre separation (e.g. Wertheim

1894; Weymouth 1958; Rovamo 1978). The optimum foveal stimulus was closely compatible with psychophysical data (see section 5.4), and also with known ganglion cell receptive and dendritic field dimensions. However data regarding the variation of different classes of ganglion cell with eccentricity is variable and incomplete thus a relationship between PSR and ganglion cell type could not be confidently inferred. (e.g. Perry et al 1984; Rodieck et al 1985; Shapley and Perry 1986).

A more direct comparison of the relative amplitudes of the corrected PSR and computed RIR from the three stimulus fields has been made with the corresponding volumes of three retinal cell lamina; the outer nuclear layer containing rod and cone nuclei, the inner nuclear layer containing horizontal, bipolar and amacrine cells and the ganglion cell layer containing ganglion cell nuclei. The thicknesses of the three nuclear layers have characteristically different distributions with retinal eccentricity: the outer nuclear layer remains fairly constant across the retina, the ganglion cell layer declines rapidly in the periphery whilst the inner nuclear layer declines at an intermediate rate (Polyak 1941). The variations in layer thickness, averaged across meridians were assessed from the radial sections of Van Buren (1963) and the volumes relating to each stimulus zone were calculated by spherical integration. The nuclear volumes were normalised on the central value for comparison with corresponding PSR and RIR amplitude data and displayed as histograms in Fig 5.16. The histograms illustrate the trend for the retinal illuminance response to relate to distal and inner nuclear retinal layers, as would be expected from flash ERG component analysis (Ripps and Witkovsky 1985). The corrected pattern specific response relates most strongly to the proximal layers. However there is also a correspondence between the negative transient of the RIR and the ganglion cell layer which suggests the conventionally recorded flash ERG may also contain ganglion cell activity. These findings provide further support for a proximal cell contribution to the pattern evoked retinal potential, particularly when the negative peak to peak response amplitude is considered. Armington's (1974) observation that the negative 'afterpotential' is greater with periodic patterns may therefore relate to the preferential stimulation of proximal retinal

elements. The latency of the negative component is also compatible with a more proximal locus of generation; it could relate to the delayed onset of inhibition of antagonistic receptive fields or because the negative component is due to the ganglion cells which are further along the neural chain of excitation.

The analysis technique to extract a pattern specific response from the PERG rests on a number of assumptions which are examined in the final three studies. Linearity and fixed response latency with contrast were demonstrated experimentally in the study described in Chapter 5. In Chapter 6 the retinal illuminance response (RIR) was shown to be a rectified response that seems to be approximately proportional to temporal contrast, as defined for pattern onset-offset stimulation by the Michelson equation (1891). It would therefore appear reasonable to use the retinal illuminance computations in the extraction of the pattern specific response.

A stimulation paradigm designed to examine the confounding effects of adaptation and afterimages inherent in the appearance mode of presentation was described in Chapter 7. The results suggest that at high spatial frequencies the presentation of a pattern that reverses position every alternate appearance cycle elicits a response of intermediate amplitude compared with responses evoked by 'static' pattern appearance and 'pattern appearance with a phase reversal every cycle'. The results were more ambiguous for lower spatial frequency patterns, and generally the local adaptation effects of pattern appearance stimulation did not appear significant. However the designed stimulation paradigm was used as a presentation method for examining the effect of pupil size on the PERG. The results are reported in Chapter 8. This experiment tested the validity and accuracy of the MTF derived correction factors used in the analysis technique. If the premise was incorrect pupil size, with equated retinal illuminance, would have a minimal effect on PERG amplitude. This was not the case. As anticipated the increase in retinal image contrast with smaller pupil sizes resulted in larger amplitude PERGs particularly at the higher spatial frequency end of the tested spectrum. Also the analysis technique demonstrated that the extracted PSRs, when finally corrected for

spatial contrast attenuation, would be similar in both conditions. However smaller computational errors are incurred as the MTF correction diminishes for smaller pupil sizes.

All these experiments suggest the technique described is an effective method of assessing the pattern specific component of the composite PERG. In a similar manner to the original ERG component analysis, e.g. Granit (1933), where the recorded response is viewed as an envelope of summated responses from different generators, the PERG is also regarded as a summation of activity from different retinal loci whose individual contribution may be selectively enhanced by certain stimulus parameters. Thus patterns of optimal spatial frequencies would promote response contributions from spatially selective retinal elements.

In summary this thesis reports the development of an analysis technique designed to extract a pattern specific response component from the recorded PERG signal. The pattern specific response is considered to reflect proximal retinal cell activity. In the present state of refinement the correspondence with ganglion cell data is tentative, but nonetheless striking.

9.2 PROPOSALS FOR FUTURE WORK

Evidence of human receptive field dimensions is significant in relation to many aspects of vision. A method for obtaining more accurate data of receptive field size has been described using the PERG and may be employed more rigorously by investigating the spatial sensitivity of the PERG and PSR with miotic pupils to minimise theoretical errors and presenting the stimulus in the way that reduces the possibility of spurious tuning due to the local adaptation effects. Stimulus fields may be selected to account for the marked naso-temporal asymmetry in retinal topography (e.g.the use of half field stimulation or obliquely oriented quadrants), and additional smaller, more specific areas stimulated. Field size would however be necessarily constrained by the areal dependence of the PERG amplitude. From this data a pattern whose spatial elements are scaled for optimum stimulation along the four principle meridians might be compiled. Concentric patterns composed of elements whose sizes increase with eccentricity have already been designed, but will require many experimental comparisons to elicit the optimal spatially varying gradient.

The complementary recording of visual field sensitivity and contrast sensitivity with the PERG would also glean information about the relative scaling of spatial detection in the visual pathway. Although the former are psychophysical assessments they have bases in ganglion cell representation and sampling. Additionally the correlation of positive field defects, of retinal or optic nerve origin, with amplitude, latency and morphology differences in different retinal locations would add important data to the nature of the pattern evoked response.

Pattern appearance presentation is not as clinically robust as pattern reversal presentation for which the contrast changes are greater and the PERGs evoked consequently larger. However pattern appearance presentation appears to be a more analytical method as exemplified by the difference in PERG ónset-offset behaviour and morphology. Response morphology alters with eccentricity and investigations under different luminance conditions and adaptation levels could elucidate the reasons for the

greater negative transient in the PERG in the central region.

Parametric manipulation of temporal factors, e.g. ramp time of stimulus presentation, rates of presentation, difference in appearance and disappearance duration, would be valuable in the further examination of the effects of after-images and response depression and also as a preferential stimulus for certain classes of retinal cell. Parallel pathways subserve the chromatic and achromatic systems, (e.g. Shapley and Perry 1986). Coloured stimuli could therefore distinguish the P-beta or parvo-cellular pathway from the P-alpha or magno-cellular pathway. Experiments designed to investigate the colour mechanisms of PERG recording through selective adaptation and isoluminance would also be interesting in the light of research that suggests that colour deficiencies may occur early on in some ophthalmological conditions. Different retinal networks may also be isolated in clinical conditions requiring medication known to effect the action or metabolism of retinal neurotransmitters; for example those subserving On /Off pathways (Ikeda and Robbins 1987). Application of the PERG in such conditions and the examination of the retinal response to illuminance decrements might elucidate the relative importance of the parallel On and Off retinal pathways in the generation of the PERG (Korth 1983; Evers and Gouras 1986; Porciatti et al 1987).

In conclusion a method of PERG analysis has been developed which separates the pattern specific and retinal illuminance responses so that their individual properties can be examined and manipulated parametrically. This should lead to a greater understanding of retinal circuitry under different conditions of stimulation and ultimately produce a more refined clinical test for retinal layer pathology.

APPENDIX 1.

SECTION 4.1.2 PATTERN STIMULATOR

Optical pathway

The optical system was mounted on a trolley designed for preferential looking assessment of newborns by C M Thompson (1987) and was equipped with a Rollei projector (model P353) with a 85mm focal length lens and halogen 24 volt, 150 watt bulb.

Images were projected onto the stimulus screen following reflection in a series of surface-silvered mirrors. The screen was made of clear perspex sheet covered with 'Intervue' rear projection PVC screen material *. Three reflections were required to provide adequate pathlength for a large stimulus screen, whilst maintaining a reasonably compact apparatus. The optical elements were positioned so that the total pathlength was 114 centimetres. Distances between successive elements were as follows; projector (nodal point) to M 1 = 7.5 cm., M 1 to M 2 = 22.5 cm., M 2 to M 3 = 31.0 cm., M 3 to screen = 53.0 cm.

Figures A.1 and A.2 drawn to approximately one-tenth scale, (by C.M Thompson), clarify the arrangement of components.

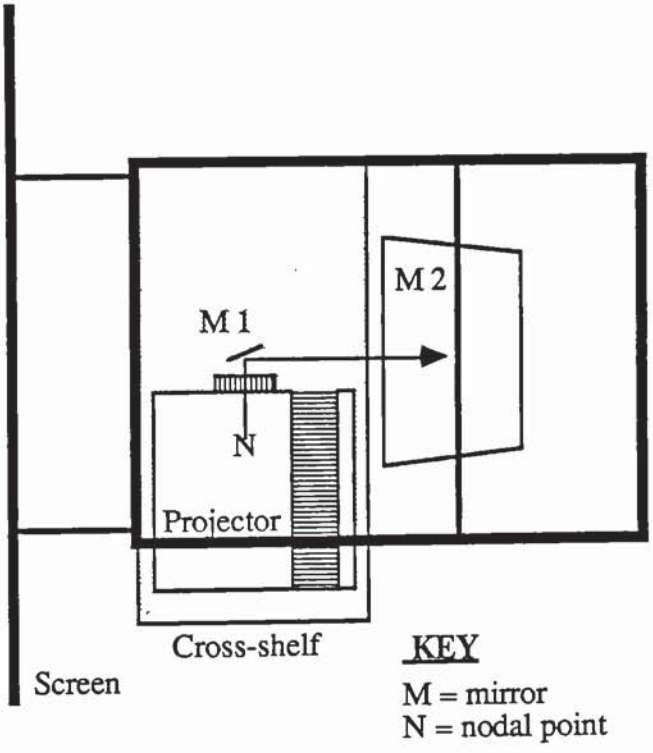

A.1 View of optical system from above.

*available from Chiltern Photographic Company Ltd, 92 Stroud Green Road, London

Mirror M 1 (measuring 3 x 4 cm) was positioned on a cross-shelf close to the projector lens and was mounted on a penmotor spindle and hence could be rotated around its vertical axis (a refinement required for pattern reversal stimulation). The projector protruded through the side of the trolley to facilitate slide access. Mirror M 2 was mounted vertically above M 3. Both mirrors measured 30 cm. square and were attached to round bars mounted through the side walls. They were adjustable about their horizontal axes.

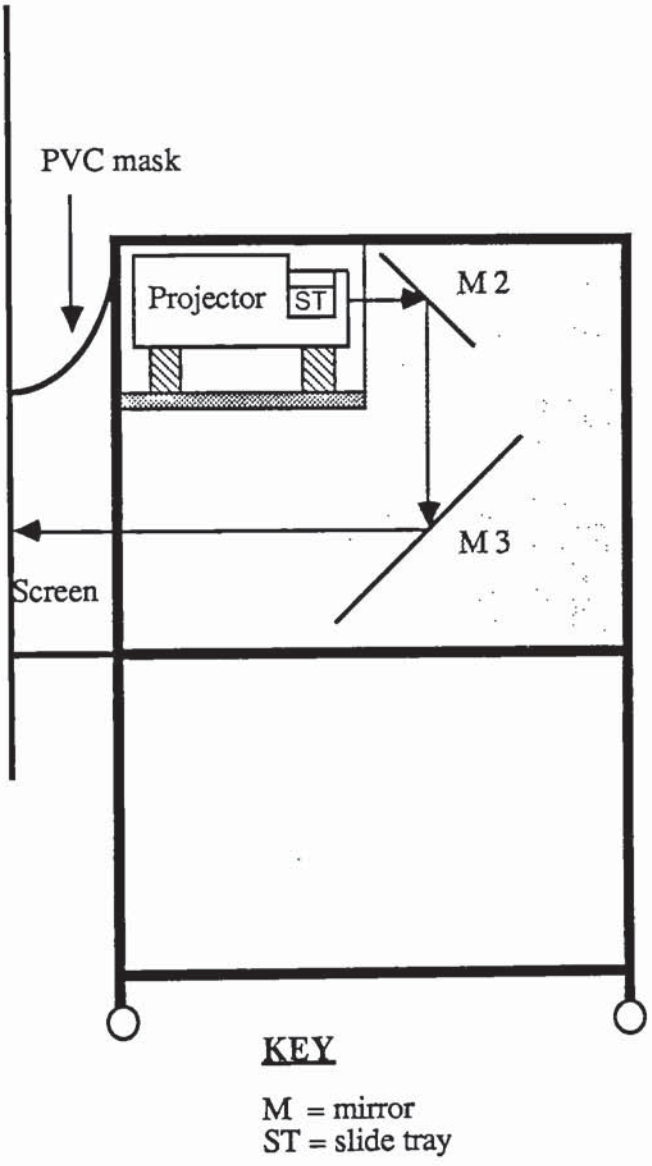

Fig 4.2 Side view of apparatus

SECTION 4.14 AMPLIFIER AND AVERAGER SETTINGS

Pattern onset ERG trace recorded to a chequerboard stimulus are shown in figure A.3 with the simultaneously recorded electrooculogram. The results were averaged an a Nicolet compact series averager between a bandpass of 1-100 Hz. The EOG was recorded with Ag cup electrodes positioned on the inner and outer canthi (Galloway 1975). The eye movement contamination that accompanies fixation was observed to be minimal. The effect of amplifier sensitivity was examined for the rejection of eye movement artefact and can be seen in the traces that the PERG is unlikely to be confounded by the EOG even at the lower sensitivity of 100 μV. An amplifier sensitivity was used throughout the study. The trace was selected as a typical individual example.

SECTION 4.2 METHOD

Experimental controls

a) A monocular stimulus run was incorporated to check for confounding volume conducted visually evoked cortical potentials. A.4. shows an example. This was conducted in all subjects and only one volunteer was rejected from the experiments because of a large contamination.

b) A run with a 50% transmission neutral density filter was carried out to examine any luminance fluctuation due to the diffusing shutter scattering light. This was most noticeable in the peripheral zone A.5. However the error incurred is minimised by the subtraction procedure. If compared with the trace from the occluded eye in A.4.which is displayed on the same gain the spurious signal is relatively small.

APPENDIX 2

SECTION 5.3.2

The normalised space averaged temporal contrasts for the pattern appearing 10', 30' and 7° 30' chequerboards for the range of stimulus contrasts used in this study are given below. The computed RIR and PSR waveforms in each condition are shown in A.6.

STIMULUS CONTRAST	7° 30' check	30'check	10' check
80%	0.901	0.617	0.229
65%	0.693	0.487	0.186
50%	0.515	0.367	0.142
30%	0.298	0.216	0.086
13%	0.126	0.092	0.037

Table shows normalised space averaged temporal contrast factors (STCAF) for pattern onset-offset checks of different stimulus contrast.

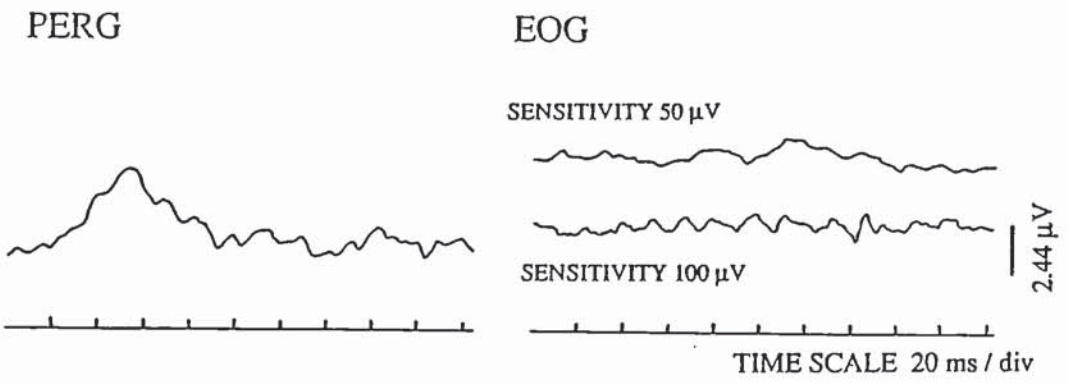

Figure A.3 Traces demonstrating the minimum contamination of pattern onset ERG by EOG at different amplifier sensitivities

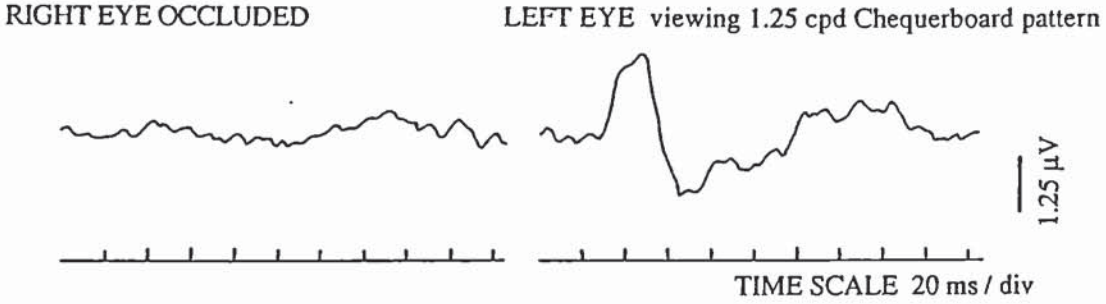

Figure A.4 Waveform recorded when eye is occluded. A control check for the confounding presence of volume conducted visual evoked cortical potential.

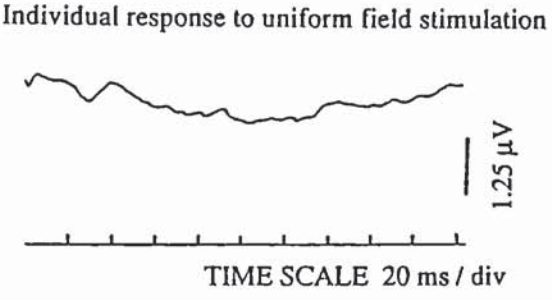

Figure A.5 A stimulus run without a pattern, but with the shutter in operation.

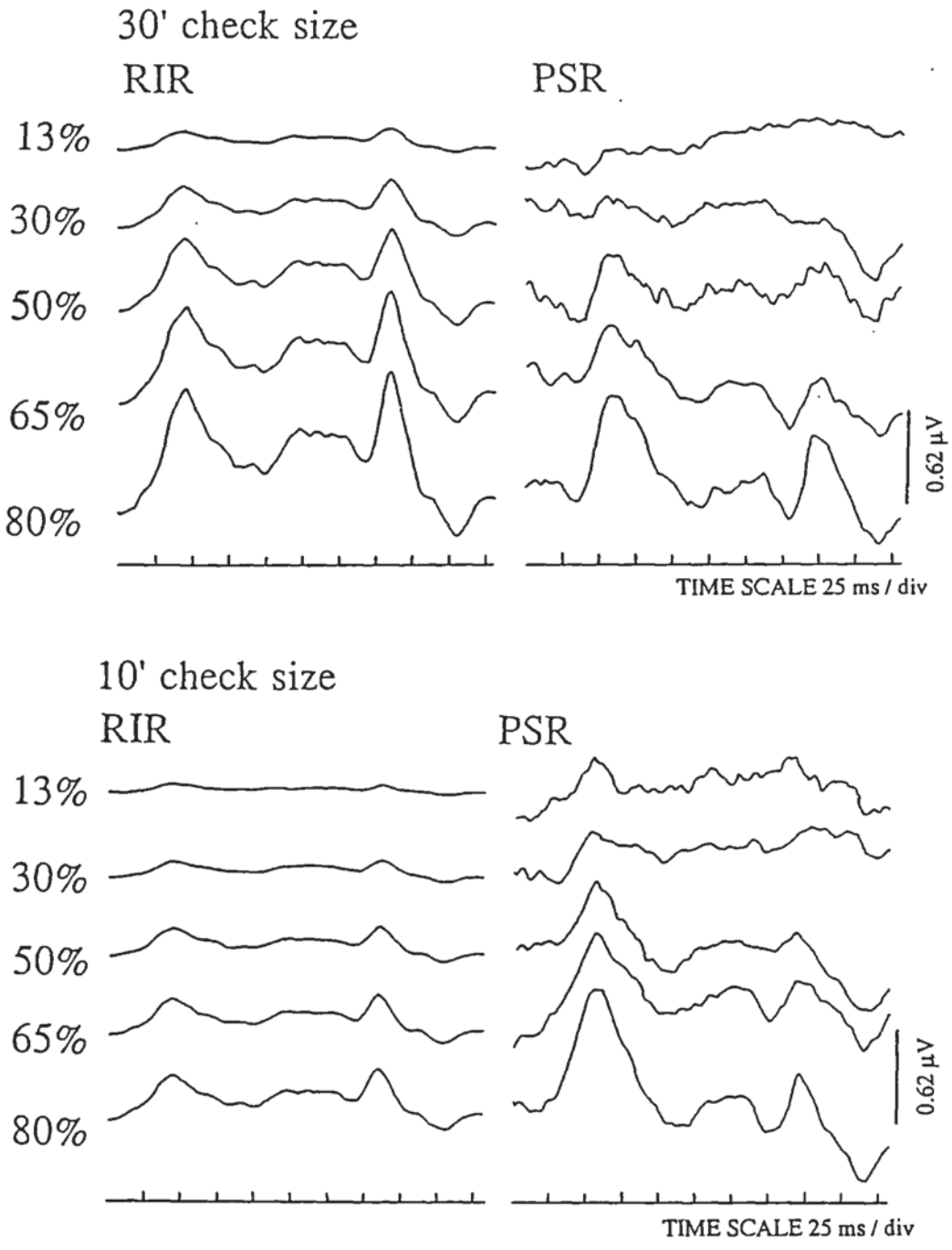

Figure A.6 Montage of group averaged traces displaying the computed RIR and PSR waveforms from pattern onset offset ERGs illustrated in Figure 5.1 in response to the presentation of 10' and 30' size chequerboard patterns at different levels of stimulus contrast.

APPENDIX 3

SUPPORTING PUBLICATIONS

1. Drasdo, N., **Thompson, D.A.**, Thompson, C.A. and Edwards, L.E. (1987)
   Complementary components of the pattern electroretinogram.
   Invest. Ophthal. Vis. Sci. 28, 158-162.

2. **Thompson, D.A.** and Drasdo, N. (1987)
   An improved method of using the DTL fibre in electroretinography.
   Ophthal. Physiol. Opt. 7. 315-319.

3. **Thompson, D.A.** and Drasdo, N. (accepted in press 1987)
   Computation of the luminance and pattern specific components of the bar pattern electroretinogram.
   Docum.Ophthalmol.,
   Presentation at the XXIV ISCEV Symposium, Palermo, Italy 1986.

4. Drasdo, N., Cox, W. and **Thompson, D.A.** (accepted in press 1987)
   The effects of image degradation on retinal illuminance and pattern responses.
   Docum. Ophthalmol.,
   Presentation at the XXIV ISCEV Symposium, Palermo, Italy 1986.

5. **Thompson, D.A.** and Drasdo, N. (1987)
   Evidence of spatial tuning in peripheral vision from the pattern electroretinogram.
   Ophthal. Physiol. Opt. 7, 93-94.

6. **Thompson, D.A.** and Drasdo, N. (1987)
   The pattern specific component of the pattern ERG and its spatial selectivity in peripheral vision.
   Abstr. poster presented at the Third International symposium of the Northern Eye Institute 1987, "Seeing, Colour and Vision".

REFERENCES

Adolph, A.R. (1985) Temporal transfer and nonlinearity properties of turtle ERG: tuning by temperature pharmocology, and light intensity. *Vision. Res.*, **25**, 4, 483-492.

Algvere, P. and Westbeck, S. (1972) Human ERG in response to double flashes of light during the course of dark adaptation: a Fourier analysis of the oscillatory potentials. *Vision. Res.*, **12,** 195-214.

Anstis, A.M. (1974) A chart demonstrating variations in acuity with retinal position. *Vision Res.*, **14**, 589-592.

Arden, G.B. Three components of the photocurrent generated in the receptor layer of the rat retina. In: vertebrate photoreception, (Eds, Barlow, H. and Fatt, P.) 141-158, Academic Press , New York. 1977.

Arden, G.B. (1985) Pattern ERG in amblyopia: clinical evidence of mode of generation. *Invest. Ophthal. Vis. Sci.*, **26**, 1649.

Arden, G.B. (1986) Uniocular recording of pattern ERG. *Vision. Res.*, **26,** 2, 281-286.

Arden, G.B., Carter, R.M., Hogg, C.R., Siegel, I.M. and Margolis, S. (1979) A gold foil electrode extending the horizons for clinical electroretinography. *Invest. Ophthal. Vis. Sci.*, **18**, 421-426.

Arden, G.B., Carter, R.M. and Macfarlan, A. (1984) Pattern and ganzfield electroretinograms in macular disease. *Brit. J. Ophthal.*, **68**, 878-884.

Arden, G.B., Granit, R. and Ponte, F. (1960) Phase of suppression following each retinal b-wave in flicker. *J. Neurophysiol.*, **23**, 305-314.

Arden, G.B., Hamilton, A.M.P., Wilson-Holt, J., Ryan, S., Yudlein, J.S. and Kurtz, A. (1986) Pattern electroretinograms become abnormal when background diabetic retinopathy deteriorates to a pre-proliferative stage: possible use as a screening test. *Brit. J. Ophthal.*, **70,** 330-335.

Arden, G.B. and Vaegan. (1983) Electroretinograms evoked in man by local uniform or patterned stimulation. *J. Physiol.*, **341**, 85-104.

Arden, G.B., Vaegan, and Hogg, C.R. (1982) Clinical and experimental evidence that the pattern electroretinogram (PERG) is generated in more proximal retinal layers than the focal electroretinogram (FERG). *Annals. N. Y. Acad. Sci.*, **388** 580-601.

Arden, G.B., Vaegan, Hogg, C.R., Powell, D.J. and Carter, R.M. (1980) Pattern ERGs are abnormal in many amblyopes. *Trans. Ophthal. Soc. UK.*, **100,** 453-460.

Arden, G.B. and Wooding, S.L. (1985) Pattern ERG in amblyopia. *Invest. Ophthal. Vis. Sci.*, **26,** 88-96.

Ariel, M. and Daw, N.W. (1982a) Effects of cholinergic drugs on receptive field properties of rabbit retinal ganglion cells. *J. Physiol.*, **324,** 161-185.

Ariel, M. Daw, N.W. (1982b) Pharmacological analysis of directionally sensitive rabbit retinal ganglion cells. *J. Physiol.*, **324,** 161-185.

Armington, J.C. The electroretinogram. Academic Press. 1974.

Armington, J.C. and Brignell, M. (1981) Effects of stimulus location and pattern upon the visually evoked cortical potential and the electroretinogram. *Intern. J. Neurosci.*, **14,** 169-178.

Armington, J.C., Corwin, T.R. and Marsetta, R. (1971) Simultaneously recorded retinal and cortical responses to patterned stimuli. *J. Opt. Soc. Am.*, **61,** 1514-1521.

Armington J.C., Gaarder K. and Schick A.M.L. (1967) Variation of spontaneous ocular and occipital responses with stimulus patterns. *J. Opt. Soc. Am.* **57,** 1534-1539.

Armington, J.C., Tepas, D.I., Kropf, W.J. and Henst, W.H. (1961) Summation of retinal potentials. *J. Opt. Soc. Am.*, **51,** 877-886.

Asher, H. (1951) The electroretinogram of the blind spot. *J. Physiol.*, **112,** 40P.

Baker, C.L. and Hess, R.F. (1984) Linear and nonlinear components of human electroretinogram. *J. Neurophysiol.*, **51,** 5, 952-967.

Barber, C., Cotterill, D.J. and Larke, J.R. (1976) A new contact lens electrode. *Doc. Ophthal. Proc. Ser.*, **13,** 385-392.

Barber, C. and Galloway, N.R. (1974) A pattern stimulus for optimum response from the retina. *Doc. Ophthal. Proc. Ser.*, **10,** 77-86.

Barlow, H.B., Derrington, A.M., Harris, L.R. and Lennie, P. (1977) The effects of remote retinal stimulation on the responses of cat retinal ganglion cells. *J. Physiol.*, **269,** 177-194.

Barlow, H.B., Fitzhugh, R. and Kuffler, S.W. (1957) Change of organisation in the receptive field of the cat's retina during dark adaptation. *J. Physiol.*, **137,** 338-354.

Baylor, D.A., Fuortes, M.G.F. and O'Bryan, P.M. (1971) Receptive fields of cones in the retina of the turtle. J. Physiol. 214; 265-294.

Bennett, A.G. and Rabbetts R.B. Clinical Visual Optics. pubs Butterworths 1984.

Berger, S.J., McDaniel, M.L., Carter, J.G. and Lowry, O.H. (1977) Distribution of four potential transmitter amino acids in monkey retina. *J. Neurochem.*, **28,** 159-163.

Berson, E.L. (1987) Electrical phenomena in the retina. in Adler's physiology of the eye - clinical application. 21, 506-567. eds Moses, R.A. and Hart, W.M. pubs. Mosby Co. 1987.

Berninger, T. and Schuurmans, R.P. (1985) Spatial tuning of the pattern ERG across temporal frequency. *Doc. Ophthalmol.*, **61,** 17-25.

Blakemore, C. (1978) Maturation and modification in the developing visual system, in Handbook of sensory physiology 8, Perception (Eds, Held, R., Liebowitz, H.W. and Tenber, H.L. Chapter 12, 377, Springer, Berlin.

Blakemore, C. and Vital-Durand, F. (1979) Development of the neural basis of visual acuity in monkeys. Speculation on the origin of deprivation amblyopia. *Trans. Ophthal. Soc. UK.*, **99,** 363-368.

Blakemore, C., Garey, L.J. and Vital-Durand, F. (1978) The physiological effects of monocular deprivation and their reversal in the monkey's visual cortex. *J. Physiol.*, **283,** 223-262.

Bloom, B.H. and Sokol, S. (1977) A corneal electrode for patterned stimulus electroretinography. *Am. J. Ophthal.*, **83,** 2, 272-275.

Bloomhardt, F.J.J. and Roufs, J.A.J. (1981) The foveal point spread function as a determinant for detail vision. *Vision Res.*, **21**, 1223-1233.

Bobak, P., Bodis-Wollner, I., Harnois, C., Maffei, L., Mylin, L., Podos, S. and Thornton, J. (1983) Pattern electroretinograms and visual evoked potentials in glaucoma and multiple sclerosis. *Am. J. Ophthal.*, **96,** 72-83.

Bonadventure, N., Roussel, G. and Wioland, N. (1981) Effects of DL-alpha-amino adipic acid on Müller cell and chicken retinal in vivo: relation to ERG, ganglion cell discharge and tectal evoked response. *Neurosci., Lett.* **27,** 81-87.

Bonadventure, N. and Wioland, N. (1978) GABA and taurine: implications in organisation of receptive fields of ganglion cells in the frog retina. *Doc. Ophthal. Proc. Ser.*, **15,** 251-255.

Borda, R.P., Gilliam, R.M. and Coats, A.C. (1978) Gold-coated mylar (GCM) electrode for electroretinography. *Doc. Ophthal. Proc. Ser.*, **15,** 339-354.

Borwein, B., Borwein, D., Mederios, J. and McGowan, J.W. (1980) The ultrastructure of monkey foveal photoreceptors with special reference to the structure, shape and size and spacing of the foveal cones. *Am. J. Anat.*, **159,** 125-146.

Boycott, B.B. and Dowling, J.R. (1969) Organisation of the primate retina: light microscopy. *Phil. Trans. R. Soc. B.*, **253,** 109-184.

Boycott, B.B., Hopkins, J.M. and Sperling, H.G. (1987) Cone connections of the horizontal cells of the rhesus monkeys retina. *Proc. Royal. Soc. Ser. B.*, **1257,** 229, 345-379.

Boycott, B.B. and Wassle, H. (1974) The morphological types of ganglion cells of the domestic cats retina. *J. Physiol.*, **240,** 397-419.

Brindley, G.S. (1959) The discrimination of after-images. *J. Physiol.* **147,** 194-203.

Brindley, G.S. and Westheimer, G. (1965) The spatial properties of the human electroretinogram. *J. Physiol.*, **179,** 518-536.

Brown, K.T. (1968) The electroretinogram: its components and their origins. *Vision Res.*, **8,** 633-677.

Brown, K.T. and Murakami, M. (1964) A new receptor potential of the monkey retina with no detectable latency. *Nature.*, **201,** 626-628.

Brown, K.T. and Tasaki, K. (1961) Localisation of electrical activity in the cat retina by an electrode marking method. *J. Physiol.*, **158,** 281-295.

Brown, K.T. and Watanabe, K. (1962) Isolation and identification of a receptor potential from the pure cone fovea of the monkey retina. *Nature*, **193,** 958-960.

Brown, K.T., Watanabe, K. and Murakami, M. (1965) The early and late receptor potentials of monkey cones and rods. *Cold. Spr. Harb. Symp. Quant. Biol.*, **30,** 457-482.

Brown, K.T. and Wiesel, T.N. (1961a) Analysis of the intra-retinal electroretinogram in the intact cat eye. *J. Physiol.*, **158,** 229-256.

Brown, K.T. and Wiesel, T.N. (1961b) Localisation of origins of electroretinogram components by intra-retinal recording in the intact cat eye. *J. Physiol.*, **158**, 257-280.

Burian, H.M. and Allen, L.A. (1954) A speculum contact lens electrode for electroretinography. *Electroenceph. clin. Neurophysiol.*, **6**, 509-511.

Burian, H.M. and Spivey, B.E. (1959) The effect of twin flashes and of repetitive light stimuli on the human electroretinogram. *Am. J. Ophthal.*, **48**, 274-286.

Burkhardt, D.A. (1970) Proximal negative response of frog retina. *J. Neurophysiol.*, **33**, 405-420.

Cajal, S.R. (1893) La retine des vértèbres. La Cellule 9, 17-257. cited by Granit 1963.

Cajal, S.R. (1933) The structure of the retina. (translated by Thorpe, S.A. and Glickstein, M.) Thomas Springfield 1972.

Campbell, F.W. and Green, D.G. (1965) Optical and retinal factors affecting visual resolution. *J. Physiol.*, **181**, 576-593.

Campbell, F.W. and Gubisch, R.W. (1966) Optical quality of the human eye. *J. Physiol.*, **186**, 558-578.

Campbell, F.W. and Robson, J.G. (1968) Application of Fourier analysis of the visibility of gratings. *J. Physiol.*, **197**, 551-566.

Carr, R.E. and Siegel, I.M. Visual electrodiagnostic testing. A practical guide for the clinician. Williams and Wilkins 1982.

Caruso, R.C. and Higgins, K.E. (1987) Origin of the PERG evidence provided by the hemianopic retina. *Invest. Ophthal. Vis. Sci. Suppl.*, **28**, 62.

Celesia, G.G. and Kaufman, D. (1985) Pattern ERGs and visual evoked potentials in maculopathies and optic nerve diseases. *Invest. Ophthal. Vis. Sci.*, **5**, 26, 726-735.

Chan, R.Y. and Naka, K.I. (1976) . The amacrine cell. *Vision Res.*, **16**, 1119-1929.

Chase, W.W., Fradkin, N.E. and Tamda, S. (1976) A new electrode for electroretinography. *Am. J. Optom. Physiol. Opt.*, **53**, 668-671.

Charman, W.N. (1983) The retinal image in the human eye. In: Progress in retinal research, **2**, 1-50.

Charman,W.N. and Walsh, G. (1985) The optical phase transfer function of the eye and the perception of spatial phase. *Vision Res.*, **25**, 619-623.

Cleland, B., Dubin, M. and Levick, W. (1971) Sustained and transient neurons in the cat's retina and lateral geniculate nucleus. *J. Physiol.*, **217**, 473-496.

Cleland, B.G., Harding, Th. and Kulunay-Keesey, V. (1979) Visual resolution and receptive field size: Examination of two kinds of cat retinal ganglion cell. *Science*, **205**, 1015-1017.

Cleland, B.G. and Levick, W.R. (1974) Brisk and sluggish concentrically organised ganglion cells in the cat's retina. *J. Physiol.*, **240**, 421-456.

Cleland, B.G., Levick, W.R. and Wassle, H. (1975) Physiological identifications of a morphological class of ganglion cell. *J. Physiol.*, **248**, 151-171.

Cohen, A.T. The retina. In: Adler's Physiology of the eye - clinical application. eds Moses,R.A. and Hart,W.M. 8th edition, ch. 19, 458-490. pubs. Mosby Co. 1987.

Cone, R.A. and Cobbs, W.H. (1969) Rhodopsin cycle in the living eye of the rat. *Nature*, **221**, 820-822.

Conner, J.D., Detwiler, P.B. and Sarthy, P.V. (1985) Ionic and electrophysiological properties of retinal Müller (glial) cells of the turtle. *J. Physiol.*, **362**, 79-92.

Conte, M.M. and Brodie, S.E. (1987) Altered contrast and luminance contributions to the pattern ERG in glaucoma. *Invest. Ophthal. Vis. Sci. Suppl.*, **28**, 129.

Cornsweet, T.N. (1956) Determination of the stimuli for involuntary drifts and saccadic eye movements. *J. Opt. Soc. Am.* **46**, 987-993.

Crawford, B.H. (1947) Visual adaptation in relation to brief conditioning stimuli. *Proc. R. Soc. Lond. B.* **134**, 283-302.

Curcio, C., Hendrickson, A. and Kalina, R. (1985) Topographic distribution of human photoreceptors. *Invest. Ophthal. Vis. Sci. Suppl.*, **26**, 261.

Curcio, C., Sloan, K.R., Packer, O., Hendrickson, A.E. and Kalina, R.E. (1987) Distribution of cones in human and monkey retina: individual variability and radial asymmetry. *Science*, **236**, 579-582.

Davis, G.W. and Naka, K.I. (1980) Spatial organisation of catfish retinal neurons 1 - single and random-bar stimulation. *J. Neurophysiol.*, **43**, 807-831.

Davson, H. The physiology of the eye. 4th Edition, Churchill Livingstone 1980.

Dawson, G.D. (1951) A summation technique for the detection of small signals in an irregular background. *J.Physiol.* Lond. **115**, 2P.

Dawson, W., Maida, T. and Rubin, M. (1982) Human pattern evoked retinal responses are altered by optic atrophy. *Invest. Ophthal. Vis. Sci.*, **22**, 796-803.

Dawson, W.W., Stratton, R.D., Hope, G.M., Parmer, R., Harry, M., Engel, and Kessier, M.J. (1986) Tissue responses of the monkey retina : tuning and dependence on inner layer integrity. *Invest. Ophthal. Vis. Sci.*, **27**, 734-745.

Dawson, W.W., Trick, G.L. and Litzkow, C.A. (1979) Improved electrode for electroretinography. *Invest. Ophthal. Vis. Sci.*, **18**, 988-991.

Dawson, W.W., Trick, G.L. and Maida, T.M. (1982) Evaluation of the DTL corneal electrode. *Doc. Ophthal. Proc. Ser.*, Vol. **31**, 81-88.

Dawson, W.W., Zimmerman, T.J. and Houde, W.L. (1974) A method for more comfortable electroretinography. *Arch. Ophthal.*, **91**, 1-2.

Deeley, R. and Drasdo, N. (1987) The effect of optical degradation on the contrast sensitivity function measured at the fovea and in the periphery. *Vision Res.* **27**, 7, 1179-1186.

Denden, A. (1978) Influence of adaptation level upon oscillatory potential in the electroretinogram. *Albrecht Von Graefes Arch. Klin. Exp. Ophthal.*, **205**, 279-288.

De Lange, D. (1958) Research into the dynamic nature of the human fovea - cortex systems with intermittent and modulated light.1 attenuation characteristics with white and coloured light *J. Opt. Soc. Am.* **48**, 777-779.

Derrington, A.M., Lennie, P. and Wright, M.J. (1979) The mechanism of peripherally evoked responses in retinal ganglion cells. *J. Physiol.*, **289**, 299-310.

Dewar, J. and M'Kendrick, J.G. (1873) On the physiological action of light. Trans. Roy. Soc. Edinb. 27, 141-166. cited by Granit 1963.

Dick, E. and Miller, R.F. (1978) Light-evoked potassium activity in mudpuppy retina: its relationship to the b-wave of the electroretinogram. *Brain. Res.*, **154**, 388-394.

Diehl, R. and Zrenner, E. (1980) Multispot stimuli reveal spatial organisation in the human electroretinogram. *Doc. Ophthal. Proc. Ser.*, **23**, 209-216.

Dowling, J.E. (1970) Organisation of vertebrate retinas. *Invest. Ophthal. Vis. Sci.*, **9**, 655-680.

Dowling, J.R. and Boycott, B.B. (1966) Organisation of the primate retina: electron microscopy. *Proc. R. Soc.*, **166**, 80-111.

Drasdo, N. (1977) The neural representation of visual space. *Nature.*, **266**, 5602, 554-556.

Drasdo, N. (1982) Optical techniques for enhancing the specificity of visual evoked potentials. *Doc. Ophthal. Proc. Ser.*, **31**, 327-336.

Drasdo, N. and Cox, W. (1987) Local luminance effects of degraded pattern stimulation. *Clin. Vision Sci.*, **1**, 4, 317-325.

Drasdo, N., Thompson, D.A., Thompson, C.M. and Edwards, L. (1987) Complementary components of the pattern electroretinogram. *Invest. Ophthal. Vis. Sci.*, **28**, 158-162.

Dreher, B., Fukuda, Y. and Rodieck, R.W. (1976) Indentification, classification and anatomical segregation of cells with X-like and Y-like properties in the lateral geniculate nucleus of old world primates. *J. Physiol.*, **258**, 433-452.

Du Bois Reymond (1849) Untersuchungen uber thierische Electricitat. Berlin, 2/1, 256-257. cited by Granit, R. 1963.

Duke-Elder, S. and Scott, G.I. Neuro-ophthalmology. In: System of ophthalmology, vol XII, ed. Duke-Elder, S., pubs. Henry Kimpton, London. 1971.

Duke-Elder, S. and Wybar, K.C. Anatomy of the visual system. In: System of ophthalmology, vol, II, ed. Duke-Elder, S., pubs. Henry Kimpton, London. 1961

Duke-Elder, S. and Weale, R.A. Physiology of vision. In: System of ophthalmology, vol,IV. ed. Duke-Elder, S., pubs. Henry Kimpton, London. 1968.

Dunne, M.C. (1987) An optical study of human ocular dimensions. PhD Thesis , University of Aston in Birmingham.

D'Zmura, M. and Lennie, P. (1987) Shared pathways for rod and cone vision. *Vision Res.*, **26**, 8, 1273-1280.

Ehinger, B. (1983) Connections between retinal neurons with identified neurotransmitters. *Vision Res.*, **23**, 11, 1281-1291.

Einthoven, J. and Jolly, W.A. (1908) The form and magnitude of the electrical response of the eye to stimulation by light at various intensities. Quart. J.exp. Physiol.,1,373-416. cited by Granit, R. 1963.

Enroth-Cugell, C. and Robson, J.G. (1966) The contrast sensitivity of retinal ganglion cells of the cat. *J. Physiol.*, **187**, 517-552.

Enroth-Cugell, C. and Robson, J.G. (1984) Functional characteristics and diversity of cat retinal ganglion cells. Basic characteristics and quantitative description. *Invest.Ophthal.Vis.Sci.* **25**, 250-267.

Enroth-Cugell, C., Robson, J.G., Schweitzer-Tong, D. and Watson, A.B. (1983) Spatio-temproal interactions in cat retinal ganglion cells showing linear spatial summation. *J. Physiol.*, **341**, 279-307.

Evers, H.U. and Gouras, P. (1986) Three cone mechanisms in the primate electroretinogram : two with one without off center bipolar responses. *Vision Res.*, **26**, 2, 245-254.

Eysel, UTh. and Grusser, O.J. (1974) Simultaneous recording of pre- and post-synaptic potentials during degeneration of the optic tract fiber input to the lateral geniculate nucleus of rats. *Brain Res.* **81**, 552-557.

Faber, D.S. (1969) Analysis of the slow retinal potentials in response to light. PhD Thesis, State University of New York at Buffalo.

Famiglietti, E.V. (1981) Functional architecture of cone bipolar cells in mammalian retina. *Vision Res.*, **21**, 1559-1563.

Famiglietti, E.V. (1983) On and off pathways through amacrine cells in mammalian retina : the synaptic connections of 'starburst' amacrine cells. *Vision Res.*, **23**, 11, 1265-1279.

Famiglietti, E.V. and Kolb, H. (1975) A bistratified amacrine cell and synaptic circuitry in the inner plexiform layer of the retina. *Brain. Res.*, **84**, 293-300.

Famiglietti, E.V. and Kolb, H. (1976) Structural basis for 'on' and 'off' centre responses in retinal ganglion cells. *Sciences*, **194**, 193-195.

Fazio, D.T., Heikenlively, J.R., Martin, D.A. and Christensen, R.E. (1986) The electroretinogram in advanced open angle glaucoma. *Doc. Ophthalmol.*, **63**, 45-54.

Feinsod, M., Rowe, H. and Averbach, E. (1971) Changes in the electroretinogram in patients with optic nerve lesions. *Doc. Ophthalmol.*, **29**, 169-200.

Flamant (1955) Etude de la repartition de la lumiere dans l'image rétinienne d'une fente. Revue Opt. théor. instrum. 34, 433-459. (cited by Charman 1983)

Flamm, L. (1971) The effect of image displacement with paced saccades in the human ERG and VECP. Unpublished doctoral dissertation, Northeastern Univ.

Frederick, J.M., Rayborn, M.E., Laties, A.M.,Lam, D. and Hollyfield, J.G.(1982) Dopaminergic neurons in the human retina. *J. Comp. Neurol.* **210**, 65-79.

Frisen, L. and Hoyt, W. (1974) Insiduous atrophy of retinal nerve fibres in multiple sclerosis. *Arch. Ophthal.*, **92**, 91-97.

Fiorentini, A., Maffei, L., Pirchio, M, Spinelli, D. and Porciatti, V. (1981) The ERG in response to alternating gratings in patients with diseases of the peripheral visual pathway. *Invest. Ophthal. Vis. Sci.*, **22**, 490-493.

Fiorentini, A., Maffei, L., Pirchio, M., Porciatti, V. and Spinelli, D. (1982) Pattern ERG in patients with unilateral alterations of the retinal ganglion cells. *Doc. Ophthal. Proc. Ser.*, **31**, 131-133.

Fukuda, Y., Hsiao, C. and Watanabe, M. (1985) Morophological correlates of Y, X and W type ganglion cells in cat's retina. *Vision Res.*, **24**, 3, 319-327.

Gallego, A. (1971) Horizontal and amacrine cells in the mammal's retina. *Vis. Res.* **3**, (Suppl.) 33-50.

Galloway, N.R. (1967) Early receptor potentials in the human eye. *Brit. J. Ophthal.*, **51**, 261-264.

Galloway, N. Ophthalmic electrodiagnosis Major problems in Ophthalmology ,1. ed Trevor-Roper, pubs W.B. Saunders Co 1975.

Galloway, N.R., Tolia, J. and Barber, C. (1986) The pattern evoked response in disorders of the optic nerve. *Doc. Ophthalmol.*, **63**, 31-36.

Gills, J.P. (1966) The electroretinogram after section of the optic nerve in man. *Am. J. Ophthal.*, **62**, 287-291.

Giltrow-Tyler, J.F., Crews, S.J. and Drasdo, N. (1978) Electroretinography with non-corneal and corneal electrodes. *Invest. Ophthal. Vis. Sci.*, **17**, 1124-1127.

Gjotterberg, M. (1986) Electrodes for electroretinography. A comparison of four different types. *Arch. Ophthal.*, **104**, 569-570.

Glezer, V.D. (1965) The receptive fields of the retina. *Vision Res.*, **5**, 487-525.

Gottlob, I. and Wedge-Lussen, L. (1987) Normal pattern electroretinograms in amblyopia. *Invest. Ophthal. Vis. Sci.*, **28**, 187-191.

Gottlob, I., Wundsch, L. and Pflug R. (1985) Possible role of amacrine cells in the generation of the mammalian ERG b-wave. *Doc. Ophthalmol.*, **61**, 55-63.

Granit, R. (1933) The components of the retinal action potential and their relation to the discharge in the optic nerve. *J. Physiol.*, **77**, 207-240.

Granit, R. (1935) Two types of retina and their electrical responses to intermittent stimuli in light and dark adaptation. *J. Physiol.*, **85**, 421-438.

Granit, R. (1962) Neurophysiology of the retina. In the eye, Vol 2, (Ed) Davson , H. Academic Press., 575-691.

Granit, R. Sensory mechanisms of the retina. 2nd ed. Oxford University Press, London. 1963.

Granit, R. and Munsterhjelm, A. (1937) The electrical response of dark-adapted frogs eyes to monochromatic stimuli. *J. Physiol.*, **88**, 436-458.

Green, D.G. (1970) Regional variations in the visual acuity for interference fringes on the retina. *J. Physiol.*, **207**, 351-356.

Groneberg, A. (1980) Simultaneously recorded retinal and cortical potentials elicited by checkerboard stimuli. *Doc. Ophthal. Proc. Ser.*, **23**, 255-262.

Groneberg, A. and Teping, C. (1980) Topodiagnostile von sehstorungen durch ableitung retinaler und kortikaler antworten auf vmkehr-kontrastmuster. *Der. Dtsch. Ophthal. Ges.*, **77**, 409-417.

Grüsser, O.J. (1979) Cat ganglion cell receptive fields and the role of horizontal cells in their generation. The Neurosciences fourth study program, (Eds) Schmitt, F.O. and Worden, F.G.15, 247-273.

Gur, M., Seevi, Y., Bielik, M. and Neumann, E. (1987) Changes in the oscillatory potentials of the electroretinogram in glaucoma. *Current Eye Res.*, **6**, 457-466.
Hallett, P.E. (1963) Spatial summation. *Vision Res.*, B, 9-24.

Halliday, A.M. (1982) Clinical neurology and neurosurgery monograms. Ed Evoked potentials in clinical testing, Edinburgh Churchill Livingstone, 187-234.

Harrison, J.M. and O'Conner, P.S., Young, S.L., Kincaid, M. and Bentley, R. (1987) The pattern ERG in man following surgical resection of the optic nerve. *Invest. Ophthal. Vis. Sci.*, **28**, 492-499.

Hart, W.M. The temporal responsiveness of vision. In: Adler's physiology of the eye - clinical applications. eds Moses, R.A. and Hart, W. pubs. Mosby Co.

Hartline, H.K. (1925) The electrical response to illumination of the eye in intact animals, including the human subject; and in decerebrate preparations. *Am. J. Physiol.*, **73**, 600-611.

Hartline, H.K. (1968,69) Visual receptors and retinal interaction. Les Prix Nobel en 1967, The Nobel Foundation, 1968, 242-269. In: Studies on excitation and inhibition in the retina. Ed. Ratliff, R., pubs Chapman and Hall 1974; 643-660.

Henkes, H.E. (1951) The use of the electroretinogram in measuring the effect of vasodilation. *Angiology*, **2**, 125-131.

Henkes, H.E. A history of human electroretinography. In: Developments in Ophthalmology; Special tests of visual function, basic problems and clinical application, **9**, 11-19, 1984.

Hess, R.F. and Baker, C.L. (1984a) Human pattern-evoked electroretinogram. *J. Neurophysiology*, **51**, 5, 939-951.

Hess, R.F. and Baker, C.L. (1984b) Assessment of retinal function in severely amblyopic individuals. *Vision Res.*, **24**, 10, 1367-1376.

Hess, R.F., Baker, C.L., Verhoeve, J.N., Keesey, U.T. and France, T.D. (1985) The pattern evoked electroretinogram: its variability in normals and its relationship to amblyopia. *Invest. Ophthal. Vis. Sci.*, **26**, 1610-1623.

Hess, R.F., Baker, C.L., Zrenner, E. and Schwarzer, J. (1986) Differences between electroretinograms of cat and primate. *J. Neurophysiol.*, **56**, 3, 747-768.

Heynen, H. and Van Norren, D. (1985a) Origin of the electroretinogram in the intact macaque eye - 1 principal component analysis. *Vision Res.*, **25**, 5, 697-707.

Heynen, H. and Van Norren, D. (1985b) Origin of the electroretinogram in the intact macaque eye - II current source-density analysis. *Vision Res.*, **25**, 5, 709-715.

Heynen, H., Wachtmeister, L. and Van Norren, D. (1985) Origin of the oscillatory potentials in the primate retina. *Vision Res.*, **25**, 10, 1365-1373.

Hilt, R. and Cavonius, C.R. (1974) Functional organisation of the peripheral retina : Sensitivity to penodic stimuli. *Vision Res.*, **14**, 1333-1337.

Hirsch, J. and Hylton, R. (1984) Quality of the primate photoreceptor lattice and limits of spatial vision. *Vision Res.*, **24**, 357-385.

Hobson, R., Odom, J., Maida, T. and Dawson, W. (1984) Effects of reference electrode position on the amplitude variability of the pattern evoked retinal potential. *Invest. Ophthal. Vis. Sci. Supp.*, **25**, 180.

Hochstein, S. and Shapley, R.M. (1976) Linear and non-linear spatial subunits in Y cat retinal ganglion cells. *J. Physiol.*, **262**, 265-284.

Holden, A.L. and Vaegan, (1983a) Comparison of the focal electoretinogram and the pattern electroretinogram in the pigeon. *J. Physiol.*, **344**, 11-23.

Holden, A.L. and Vaegan, (1983b) Vitreal and intraretinal responses to contrast reversing patterns in the pigeon eye. *Vision Res.*, **23**, 5, 561-572.

Holden, A.L. and Vaegan, (1983c) Artefacts of intrusion in the pattern electroretinogram. *Ophthal, Res.*, **15**, 289-292.

Holder, G.E. (1987) Significance of abnormal pattern electroretinography in anterior visual pathway dysfunction. *Brit. J. Ophthal.*, **71**, 166-171.

Holder, G.E. and Huber, M.J.E. (1984) The effects of miosis on pattern and flash ERG and pattern visual evoked potentials. *Doc. Ophthal. Proc. Ser.*, **40**, 109-116.

Hollander, H., Bisti, S., Maffei, L. and Hebel, R. (1984) Electroretinographic responses and retrograde changes of retinal morphology after intracranial optic nerve section. A quantitative analysis in the cat. *Exp. Brain. Res.*, **55**, 483-493.

Holmgren, F. (1865/6) Method att objectivera effecten av ljusintryck pa retina. Upsala Lakaref. forh.1, 177-191. cited by Granit, R. 1963.

Honda, Y., Nao, I.N., Kim, S., Sakaue, E. and Nambu, M. (1986) New disposable ERG electrode made of anomalous polyvinyl alcohol gel. *Doc. Ophthalmol.*, **63**, 205-207.

Hubel, D.H. and Wiesel, T.N. (1965) Binocular interaction in striate cortex of kittens reared with artificial squint. *J. Neurophysiol.*, **28**, 1041-1059.

Hughes, A. (1981) Cat retina and the sampling theories : the relation of transient and sustained brisk unit cut-off frequency to alpha and beta mode cell density. *Exp. Brain. Res.*, **42**, 196-202.

Hughes, A. (1981) Population magnitudes and distribution of the major modal classes of cat retinal ganglion cell as estimated from HRP filling and a systematic survey of the soma diameter spectra for classical neurones. *J. Comp. Neurol.*, **197**, 303-339.

Hutchins, J.B. and Hollyfield, J.G. (1985) Acetylcholine receptors in the human retina. *Invest. Ophthal. Vis. Sci.*, **26**, 1550-1557.

Ikeda, H. (1976) Electrophysiology of the retina and visual pathway. In: Medical ophthalmology, (Eds) Rose, F., Chapman and Hill, 38-55.

Ikeda, H. (1980) Visual acuity, its development and amblyopia. *Proc. Royal. Soc. Med.*, **73**, 546-555.

Ikeda, H. (1985) Transmitter action at cat retinal ganglion cells. In: Progress in retinal research, (Eds) Osborne, N. and Chader, G., 4, 2-28

Ikeda, H. and Robbins, J. (1987) Development of neurochemical segregation of ON and OFF retinal channels which subserve contrast vision. Abstr. Satellite Symp. 2nd World Congr. Neuroscience.

Ikeda, H. and Sheardown, M.J. (1983) Functional transmitters at retinal ganglion cells in the cat. *Vision Res.*, **23**, 10, 1161-1174.

Ikeda, H. and Tremain, K.E. (1978) Amblyopia resulting from penalisation : neurophysiological studies on kittens reared with atropinisation of one or both eyes. *Brit. J. Ophthal.*, **62**, 21-28.

Ikeda, H., Tremain, K.E. and Saunders, M.D. (1978) Neurophysiological investigation in optic nerve disease : combined assessment of the visual evoked response and electroretinogram. *Brit. J. Ophthal.*, **62**, 227-239.

Ikeda, H. and Tremain, K.E. (1979) Amblyopia occurs in retinal ganglion cells in cats reared with convergent squint without alternating fixation. *Exp. Brain. Res.*, **35**, 559-582.

Ikeda, H. and Wright, M.J. (1972) Receptive field organisation of 'sustained' and 'transient' retinal cells which subserve different functional roles. *J. Physiol.*, **227**, 769-800.

Imaizumi, K., Tazawa, Y. and Kobayashi, H. (1972) Electrophysiological and histopathological studies on the rabbit retina treated with sodium iodate and sodium l - glutamate. *Doc. Ophthal. Proc. Ser.*, **2**, 105-118.

Jacobson, J.H. and Gestring, G.F. (1958) Centrifugal influence on the electroretinogram. *Arch. Ophthal.*, **60**, 295-302.

Jacobson, J.H., Throse, T. and Popkin, A.B. (1966) Independence of the oscillatory potential, photopic and scotopic b-wave of the human electroretinogram. The clinical value of electroretinogram. ISCERG. Symp., 8-20.

Jacobson, S.G., Sandberg, M.A., Effron, M.H. and Berson, E. (1979) Foveal cone electroretinograms in strabismic amblyopia. Comparison with juvenile macular degeneration, macular scars and optic atrophy. *Trans. Ophthal. Soc. UK.*, **99**, 353-356.

Jennings, J.A.M. and Charman, W.N. (1981) Off-axis image quality in the human eye. *Vision Res.*, **21**, 445-455.

Jennings, J.A.M. and Charman, W.N. (1974) An analytical approximation for the modulation transfer function of the eye. *Brit. J. Physiol. Opt.*, **29**, 64-72.

Johnson, E.P., Riggs. L.A. and Schick, A.M.L. (1966) Photopic retinal potentials evoked by phase alternation of a barred pattern. In: Clinical electroretinography. (Eds) Burian and Jacobson, J.H., 75-91.

Johnson, C.B. (1970) A method of characterising electro-optical device modulation transfer functions. *Photogr. Sci. Engng.*, **14**, 413-415.

Johnson, C.B. (1973) A convenient form of graph paper for the determination of electro-optical device modulation transfer function parameters. IEEE. *Trans. Electron. Devices.*, **20**, 80-81.

Kamp, C.W. and Morgan, W.W. (1981) GABA antagonists enhance dopamine turnover in the rat retina in vivo. *Eur. J. Pharmac.*, **69**, 273-279.

Kandel, E. and James, J. Principles of neural science. pubs, Edward Arnold, New York. 1985.

Kaneko, A. (1973) Receptive field organisation of bipolar and amacrine cells in the goldfish retina. *J. Physiol.*, **235**, 133-153.

Kaplan, E. and Shapley, R.M. (1986) The primate retina contains two types of ganglion cells with high and low contrast sensitivity. *Proc. Natl. Acad. Sci. USA.*, **83**, 2755-2757.

Karpe, G. (1945) The basis of clinical electroretinography. *Acta. Ophthal. Suppl.*, **24**, 1-118.

Karten, H.J. and Brecha, N. (1983) Localisation of neuroactive substances in the vertebrate retina: evidence for lamination in the inner plexiform layer. *Vision Res.*, **23**, 10, 1197-1205.

Karwoski, C.J. and Newman, E.A. (1987) Generation of the e-wave of the electroretinogram in frog retina. *Invest. Ophthal. Vis. Sci. Suppl.*, **28**, 407.

Karwoski, C.J. and Proenza, L.M. (1977) Relationship between Müller cell responses, a local transretinal potential and potassium flux. *J. Neurophysiology.*, **40**, 244-259.

Karwoski, C.J. and Proenza, L.M. (1978) Light evoked changes in extracellular potassium concentration in Mudpuppy retina. *Brain Res.* **142**, 515-530.

Karwoski, C.J. and Proenza, L.M. (1980) Neurons, potassium and glia in proximal retina of Necturus. *J.gen. Physiol.* **75**, 141-162.

Kelly, D.H. (1976) Pattern detection and the two dimensional Fourier transform: flickering chequerboards and chromatic mechanisms. *Vision Res.* **16**, 277-287.

Kirkby, A.W. and Enroth-Cugell, C. (1976) The involvement of gamma-aminobutyric acid in the organisation of cat retinal ganglion cell receptive fields: a study with picrotoxin and bicuculline. *J. Gen. Physiol.*, **68**, 465-484.

Kirkham, T.H. and Coupland, S.G. (1981) Abnormal pattern electroretinograms with macular cherry - red spots; evidence for selective ganglion cell damage. *Curr. Eye. Res.*, **1**, 6, 367-372.

Kirkham, T.H. and Coupland, S.G. (1982/3) Pattern ergs and check size: absence of spatial frequency tuning. *Curr. Eye. Res.*, **2**, 8, 511-521.

Kline, R.P., Ripps, H. and Dowling, J.E. (1978) Generation of b-wave currents in the skate retina. *Proc. Natn. Acad. Soc. USA.*, **75**, 5727-5731.

Knapp, A.G. and Schiller, P.H. The contribution of on-bipolar cells to the electroretinogram of rabbit and monkey - a study using 2-amino-4-phosphonobutyrate APB. Vision Res. 24, 1841-1846.

Kolb, H. Cone pathways in the mammalian retina. in Molecular and cellular basis of visual acuity. eds. Hilfer, S.R. and Sherrield, J.R. pubs. Springer-Verlag 1984.

Kolb, H., Boycott, B.B. and Dowling, J. (1969) A second type of midget bipolar cell in the primate retina. Appendix. *Phil. Trans. Royal. Soc.*, **255**, 177-184.

Kolb, H., Mariani, A. and Gallego, A. (1986) A second type of horizontal cell in the monkey retina. *J. Comp. Neurol.*, **183**, 31-44.

Kolb, H. and Nelson, R. (1981) Amacrine cells of the cat retina. *Vision Res.*, **21**, 1625-1633.

Kolb, H., Nelson, R. and Mariani, A,. (1981) Amacrine cells, bipolar cells and ganglion cells of the cat retina.: A Golgi study. *Vision. Res.*, **21**, 1081-1114.

Kolker, A.E., Trick, G.L., Cooper, D.G., Garden, M.O. and Kass, M.A. (1987) Steady state pattern reversal ERGs in ocular hypertension: the association with risk factors for glaucoma. *Invest. Ophthal, Vis. Sci. Suppl.*, **28**, 129.

Kooijman, A.C. (1987) Comparison of electrodes for electroretinography. *Arch. Ophthal.*, **105**, 23.

Korth, M. (1983) Patttern-evoked responses and luminance-evoked responses in human electroretinogram. *J. Physiol.*, **337**, 451-469.

Korth, M. (1984) Nasopharyngeal recordings separate retinal from optic nerve potentials. *Curr. Eye. Res.*, **3**, 6, 873-886.

Korth, M., Horn, F., Storck, B. and Jonas, J. (1987a) Pattern electroretinograms (PERGs) in normal and glaucoma eyes. *Invest. Ophthal.Vis.Sci. Suppl.*, **28**, 6, 129.

Korth, M. and Ilschner, S. (1986) The spatial organisation of retinal receptive fields in light and darkness as revealed by the pattern electroretinogram. *Doc. Ophthalmol.*, **63**, 143-149.

Korth, M., Ilschner, S. and Sembritzki, O. (1987b) Retinal receptive fields under different adaptation levels studied with the pattern evoked ERG. *Albrecht Graefe's Arch. Klin. Exp. Ophthal.*, **225**, 63-69.

Korth, M. and Rix, R. (1983) The pattern electroretinogram under different conditions of stimulus luminance and contrast. *Doc. Ophthalmol.*, **40**, 20-28.

Korth, M. and Rix, R. (1984) Effects of stimulus intensity and contrast on the pattern ERG. *Ophthal. Res.*, **16**, 60-66.

Korth, M. and Rix, R. (1985) Changes in spatial selectivity of pattern-ERG components with stimulus contrast. *Albrecht Graefe's Arch. Klin. Exp. Ophthal.*, **223**, 23-28.

Korth, M. and Rix, R. (1987) The pattern ERG in response to colored stimuli. *Doc. Ophthalmol.*, **65**, 71-77.

Korth, M. Rix, R. and Sembritzki, O. (1985) Spatial contrast transfer functions of the pattern evoked electroretinogram. *Invest. Ophthal. Vis. Sci.*, **26**, 303-308.

Kosnik,W., Fikre, J. and Sekule, R. (1986) Visual fixation stability in older adults. I*nvest. Ophthal. Vis. Sci.* **27**, 1720-1725.

Kruger, J. and Fisher, B. (1973) Strong periphery effect in cat retinal ganglion cells. Excitatory responses in on and off centre neurones to single grid displacements. *Exp. Brain. Res.*, **18**, 316-318.

Kuffler, S.W. (1953) Discharge patterns and functional organisation of mammalian retina. *J. Neurophysiol.*, **16**, 37-68.

Lachapelle, P. (1985) Pattern and focal ERG in amblyopia. *Invest. Ophthal. Vis. Sci.* **26**, 1648.

Lachapelle, P. (1985) Oscillations on the electroretinogram: a synthetic approach. *Can. J. Ophthal.*, **20**, 6, 216-219.

Lachapelle, P. and Molotchnikoft, S. (1986) Components of the electroretinogram; a reappraisal. *Doc. Ophthalmol.*, **63**, 337-348.

Lamb, T.D. (1976) Spatial properties of horizontal cell responses in the turtle retina. *J. Physiol.* **263,** 239-255.

Lamb, T.D. (1986) Transduction in vertebrate photoreceptors, the roles of cyclic GMP and calcuim. *TINS.*, **9**, 224-228.

Lawwill, T. (1974) The bar pattern electroretinogram for clinical evaluation of the central retina. *Am. J. Ophthal.*, **78**, 121-126.

Lawwill, T. (1984) The bar pattern electroretinogram. *Doc. Ophthalmol.*, **40**, 1-10.

Lee, B.B., Crook, J.M. and Valberg, A. (1985) The relation between visual resolution and eccentricity for the ganglion cells of the monkey retina. *Soc. Neurosci. Abstr.*, **11**, 339.

Lee, D.A., Rimele,T.J., Brubaker, R.F., Nagataki, S. and Van Houtte, P.M. (1983) Effect of thymoxamine on the human pupil. *Exp. Eye Res.* **36**, 655-662.

Le Grand, Y. Light, colour and vision. 2nd ed. pubs. Chapman and Hall, London. 1968.

Leguire, L.E. and Rogers, G.L. (1985) Pattern electroretinogram: use of non-corneal skin electrodes. *Vision Res.* **25**, 867-870.

Lennie, P. (1980) Parallel visual pathways: a review. *Vision Res.*, **20**, 561-594.

Lovasik, J.V. and Kothe, A.C. (1986) The pattern evoked electroretinogram: origin, characteristics and clinical usage. *Can. J. Optom.*, **48**, 28-46.

Lurie, M. (1976) Some observations on the c-wave of the electroretinogram in the intact frog eye. *Exp, Eye Res.*, **23**, 197-207.

McBrien, N.A. and Millodot, M. (1985) Clinical evaluation of the Canon Autoref R-1. *Am. J. Optom. Physiol. Opt.* **62**, 786-792.

McDonald, W.I. (1983) Doyne lecture: The significance of optic neuritis. *Trans. Ophthal. Soc. UK.*, **103**, 230-246.

McDonald, W.I. The pathogenesis of optic neuritis in Optic neuritis. Ch 3, 42-50. eds. Hess, R.F. and Plant, G.T., pubs. Cambridge University press 1986.

McIlwain, J.T. (1966) Some evidence concerning the physiological basis of the peripheral effect in the cats retina. *Exp. Brain. Res.*, **1**, 265-271.

MacNichol, E.F. and Svaetchin, G. (1958) Electrical responses from the isolated retinas of fishes. *Am. J. Ophthal.* **46**, 26-46.

Madison, R., Moore, M.R. and Sidman, R.L. (1984) Retinal ganglion cells and axais survive optic nerve transection. *Inter. J. Neurosci.*, **23**, 15-32.

Maffei, L and Florentini, A. (1981) Electroretinographic responses to alternating gratings before and after section of the optic nerve. *Science.*, **211**, 953-955.

Maffei, L., Florentini, A., Bisti, S. and Hollander, H. (1985) Pattern ERG in the monkey after sections of the optic nerve. *Exp. Brain. Res.*, **59**, 2, 423-425.

Maguire, G.W. and Smith, E. (1985) Cat retinal ganglion receptive-field alterations after 6-hydroxydopamine induced dopaminergic amacrine cell lesion. *J. Neurophysiol.*, **3**, 6, 1431-1443.

Maksimova, E.M. (1969) The effect of intracellular polarisation of horizontal cells on the ganglion cell activity of fish retina. *Biolizika*, **14**, 537-544.

Marc, R.E. (1986) Neurochemical stratifications in the inner plexiform layer of the vertebrate retina. *Vision Res.*, **26**, 2, 223-238.

Marg, E. (1953) The effect of stimulus size and retinal illuminance on the human electroretinogram. *Am. J. Optom. and Arch. Am. Acad. Optom.* **30**, 417-433.

Mariani, A.P. (1981) Biplexiform cells: ganglion cells of the primate retina that contact photoreceptors. *Science.*, **216**, 1134-1136.

Mariani, A.P. (1982) Newly identified bipolar cells in monkey retina. *Invest. Ophthal. Vis. Sci.Suppl.*, **22**, 247.

Mariani, A.P. (1984) Bipolar cells in monkey retina selective for the cones likely to be blue sensitive. *Nature.*, **308**, 184-186.

Mariani, A.P., Kolb, H. and Nelson, R. (1984) Dopamine - containing amacrine cells of rhesus monkey retina parallel rods in spatial distribution. *Brain. Res.*, **322**, 1-7.

Marmarelis, P.Z. and Naka, K.I. (1973) Non-linear analysis and synthesis of receptive field responses in the catfish retina III, two imput white-noise analyses *J. Neurophysiol.*, **36**, 634-368.

Marx, M.S., Podos, S.M., Bodis-Wollner, I., Howard-Williams, J.R., Siegel, M.J., Teitelbaum, C.S., Macun, E.L. and Severin, C. (1986) Flash and pattern electroretinograms in normal and laser induced glaucomatous primates eyes. *Invest. Ophthal, Vis. Sci.*, **27**, 378-386.

Mashima, Y. and Oguchi, Y. (1985) Clinical study of the pattern electroretinogram in patients with optic nerve damage. *Doc. Ophthalmol.*, **61**, 91-96.

Masland, R.H. (1980) Acetylcholine in the retina. *Neurochem.*, **1**, 501-518.

Masland, R.H. and Ames, A. (1975) Dissociation of field potential from neuronal activity in the isolated retina: failure of the b-wave with normal ganglion cell responses. *J. Neurobiol.*, **6**, 305-312.

Masland, R.H. and Tauchi, M. (1986) The cholinergic amacrine cell. *TINS.*, **95** 218-223.

Massey, S.C., Retlbum, D.A. and Crawford, M.J.C. (1983) The effects of 2-amino 4-phosphonobutyric, APB, in the ERG and ganglion cell discharge of rabbit retina. *Vision. Res.*, **23**, 1607-1613.

Matsuura, T., Miller, W.H. and Tomita, T. (1978) Cone specific c-wave in the turtle retina. *Vision. Res.*, **18**, 767-775.

May, J., Ralston, J., Reed, J. and Van Dyk, H. (1982) Loss in pattern elicited electroretinograms in optic nerve dysfunction. *Am. J. Ophthal.*, **93**, 418-422.

Merigan, W.H. (1987) Role of P and M pathways in the chromatic and achromatic vision of macaques. Abstr. Satellite Symp. 2nd World Congr. Neurosci.

Merigan, W.H. and Eskin, T.A. (1986) Spatio-temporal vision of macaques with severe loss of Pß retinal ganglion cells. *Vision Res.*, **26**, 1751-1756.

Michelson, A.A. (1891) On the application of interference methods to spectroscopic measurements. *I.Phil. Mag.*, **31**, 338-348.

Miller, R.F., Dacheux, R. and Frumkes, T.E. (1977a) Amacrine cells in Necturus retina: evidence for independent gamma-aminobutyric acid and glycine releasing neurones. *Science.*, **198**, 748-750.

Miller, R.F., Dacheux, R. and Proenza, L. (1977b) Müller cell depolarisation evoked by antidromic optic nerve stimulation. *Brain. Res.*, **121**, 162-166.

Miller, R.F. and Dowling, J.E. (1970) Intracellular responses of the Müller (glial) cells of mudpuppy retina. Their relationship to the b-wave of the electroretinogram. *J. Neurophysiol.*, **33**, 323-341.

Miller, R.F., Frumkes, T.E., Slaughter, M. and Dacheux, R.F. (1981) Physiological and pharmacological basis of GABA and glycine On-neurons of mudpuppy retina - II; amacrine and ganglion cells. *J. Neurophysiol.*, **45**, 764-781.

Miller, W.H. (1979) Intra-ocular filters. In: Handbook of sensory physiology. ed. Autrum H. vol VII/6A ch.3. pubs. Springer Verlag.

Missotten, L. (1974) Estimation of the ratio of cones to neurons in the fovea of the human retina. *Invest. Ophthal. Vis. Sci.*, **13**, 1045-1049.

De Monasterio, F.M. (1978a) Properties of concentrically organised X and Y ganglion cells of macaque retina. *J. Neurophysiol.*, **41**, 1394-1417.

De Monasterio, F.M. (1978b) Centre and surround mechanisms of opponent colour X and Y ganglion cells of retina of macaques. *J. Neurophysiol.*, **41**, 1418-1434.

De Monasterio, F.M. (1978c) Properties of ganglion cells with atypical receptive field organisation in retina of macaque. *J. Neurophysiol.* **41**, 1435-1449.

De Monasterio, F.M. and Gouras, P. (1975) Functional properties of ganglion cells of the rhesus monkey. *J. Physiol.*, **251**, 167-196.

De Monasterio, F.M., Gouras, P. and Tolhurst, D.J. (1975) Trichromatic colour opponency in ganglion cells of the rhesus monkey. *J. Physiol.*, **251**, 197-216.

Mullen, K.T. (1982) The effects of spatial frequency on opponent colour contributions to modulation thresholds. *Invest. Ophthal. Vis. Sci. Suppl.*, **22**, 77.

Mullen, K.T. (1985) The contrast sensitivity of human colour vision to red/green blue/yellow chromatic gratings. *J. Physiol.* **359**, 381-400.

Murakami, M. and Kaneko, A. (1966) Differentiation of PIII subcomponents in cold blooded vertebrate retinas. *Vision. Res.*, **6**, 627-636.

Nachmias, J. Two-dimensional motion of the retinal image during monocular fixation. *J. Opt. Soc. Am.* **49**, 901-908.

Naka, K.I. (1976) Neuronal circuitry in the catfish retina. *Invest. Ophthal. Vis. Sci.* **15**, 926-935.

Naka, K.I. (1982) The cells horizontal cells talk to. *Vision. Res.*, **22**, 6, 653-660.

Naka, K.I. and Rushton, W.A.H. (1967) The generation and spread of S-potentials in fish (cyprinidae). *J. Physiol.*, **185**, 536-555.

Nakatsuka, K. and Harnasaki, D.I. (1985) Destruction of the indoleamine - accumulating amacrine cells alters the ERG of rabbits. *Invest. Ophthal. Vis. Sci.*, **26**, 1109-1116.

Nelson, R. (1977) Cat cones have rod input: a comparison of the response properties of cones and horizontal cell bodies in the retina of the cat. *J. Comp. Neurol.*, **172**, 109-136.

Nelson, R., Famiglietti, E. and Kolb, H. (1978) Intra-cellular staining reveals different levels of stratification for on and off centre ganglion cells in the cat retina. *J. Neurophysiol.*, **41**, 472-483.

Nelson, R., Kolb, H., Robinson, M.M. and Mariani, A.P. (198l) Neural circuitry of the cat retina: cone pathways to ganglion cells. *Vision. Res.*, **21**, 1527-1536.

Nelson, R. and Kolb, H. (1983) Synaptic patterns and response properties of bipolar and ganglion cells in the cat retina. *Vision. Res.*, **23**, 10, 1183-11983.

Nelson, R., von Litzow, A., Kolb, H. and Gouras, P. (1975) Horizontal cells in cat retina with independent dendritic systems. *Science.*, **189**, 137-139.

Nelson, R., Zrennner, E. and Gouras, P. (1979) Patterened stimuli reveal spatial organization in the electroretinogram. ISCEV. Symp., 161-169.

Newman, E.A. (1980) Current source density analysis of the b-wave of frog retina. *J. Neurophysiol.*, **43**, 1355-1366.

Newman, E.A. (1984) Regional specialisation of retinal ganglion cell membrane. *Nature.*, **309**, 155-157.

Newman, E.A. and Odette, L.L. (1984) Model of electroretinogram b-wave generation, a test of the K^+ hypothesis. *J. Neurophysiol.*, **51**, 1, 164-182.

Nightengale, S., Mitchell, K. and Howe, J. (1986) Visual evoked cortical potentials and pattern electroretinograms in Parkinson's disease and control subjects. *J. Neurol. Neurosurg. Psychiat.*, **49**, 1280-1287.

Nilsson, S.E.G. Interactions between Pl and slow Plll in the generation of the electroretinogram c-wave. In: Developments in Ophthalmology; Special tests of visual function, basic problems and clinical application, **9**, 53-58. 1984.

Noell, W.K. (1954) The origin of the electroretinogram. *Am. J. Ophthal.*, **38**, 78-90.

O'Connor Davies, P.H. The action and uses of ophthalmic drugs. pubs. Butterworths, London. 1976.

Odom, J.V., Maida, T.M. and Dawson, W. (1982/3) Pattern evoked retinal response (PERR) in human: effects of spatial frequency, temporal frequency, luminance and defocus. *Curr. Eye. Res.*, **2**, 2, 99-108.

Odom, J.V. and Norcia, A.M. (1984) Retinal and cortical potentials. Spatial and temporal characteristics. *Doc. Ophthal. Proc.Ser.*, **40**, 29-38.

Oehler, R. (1983) Perzeptive Feldmessungen biem Rhesusaffen: Ein Verhatensexperiment mit dem Westheimer Paradigma. Dissertation. Freiberg i. Br. cited by Perry, V. H., Oehler, R. and Cowey, A. (1984) Neuroscience 12; 1101-1123.

Ota, I. and Miyake, Y. (1986) The pattern electroretinogram in patients with optic nerve disease. *Doc. Ophthalmol.*, **62**, 53-59.

Ogden, T.E. (1973) The oscillatory waves of the primate electroretinogram. *Vision Res.*, **13**, 1059-1074.

Østerburg, G. (1935) Topography of the layer of rods and cones in the human retina. *Acta. Ophthal., Supp.*, 61-103.

Padmos, P., Haaijman, J.J. and Spekreijse, H. (1973) Visually evoked cortical potentials to patterned stimuli in monkey and man. *Electroenceph. Clin. Neurophys.*, **35**, 153-163.

Papst, N., Bopp, M. and Schnaudigel, O.E. (1984a) Pattern electroretinogram and visually evoked cortical potentials in glaucoma. *Graefe's Arch. Clin. Exp. Ophthal.*, **222**, 29-33.

Papst, N., Bopp, M. and Schnaudigel. O.E. (1984b) The pattern evoked electroretinogram associated with elevated intraocular pressure. *Graefe's Arch. Clin. Exp. Ophthal.*, **222**, 34-37.

Peachey, N.S., Sokol, S. and Moskowitz, A. (1983) Recording the contralateral PERG: effect of different electrodes. *Invest. Ophthal. Vis. Sci.*, **24**, 1, 1514-1516.

Peichl and Wässle, H. (1979) Size, scatter and coverage of ganglion cell receptive field centres in the cat retina. *J. Physiol.*, **291**, 117-141.

Penn, R.D. and Hagins, W.A. (1969) Signal transmission along retinal rods and the origin of the electroretinographic a-wave. *Nature.*, **223**, 201-205.

Perry, V.H. and Cowey, A. (1984b) Retinal ganglion cells that project to the superior colliculus and pretectum in the macaque monkey. *Neurosci.*, **12**, 4, 1125-1137

Perry, V.H. and Cowey, A. (1985) The ganglion cell and cone distributions in the monkey's retina: implications for central magnification factors. *Vision. Res.*, **25**, 12, 1795-1810.

Perry, V.H., Oehler, R. and Cowey, A. (1984a) Retinal ganglion cells that project to the dorsal lateral geniculate nucleus in the macaque monkey. *Neurosci.*, **12**, 4, 1101-1123.

Persson, H.E. and Wanger, P. (1982) Pattern-reversal electroretinogram in squint amblyopia, artificial anisometropia and simulated eccentric fixation. *Acta. Ophthal.*, **60**, 123-132.

Persson, H.E. and Wanger, P. (1984) Pattern-reversal electroretinograms and visual evoked cortical potentials in multiple sclerosis. *Brit. J. Ophthal.*, **68**, 760-764.

Piéron, H. and Siegal, J. (1939) Des variations de latence des responses électriques oculaires et d'une dissociation nécessaire de l'onde négative initiale et de l'onde positive terminale de l'électrorétinogram. *C.R. Soc., Biol.*, Paris, **131**, 1048-1050. cited by Granit , R. 1963.

Piper, H. (1911) Ueber die netzhautströme. *Arch. Anat. Physiol. Lpz.* 85-132. cited by Granit, R. 1963.

Plant, G.T. and Hess, R.F. (1986) The electrophysiological assessment of optic neuritis. In: Optic neuritis Hess, R.F. and Plant, G.T., (Eds) 9, 192-229. Cambridge Unversity Press, Cambridge.

Polyak, S.L. (1941) The retina. University of Chicago Press, Chicago.

Polyak, S.L. (1957) The vertebrate visual system. University of Chicago Press, Chicago.

Porciatti, V (1987) Non-linearities in the focal ERG evoked by pattern and uniform field stimulation; their variation in retinal and optic nerve dysfunction. *Invest. Ophthal. Vis Sci* **28**.8, 1306-1313.

Porciatti, V. and von Berger, G.P. (1984) Pattern electroretinogram and visual evoked potential in optic nerve disease, early diagnosis and prognosis. *Doc. Ophthal. Proc. Ser.*, **40**, 118-126.

Porciatti, V., Bagnoli, P. Alesci, R. and Sebastiani, L. (1987) Pattern evoked retinal and tectal responses. Are they from off channels? Abstr. Satellite Sympos. 2nd World Congr. Neurosci.

Potts, A.M., Modrell, R.W. and Kingsbury, C. (1960) Permanent fractionation of the electroretinogram by sodium glutamate. *Am. J. Ophthal.*, **50**, 900-907.

Potter, D.E. (1981) Adrenergic pharmacology of aqueous humour dynamics. *Pharmacol. Rev.* **33**, 133-153.

Pourcho, R.G. (1982) Dopaminergic amacrines in the cat retina. *Brain. Res.*, **252**, 1001-109.

Pugh, E.N. and Cobbs, W.H.(1986) Visual transduction in vertebrate rods and cones, a tale of two transmitters, calcium and cyclic GMP - a review. *Vision Res.* **26**, 1613-1643.

Pycock, C.J. (1985) Retinal neurotransmission. *Sur. Ophthal.*, **29**, 5, 355-365.

Quigley, H.A. and Addicks, E.M. (1980) Chronic experimental glaucoma in primates II. Effect of extended intraocular pressure elevation on optic nerve head and axonal transport. *Invest. Ophthal. Vis. Sci.*, **19**, 137-152.

Quigley, H.A., Hohman, R.M., Addicks, E.M., Massof, R.W. and Green, W.R. (1983) Morphological changes in the lamina cribrosa correlated with neural loss in open angle glaucoma. *Am. J. Ophthal.*, **95**, 675-691.

Ransom-Hogg, A. and Spillman, L. (1980) Perceptive field size in fovea and periphery of the light-and dark- adapted retinta. *Vision Res.*, **20**, 221-228.

Regan, D. (1972) Assessment of visual acuity by evoked potential recordings: ambiguity caused by temporal dependence of spatial frequency selectivity. *Vis. Sci.*, **18**, 439-443.

Regan, D. and Spekreijse, H. (1986) Evoked potentials in vision research 1961-86. *Vision Res.* **26**, 9,1461-1480.

Riemslag, F.C.C. and Heynen, H.G.M. (1984) Depth profile of pattern local electroretinograms in macaque. *Doc. Ophthal. Proc. Ser.*, **40**, 143-48.

Riemslag, F.C.C., Ringo, J.L., Spekreijse, H. and Verduyn Lunel, H. (1983) The distinction between luminance and spatial contrast components in the pattern ERG. *Doc. Ophthal. Proc. Ser.*, **37**, 255-264.

Riemslag, F.C.C., Ringo, J.L., Spekreijse, H. and Verduyn Lunel, H. (1985) The luminance origin of the pattern electroretinogram in man. *J. Physiol.*, **363**, 191-209.

Riggs, L.A. (1941) Continuous and reproducible records of the electrical activity of the human retina. *Proc. Soc. Exp. Biol. Med.*, **48**, 204-207.

Riggs, L.A. (1977) Electrophysiological techniques for studying visual function in man: a historical overview. *J. Opt. Soc. Am.*, **67**, 11, 1451-1457.

Riggs, L.A. (1986) Electroretinography. *Vision. Res.*, **26**, 9, 1443-1459.

Riggs, L.A., Johnson, E.P. and Schick, A.M.L. (1964) Electrical responses of the human eye to moving stimulus patterns. *Science.*, **144**, 567.

Riggs, L.A., Johnson, E.P. and Schick, A.M.L. (1966) Electrical responses of the human eye to changes in wavelength of the stimulating light. *J. Optom. Soc. Am.*, **56**, 1621-1627.

Ringens, P.J., Vijfvinkel-Bruinenga, S. and Van Lith, G.H.M. (1986a) The pattern-elicited electroretinogram I - a tool in the early detection of glaucoma. *Ophthalmol*, **192**, 171-175.

Ringens, P.J., Van Lith, G.H.M. and Poel, H.V.D. (1986b) The pattern-elicited electroretinogram II - retinal responses in retrobulbar neuritis. *Ophthal.*, **192**, 217-219.

Ringo, J., Van Duk, B. and Spekreijse, H. (1984) Pattern ERG of the cat. *Vision. Res.*, **24**, 8, 859-865.

Ripps, H. and Witkovsky, P. (1985) Neuron-glia interaction in the brain and retina. In: Progress in retinal research, (Eds) Osbourne, N. and Chader, G. , Vol, 4, Chp 7, 181-212.

Robson, J.G. The neurophysiology of retinal ganglion cells and optic nerve. In: Optic neuritis (Eds) Hess, R.F. and Plant, G.T. , Chp 2, 19-41. 1986.

Rodieck, R.W. (1979) Visual pathways. *Ann. Rev. Neurosci.*, **2**, 193-225.

Rodieck, R.W., Binmoeller, K.F. and Dineen, J. (1985) Parasol and midget ganglion cells of the human retina. *J. Comp. Neurol.*, **233**, 115-132.

Rodieck, R.W. and Stone, J. (1965a) Response of cat retinal ganglion cells to moving visual pattterns. *J. Neurophysiol.*, **28**, 819-832.

Rodieck, R.W. and Stone, J. (1965b) Analysis of receptive fields of cat retinal ganglion cells. *J. Neurophysiol.*, **28**, 833-849.

Rovamo, J. (1978) Receptive field density of retinal ganglion cells and cortical magnification factor in man. *Med. Biol.*, **56**, 97-102.

Rovamo, J. and Virsu, V. (1979) An estimation and application of the human cortical magnification factor. *Exp. Brain. Res.*, **37**, 495-510.

Ryan, M.K. and Hendrickson, A.E. (1987) Interplexiform cells in macaque monkey retina. *Exp. Eye. Res.*, **45**, 57-66.

Saheb, N.E., Lorenzetti, D. East, D. and Salpter-Carlton, S. (1982) Thymoxamine versus pilocarpine in the reversal of phenylephrine-induced mydriasis. *Can. J. Ophthalmol.* **17**, 6, 266-267.

Sakai, H.M., Naka, K.I. and Dowling, J.E. (1986) Ganglion cell dendrites are presynaptic in catfish retina. *Nature.*, **319**, 495-497.

Sanchez, R.M., Dunkelberger, G.R. and Quigley, H.A. (1986) The number and diameter distribution of axons in the monkey optic nerve. *Invest. Ophthal. Vis. Sci.* **27**, 1342-1350.

Sarthy, P.V. (1983) ^{3}H-GABA release from Müller glia cells in the rat retina. *J. Neurophysiol.*, **3**, 2494-2503.

Schneider, T. and Zrenner, E. (1987) Double flash responses in different retinal layers. *Ophthal. Res.*, **19**, 193-199.

Schiller, P.H. (1984) The connections of the retinal on and off pathways to the lateral geniculate nucleus of the monkey. *Vision. Res.*, **24**, 9, 923-932.

Schiller, P.H. and Malpeli, J.G. (1978) Functional specificity of lateral geniculate nucleus laminae of the rhesus monkey. *J. Neurophysiol.*, **41**, 788-797.

Schiller, P.H. and Malpeli, J.G. (1977) Properties of tectal projections of monkey retinal ganglion cells. *J. Neurophysiol.*, **40**, 428-445.

Schultze, M. (1866) Zur anatomie und physiologie der retina. *Arch mikr. Anat.*, **2**, 175-286. cited by Granit R. 1963.

Schuurmans, R.P. and Berninger, T. (1984) Pattern reversal responses in man and cat: a comparison. *Ophthal. Res.*, **16**, 67-72.

Seiple, W.H. and Siegel, I.M. (1983) Recording the pattern electroretinogram: a cautionary note. *Invest. Ophthal. Vis. Sci.*, **24**, 796-798.

Seiple, W.H., Price, M.J., Kupersmith, M., Siegel, I. and Carr, R. (1983) The pattern electroretinogram in optic nerve disease. *Ophthalmol.*, **90**, 9, 1127-1132.

Serra, G., Carreras, M., Tugnoli, V., Manca, M. and Christofori, M.C., (1984) Pattern electroretinogram in multiple sclerosis. *J. Neurol. Neurosurg. Psychiat.*, **47**, 879-883.

Shapero, M. (1971) Amblyopia. Chiltern Book Co. London.

Shapley, R. (1982) Parallel pathways in the mammalian visual system. *Annals N.Y.Acad. Sci.* **388** 11-20.

Shapley, R. and Enroth Cugell, C. (1984) Visual adaptation and retinal gain controls. In: Progress in retinal research. (Eds) Osbourne, N. and Chader, G.J., Pergammon press.Ch 9, 263-346.

Shapley, R.M. and Lennie, P. (1985) Spatial frequency analysis in the visual system. *Ann. Rev. Neurosci.*, **8**, 547-583.

Shapley, R.M. and Perry, V.H. (1986) Cat and monkey retinal ganglion cells and their visual functional roles. *TINS.*, **95**, 229-235.

Shapley, R.M. and Victor, J.D. (1979) Nonlinear spatial summation and the contrast gain control of cat retinal ganglion cells. *J. Physiol.*, **290**, 141-161.

Shepherd, G.M. (1986) Microcircuits to see by. *Nature.*, **319**, 452-453.

Sherman, J. (1982) Simultaneous pattern reversal electroretinograms and visual evoked potentials in diseases of the macula and optic nerve. *Annals N. Y. Acad. Sci.*, **388**, 214-226.

Sherman, J. and Richardson, V. (1982) What is the origin of the pattern reversal electroretinogram in humans. *Invest. Ophthal. Vis. Sci. Suppl.*, **22**, 138.

Sierpinski-Bart, J., Moran, A., Hocherman, S. and Neumann, E. (1978) Non-corneal electroretinography for pediatric ophthalmology. *Metabolic Ophthalmol.*, **2**, 387-388.

Sieving, P.A., Frishman, L.J. and Steinberg, R.H. (1986) M-wave of proximal retina in cat. *J. Neurophysiol.*, **56**, 1039-1048.

Sieving, P.A., Linsenmeir, R.A. and Steinberg, R.H. (1984) Current source density (CSD) analysis shows main pattern ERG (PERG) source in proximal retina. *Invest. Ophthal. Vis. Sci. Suppl.*, **25**, 259.

Sieving, P.A. and Steinberg, R.H. (1985) Contribution from proximal retina to intraretinal pattern ERG : The M-wave. *Invest. Ophthal. Vis. Sci.*, **26**, 1642-1647.

Skalka, H.W. (1979) Computer averaged ERG's using skin electrodes. ISCEV Symp., 259-263.

Skrandies, W., Leipert, K.P. and Dodt, E. (1987) Alterations of retinal and cortical evoked potentials in patients with visual field defects. *Invest. Ophthal. Vis. Sci. Suppl.*, **28**, 409.

Slaughter, M.M. and Miller, R.F. (198l) 2-amino - 4-phosphonobutyric acid: a new pharmacological tool for retina research. *Science.*, **211**, 182-184.

Slaughter, M.M. and Miller, R.F. (1983) An excitatory amino acid antagonist blocks cone input to sign conserving second order retinal neurons. *Science* , **219**, 1230-1232.

Slooter, J. and Van Norren, D. (1980) Visual acuity measured with pupil responses to checkerboard stimuli. *Invest. Ophthal. Vis. Sci.*, **19**, 105-108.

Snyder, A.W., Bossomaier, T.R.J. and Hughes, A. (1986) Optical image quality and the cone mosaic. *Science.*, **23**, 499-500.

Sokol, S. (1978) Pattern elicited ERGs and VECPs in amblyopia and infant vision. *Vis. Psychophys. Physiol.*, 453-463.

Sokol, S. and Bloom, B.H. (1977) Macular ERGs elicited by checkerboard pattern stimuli. *Doc. Ophthal. Proc. Ser.*, **13**, 299-305.

Sokol, S., Jones, K. and Nadler, D. (1983) Comparison of the spatial response properties of the human retina and cortex as measured by simultaneously recorded pattern ERGs and VEPs. *Vision. Res.*, **23**, 7, 723-727.

Sokol, S. and Nadler, D. (1979) Simultaneous electroretinograms and visually evoked potentials from adult amblyopes in response to a patterened stimulus. *Invest. Ophthal. Vis. Sci.*, **24**, 848-855.

Soodak, R.E., Shapley, R.M. and Kaplan, E. (1987) Functional subunits of receptive field centres in cat X and Y cells. *Invest. Ophthal. Vis. Sci. Suppl.*, **28**, 240.

Spalton, D.J., Hitchings, R.A., and Hunter, P.A. Atlas of clinical ophthalmology. pubs. Churchill Livingston, Edinburgh. 1986.

Spekreijse, H. (1966) Analysis of EEG responses in man evoked by sine wave modulated light. pubs. Junk, The Hague.

Spekreijse, H. and Apkarian, P. (1986) The use of a system analysis approach to electrodiagnostic (ERG and VEP) assessment. *Vision. Res.*, **26**, 1, 195-219.

Spekreijse, H., Estevez, O. and Van Der Tweel, H. (1973a) Luminance responses to pattern reversal. *Doc. Ophthal. Proc. Ser.*, **2**, 205-211.

Spekreijse, H., Van Der Tweel, H. and Zuidema, Th. (1973b) Contrast evoked responses in man. *Vision. Res.*, **13**, 1577-1601.

Spillman, L. (1971) Foveal receptive fields in the human visual system measured with simultaneous contrast in grids and bars. *Pflügers Arch. ges Physiol.* **326,** 281-299.

Steinberg, R.H., Schmidt, R. and Brown, K.T. (1970) Intracellular responses to light from cat pigment epithelium: origin of the elctroretinogram c-wave. *Nature.*, **227**, 728-730.

Sterling, P., Freed, M. and Smith, R.G. (1986) Microcircuitry and functional architecture of the cat retina. *TINS*, **95**, 186-192.

Stockton, R.A. and Slaughter, M.M. (1987) On-bipolar cell potassium fluxes are uniquely associated with the ERG b-wave. *Invest. Ophthal. Vis. Sci. Suppl.*, **28**. 406.

Stoerig, P. and Zrenner, E. (1987) The pattern-ERG after post-geniculate lesions: functional aspects of trans-synaptic retrograde degeneration in man. *Invest. Ophthal. Vis. Sci. Suppl.*, **28**, 409.

Stone, J., Dreher, B. and Leventhal, A. (1979) Hierarchical and parallel mechanisms in the organisation of the visual cortex. *Brain. Res.*, 345-395.

Stone, J. and Fukuda, Y. (1974) Properties of cat retinal ganglion cells: a comparison of W-cells with X- and Y- cells. *J. Neurophysiol.*, **37**, 722-748.

Stone, J. and Hoffman, K.P. (1972) Very slow conducting ganglion cells in the cat retinal, a major new functional type. *Brain. Res.*, **43**, 610-616.

Stone, J. and Johnston, E. (1981) The topography of primate retina: a study of the human, bushbaby, and new and old world monkeys. *J. Comp. Neurol.*, **196,** 205-223.

Sundmark, E. (1959) The contact glass in human electroretinography. *Acta. Ophthal. Suppl.*, **52**, 1-40.

Svaetchin, G. (1956) The cone function related to the activity of retinal neurones. *Acta Physiol. Scand.* **39** (Suppl. 134) 67-92.

Svaetchin, G. and MacNichol, E.F. (1958) Retinal mechanism for chromatic and achromatic vision. *Annals N. Y. Acad. Sci.* **74**, 385-404 .

Szamier, R.B., Ripps, H. and Chappell, R.L. (1980) On the glial cell origin of the ERG b-wave. *Invest. Ophthal. Vis. Sci. Suppl*, **19**, 39.

Thier, P. and Alder, V. (1984) Action of iontophoretically applied dopamine on cat retinal ganglion cells. *Brain. Res.*, **292**, 109-121.

Thompson. C.M. (1987) Objective and psychophysical studies of infant visual development. PhD Thesis, Aston Unversity.

Thompson, D.A. and Drasdo, N. (1987) An improved method for using the DTL fibre in electroretinography. *Ophthal. Physiol. Opt.*, **7**, 315-320.

Tomita, T. (1970) Electrical activity of vertebrate photoreceptors. *Quart. Rev. Biophys.*, **3**, 179-222.

Tomita, T. (1986) Retrospective review of retinal circuitry. *Vision. Res.*, **26**, 1339-1350.

Trick, G.L. (1985) Retinal potentials in patients with primary open angle glaucoma: physiological evidence for temporal frequency tuning deficits. *Invest. Ophthal. Vis. Sci.*, **26**, 1750-1758.

Trick, G.L. and Wintermeyer, D.H. (1982) Spatial and temporal frequency tuning of pattern reversal retinal potentials. *Invest. Ophthal. Vis. Sci.*, **23**, 6, 774-779.

Troscianko, T. (1982) A given visual field location has a wide range of perceptive field sizes. *Vision Res.*, **22**, 1363-1369.

Tuttle, D.R. (1973) Electrophysiological studies of functional amblyopia utilizing pattern reversal techniques. Masters thesis, Unversity of Louisville.

Vaegan and Arden, G.B. (1987) Effect of pattern luminance profile on the pattern ERG in man and pigeon. *Vision Res.* **27**, 883-892.

Vaegan, Arden, G.B. and Hogg, C.R. (1982) Properties of normal electroretinograms evoked by patterned stimuli in man. *Doc. Ophthal. Proc. Ser.*, **31**.111-129.

Valeton, J.M. and Van Norren D. (1982) Fractional recording and component analysis of primate ERG: separation of photoreceptor and other retinal potentials. *Vision Res.*, **22**, 381-391.

Van Blokland, G.J. (1986) Directionality and alignment of the foveal receptors, assessed with light scattered from the human fundus in vivo. *Vision Res.*, **26**, 3, 495-500.

Van Buren, J.M. (1963a) The retinal ganglion cell layer. pubs. C. Thomas, Springfield, Illinois.

Van Buren, J.M. (1963b) Trans-synaptic retrograde degeneration in the visual system of primates. *J. Neurol. Neurosurg. Psychiat.*, **26**, 402.

Van Den Berg, T.J.T.P., Riemslag, F.C.C., De Vos, G.W.G.A and Verduyn Lunel, H.F.E. (1986) Pattern ERG and glaucomatous visual field defects. *Doc. Ophthalmol.*, **61**, 335-341.

Van Der Tweel, I.H. (1961) Some problems in vision regarded with respect to linearity and frequency responses. *Annals. N.Y. Acad. Sci.*, **89**, 829-856.

Van Essen, D.C. and Anderson, C.H. (1986) Sampling of the visual image in the retina and LGN of the macaque. *Invest. Ophthal. Vis. Sci. Suppl.*, **94**, 2.

Van Lith, G., Ringens, P. and De Heer, L.J. (1984) Pattern electroretinogram and glaucoma. In: Developments in Ophthalmology; Special tests of visual function, basic problems and clinical application, **9**, 133-139, 1984.

Van Meeteren, A. (1974) Calculations on the optical modulation transfer function of the human eye for white light. *Acta. Ophthal.*, **21**, 5, 395-412.

Virsu, V. and Rovamo, J. (1979) Visual resolution, contrast sensitivity, and the cortical magnification factor. *Exp. Brain. Res.*, **37**, 475-494.

Vogel, D.A. and Green, D.A. (1980) Potassium release and b-wave generation : A test of the Müller cell hypothesis. *Invest. Ophthal. Vis. Sci.*, **19**, 39.

Vos, J.J., Walraven, J. and Van Meeteren, A. (1976) Light profiles of the foveal image of a point source. *Vision Res.*, **16**, 215-216.

Wachmeister, L. (1972) On the oscillatory potentials of the human electroretinogram in dark and light adaptation. *Acta. Ophthal.*, **116**.

Wachtmeister, L. (1974) Incremental thresholds of the oscillatory patentials of the human electroretinogram in response to coloured light. *Acta. Ophthal.*, **52**, 378-389.

Wachtmeister, L. and Azazi, M. (1985) Oscillatory potentials of the electroretinogram in patients with unilateral optic atrophy. *Ophthalmol.*, **191**, 39-50.

Wachtmeister, L. and Dowling, J.E. (1979) Laminar profile study of the oscillatory potentials of the vertebrate electroretinogram (ERG). ISCEV Symp., 355-360.

Wässle, H., Piechl, L. and Boycott, B.B. (1981) Dendritic territories of cat retinal ganglion cells. *Nature*, **292**, 344-345.

Watnabe, I. and Toyama, K. (1979) The oscillatory potentials and the rhythmic wavelets superimposed upon the off effect of the ERG. ISCEV Symp., 101-105.

Wanger, P. and Persson, H.E. (1983) Pattern reversal electroretinogram in unilateral glaucoma. *Invest. Ophthal. Vis. Sci.*, **24**, 749-753.

Wanger, P. and Persson, H.E. (1984) Oscillatory potentials, flash and pattern reversal electroretinogram in amblyopia. *Acta. Ophthal.*, **62**, 643-650.

Wanger, P. and Persson, H.E. (1985) Pattern reversal ERGs in ocular hypertension. *Doc. Ophthal.*, **61**, 27-31.

Welinder, E. (1982) Effects of intravitreally injected DL- alpha-amino adipic acid on the c-wave of the D.C. recorded electroretinogram in albino rabbit. *Invest. Ophthal. Vis. Sci.*, **23**, 240-245.

Wertheim, T. (1894) Ueber die indirekte Sehschärfe. *Z. für Psychol.Physiol. Sinnesorg.* **7**, 172-189.

Westheimer, G. (1965) Spatial interaction in the human retina during scotopic vision. *J. Physiol.*, **181**, 881-894.

Westheimer, G. (1985) The oscilloscopic view: retinal illuminance and contrast of point and line targets. *Vision. Res.*, **25**, 1097-1103.

Weymouth, F.W. (1958) Visual sensory units and the minimum angle of resolution. *Am. J. Ophthalmol.* **46**, 102-113.

Wiesel, T.N. and Hubel, D.H. (1965) Extent and recovery from the effects of visual deprivation in kittens. *J. Neurophysiol.*, **28**, 1060-1072.

Wiesel, T.N. and Hubel, D.H. (1966) Spatial and chromatic interactions in the lateral geniculate body of the rhesus monkey. *J. Neurophysiol.*, **29**, 1115-1156.

Williams, D.R. (1985) Aliasing in human foveal vision. *Vision. Res.*, **25**, 2, 195-205.

Williams, D.R. (1986) Seeing through the photoreceptor mosaic. *TINS*, **95**, 193-198.

Williams, D.R., Colett, A. and Korte, R. (1986) Extrafoveal grating resolution and sampling theory. *Invest. Ophthal. Vis. Sci.*, **27**, 3, 94.

Wilson, H.R. (1978) Quantitative prediciton of line spread function measurements: implications for channel band widths. *Vision Res.*, **18**, 493-496.

Wilson, H.R. and Bergen, J.R. (1979) A four mechanism model for threshold spatial vision. *Vision. Res.*, **19**, 19-32.

Wirth, A., Cavallacci, G. and Genovesi Ebert, F. (1984) The advantages of an inverted retina. *Dev. Ophthalmol.*, **9**, 20-28.

Wolter, J.R. (1978) Centrifugal fibres in adult human optic nerve 16 days after enucleation. *Trans. Am Ophthal. Soc.* **76** 140-155.

Yau, K.W. and Nakatani, K. (1985) Light-suppressible cyclic GMP-sensitive conductance in the plasma membrane of a truncated rod outer sement. *Nature,* **317**; 252.

Yellot, J.I. (1982) Spectral analysis of spatial sampling by photoreceptors: topological disorder prevents aliasing. *Vision. Res.*, **22**, 9, 1205-1210.

Yonemura, D. and Kawasaki, K. (1979) New approaches to ophthalmic electrodiagnosis by retinal oscillatory potential, drug induced responses from retinal pigment epithelium and cone potential. *Doc. Ophthalmol.*, **48**, 163-222.

Yonemura, D., Kawasaki, K., Yanagda, T., Tanak, J, Kawaguchi, H, and Nakata, Y. (1979) Effects of Ω - amino acids on oscillatory activities of the light evoked potentials in the retina and visual pathways. ISCEV Symp., 339-353.

Yuodelis, C. and Hendrikson, A. (1986) A qualitative and quantitative analysis of the human fovea during development. *Vision. Res.*, **26**, 847-855.

Ziv, B. (1961) The gold ring electrode in electroretinography. *Arch. Ophthal.*, **65**, 582-583.